INFORMATION TO USERS

This manuscript has been reproduced from the microfilm master. UMI films the text directly from the original or copy submitted. Thus, some thesis and dissertation copies are in typewriter face, while others may be from any type of computer printer.

The quality of this reproduction is dependent upon the quality of the copy submitted. Broken or indistinct print, colored or poor quality illustrations and photographs, print bleedthrough, substandard margins, and improper alignment can adversely affect reproduction.

In the unlikely event that the author did not send UMI a complete manuscript and there are missing pages, these will be noted. Also, if unauthorized copyright material had to be removed, a note will indicate the deletion.

Oversize materials (e.g., maps, drawings, charts) are reproduced by sectioning the original, beginning at the upper left-hand corner and continuing from left to right in equal sections with small overlaps. Each original is also photographed in one exposure and is included in reduced form at the back of the book.

Photographs included in the original manuscript have been reproduced xerographically in this copy. Higher quality 6" x 9" black and white photographic prints are available for any photographs or illustrations appearing in this copy for an additional charge. Contact UMI directly to order.

UMI

THE UNIVERSITY OF ALBERTA

REFERENCE SYMBOL ASSISTED MULTISTAGE SUCCESSIVE INTERFERENCE

CANCELLING RECEIVER FOR CODE DIVISION MULTIPLE ACCESS WIRELESS

COMMUNICATION SYSTEMS.

BY

ANTHONY C.K. SOONG ©

A THESIS

SUBMITTED TO THE FACULTY OF GRADUATE STUDIES AND RESEARCH IN

PARTIAL FULFILLMENT OF THE REQUIREMENTS FOR THE DEGREE OF

DOCTOR OF PHILOSOPHY

DEPARTMENT OF ELECTRICAL AND COMPUTING ENGINEERING

EDMONTON, ALBERTA

SPRING, 1997

0-612-21639-X

Canada

THE UNIVERSITY OF ALBERTA

RELEASE FORM

NAME OF AUTHOR: Anthony C.K. Soong

TITLE OF THESIS: Reference symbol assisted multistage successive interference cancelling receiver for code division multiple access wireless communication systems.

DEGREE: Doctor of Philosophy

YEAR THIS DEGREE GRANTED: 1997

Permission is hereby granted to THE UNIVERSITY OF ALBERTA LIBRARY to reproduce single copies of this thesis and to lend or sell such copies for private, scholarly or scientific research purposes only.

The author reserves other publication rights, and neither the thesis nor extensive extracts from it may be printed or otherwise reproduced without the author's written permission.

Anthony C.K. Soong
QUALCOMM Incorporated
5450 Western Avenue
Boulder, CO
U.S.A.

Date: April 8, 1997

THE UNIVERSITY OF ALBERTA

FACULTY OF GRADUATE STUDIES AND RESEARCH

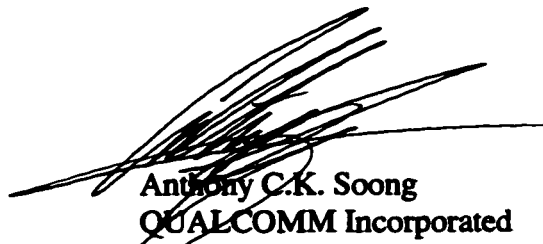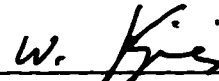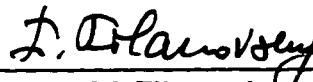The undersigned certify that they have read, and recommend to the Faculty of Graduate Studies and Research for acceptance, a thesis entitled *Reference symbol assisted multistage successive interference cancelling receiver for code division multiple access wireless communication systems* submitted by Anthony C.K. Soong in partial fulfillment of the requirements for the degree of Doctor of Philosophy.

Supervisor, Dr. Witold A. Krzymień
Department of Electrical and Computer Engineering

Dr. Paul K.M. Ho
School of Engineering Science
Simon Fraser University

Dr. Igor M. Filanovsky
Department of Electrical and Computer Engineering

Dr. Zoltan J. Koles
Department of Biomedical Engineering

Dr. Raymond E. Rink
Department of Electrical and Computer Engineering

Date: 7 April 1997

Abstract

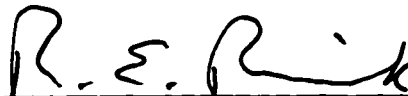This thesis investigates the performance of the reference symbol assisted successive interference cancelling (RAMSIC) receiver for CDMA wireless communication systems. The reverse link of a CDMA system with binary antipodal modulation and coherent detection is considered. The results with biphase spreading of the modulated signal show that the initial capacity improvement is relatively small. This is because interference from symbols not yet detected by the receiver significantly corrupts the channel estimates. Therefore, the transmitted signal structure has been modified to include guard intervals around the reference symbols to minimize this interference. Single cell analysis shows that the proposed technique results in a system with capacity approaching 80% that of the system with successive interference cancellation operating with perfect channel estimates. Multi-cell performance results demonstrate that without any forward error correction, the capacity of the proposed system with the RAMSIC receiver compares very favourably with that of comparable CDMA systems employing conventional detection and coding even when the path loss exponent is two. Further analysis shows that the RAMSIC receiver with quadriphase spreading performs significantly better than that with biphase spreading which in turn is superior to the conventional matched filter receiver. Performance analysis with imperfect parameter estimation shows that chip synchronization errors of the order to be expected in a properly designed conventional CDMA system have only minimal effect on performance but power control error, on the other hand, significantly affects performance. Hence, additional diversity should be employed to minimize the power control error. Consequently, the application of antenna diversity is then investigated. The results show that with a realistic feedback power control algorithm

and in fast fading the capacity of the system with dual receive antenna diversity can be increased 1.6 times over that of the IS-95 system. It is also demonstrated that the capacity of the system in slow fading environment increases dramatically over that under fast fading. Therefore, the 1.6 fold advantage of the RAMSIC receiver may be interpreted as the worst case performance advantage. Investigation of transmitter antenna diversity shows that in systems requiring lower BER (10^{-4} or less), such as in image and video communication, artificial multipath created by two transmitting antennas should also be considered as one possible way to increase capacity.

Acknowledgement

There are many people to whom I am grateful for their support: my wife Sherry and my children Micheli and Madeline for putting up with me; my mother, Christina, without whom this work could never have been done; my late father; the rest of my extended family for their unending support; my supervisor Dr. Witold A. Krzymień for his excellent guidance and encouragement; Dr. Zoltan Koles for his friendship and enlightening discussions; Drs. Igor Filanovsky, Paul Ho and Ray Rink for their excellent comments. The financial support from TR *Labs* is much appreciated.

Further thanks go out to all my friends and everyone at TR *Labs* and The Clinical Diagnostics and Research Centre at Alberta Hospital Edmonton for their friendship.

Table of Contents

List of Tables

List of Figures

List of Abbreviations

AWGN	additive white Gaussian noise
BER	bit error rate
BPSK	binary phase shift keying
CDMA	code division multiple access
CLPC	closed loop power control
DS-CDMA	direct sequence code division multiple access
DS-SS	direct sequence spread-spectrum
DS-SSMA	direct sequence spread-spectrum multiple access
FDMA	frequency division multiple access
FH	frequency-hop
FM	frequency modulation
IID	independent and identically distributed
LMS	least mean square
MAI	multiple access interference
MLSE	maximum likelihood sequence estimation
MMSE	minimum mean square error
MSE	mean square error
MSK	minimum shift keying
MTSO	mobile telephone switching office
NOMAC	noise modulation and correlation
O^3-BPSK	orthogonal on-off BPSK
PCS	personal communication system
PIC	parallel interference cancellation
QPSK	quadrature phase shift keying
RAMSIC	reference symbol assisted multistage successive interference cancelling
RF	radio frequency
RLS	recursive least squares
SIC	successive interference cancellation
SS	spread-spectrum
TDMA	time division multiple access
US	uncorrelated scattering
WSS	wide sense stationary
WSSUS	wide sense stationary uncorrelated scattering

Chapter 1: Introduction

1.1 Introduction

One of the great thrusts in the telecommunication industry today is wireless communications. Its main attraction is obvious: it gives users the freedom of mobility while still being able to transmit and receive information. The explosion of the cellular communication industry is a testimony to the utility of wireless telephony with the public. This explosion in the demand for cellular services has resulted in traffic congestion over the allotted spectrum. In some cases, the number of potential users far exceeds the current capabilities of some cellular systems. Therefore, increasing the number of simultaneous users over the current allotted spectrum is a *desideratum* of the telecommunication industry.

There are, at present, basically three different methods of providing deterministic multiple access: frequency division multiple access (FDMA)[1], time division multiple access (TDMA)[2] and code division multiple access (CDMA). The current interest in CDMA by the telecommunication industry is mainly due to its potentially higher traffic carrying capabilities. The capacity of CDMA cellular telephone systems can theoretically be significantly increased when compared to analog FDMA and digital TDMA (Schilling, 1991). Furthermore, CDMA offers inherent communication privacy and it may be easier to

---

[1] FDMA systems take advantage of the fact that the spectrum usually allotted for a particular service is much larger than is necessary for the transmission of a single user's data. Therefore, the allotted spectrum can be divided into several channels whose bandwidth is just sufficient for the transmission of a single user's data. In so doing, the allotted frequencies are divided among several users.

[2] TDMA systems take advantage of the fact that the bit rate capacity of the RF channel is much larger than the bit rate of any particular user. Therefore, several users may use the same RF channel if they transmit their data at different time. In so doing the RF channel is time shared between several users. It should be noted that systems that combine both FDMA and TDMA are common.

implement (Tse, 1993).

It is the intent of this thesis to investigate techniques for increasing the multiple access capabilities of the CDMA system. Before we go into a discussion about the scope of the thesis, a short discussion of the concepts of cellular mobile telephone system will be given.

1.2 Cellular Mobile Telephone System

The conventional (non-cellular) mobile telephone system was designed to provide service to a relatively small number of users and operated with about 100 radio frequency (RF) channels from a number of base stations. The zone of coverage for each base station was normally planned to be as large as possible. Therefore, the transmitted power was as high as possible. Channel reuse was not possible except at base stations separated by a very large distance. The only way to increase capacity in such system was to increase the number of allotted RF channels. Hence, the capacity of the system was limited by the number of RF channels available. Since additional spectral allocations were increasingly difficult to obtain, a new system with more efficient usage of the spectrum was necessary.

The necessity of providing high capacity mobile radio telephone systems that did not require very large number of channels led to the development of base stations serving a small area or cell. The same channels may then be re-used within a relatively small distance. The capacity of the system can be increased by decreasing the size of the cell and re-using existing channels. This mobile communication system is known as cellular mobile communication system.

2

On January 4, 1979, the FCC authorized Illinois Bell Telephone Co. to conduct a trial of a developmental cellular system and to offer cellular service to the public in the Chicago area. At around the same time, American Radio Telephone Service Inc. was authorized to operate a cellular service in the Washington - Baltimore area. These systems demonstrated the feasibility and affordability of cellular service and full commercial service began first in Chicago in October of 1983.

There are three parts to a basic cellular system: mobile units, cell sites (or base station) and mobile telephone switching offices (MTSO). The mobile telephone unit contains a control unit, a transceiver and an antenna system. The cell site provides the interface between the mobile units and the MTSO. It consists of a control unit, radio cabinets, antennas, a power plant and data terminals. The MTSO is the central coordinating element for all cell sites in a given system. It interfaces with the telephone company zone offices, controls call processing and handles billing activities. The MTSO consists of the cellular processor and the cellular switch. The cellular processor provides central coordination and cellular administration. The cellular switch can be either analog or digital. It switches calls to connect mobile subscribers to other mobile subscribers and to the telephone network.

The operation of the cellular mobile system, from a customer's perspective, can be divided into five parts: mobile unit initialization, mobile originated calls, network originated calls, and call termination and handoff procedure. Mobile unit initialization occurs when a user activates the receiver of the mobile unit. The receiver scans a number of set-up channels (21 or three per cell, in the first generation North-American cellular

3

service). It selects the strongest of these set-up channels and locks on to it. Since each cell site is assigned a different set-up channel, locking onto the strongest set-up channel usually means selecting the closest[3] cell site. Since this self locking scheme is used in the idle stage, it is user independent. Self locking also eliminates the load on the transmission at the cell site for locating the mobile unit. The disadvantage is that no location information of idle mobile units appears at each cell site. Thus the paging process for calls initiated from the land line to the mobile unit is longer. Self locking is, however, still an advantage for the system because most of the calls are initiated by the mobile. But if in the future, when land-line originated calls are more prevalent, a feature called "registration" can be used (Lee, 1989).

For mobile originated calls, the mobile user places the called number into an originating register in the mobile unit and pushes the "send" button. A request for service is then sent on the selected set-up channel. The cell site, upon receiving the service request, selects the best directional antenna for the voice channel. At the same time, the cell site sends a request for a voice channel, via a high speed link to the MTSO. The MTSO selects an appropriate voice channel for the call. The cell site then links the mobile user through the selected channel and antenna. The MTSO also connects the wire-line party via the telephone zone office.

For network originated calls, a land line party dials a mobile user's number. The telephone zone office, recognizing that the number is of a mobile user, forwards the call to the MTSO. The MTSO then sends a paging signal to certain cell sites based upon the

---

[3] In some cases, because of multipath fading, the strongest set-up channel is not associated with the closest cell site. A more detailed description of cell membership will be discussed later but for now we can assume that it is the closest.

mobile unit number and the search algorithm. The paging signal is then transmitted by each paged cell site. The mobile unit, recognizing that it is being paged, locks onto the strongest set-up channel and responds to the page. At the same time, the mobile unit also follows instruction to tune to an assigned voice channel and initiates user alert.

Call termination occurs when the mobile user turns off the voice transmitter. A particular signal (signaling tone) is then transmitted to the cell site and both sides free the voice channel. The mobile user then resumes monitoring pages through the strongest set-up channel.

Handoffs occur when a mobile unit, during a call, moves out of the coverage area of a particular cell site. At that point, the reception becomes weak and the present cell site requests a handoff. The system switches the call to a new frequency channel in a new cell site without either interrupting the call or alerting the user.

The above discussion of cellular communication system is intended to give a flavour of cellular telephony for those unfamiliar with the concept. It is by no means a comprehensive survey of the topic. The interested reader is asked to consult the excellent treatise of the area in Lee (1989). We now move onto a discussion about the objective and scope of the thesis.

1.3 Scope of the thesis

This thesis is singularly concerned with improving the traffic capacity of CDMA wireless communication systems. A review of the current technologies available for increasing traffic capacity is given in Chapter 2. It will be shown that receiver structures

that are capable of mitigating multiple access interference will significantly enhance capacity because the capacity of CDMA systems is limited by this interference. Chapter 3 will introduce a relatively simple receiver structure, the reference symbol assisted multistage successive interference cancelling (RAMSIC) receiver, that has the potential of mitigating the multiple access interference. The performance of this receiver with biphase spreading will then be determined in both single cell and multiple cell system. The results will show that significant capacity improvement over that with the conventional matched filter receiver is possible even under worst-case propagation conditions. Chapter 4 will investigate the sensitivity of the receiver to imperfect parameter estimation. The performance with biphase as well as quadriphase spreading will be examined. The results will show that synchronization algorithms that are acceptable for conventional direct-sequence spread spectrum communication will be sufficient for the RAMSIC receiver. But they also demonstrate that the RAMSIC receiver is extremely sensitive to power control errors and that additional diversity should be exploited if tight power control cannot be achieved. Chapter 5 investigates the performance of the RAMSIC receiver with antenna diversity. The results show that even without tight power control, significant capacity improvement (of the order of 1.7 times that of the current commercial CDMA system) is possible with the RAMSIC receiver using dual antenna diversity. Major conclusions of the work will be given in Chapter 6 along with a short discussion about possible extensions of the work.

6

1.4 Conclusion

The objective of this thesis is to investigate the performance of the reference symbol assisted successive interference cancelling receiver for CDMA wireless communication system. The receiver structure is of interest because it is capable of mitigating the multiple access interference which severely limits the capacity of CDMA systems, and at the same time it arguably is the easiest multi-user detector to implement because of its simple structure.

1.5 References

Lee, W.C.Y. (1989): *Mobile Cellular Telecommunications Systems*, New York: McGraw Hill Book Co..

Schilling, D.L., Milstein, L.B., Pickholtz, R.L., Kullback, M.and Miller, F. (1991): Spread Spectrum for Commercial Communications. *IEEE Communications Magazine*, vol. 29, no. 4, pp. 66-79.

Tse, R.T.S. (1992): *Spread Spectrum Multiple Access with Orthogonal Convolutional Codes for Indoor Digital Radio*, M.Sc. dissertation, University of Alberta.

Chapter 2: Background

2.1 Introduction

As it was stated in Chapter 1, the intent of this thesis is to investigate a receiver structure capable of increasing the multiple access capabilities of the CDMA wireless communication. Before we go into a discussion about the proposed receiver, the concepts of spread spectrum communication, the properties of the transmission channel, the notion of power control as well as current developments in multi-user detectors for CDMA systems must be fully understood.

2.2 Spread-Spectrum Communication

It has been well over forty years since the terms spread-spectrum (SS) and noise modulation and correlation (NOMAC) were first used to describe a class of signalling techniques that has desirable attributes for communication and navigation applications particularly in interference environments. Indeed it was mainly because of the anti-jamming capabilities of SS that the early works on this discipline were cloaked in secrecy. Most of the studies were conducted for the military and could thus only be found in classified documents. It is only in the last fifteen years that commercial uses of SS communications were contemplated.

The designation "spread spectrum" is used for signals which share the following two characteristics: 1) the energy transmitted must occupy a bandwidth that is both larger (often much larger) than and independent of the information bit rate; 2) demodulation must involve, at least in part, the correlation of the received signal with a replica of the signal used to spread the information signal in the transmitter (Simon *et al.*, 1985). It

9

should be noted that modulation techniques exist that result in a wide bandwidth transmission that are not spread-spectrum modulation.

One method of spread-spectrum modulation is to modulate the modulated information signal with another very wide band signal. Although in principle analog modulation can be used for this second modulation, it is usually digital phase modulation. The spreading signal is chosen to both facilitate demodulation by the intended receiver and make demodulation by unintended receivers as difficult as possible. These same properties of the modulated signal also allow the intended receiver to discriminate between the intended signal and a jamming signal. Spreading of the bandwidth by direct modulation of a data modulated carrier is called direct sequence spread-spectrum (DS-SS).

The simplest form of DS-SS is obtained using binary phase shift keying (BPSK) as the modulation technique. Consider a constant-envelope data-modulated carrier that has power P, radian frequency ω_0, and data phase modulation $\theta_d(t)$ given by

$$s_d(t) = \sqrt{2P} \cos[\omega_o t + \theta_d(t)] \ . \tag{2.1}$$

BPSK spreading is then accomplished by multiplying with a function, $c(t)$, taking on values of ± 1. In order for the function $c(t)$ to spread the energy of the signal s_d, the symbol duration of the spreading code, T_c, must be smaller than the data symbol duration, T_s. The spreading code symbol element is often referred to as the spreading code chip and the ratio of the symbol duration over the chip duration is known as the processing gain, G. It should be noted here that although the analysis of the system is greatly simplified if T_s is some integer multiple of T_c, it is not a requirement of SS systems. The transmitted signal is then

$$s_t(t) = \sqrt{2P}c(t)\cos[\omega_o t + \theta_d(t)] \; . \tag{2.2}$$

If this signal is transmitted via a distortionless additive white Gaussian noise (AWGN) channel having transmission delay T_d, then the received signal is given by:

$$s_r(t) = \sqrt{2P}c(t-T_d)\cos[\omega_o(t-T_d) + \theta_d(t-T_d) + \varphi] + n(t) \; , \tag{2.3}$$

where $n(t)$ denotes the AWGN component. Demodulation of the received signal at the receiver is accomplished, in part, by correlating it with the appropriately delayed spreading code. This correlation of the received signal is called despreading and is a critical function in SS systems. If the delay estimated by the receiver is denoted as $\hat{T}_d$ then the signal component of the output of the despreader mixer is

$$s_{rd}(t) = \sqrt{2P}c(t-T_d)c(t-\hat{T}_d)\cos[\omega_o(t-T_d) + \theta_d(t-T_d) + \varphi] \; . \tag{2.4}$$

If the spreading code at the receiver is perfectly synchronized with the spreading code at the transmitter (i.e. $T_d = \hat{T}_d$), the product $c(t-T_d)c(t-\hat{T}_d)$ is unity because $c(t) = \pm 1$. Therefore when correctly synchronized, the output of the despreader is the same as $s_d(t)$ except for a random phase φ, and thus can be demodulated with a conventional coherent phase demodulator.

It can be seen from the above that despreading of the received signal will only occur if the correct spreading sequence is used in the despreader. Thus, by giving each user a unique spreading code, multiple users may transmit on the same RF channel. The receiver will only despread the intended signal by demodulating with the intended signal's spreading code. The signals from the other users will not be despread but they will add to the interfering noise corrupting the desired signal. This additional interference with the desired

signal is known as multiple access interference (or noise). The amount of multiple access interference is dependent upon the cross-correlation between the intended spreading code sequence and the other users' spreading code sequences. The larger the cross correlation, the larger the multiple access interference. Since only the intended receivers have the spreading code for despreading of the signals, transmissions with SS systems are inherently difficult to intercept.

Furthermore, despreading of the intended signal depends upon the synchronization of the receiver spreading code with the transmitter spreading code. Many methods exist to achieve synchronization (e.g. see chapters 10 and 11 in Ziemer and Peterson, 1985). It is, nevertheless an active area of research and beyond the scope of this thesis to give a review of the current developments.

The anti-jamming property of SS communications can now be easily understood. Consider the case that the received signal given by (2.3) is intentionally jammed by a signal $J(t)$. The output of the despreading mixer, ignoring the AWGN term, is then given by

$$s_{rdj}(t) = \sqrt{2P} \cos[\omega_o(t - T_d) + \theta_d(t - T_d) + \varphi] + J(t)c(t - \hat{T}_d) \ . \qquad (2.5)$$

We can clearly see from (2.5) that the energy of the jamming signal is spread by the despreader. If the output of the despreader is now demodulated with a conventional coherent phase detector, the narrowband intermediate frequency filter will then filter out most of the energy of the jamming signal. Hence the effectiveness of the jamming signal is significantly reduced. Moreover, it has been shown that if small probability of bit error is required, then no other binary signalling scheme or receiver can substantially improve upon the performance of DS-SS with a correlation receiver for the same power and

bandwidth (Hizlan and Hughes, 1991). The preceding was intended to give an intuitive understanding of the anti-jamming property of SS systems, the interested reader is encouraged to consult the detailed discussion of the topic in Peterson *et al.* (1995), Simon *et al.* (1985), Wang and Milstein (1988) and Vijayan and Poor (1990).

So far we have discussed DS-SS system that is generated via BPSK modulation with a spreading sequence. It is no surprise that other modulation techniques, such as quadrature phase keying (QPSK) and minimum phase shift keying (MSK), can be employed. The advantage of QPSK DS-SS over BPSK DS-SS is that quadrature modulations are more difficult to detect[1] in low probability of detection applications and are less sensitive to some types of jamming. The advantage of MSK DS-SS over BPSK DS-SS is the theoretical benefit of a QPSK system together with hardware only slightly more complex than BPSK. It should be noted that the traditional reason for quadrature modulation, to conserve spectrum, is not usually of primary importance in a SS system.

It is intuitively obvious that a second method of widening the spectrum is to change the carrier frequency periodically. This type of spread spectrum is known as frequency-hop (FH) spread spectrum because the transmitted signal appears as a data-modulated carrier that is hopping from one frequency to the next. Although not absolutely necessary, each carrier frequency is usually chosen from a set of 2^k frequencies spaced approximately the width of the data modulation spectrum apart. To despread the transmitted signal, a local oscillator at the receiver is hopping synchronously with the received signal. The

---

[1]This is because the bandwidth requirement for transmitting the same information is less with QPSK than with BPSK modulation. Therefore, if we are to spread the signal over the same RF bandwidth, the processing gain will be larger for QPSK than with BPSK. Note that this is not true for the QPSK system proposed by Qualcomm where both the quadrature and in-phase signals transmit the same symbol.

difficulties of building truly coherent frequency synthesizers as well as the code tracking requirements, however, preclude the use of coherent data demodulation schemes. As a result, most FH SS systems use either noncoherent or differentially coherent data modulation.

Two different types of FH SS systems are possible. If the carrier frequency changes more slowly than the symbol rate, the system is known as a slow FH system. If, on the other hand, the carrier frequency changes faster than the symbol rate, the system is known as a fast FH system. A significant benefit of fast FH system is that frequency diversity gain is seen on each transmitted symbol. Therefore, fast FH system performs better in a partial-band jamming environment (Robertson and Ha, 1992). Moreover, frequency diversity has distinct advantages in a fading environment (Peterson *et al.*, 1995).

In order that some of the advantages of both FH and DS spread spectrum systems are combined in a single system, hybrid direct-sequence/frequency-hop systems that employ both DS and FH spreading techniques are employed. Hybrid systems are widely used in the military and are currently the only practical way of achieving extremely wide spectrum spreading. There exist, in the literature, a wide variety of methods for combining FH and DS spreading (Peterson *et al.*, 1985).

The preceding discussion of FH and hybrid systems was included here for completeness. Since a high capacity FH-SSMA system requires many filters tuned to specific hopping frequencies in the receiver and a frequency synthesizer that is capable of abrupt and, perhaps, high speed frequency hops at the transmitter, it is not suitable for high volume consumer products (Tse, 1992). Therefore, we will restrict ourselves to DS-SSMA systems in this thesis and we will not discuss FH and hybrid systems in any greater

detail. The interested reader may consult the more detailed discussion of these systems in Peterson *et al.* (1995), Simon *et al.* (1985), Robertson and Ha (1992), Maric and Titlebaum (1992) and Nemsic and Geraniotis (1992).

2.3 The Mobile Radio Channel

We digress here for a discussion of the interaction between the mobile communication channel and the transmitted signal. The properties of the channel that will be presented are independent of the type of multiple access scheme employed. Nevertheless if we are to significantly improve the traffic capacity of the CDMA system, a solid understanding of the channel is required. This discussion will be deeper in the small scale characteristics of the channel than on the large scale characteristics because power control can be used to easily mitigate the large scale effects.

One major problem in mobile communication is that a line-of-sight path between the transmitting and receiving antennas rarely exists. Propagation is, therefore, mainly by way of scattering from the surfaces of obstacles and by diffraction around and/or over them. Hence, the received signal arrives at the receiver via several different paths simultaneously. This is the so called multipath phenomenon where radio waves arrive from different directions with different time delays. These radio waves combine vectorially at the receiver. Depending on the phase relationship among the component waves, the resulting signal may be large or small. In such an environment, the transmission channel may be modelled as random multiple propagation paths varying with the movement of the mobiles that are characterized by three approximately separable effects: multipath fading, shadowing and path loss. Multipath fading can be further divided into nonselective

15

(envelope fading), time selective (Doppler spread) and frequency selective (time-delay spread) fading.

When the received single-tone signal is measured over a distance of a few hundred wavelengths, variations occur in the signal envelope that may be both fast and deep. These fluctuations in the signal envelope are known as nonselective fading (or envelope fading). When the number of plane waves composing the received signal is large, the received complex low-pass equivalent signal in the absence of a line of sight or specular component can be modelled as a zero mean complex Gaussian random process (Ossana, 1964; Gilbert, 1965; Clark, 1968; Gans, 1972). The received envelope thus has a Rayleigh distribution. In the presence of a line of sight or specular component, the inphase and quadrature parts of the received signal have non-zero mean and the envelope has a Ricean distribution (Stüber, 1996). The fading rate is shown to be proportional to the vehicle speed and the carrier frequency.

Fast nonselective fading is accompanied by fast phase changes, which induce random FM noise on the received carrier. The baseband spectrum of this random FM noise after envelope detection of the Doppler-shifted signal extends to twice the maximum Doppler frequency (Jakes, 1974). This effect, which can be considered as a temporal decorrelation of the multipath fading, is called time selective fading. It is time selective because the characteristic of the channel is changing with time. Furthermore, it can be shown (Steele, 1992) that when the channel is time variant, Doppler spreading (frequency dispersion) occurs. Frequency dispersion causes the bandwidth of the received signal to be different than that of the transmitted signal.

If the signal has a short duration then it is passed through the channel before the

channel characteristics can significantly change. As the signal duration is lengthened, the characteristics of the channel change while the signal is in flight and distortion results. This is because the channel as seen by the leading edge of the signal is different than that seen by the trailing edge. At the same time, Doppler spreading occurs until it is possible to observe significant widening of the received signal. The minimum signal duration at which frequency dispersion becomes noticeable is inversely proportional to the maximum Doppler shift experienced by the signal. The coherence time is a measure of the maximum length of the signal before distortion becomes noticeable. It is often defined as the time interval over which the envelope correlation is greater than 0.5.

Consider now the case of two frequency components within the message bandwidth. If these frequencies are close together, the electrical lengths of each path are approximately the same for both frequencies. That is, although there is multipath fading, the two frequency components will behave very similarly. Hence, provided that the message bandwidth is small, all frequency components within it behave similarly and flat fading is said to exist. The bandwidth in which different frequencies can be considered to fade similarly is defined as the coherence bandwidth. This bandwidth is inversely proportional to the root mean square value of the time-delay spread which is a measure of the temporal width of a received multiple-impulsive carrier that is transmitted through a multipath fading channel. As the frequency separation increases beyond the coherence bandwidth, the electrical lengths of each path are different for each frequency. The behaviour of the two frequency components will thus become uncorrelated. The extent of the decorrelation will depend upon the spread of the delay times because the phase shifts arise from the excess path lengths (excess over that of the first path). For very large delay

spreads, the electrical length difference may be a significant fraction of a wavelength even if the frequency separation is small. For the case of wideband signals in spread spectrum applications, the bandwidth of the signal is larger than the coherence bandwidth. The amplitude and phase relations of the various spectral components in the received signal are, therefore, not the same as they were in the transmitted signal. This phenomenon is known as frequency selective fading and appears as a variation in the received signal strength as a function of frequency.

Time dispersion and frequency selective fading are both manifestations of multipath propagation with delay spread. The presence of one implies the presence of the other. Time dispersion refers to the signal being stretched in time so that the duration of the received signal is greater than that of the transmitted signal. It is a result of the signals taking different times to cross the channel by different paths.

Even after the small-scale multipath fading described above is removed by averaging over distances of a few tens of wavelengths, large-scale variations of the signal strength remain. These fluctuations are known as shadowing and are caused mainly be terrain features of the mobile radio propagation environment. They impose a slowly changing average upon the Rayleigh fading statistics. A comprehensive mathematical model for shadowing does not exist in the literature but a log-normal distribution with a standard deviation of 5 to 12 dB has been found to fit experimental data in a typical urban environment (Okumura *et al.*, 1968; Egli, 1957; Black and Reudink 1972).

The average value of log-normal shadowing is determined by the path loss. The loss for each path in a multipath environment varies with the propagation distance between the transmitter and the receiver. The variation of the path loss has been shown experimentally

to obey the inverse square to fourth power law (Young, 1972; Rappaport and Milstein 1992).

Insights into how the channel appears to transmitted signal may be obtained from the coherence time and coherence bandwidth. If the bandwidth of the signal is less than the coherence bandwidth of the channel, frequency selective fading and, therefore, time dispersion of the signal do not appear. The channel is thus frequency flat for that particular system. Similarly when the time duration of the received signal is less than the coherence time, the channel will, as seen by the signal, be time invariant. The channel is thus time flat for that particular system.

When the channel is both time and frequency flat, it is known as a flat-flat channel. When the channel is both frequency dispersive and time dispersive, it is known as a doubly dispersive channel. The flat-flat channel does not fade with either time or frequency. An additive white Gaussian noise channel is an example of a flat-flat channel. The frequency flat channel (commonly called the flat fading channel) is observed by narrowband mobile systems. Wide band mobile systems, on the other hand, often operate on the doubly dispersive channel (commonly called the frequency selective fading channel).

Bello (1963) proposed a set of system functions that can describe linear time variant channels. Each function constitutes a complete description of the channel and all of the other functions may be calculated with only the full knowledge of any one particular function. Bello system functions are not only dependent upon the usual time and frequency variables, t and f, which are dual network variables (Bello, 1964), but are also dependent on the delay and Doppler shift variables, τ and v, which are dual variables describing time

and frequency translation. Time and frequency are dual network variables because they are used to describe input and output signals in the time and frequency domain respectively. Delay and Doppler shifts are dual network variables because they are used to describe dispersion in the time and frequency domain respectively. In general, variables are duals when they are used to describe similar concepts or behaviours in their respective domains[1].

It should be noted that although delay and time are both measured in seconds, the delay variable is independent of the time variable and as such can be drawn on a set of Cartesian coordinates. The easiest way to understand why these variables are independent is to consider the electrical lengths of the propagation paths. The electrical length of a particular propagation path, l_e, is the distance traversed by the electromagnetic wave going from the transmitter to the receiver following that path and is related to the delay by the following expression:

$$l_e = c\tau \qquad (2.6)$$

where c is the speed of light. Therefore, a path still possesses an electrical length and hence an associated delay even if the time variable is frozen. In general, at any instant in time, there may exist a path with any positive electrical length and so the two variables are independent of each other.

Since both frequency and Doppler shifts are measured in Hz, it is also not clear whether these two variables are independent. To understand why they are independent, recall that the Doppler shift is actually the rate of change of the physical length of the path

---

[1]The concept of duality is not discussed in detail here because of space limitations. The interested reader is encouraged to consult the detailed development of the concept in Bello (1964).

$\dfrac{dl}{dt}$, scaled by the signal's frequency. Frequency scaling is necessary because signals

perceive lengths in terms of wavelengths and not absolute measures. Since $\dfrac{dl}{dt}$ is

independent of frequency, it is possible for a path to exist possessing any Doppler shift

value at any particular frequency. Therefore, the two variables are also independent of

each other.

Although the previous discussion stated that the mobile radio channel have

characteristics that vary randomly, it is easier to introduce the Bello functions by assuming

that the channel is deterministic. Moreover, for convenience, we will also represent real

bandpass signals by their complex envelopes.

Let $h_\sigma(t)$ be the response of a linear time variant system at time t to the unit impulse

input $\delta(t\text{-}\sigma)$ located at time σ. The input delay spread function, $h(t,\tau)$, is then defined as

$$h(t,\tau) \equiv h_{t-\tau}(t) .\qquad(2.7)$$

It may be interpreted as the response of the channel at time t to a unit impulse input τ

seconds in the past. Note that $h(t,\tau) = 0$ for $\tau < 0$ because of causality. In other words, the

channel cannot have an output before any input is applied. To derive the input-output

relationship, let $u(t)$ be the complex low pass input. Recall that the sifting property of the

unit impulse function can be used to represent $u(t)$ as

$$u(t) = \int_{-\infty}^{\infty} u(\sigma)\delta(t-\sigma)d\sigma .\qquad(2.8)$$

The low pass output $z(t)$ can be obtained via superposition as

$$z(t) = \int_{-\infty}^{\infty} u(\sigma)h_\sigma(t)\,d\sigma .\qquad(2.9)$$

With $\sigma = t - \tau$ we get:

$$z(t) = \int_{-\infty}^{\infty} u(t-\tau)h_{t-\tau}(t)\,d\sigma \;, \tag{2.10}$$

and from (2.7)

$$z(t) = \int_{-\infty}^{\infty} u(t-\tau)h(t,\tau)\,d\tau \;. \tag{2.11}$$

Hence $h(t,\tau)$ is a Bello system function that relates the complex low pass input and output time waveforms. It is called the input delay-spread function because the delay is associated with the input port of the channel.

If the convolution in (2.11) is approximated as a sum, then

$$z(t) = \sum_{m=0}^{\infty} u(t-m\Delta\tau)h(t,m\Delta\tau)\Delta\tau \;. \tag{2.12}$$

This allows us to visualize the channel as a transversal filter with tap spacing $\Delta\tau$ and time varying tap gains of $h(t, m\Delta\tau)\Delta\tau$. This description provides a convenient way for a computer simulation to describe the channel because the channel can then be modelled as a tapped delay line.

The delay-Doppler-spread function $S(\tau,v)$ is defined as

$$S(\tau,v) = \mathcal{F}_{t,v}(h(t,\tau)) \tag{2.13}$$

where $\mathcal{F}_{t,v}(\circ)$ denotes the Fourier transform mapping signal from the t domain to the v domain. The fact that the time domain Fourier transformation transforms into the Doppler spread domain may seem a little peculiar. It should, however, be noted that it is a change in the channel's behaviour as a function of time that causes a Doppler shift whereas the channel spectrum is the frequency response of the channel at a specific time as a function

of the delay variable.

To obtain the input-output relationship associated with $S(\tau,v)$, we substitute (2.13) into (2.11)

$$z(t) = \int_{-\infty}^{\infty} \mathcal{F}_{v,t}^{-1}(S(\tau,v))u(t-\tau)d\tau$$

$$= \int_{-\infty}^{\infty}\int_{-\infty}^{\infty} S(\tau,v)u(t-\tau)e^{j2\pi vt}dvd\tau \quad . \tag{2.14}$$

Thus, $S(\tau,v)$ can be interpreted as the gain experienced by signals suffering first delay in the range $[\tau,\tau+d\tau]$ and then Doppler shift in the range $[v,v+dv]$. In other words, it is a measure of the scattering amplitude of the channel in terms of τ and v. Since double integration is computationally more complex than single integration, this function is seldom used in computer simulations. It is, however, commonly used to display the dispersive characteristics of a channel because it explicitly shows both time and frequency dispersion.

The time-variant transfer function, $T(f,t)$, is defined as

$$T(f,t) = \mathcal{F}_{\tau,f}(h(t,\tau)) \quad . \tag{2.15}$$

The input-output relationship associated with this Bello function is obtained by first replacing $u(t\text{-}\tau)$ in (2.11) with the inverse Fourier transformation of its Fourier transform, $\mathcal{F}_{t,f}^{-1}\{\mathcal{F}_{t,f}(u(t-\tau))\}$, to obtain

$$z(t) = \int_{-\infty}^{\infty} h(t,\tau)\int_{-\infty}^{\infty} U(f)e^{j2\pi f(t-\tau)}\, df\, d\tau$$

$$= \int_{-\infty}^{\infty}\left\{\int_{-\infty}^{\infty} h(t,\tau)e^{-j2\pi f\tau}\, d\tau\right\}e^{j2\pi ft}U(f)\, df \quad . \tag{2.16}$$

Substituting in (2.15) yields

$$z(t) = \int_{-\infty}^{\infty} T(f,t) U(f) e^{j2\pi ft} df \ . \tag{2.17}$$

From (2.17), $T(f,t)$ can be interpreted as the complex envelope of the received signal for a complex exponential input at the carrier frequency f. Physically, it is the time variant version of the conventional time invariant system transfer function.

The output Doppler-spread function, $H(f,v)$, is defined as

$$H(f,v) = \mathcal{F}_{t,v}(T(f,t)) \ . \tag{2.18}$$

Its input-output relationship can be obtained by substituting (2.18) into (2.17) to give

$$z(t) = \int_{-\infty}^{\infty}\int_{-\infty}^{\infty} H(f,v) e^{j2\pi vt} dv\, U(f) e^{j2\pi ft} df$$

$$= \int_{-\infty}^{\infty}\int_{-\infty}^{\infty} H(f,v) U(f) e^{j2\pi ft} df\, e^{j2\pi vt} dv \ . \tag{2.19}$$

Let $f = f_l - v$. Equation (2.19) can now be written as

$$z(t) = \int_{-\infty}^{\infty}\int_{-\infty}^{\infty} H(f_l - v, v) U(f_l - v) e^{j2\pi(f_l - v)t} df_l\, e^{j2\pi vt} dv$$

$$= \int_{-\infty}^{\infty}\int_{-\infty}^{\infty} H(f_l - v, v) U(f_l - v) e^{j2\pi f_l t} df_l\, dv$$

$$= \int_{-\infty}^{\infty}\int_{-\infty}^{\infty} H(f - v, v) U(f - v) dv\, e^{j2\pi ft} df \tag{2.20}$$

where for convenience, the subscript was dropped in the last step. Taking the Fourier transform of both sides of (2.20) gives

$$\mathcal{F}_{t,f}[z(t)] = Z(f) = \int_{-\infty}^{\infty} U(f - v) H(f - v, v)\, dv \ . \tag{2.21}$$

Hence, $H(f,v)$ can be interpreted as the frequency response of the channel at a frequency v Hz above a complex exponential input at f Hz. It is called the output Doppler-spread function because it explicitly shows the effect of the Doppler shift or spectral broadening on the output spectrum. In physical terms, the frequency shift variable v can be interpreted

as the Doppler shift that is introduced by the channel. The integral in (2.21) may be approximated by the discrete sum

$$Z(f) = \sum_{m=-\infty}^{\infty} U(f - m\Delta v)H(f - m\Delta v, m\Delta v)\, \Delta v \ . \tag{2.22}$$

Hence, the channel can be represented as a bank of matched filters with transfer function $H(f - m\Delta v, m\Delta v)\Delta v$ followed by a frequency conversion chain that produces the Doppler shift. An alternative description of the channel for computer simulation is thus offered by (2.22).

Another Fourier transform relationship of the output Doppler-spread function can be obtained as follows. Taking the Fourier transform of both sides of (2.14) gives

$$\begin{aligned}\mathcal{F}_{t,f}[z(t)] = Z(f) &= \int_{-\infty}^{\infty}\int_{-\infty}^{\infty}\int_{-\infty}^{\infty} S(\tau,v)u(t-\tau)e^{j2\pi(v-f)t}\, dv\, d\tau\, dt \\ &= \int_{-\infty}^{\infty}\int_{-\infty}^{\infty} S(\tau,v)\int_{-\infty}^{\infty} u(t-\tau)e^{j2\pi(v-f)t}dt\, dv\, d\tau \ . \end{aligned} \tag{2.23}$$

With $v - f = -\rho$, (2.23) can be written as

$$\begin{aligned}z(f) &= \int_{-\infty}^{\infty}\int_{-\infty}^{\infty} S(\tau, f-\rho)\int_{-\infty}^{\infty} u(t-\tau)e^{-j2\pi\rho t}dt d\rho d\tau \\ &= \int_{-\infty}^{\infty}\int_{-\infty}^{\infty} S(\tau, f-\rho)U(\rho)e^{-j2\pi\tau\rho}d\rho d\tau \ . \end{aligned}$$

But $\rho = f - v$ and $v = f - \rho$. Hence

$$\begin{aligned}z(f) &= \int_{-\infty}^{\infty}\int_{-\infty}^{\infty} S(\tau,v)U(f-v)e^{j2\pi(v-f)\tau}dv d\tau \\ &= \int_{-\infty}^{\infty} U(f-v)\int_{-\infty}^{\infty} S(\tau,v)e^{-j2\pi(f-v)\tau}d\tau dv \ . \end{aligned} \tag{2.24}$$

Now observe that if

$$\mathcal{F}_{\tau,f}^{-1}[H(f,v)] = S(\tau,v)$$

then, by the frequency shifting property of the Fourier transform,

25

$$\mathcal{F}_{\tau,f}^{-1}[H(f-\nu,\nu)] = S(\tau,\nu)e^{j2\pi\nu\tau} \ .$$

Hence

$$\int_{-\infty}^{\infty} S(\tau,\nu)e^{-j2\pi(f-\nu)\tau}d\tau = \mathcal{F}_{\tau,f}\left[S(\tau,\nu)e^{j2\pi\nu\tau}\right] = H(f-\nu,\nu) \ . \qquad (2.25)$$

Substituting (2.25) into (2.24) yields (2.21). Therefore,

$$H(f,\nu) = \mathcal{F}_{\tau,f}[S(\tau,\nu)] \qquad (2.26)$$

and is an alternative definition of the output-Doppler-spread function.

Four other Bello system functions can be defined which are the duals of the four functions already discussed. These are the input Doppler-spread function, output delay-spread function, the Doppler delay-spread function and frequency dependent modulation function. The input Doppler-spread function, denoted by $G(f,\nu)$ is defined as the dual of $h(t,\tau)$. Its input-output relationship can be obtained as

$$Z(f) = \int_{-\infty}^{\infty} G(f,\nu)U(f-\nu)d\nu, \qquad (2.27)$$

by applying duality relationships (given in Bello (1964)) to (2.11). Physically, $G(f,\nu)$ represents the spectral response of the channel at a frequency f Hz due to a complex exponential input ν Hz below f. Comparing (2.27) with (2.21) it becomes clear that

$$H(f,\nu) = G(f+\nu,\nu). \qquad (2.28)$$

The output Doppler-spread function $g(t,\tau)$ is defined as the dual of the output Doppler-spread function. By applying duality relationships to (2.21), the following input-output relationship can be obtained:

$$z(t) = \int_{-\infty}^{\infty} u(t-\tau)g(t-\tau,\tau)d\tau \ . \qquad (2.29)$$

It can be interpreted as the channel response τ seconds in the future to a unit impulse input

26

at a time t. Comparing (2.29) with (2.11), we see the following relationship:

$$h(t,\tau) = g(t-\tau,\tau).$$

(2.30)

The Doppler delay-spread function, $V(v,\tau)$, is defined as the dual of the delay Doppler-spread function. Its input-output relationship,

$$Z(f) = \int_{-\infty}^{\infty}\int_{-\infty}^{\infty} V(v,\tau)U(f-v)e^{-j2\pi\tau f}d\tau \, dv,$$

(2.31)

is obtained by applying duality relationships to (2.14). The physical interpretation of $V(v,\tau)$ is the gain afforded to signals suffering first Doppler shift in $[v,v+dv]$ then delay in $[\tau,\tau+d\tau]$. Taking the inverse Fourier transform of (2.31) gives

$$z(t) = \mathcal{F}_{t,f}^{-1}[Z(f)] = \int_{-\infty}^{\infty}\int_{-\infty}^{\infty}\int_{-\infty}^{\infty} V(v,\tau)U(f-v)e^{-j2\pi\tau f}e^{j2\pi ft}df \, d\tau \, dv.$$

Let $f_1 = f - v$, then

$$z(t) = \int_{-\infty}^{\infty}\int_{-\infty}^{\infty} V(v,\tau)\int_{-\infty}^{\infty}U(f_1)e^{-j2\pi\tau(f_1+v)}e^{j2\pi(f_1+v)t}df_1 \, d\tau \, dv$$

$$= \int_{-\infty}^{\infty}\int_{-\infty}^{\infty} V(v,\tau)e^{-j2\pi vt}e^{j2\pi vt}\int_{-\infty}^{\infty}U(f_1)e^{-j2\pi\tau f_1}e^{j2\pi f_1 t}df_1 \, d\tau \, dv$$

$$= \int_{-\infty}^{\infty}\int_{-\infty}^{\infty} V(v,\tau)e^{-j2\pi v\tau}e^{j2\pi vt}u(t-\tau)dv \, d\tau \quad .$$

(2.32)

Comparing (2.32) with (2.14), the following relationship becomes evident:

$$S(\tau,v) = V(v,\tau)e^{-j2\pi v\tau}$$

(2.33)

The last Bello function is the frequency dependent modulation function, $M(t,f)$, which is defined as the dual of the time-variant transfer function. Its input-output relationship is given by:

$$Z(f) = \int_{-\infty}^{\infty} M(t,f)u(t)e^{-j2\pi ft}dt$$

(2.34).

which is obtained by applying duality relationships to (2.17). Physically, $M(t,f)$ is the

27

complex amplitude spectrum of the received signal for a unit impulse input at $t = 0$. Comparing (2.34) with (2.17), it can be shown that

$$T(f,t) = \int_{-\infty}^{\infty}\int_{-\infty}^{\infty} M(t',f')e^{-j2\pi(f-f')(t-t')}\,df'dt' \qquad (2.35)$$

(Steele, 1992). Since this second set of Bello system functions is the dual of the first set, it can also be arranged symmetrically with respect to the Fourier transforms.

The Bello system functions can be used to fully describe a deterministic time-variant channel. The mobile radio channel, however, is a randomly time-variant channel. Such channels cannot be described with just Bello system functions because the functions become stochastic processes. A full statistical description of the system functions requires the determination of multidimensional probability density functions associated with each function. This is not a trivial task. A more practical, but less stringent method for characterizing random time-variant channels is to obtain statistical correlation functions for the individual Bello system functions. If we assume that the underlying processes are zero mean Gaussian processes, then a complete statistical description is obtained with the determination of the autocorrelation functions. Since there are two sets of Bello system functions, one set being the dual of the other, only four autocorrelation functions are of interest:

$$R_h(t_1,t_2;\tau_1,\tau_2) = \frac{1}{2}\left\langle h(t_1,\tau_1)h^*(t_2,\tau_2)\right\rangle, \qquad (2.36)$$

$$R_S(\tau_1,\tau_2;v_1,v_2) = \frac{1}{2}\left\langle S(\tau_1,v_1)S^*(\tau_2,v_2)\right\rangle, \qquad (2.37)$$

$$R_T(f_1,f_2;t_1,t_2) = \frac{1}{2}\left\langle T(f_1,t_1)T^*(f_2,t_2)\right\rangle, \qquad (2.38)$$

$$R_H(f_1,f_2;v_1,v_2) = \frac{1}{2}\left\langle H(f_1,v_1)H^*(f_2,v_2)\right\rangle, \qquad (2.39)$$

where $\langle \circ \rangle$ denotes expectation and x^* denotes the complex conjugate of x. It can be shown (see Steele, 1992) that these autocorrelation functions are related to each other through the double Fourier transform pairs. The autocorrelation functions given by (2.36) to (2.39) may be used to describe any randomly time-variant channel. However, if the channel is wide sense-stationary in the time domain and/or the frequency domain, then its correlation functions can be simplified.

A channel that exhibits time-shift invariance of its second order statistics is known as the wide sense stationary (WSS) channel. The correlation function for a WSS channel, hence, depends on the time difference and not absolute time. The correlation functions for WSS channels then become

$$R_h(t_1,t_2;\tau_1,\tau_2) = R_h(\Delta t;\tau_1,\tau_2), \tag{2.40}$$

$$R_S(\tau_1,\tau_2;v_1,v_2) = P_S(\tau_1,\tau_2;v_1)\delta(v_1-v_2), \tag{2.41}$$

$$R_T(f_1,f_2;t_1,t_2) = R_T(f_1,f_2;\Delta t), \tag{2.42}$$

$$R_H(f_1,f_2;v_1,v_2) = P_H(f_1,f_2;v_1)\delta(v_1-v_2), \tag{2.43}$$

where

$$P_S(\tau_1,\tau_2;v) = \int_{-\infty}^{\infty} R_h(\Delta t;\tau_1,\tau_2)e^{-j2\pi v\Delta t}d(\Delta t) \tag{2.44}$$

and

$$P_H(f_1,f_2;v) = \int_{-\infty}^{\infty} R_T(f_1,f_2;\Delta t)e^{-j2\pi v\Delta t}d(\Delta t) . \tag{2.45}$$

(2.41) and (2.43) show that a characteristic of the WSS channel is that signals arriving with different Doppler shift values are uncorrelated. This implies the attenuations and phase shifts associated with signal components having different Doppler shifts are

uncorrelated.

The dual of the WSS channel is the uncorrelated scattering (US) channel. For this channel, the attenuation and phase shift with paths of different delays are uncorrelated. The autocorrelation functions become

$$R_h(t_1,t_2;\tau_1,\tau_2) = P_h(t_1,t_2;\tau)\delta(\tau_1 - \tau_2) \tag{2.46}$$

$$R_S(\tau_1,\tau_2;v_1,v_2) = P_S(\tau;v_1,v_2)\delta(\tau_1 - \tau_2) \tag{2.47}$$

$$R_T(f_1,f_2;t_1,t_2) = R_T(\Delta f;t_1,t_2) \tag{2.48}$$

$$R_H(f_1,f_2;v_1,v_2) = R_H(\Delta f;v_1,v_2) \tag{2.49}$$

where

$$P_S(\tau;v_1,v_2) = \int_{-\infty}^{\infty} R_H(\Delta f;v_1,v_2)e^{j2\pi\tau\Delta f}d(\Delta f) \tag{2.50}$$

and

$$P_h(t_1,t_2;\tau) = \int_{-\infty}^{\infty} R_T(\Delta f;t_1,t_2)e^{j2\pi\tau\Delta f}d(\Delta f) \ . \tag{2.51}$$

Thus a US channel is WSS in the frequency domain (see (2.48) and (2.49)) and exhibits uncorrelated scattering in the delay domain (see (2.46) and (2.47)). This is in contrast to the WSS channel which is WSS in the time domain and exhibits uncorrelated scattering in the Doppler domain.

The most useful channel, as far as describing realistic mobile radio channels is concerned, is a hybrid of the above two channels known as the wide sense stationary uncorrelated scattering (WSSUS) channel. The first and second order statistics of the WSSUS channel are invariant under shift in time and frequency. In other words, channels of this type display uncorrelated scattering in both the delay and Doppler shift domain. By

30

first applying the WSS criteria and then the US criteria or vise versa, the correlation functions can be easily determined as:

$$R_h(t_1,t_2;\tau_1,\tau_2) = P_h(\Delta t;\tau_1)\delta(\tau_1-\tau_2),\qquad(2.52)$$

$$R_S(\tau_1,\tau_2;v_1,v_2) = R_s(\tau_1;v_1)\delta(\tau_1-\tau_2)\delta(v_1-v_2),\qquad(2.53)$$

$$R_T(f_1,f_2;t_1,t_2) = R_T(\Delta f;\Delta t),\qquad(2.54)$$

$$R_H(f_1,f_2;v_1,v_2) = P_H(\Delta f;v_1)\delta(v_1-v_2),\qquad(2.55)$$

where

$$P_h(\Delta t;\tau) = \int_{-\infty}^{\infty} R_T(\Delta f;\Delta t)e^{j2\pi\tau\Delta f}d(\Delta f)\qquad(2.56)$$

and

$$P_H(\Delta f;v) = \int_{-\infty}^{\infty} R_T(\Delta f;\Delta t)e^{-j2\pi v\Delta t}d(\Delta t).\qquad(2.57)$$

Real mobile radio channels are not strictly WSSUS channels. They, however, generally behave like a WSSUS channel over a finite interval of time and a band of frequencies and are thus quasi-WSSUS channels. It is suggested by Bello (1963) that a useful method for describing real mobile channels is to successively apply a WSSUS model over small time and frequency intervals. The correlations for each interval in time and frequency will now be different and thus, from a global perspective (e.g. over a long time interval), they behave like random variables. Therefore to fully characterize the channel, the statistics of these correlations have to be determined.

The function $R_h(0;\tau,\tau) = P_h(0,\tau) \equiv P_h(\tau)$ is called the power delay profile (or the multipath intensity profile) of the channel. It gives the average power of the channel

31

output to a unit impulse input as a function of time delay. Two commonly found parameters used in characterizing channels are the average delay (mean excess delay) of the channel which is defined as

$$\mu_\tau = \frac{\int_0^\infty \tau P_h(\tau)d\tau}{\int_0^\infty P_h(\tau)d\tau},$$

(2.58)

and the rms delay spread which is defined as

$$\sigma_\tau = \sqrt{\frac{\int_0^\infty (\tau - \mu_\tau)^2 P_h(\tau)d\tau}{\int_0^\infty P_h(\tau)d\tau}}.$$

(2.59)

The rms delay spread for typical macrocellular applications is of the order of single μs while that of microcellular applications is of the order of tens of ns. Another measure for characterizing the delay spread that is found in the literature is the maximum excess delay spread (X dB) (sometime called the excess delay spread) and is defined as the time delay during which $P_h(\tau)$ falls to X dB below the maximum. Note that regardless of whether it is called the maximum excess delay spread or the excess delay spread, it must be specified with a threshold.

The correlation function $R_T(\Delta f; \Delta t)$ is known as the spaced-frequency spaced-time function. The frequency correlation of the channel is measured by $R_T(\Delta f;0)$. The coherence bandwidth, B_c, of the channel is the smallest value of Δf for which $R_T(\Delta f;0)$ is greater than some selected value (say 0.5). The coherence bandwidth is related to either the average delay or the rms delay spread because $R_T(\Delta f;0)$ and $P_h(\tau)$ form a Fourier transform pair (see (2.56)). In particular,

$$B_c \propto \frac{1}{\mu_\tau} \qquad \text{or} \qquad B_c \propto \frac{1}{\sigma_\tau} . \qquad (2.60)$$

$R_T(0;\Delta t)$ is a measure of the temporal correlation of the channel. The coherence time of

the channel, T_{co}, is defined as the smallest value of Δt for which $R_T(0;\Delta t)$ is greater than

some selected value (say 0.5).

The time correlation of the channel is also measured by the Doppler power spectral

density, $P_H(0;\nu)$. It gives the average power of the channel output to a complex

exponential input as a function of the Doppler frequency. The Doppler spread, B_d, is

defined as the range of values over which $P_H(0;\nu)$ is significant. The Doppler spread is

also a measure of the coherence time because of the Fourier relationship between $P_H(0;\nu)$

and $R_T(0;\Delta t)$ (see (2.57). In particular,

$$T_{co} \approx \frac{1}{B_d} . \qquad (2.61)$$

A widely used function in the characterization of multipath fading channels is the

scattering function, $R_s(\tau,\nu)$. It gives the average power output of the channel as a function

of the time delay and the Doppler shift.

For the remainder of this work, the mobile channel will be described by the input

delay-spread function and modelled as a linear time-variant filter with the impulse response

for every point in three dimensional space given by:

$$h(t,\tau) = \sum_{i=1}^{L(t)} a_i(t)\delta[\tau - \tau_i]e^{j\theta_i(t)} , \qquad (2.62)$$

which represents the response of the channel at time t due to an impulse applied at time t -

τ; $\delta(\cdot)$ is the delta impulse, $L(t)$ is the number of multipath components, $a_i(t)$ is the

attenuation coefficient, τ_i is the delay time, and $\theta_i(t)$ is the phase delay for each path. It should be noted here that if the statistics of theses variables are known, the multipath channel is then completely characterized. A detailed description of the statistical distributions of these variables is beyond the scope of this work. The interested reader is encouraged to consult the extensive discussion in Parsons (1992) and Hashemi (1993a, b).

2.4 Power Control

Now that we have some understanding of the mobile channel, we turn our attention to current methods for increasing the traffic capacity of CDMA wireless communication systems. The need for power control in CDMA systems in order to make them work, as well as to increase capacity, is well documented in the literature (Ariyavistakul and Chang, 1991; Chang and Ariyavistakul, 1991; Gilhousen et al., 1991; Joseph and Raychaudhuri, 1991; Lee, 1991; Ariyavistakul, 1992; Díaz and Agustí, 1992; Esmailzadeh et al., 1992; Milstein et al., 1992; Mokhtar and Gupta, 1992; Prasad et al., 1992). There are two main reasons for this. The first one is to mitigate the so called near-far problem. This problem occurs because the cross-correlations between different spreading sequences are typically small, but non-zero. Therefore, the despread signal from the intended user will also contain residual signals from other users that will interfere with the intended signal. Moreover, if the intended user's signal is weak because it is far away from the base station and the interfering signals are strong because they are much closer to the base station, the intended user's signal may be swamped by the interference. As a result, communication with the intended user may become impossible. One method of solving this problem is to

control the power transmitted by each mobile on the reverse link (mobile to base) so that the received powers from each user at the base station are the same.

The second reason for power control is to reduce interference to adjacent cells in the forward link (base to mobile). Since the same frequencies are reused in adjacent cells and the cross-correlations between different spreading codes are not zero, the signals transmitted by one base station will interfere with those in the adjacent cells. The interference is most severe for users that are at the periphery of a cell. This interference, however, can be minimized by controlling the power transmitted by the base station. That is, the transmitted power to a particular user from the base station is limited to the minimum that is necessary to maintain communication with that user. Thus, the total transmitted power and hence intercell interference is minimized. The effectiveness of power control in reducing the interference effects for mobiles in a cell periphery is demonstrated by Stüber and Kchao (1992).

In a single cell system, the principle of power control is straightforward, although its implementation may not be (Gilhousen et al., 1991). The mobile users can monitor the total received signal power from the cell site. They can then adjust their transmitted power according to the detected power level. This type of power control is known as open loop power control and is the simplest of the power control schemes. Further refinements in the transmitted power level of each subscriber can be commanded by the cell site depending upon the power level received by the base station. The control loop is then closed and hence this type of power control is known as closed loop power control.

Closed loop power control (CLPC) system, in addition to compensating for the path loss and shadow fading, attempts to compensate for the Rayleigh fading. CLPC systems

35

are especially interesting in indoor channels where small Doppler spreads can make temporal interleaving ineffective because of the long delay required (Díaz and Agustí, 1992). It should be noted that on microcellular channels TDMA capacity exceeds the capacity of a CDMA system if the latter is equipped only with open loop power control on the forward link while the capacity of CDMA system equipped with CLPC is greater than that of TDMA (Jalali and Mermelstein, 1994).

In multiple-cell CDMA systems, the situation is much more complicated. Firstly, for the reverse link, power control for the mobiles is under the direction of the base station of their own cell. Therefore, the interference signal due to subscribers in other cells may increase or decrease depending upon the transmitted power necessary to eliminate the near-far effect in their own cells (Gilhousen et al., 1991). Hence, from the point of view of users in one cell, the interference from users at other cell sites can increase or decrease unpredictably. Furthermore, even the question of cell membership is not simple, because it is not the minimum distance that determines which base station (cell site) the subscriber joins but rather the maximum pilot signal power that is received by the subscriber.

2.5 Multi-user receivers[1]

Power control is one approach to solving the near-far problem. Another method is to eliminate the interference due to the near-in user from the signals received from the far-out user. Moreover, any CDMA system that employs techniques for removal of multiple access interference not only mitigates the near-far problem but also significantly increases

---

[1]The term multi-user receiver has been used by some authors to denote receiver structures that detect the signals from multiple users and by others to denote receiver structures capable of mitigating multiple access interference. It will be used in the latter sense in this thesis.

the capacity of the system. This is because CDMA systems are limited by multiple access interference (MAI). Partial reviews of the recent developments in multi-user receivers can be found in Verdu (1994), Duel-Hallen *et al.* (1995) and Moshavi (1996).

2.5.1 Optimal multi-user receiver

The optimal multi-user receiver structure selects the most probable sequence of bits given the received composite signal. Although optimal detection can be attained with Bayesian estimation, it is more convenient to use maximum likelihood detection when the prior probabilities are equal (Helstrom, 1995). As we will see, the maximum likelihood detector, in essence, calculates the Euclidean distance between the received signal and all possible transmitted signals in an MxN dimensional signal space (where N is the number of bits in the packet and M is the number of users) and chooses the signal at the smallest Euclidean distance as the most likely transmitted signal.

We will consider an asynchronous CDMA system. The synchronous system can be considered as a special case of the asynchronous system where all the delays are equal. The detection problem is, of course, more difficult with the asynchronous channel because in a synchronous channel, the detector can focus on one bit interval independently of the other ones. Any decision made with an asynchronous system, on the other hand, must take into consideration the decisions on the overlapping bits.

The received signal, $r(t)$, with BPSK modulation in an AWGN channel may be expressed as

$$r(t) = \sum_{m=1}^{M} \sqrt{E_m} \sum_{i=1}^{N} b_m(i) c_m(t - iT_s - \tau_m) + n(t) \qquad (2.63)$$

where E_m is the signal energy per bit, M is the number of users, N is the length of the data sequence, the information sequence of the mth user is denoted by $\{b_m(i)\}$, T_s is the symbol duration, τ_m is the transmission delay and $n(t)$ is the additive white Gaussian noise. The spreading waveform is of the form

$$c_m(t) = \sum_{i=0}^{G-1} c_{m,i} \, \psi(t - iT_c) \tag{2.64}$$

where $c_{m,i}$ is a member of the binary pseudorandom sequence $\{c_{m,i}\}$ which can take on values of ± 1; $\psi(t)$ is the chip pulse of duration T_c $(T_c \ll T_s)$ and G is the processing gain. Without loss of generality we will assume that the energy of the chip waveform is normalized as follows:

$$\int_0^{T_c} \psi^2(t) \, dt = 1 \quad . \tag{2.65}$$

The optimum multi-user receiver computes the log likelihood function (Verdu, 1986)

$$
\begin{aligned}
\Lambda(\mathbf{b}) &= -\int_0^{NT_s + 2T_s} \left[r(t) - \sum_{m=1}^{M} \sqrt{E_m} \sum_{i=1}^{N} b_m(i) c_m(t - iT_s - \tau_m) \right]^2 dt \\
&= -\int_0^{NT_s + 2T_s} r^2(t) dt + 2\int_0^{NT_s + 2T_s} r(t) \sum_{m=1}^{M} \sqrt{E_m} \sum_{i=1}^{N} b_m(i) c_m(t - iT_s - \tau_m) dt \\
&\quad - \int_0^{NT_s + 2T_s} \sum_{m=1}^{M} \sqrt{E_m} \sum_{i=1}^{N} b_m(i) c_m(t - iT_s - \tau_m) \sum_{l=1}^{M} \sqrt{E_l} \sum_{j=1}^{N} b_l(j) c_l(t - jT_s - \tau l) \, dt,
\end{aligned}
\tag{2.66}
$$

where $\mathbf{b}$ is given by

$$
\begin{aligned}
\mathbf{b} = \Big[&\sqrt{E_1} b_1(1), \sqrt{E_2} b_2(1), \cdots, \sqrt{E_M} b_M(1), \sqrt{E_1} b_1(2), \cdots, \sqrt{E_M} b_M(2), \cdots, \sqrt{E_1} b_1(N), \\
&\cdots \sqrt{E_M} b_M(N) \Big]^T \quad .
\end{aligned}
\tag{2.67}
$$

The receiver then selects as the most probable transmitted sequence the vector $\mathbf{b}$ which maximizes the log-likelihood function. Since the first term in (2.66) is constant, it does not influence the maximization and thus can be ignored. The last term of (2.66) can be easily decomposed into terms involving the cross-correlations of the spreading waveforms.

Therefore, the log-likelihood function may be expressed in terms of the outputs of M correlators or matched filters; one for each spreading waveform. Hence the set of correlator outputs constitutes a sufficient statistic for detection. This set of MN correlator outputs can be expressed compactly using vector notation as

$$\mathbf{r} = \mathbf{R_N}\mathbf{b} + \mathbf{n} ,\qquad (2.68)$$

where

$$\mathbf{r} = \left[r_1(1), r_2(1), r_3(1), \cdots, r_M(1), r_1(2), \cdots, r_M(2), \cdots r_1(N), r_2(N), \cdots, r_M(N) \right]^T ,\qquad (2.69)$$

$$r_i(j) = \int_{jT_s - \tau_i}^{(j+1)T_s - \tau_i} r(t) c_i(t - jT_s - \tau_i)\, dt ,\qquad (2.70)$$

$$\mathbf{n} = \left[n_1(1), n_2(1), n_3(1), \cdots, n_M(1), n_1(2), \cdots, n_M(2), \cdots n_1(N), n_2(N), \cdots, n_M(N) \right]^T ,\qquad (2.71)$$

$$n_i(j) = \int_{jT_s + \tau_i}^{(j+1)T_s + \tau_i} c_i(t - jT_s - \tau_i) n(t)\, dt ,\qquad (2.72)$$

$$\mathbf{R_N} = \begin{bmatrix} \mathbf{R_a}(0) & \mathbf{R_a^T}(1) & 0 & \cdots & \cdots & 0 \\ \mathbf{R_a}(1) & \mathbf{R_a}(0) & \mathbf{R_a^T}(1) & 0 & \cdots & 0 \\ \vdots & \vdots & \vdots & \vdots & \vdots & \vdots \\ 0 & \cdots & 0 & \mathbf{R_a}(1) & \mathbf{R_a}(0) & \mathbf{R_a^T}(1) \\ 0 & \cdots & \cdots & 0 & \mathbf{R_a}(1) & \mathbf{R_a}(0) \end{bmatrix} ,\qquad (2.73)$$

and the MxM matrix $\mathbf{R_a}(k)$ is defined as

$$\mathbf{R_a}(k) = \left\{ R_{ij}(k) \right\} = \left\{ \int_{-\infty}^{\infty} c_i(t - \tau_i) c_j(t + kT_s + \tau_j)\, dt \right\} .\qquad (2.74)$$

With a block processing approach, we see that the optimum receiver must compute 2^{MN} correlation metrics and select M sequences of length N that correspond to the largest correlation metric. An alternative approach, employing the Viterbi algorithm and called the optimal maximum likelihood sequence estimation (MLSE) receiver has been developed by Verdu (1986) for CDMA systems in AWGN channel. The complexity of the receiver is

39

reduced to 2^N. The MLSE, however, requires that the detector has full knowledge of the received amplitudes and phases. Extensions of the optimal MLSE receiver to that of frequency selective fading channels are proposed by Fukawa and Suzuki (1991), Varanasi and Vasudevan (1994), Vasudevan and Varanasi (1994), Yokota *et al.* (1995) and Zvonar (1996a). Fawer and Aazhang (1995) developed algorithms for estimating the complex channel coefficients as well as detection from the sufficient statistics provided by the RAKE correlators[1] based on the maximum likelihood rule. The application of space diversity as well as time diversity to the optimal receiver are studied by Zvonar (1994; 1996b). A small simplification of the MLSE receiver can be attained by employing a local descent algorithm through the Voronoi regions instead of the Viterbi algorithm (Agrell and Ottosson, 1995). Nevertheless, the computational complexity of the optimum multi-user receiver, with either the Viterbi algorithm or the local descent algorithm, depends exponentially on the number of users and so it is only practical for systems with very small number of users. Therefore, considerable research efforts have focused on suboptimal receiver structures that retain some robustness to multi-user interference.

2.5.2 Suboptimal multi-user receivers

Many suboptimal multi-users receivers have been developed. But before discussing these suboptimal detectors in detail, it is beneficial to first discuss them from a global perspective. In so doing, one can gain an understanding of the interrelationships between these detectors.

From the preceding discussion on the MLSE receiver, it was concluded that even

----

[1] A description of the RAKE receiver can be found in Proakis (1995), pp. 797.

with the Viterbi algorithm, the optimal receiver is still highly complex. The first attempts at simplifying the optimal MLSE receivers focused on approximating the Viterbi algorithm with simpler algorithms and decentralization. However, the complexity of these receivers is still prohibitive. This prompted the search for other classes of suboptimal detectors. These detectors can be roughly classified as linear, non-linear and subtractive receivers. Linear receivers can be further classified into decorrelating, pre-decorrelating, minimum mean square error (MMSE), blind adaptive, polynomial expansion and noise whitening receivers. The non-linear receivers can be further classified into decision feedback and neural network receivers. The subtractive interference cancelling receivers can be either linear or non-linear, depending upon how the MAI is regenerated.

The decorrelating receiver applies the inverse of the correlation matrix to the conventional matched filter outputs in order to remove the MAI. This class of receivers requires the knowledge of the spreading sequences of all users and the phases of the received signal but does not require the received amplitudes. The decorrelating receiver leads to the development of two other receivers. The first is the pre-decorrelating receiver which applies the linear transformation at the transmitter instead of at the receiver. However, since this requires the prediction of the behaviour of the non-stationary channel, this method is not applicable to mobile communications. The second is MMSE receiver. Since the decorrelating receiver completely eliminates the MAI at the expense of noise enhancement, MMSE receivers utilize the additional knowledge of the received signal power and attempt to strike a balance between noise enhancement and residual interference. However, it should be noted that an MMSE receiver does not require the knowledge of the spreading sequences if it is implemented adaptively. Furthermore, blind

41

adaptive interference suppression receivers can be used to implement adaptive MMSE receivers without the need for a training sequence. Since the non-adaptive MMSE receivers and the decorrelating receiver need to perform a matrix inversion, further simplification of their structure can be obtained with the polynomial expansion receiver which provides a convenient method for approximating the inverse of the correlation matrix. The noise-whitening receiver adds, before the conventional receiver, a linear filter that maximizes signal to noise ratio with the constraint that the impulse response last only one symbol time. Thus, the noise whitening receiver is not related to the decorrelating and MMSE type receivers but rather represents a unique approach to suboptimal multi-user detection.

The decorrelating and MMSE receivers have shown that the principle of linear equalization can be adapted for multi-user detection. It is, therefore not too surprising that the principle of decision feedback equalizers has been used to derive the decision feedback multi-user receiver. The advantage of this class of receivers is that it does not require the knowledge of the spreading sequences. Another receiver that was first designed to combat intersymbol interference but has since found a role in combating MAI is neural network receivers.

A different approach to multi-user detection is the subtractive receiver. Its basic principle is that separate estimates of the MAI contributed by each user are determined at the receiver and subtracted out. If soft data outputs (e.g. the matched filter outputs) are used for the MAI, then the receiver only needs the knowledge of the spreading sequence and the receiver is linear. If, on the other hand, hard-decisions on the transmitted bits are used for MAI regeneration, then the receiver requires the knowledge of the spreading

sequences as well as the amplitude and phase of the received signal and it is non-linear. If each user's signal is successively subtracted from the received signal, then the receiver is known as a successive interference cancellation (SIC) receiver. If MAI is simultaneously subtracted from the signals of all users, then the receiver is known as a parallel interference cancellation (PIC) receiver.

The multi-stage interference cancelling receiver performs cancellation in multiple stages. Its basic principle is that the single user performance gets better after each stage of cancellation because the decisions used for interference cancellation get more reliable. With a multi-stage receiver, the MAI can be cancelled either successively, in parallel or through a combination of both.

It must be stressed that not all multi-users detectors fall into one of the above classes. There exist some multi-user detectors that do not fall into any of the classes above and some that have structures that are a combination of several types.

2.5.2.1 Suboptimal forward dynamic programming multi-user receiver

Now that we have some understanding of the global picture, let us look at each class of multi-user detectors in more detail. A suboptimal receiver structure that replaces the Viterbi algorithm in the optimal receiver with a modification of Fano's sequential-decoding algorithm in conjunction with the stack algorithm has been developed by Xie *et al.* (1990). The fundamental feature of this detector is that it searches for the most likely path based upon local metric values rather than evaluating all candidates for the best path as in the Viterbi algorithm. As a result, the complexity is linearly dependent on the number of users but the price paid for this reduction in complexity is an increase in the error

probability. It is shown that at least in AWGN channels, this detector performs nearly as well as the optimal detector.

2.5.2.2 Decentralized multi-user receiver

Since the optimal MLSE receiver requires centralized implementation, a logical simplification is decentralization. By decentralization we mean that a subset of D users, rather than all users, is demodulated simultaneously. When $D > 1$ the process is known as partial decentralization and when $D = 1$ it is known as full decentralization.

The process of decentralization of the MLSE receiver has been studied by Poor and Verdu (1988). The general form of the single-user likelihood ratio obtained has a correction term which depends on both in-phase and quadrature components of the input. However implementation of the receiver based upon the general form of the single-user likelihood ratio (the optimum one-shot single user receiver) for more than two users is as computationally burdensome as the optimal multi-user receiver. An important reduction in complexity, however, is possible if the modulation waveforms of the interfering users are signature sequences. Specifically, if the chip waveforms of all interfering users are known and the signature sequences are independent sequences of independent, equiprobable binary digits, useful approximations to the optimal single-user likelihood ratio can be obtained. These approximations are asymptotically exact as either the length of the spreading codes or the signal-to-background-noise ratio increases without bound. Furthermore, for the specific case of two users, this receiver achieves perfect demodulation in the absence of Gaussian noise regardless of the energy to the interference from the other user. Therefore this receiver may avoid the multiple access interference

limitation that plagues the conventional matched filter receiver.

A locally optimum single-user correlation receiver is also derived in (Poor and Verdu, 1988) using an asymptotic form of the log-likelihood ratio for signal detection in white Gaussian noise. This receiver uses a replica of the desired user's signal and can be used to provide a partial decentralized receiver.

2.5.2.3 Linear suboptimal multi-user receiver

Since the suboptimal multi-user receivers discussed above are still too complex to be implemented in a practical system, other classes of suboptimal receivers have been developed. We will begin our discussion with linear suboptimal receivers. The class of linear suboptimal receivers contains the decorrelating, pre-decorrelating, minimum mean square error (MMSE), blind adaptive, polynomial expansion and noise whitening receivers.

2.5.2.3.1 Decorrelating multi-user receiver

In another attempt at reducing the complexity of the optimal MLSE receiver, the decorrelating receiver was originally proposed by Schneider (1979) and Kohno *et al.* (1983) and was extensively analyzed for demodulation of synchronous (Lupas and Verdu, 1989) and asynchronous (Lupas and Verdu, 1990) CDMA systems. Recall that with BPSK modulation, the received signal vector r that represents the outputs of the M correlators is given by (2.68). The soft decision estimates of this detector, b^0, are obtained by multiplying the correlator outputs with the inverse of the correlation matrix. Thus,

$$b^0 = R_N^{-1} r = R_N^{-1} R_N b + R_N^{-1} n = b + R_N^{-1} n . \tag{2.75}$$

The detected symbols are obtained by taking the sign of each element of b^0. It should be noted that this linear transformation on r is equivalent to correlating $r(t)$ with a set of modified spreading waveforms that tunes out or decorrelates the multi-user interference. That is why this type of detector is called a decorrelating receiver. Furthermore, it can be seen from (2.75) that the decorrelating matrix completely removes the MAI at the expense of increasing the background noise. Most of the studies with the decorrelating receiver have been with coherent detection. Noncoherent detection with the decorrelating receiver has only been considered in Varanasi and Aazhang (1991b), Varanasi (1993) and Zvonar and Brady (1994).

The decorrelating receiver can also be obtained by maximizing the following log likelihood function:

$$\Lambda(b) = -(r - R_N b)^T R_N^{-1} (r - R_N b). \tag{2.76}$$

The result of this maximization is

$$b^0 = R_N^{-1} r \tag{2.77}$$

which is the same as (2.75). Therefore, the decorrelating receiver selects the most probable vector of bits given the outputs of the M correlators. Note that this is in contrast to the optimal detector which selects the most probable vectors of bits given the received signal.

Since the studies by Lupas and Verdu (1989, 1990) are focused only on the AWGN channels, more recent work has been along the line of extending the decorrelating receiver to fading channels. In order for the decorrelator to operate in fading channels, with

46

coherent detection, knowledge of the phases of the received signal is required[1]. Kajiwara *et al.* (1993) show that with perfect phase estimates, significant capacity gains over the conventional matched filter receiver can be obtained in flat fading channels. A similar result is obtained when a decorrelating receiver is combined with a RAKE receiver in frequency selective fading channels (Huang and Schwartz, 1994; Vasudevan and Varanasi, 1994; Zvonar, 1996a; Zvonar and Brady, 1995; Zvonar and Brady, 1996). Furthermore, its performance can also be dramatically improved with space diversity (Zvonar, 1994; 1996b). For a CDMA system with M users, each generating L resolvable paths, the decorrelating filter is analogous to the decorrelating filter designed for LM users transmitting in a single path CDMA channel. This type of decorrelator is referred to as path-by-path decorrelator. The multiple access interference is eliminated prior to combining. However, by passing the received signal through the decorrelating filter, the thermal noises in the L branches of the mth user are correlated. The usual approach prior to combining is to introduce the whitening operation in which the whitening filter is obtained by Cholesky decomposition of the noise covariance matrix. The optimal combiner after noise whitening is the maximal ratio combiner[2]. In order for the correlator to perform maximal ratio combining, it will need the knowledge of the amplitudes of the received signals. To avoid this, equal gain combining, which is suboptimal, can be employed. This drawback, however, pales in comparison to the fact that the asymptotic efficiency of the path-by-path decorrelator drops rapidly as the number of users increases (Kawahara and Matsumoto, 1995). Therefore, this structure is only feasible when the

---

[1] As with most multi-user detectors, if noncoherent detection is used, the need to estimate the phases can be avoided.
[2] A description of the maximal ratio combiner can be found in Proakis (1995), pp. 779.

number of users is small. This decrease in the asymptotic efficiency can be recovered if a slightly different decorrelator, the channel-matched decorrelator, is used. The major disadvantage of the channel matched decorrelator is that the decorrelation matrix is constructed based upon the convolution of the spreading sequence of each user and its corresponding channel impulse response, and thus full knowledge of the channel impulse response is required.

The above studies show that, with perfect parameter estimation, the decorrelating receiver can be used in fading channels. The next logical step is to develop methodologies for estimating the parameters and dynamically updating the decorrelation filter. Several methods for doing this have been proposed in the literature. Kawahara and Matsumoto (1995) use joint detection to estimate the channel for the channel matched decorrelator update. Wijayasuriya et al.(1993b) introduces another approach based upon the Sherman-Morrison formula (Golub and Van Loan, 1985) and exploits the sparse nature of the block tri-diagonal form of R_N. Yoon et al. (1994) suggest the use of reference symbols for the estimation of the channel. The performance of a combination of a truncated decorrelator and coherent RAKE receiver using pilot symbols for estimation of the channel impulse response is analyzed by Miki and Sawahashi (1995a). Bar-Ness et al. (1994a; b) suggest the use of a bootstrapped adaptive algorithm for updating the decorrelation filter weights which simultaneously reduces the absolute value of the correlation between the decorrelator output at time i and all other outputs of the decorrelator after decision at time i, i-1, and i+1, respectively. Chen and Roy (1994) and Roy et al. (1994) report a recursive least squares computation of the decorrelating detector coefficients for the case of synchronous DS-SS. All these methods provide estimates of the channel impulse function,

but because of the differences in the assumptions used in the analysis, direct comparison of performance is difficult. Therefore, more research is necessary to determine the best method for updating the weights of the decorrelation filter for operation in fading channels.

Another approach to handling the nonstationarity of the channel is the sliding window decorrelating algorithm (Wijayasuriya *et al.*, 1992a) combined with a RAKE receiver (Wijayasuriya *et al.*, 1993a). Instead of decorrelating a complete packet of data bits at a time, the sliding window decorrelating algorithm slides the processing window over the incoming data. It can thus process data transmission of infinite length on a real time basis with a constant delay of the order of a data bit period. The analysis shows that significant capacity improvement over the conventional matched filter receiver is possible with perfect channel estimates. However, the issue of how to update the sliding window decorrelation filter weights has not yet been addressed.

The effect of synchronization errors on the performance of the decorrelating receiver is analyzed by Ström *et al.* (1994) and Parkvall *et al.* (1995). Their results show that even with small synchronization errors of the order of a few percent of a chip duration, the performance of the decorrelating receiver degrades seriously. Therefore synchronization algorithms that are acceptable for spread spectrum communication are not of sufficient accuracy for decorrelating receivers and that new algorithms must be developed.

This discussion of the decorrelating receiver has, so far, assumed that the number of users in the system is fixed. In a real CDMA wireless communication system, the number of users in the system will always be changing. Therefore algorithms that update the

decorrelating filter weights when the number of users in the system changes are of significant interest. Juntti (1995) introduces an order-recursive algorithm for detector update. The algorithm computes either the inverse or the Cholesky factorization of the correlation matrix. An alternative approach which adaptively augments an existing conventional decorrelator to demodulate new active users in addition to existing users has been developed by Mitra and Poor (1996a; b). The approach is based upon likelihood tests for the determination of the spreading code of the new users.

The decorrelating detector has been extended recently to the case of multi-rate DS-CDMA systems (Saquib et al., 1996). The high bit rate users can be modelled as an equivalent system of low bit rate users. Thus, as far as the decorrelator is concerned, a high bit rate user is simply composed of several low bit rate users. The major disadvantage here is that this system introduces processing delays for the high rate user.

Some attempts have been made in the literature to simplify the decorrelating receiver. Most of these methods entail breaking up the detection problem into more manageable blocks (Xie et al., 1990; Kagiwara and Nakagawa, 1991; Wijayasuriya et al., 1992b; Shi et al., 1993; Kajiwara and Nakagawa, 1994; Jung and Blanz, 1995; Mili and Sawahashi, 1995b; Zheng and Barton, 1995; Klein et al., 1996). Miki and Sawahashi (1995b) suggest that since the number of interferers that are strong enough to influence the desired signal is limited, a preselection scheme in which the strongest interferers are selected for cancellation can be effective. Not only does this reduce complexity by reducing the size of the matrix for inversion, but also the enhancement of the thermal noise which is inevitable with any decorrelation receiver. Their results show that the preselection type decorrelating receiver offers better bit error rate (BER) performance than the

conventional decorrelating detector, especially when the number of the received signals approaches the processing gain. Kajiwara and Nakagawa (1991) and Shi et. al. (1993) suggest, for asynchronous systems, the use of one shot receiver instead of the sequence detection in the conventional decorrelating detector. One shot detector can be considered as the limiting case of the truncated decorrelating receiver in Miki and Sawahashi (1995a). Their results show that the one shot detector is near-far resistant but that its performance will more or less depend upon the phase delays of the active users in the system. This problem is alleviated somewhat by a new signalling scheme, orthogonal on-off BPSK (O^3-BPSK) (Zheng and Barton, 1994). In this scheme, the temporally adjacent bits from different users in the received signals are decoupled by using the on-off signalling and the data rate is maintained with no increase in transmission rate by adopting an orthogonal structure. This structure, however, will double the size of the correlation matrix resulting in increased complexity and thermal noise enhancement. Sezgin and Bar-Ness (1996) suggest the use of a bootstrapped adaptive algorithm for adapting the one shot receiver to the changing conditions of the wireless communication channel.

The decorrelating receiver can be considered as a special case of a class of multi-user detectors known as parallel group detectors (Varanasi, 1995; 1996). The performance and complexity of this class of detectors span the region with the decorrelating receiver (which corresponds to one user per group) on the one extreme and the MLSE receiver (which corresponds to all users in one group) on the other extreme.

2.5.2.3.2 Pre-decorrelating multi-user receiver

An alternative to the decorrelating receiver is the pre-decorrelating receiver

51

proposed by Tang and Cheng (1994a; b). The basic idea is that instead of applying the linear transformation at the receiver, it is applied at the transmitter. In so doing, instead of transmitting the data, linear combinations of the active user's data as determined by the inverse crosscorrelation matrix of their signature waveforms are transmitted. Because of the need to predict the behaviour of a non-stationary channel, this method is not too practical for mobile communication and has received very little attention in the literature.

2.5.3.3.3 Minimum mean square error multi-user receiver

Decorrelating receivers attempt to remove the multiple access noise completely without regard to thermal noise enhancement. This is similar to the zero forcing criterion[1] in equalizer design. Another design is the MMSE receiver which minimizes the mean square error between the detected bits and the soft decision estimates (Xie et al., 1990; Lee, 1993; Klein et al., 1994; Rapajic and Vucetic, 1994; Juntti and Aazhang, 1995; Schlegel et al., 1995). MMSE receivers attempt to strike a balance between the residual interference and noise enhancement. The performance of the MMSE receiver is generally better than that of the decorrelating receiver. In the absence of thermal noise, the MMSE receiver converges to the decorrelating receiver. Ge and Bar-Ness (1996) demonstrate that the MMSE receiver has the same performance as the bootstrap multi-user detector. Another design that tries to trade off residual interference for noise enhancement is proposed by Bar-Ness and Punt (1995). Instead of minimizing the square error, this receiver performs a linear transform that minimized the correlation of each users soft

---

[1]The *zero-forcing criterion* is a criterion for equalizer adaptation which forces the equalizer to completely suppress intersymbol interference, without regard for possible increase of the background noise.

decision estimate with all of the other users detected bits.

MMSE receivers readily allow a simple adaptive implementation. Analysis of a single cell system, however, shows that because of significant coefficient noise characteristic of long adaptive equalizers, this approach to interference cancellation will be very difficult to implement in systems with large processing gain (Madhow and Honig, 1994). Numerical analysis of the performance variability of the MMSE detection for DS-CDMA shows a spread in received SIR of approximately 10 dB (Honig and Veerakachen, 1996). The convergence of the MMSE receivers can be improved by a rapidly converging adaptive algorithm based upon orthogonal transformation (Lee, 1993).

A family of suboptimum receivers that achieve a balance between residual interference and noise enhancement is studied by Xie et al. (1990). The decision algorithm for this class of suboptimum receivers consists of a linear transformation followed by a set of threshold receivers. The linear transformations are derived based upon two different performance criteria: minimum mean squared error and weighted least squares. These criteria, though not optimum in terms of the bit error probability, are mathematically tractable and lead to elegant and simple detection structures that can be implemented using tapped delay lines. The complexity of this class of receivers increases linearly with increasing number of users. Their performance is much better than that of the conventional receiver and nearly as good as that of the MLSE receiver in many practical circumstances.

In order to extend the MMSE detectors for operation in a fading environment, joint detection and channel estimation have been proposed. With known delays, a tree search method combined with least-squares estimation for joint detection and estimation of amplitudes can be employed (Xie et al., 1993). Iltis and Mailaender (1994) propose an

algorithm for joint detection and estimation of both amplitude and delay. The algorithm is an extension of the symbol by symbol detector (Abend and Fitchman, 1970), originally derived for intersymbol interference, to multiple access interference. The likelihoods in the symbol-by-symbol metric updates are approximated using a set of extended Kalman filter innovations. A significant calculation simplification is realized when the likelihood computation and Kalman filter updates are expressed in terms of a set of cross-correlation functions which only need to be computed for a subset of the possible symbols. A metric pruning technique further reduces the number of Kalman filter updates. Turbo codes tailored to the delay requirements of the voice communications have been shown to significantly increase the performance of joint MMSE detectors (Jung et al., 1994).

2.5.2.3.4 Blind adaptive multi-user receiver

Since the adaptive MMSE detectors that were discussed above require a training sequence for adaptation, the blind adaptive multi-user receiver has recently been introduced (Honig et al., 1994). This receiver attains the same near-far resistance as the optimum receiver, the same asymptotic efficiency as the decorrelating detector and the same bit error rate as the adaptive MMSE receiver. Simplification of this receiver to a partially blind adaptive receiver is presented by Schodorf and Williams (1996). This design trades off complexity with performance. Another blind equalizer, motivated by the Wiener reconstruction-filter theory, which is a minimum-variance-distortionless-response type filter that maximizes the output signal to interference plus noise ratio is developed by Batalama and Pados (1995).

54

2.5.2.3.5 Polynomial expansion multi-user receiver

Another linear multi-user detector that has been suggested in the literature is the polynomial expansion detector (Moshavi *et al.*, 1996). This receiver provides a convenient approximation of the inverse matrix necessary for the implementation of the decorrelating and MMSE receiver because it approximates the inverse matrix with a polynomial expansion in R_N. The soft decision estimates are given by

$$\mathbf{b}_l = \mathbf{L}_{PE} \mathbf{r}$$

where

$$\mathbf{L}_{PE} = \sum_{i=0}^{N_s} w_i \mathbf{R}_N^i,$$

w_i are the polynomial weights and N_s is the order of the polynomial expansion. For a given polynomial expansion order and cross correlation matrix, the weights are chosen to optimize some performance measure. For messages of finite length, it can be shown that the polynomial expansion detector can exactly implement the decorrelating receiver. For practical values of message lengths, the polynomial expansion order necessary to exactly implement the decorrelating receiver becomes very high but good approximations can be obtained with low polynomial expansion orders. Therefore, its performance is usually slightly poorer than that of the decorrelating receiver but its structure is relatively simple.

2.5.2.3.6 Noise-whitening multi-user receiver

Monk *et al.* (1994) have developed a noise-whitening approach to multi-user rejection. The receiver is based on the analogy of detecting a bit in multiple access interference to detection of a known signal in stationary coloured Gaussian noise. This is

because the multiple access interference is the sum of independent signals so that at any point in time, for a large number of users, it is approximately Gaussian. Furthermore, if the interfering users are randomly delayed and use pseudorandom signature sequences, the multiple access interference process appears to be stationary. The resulting receiver structure does not require locking and despreading the other users signals, knowledge of the spreading codes of the other users, spreading codes be periodic in a bit time and the same set of transmitters be active across many bit times. The structure of the receiver is the conventional receiver with a linear filter that first maximizes signal-to-noise ratio. Since the general signal-to-noise ratio maximizing filter is not realizable, an additional constraint which limits the duration of impulse response to one symbol bit time is used. The results show, at least for an AWGN channel, significant performance improvement over the conventional matched filter. How this detector performs in relation to other suboptimal receivers is still an open question.

Yoon and Leib (1996) developed a receiver which is a compromise between the noise whitening matched filter and linear MMSE detectors. A new signal-to-noise ratio maximizing filter was developed by assuming that the receiver has the additional knowledge of the chip delays and signal powers of a group of strong interferers. The major advantage of this new matched filter is its ability of suppress interference from strong users without knowledge of their spreading codes. The performance of this receiver is better than or, in the degenerate case (a system where all interferers power are the same), equal to that of the noise whitening matched filter.

The performance of this class of receivers has only been analyzed in the AWGN environment. Their performance in a fading environment is still an open question.

56

2.5.2.4 Non-linear multi-user receiver

The linear multi-user receivers discussed above require a fundamentally different CDMA design philosophy that of IS-95[1] systems. In the IS-95 system, each user is encoded, modulated and spread with a very long pseudo-random sequence (2^{42} chips). Linear multi-user receivers, on the other hand, require that each user occupy a unique dimension in signal space and hence the spreading sequences are designed to be at one bit or code symbol duration. The difference, however, goes beyond the length of the spreading sequences. With linear multi-user receivers, the dimensional separation of the users is exploited in order to reduce the MAI, while in the IS-95 system, coding gain makes the system interference tolerant. Recent results have shown that coded systems outperform systems employing linear multi-user receivers both in terms of per cell capacity and robustness (Vembu and Viterbi, 1996). This is because the adaptive algorithms necessary for linear multi-user receivers to operate on non-stationary channels require a high signal to noise ratio (SNR) to converge. In fading channels the signal to noise ratio may exhibit momentary fluctuations of 10 dB or more. This problem is further compounded if forward error correction coding is used with a linear multi-user receiver because the SNR available at the symbol level is further decreased with error control coding. Hence, the SNR may not be high enough for the adaptive algorithms to converge. Note that this result does not necessary apply to non-linear multi-user receivers because, as we will see next, their design philosophy does not preclude the use of forward error

---

[1] A discussion of the IS-95 system is not included here because of space limitations. For those readers who are unfamiliar with the IS-95 system, they are encouraged to consult (TIA/EIA/IS-95, 1993).

correction coding.

2.5.2.4.1 Decision feedback multi-user receiver

We have seen the applicability of the principle of linear equalization to multi-user detection. The next logical development is the application of the principle of decision feedback equalization (Abdulrahman, 1993; Abdulrahman *et al.*, 1992; 1993; 1994; Falconer *et al.*, 1993). An advantage of this approach is that the receivers do not require the knowledge of the spreading sequences of the other users. In so doing the inherent privacy property of the SS systems is preserved. It is shown that , if the receiver is designed using the *zero-forcing criterion* and the channels and/or filter responses are strictly band limited to say

$$|f| \leq \frac{B}{T} , \qquad (2.78)$$

where T is the symbol time and B is some constant greater than 0.5, then the maximum number of possible users, N, which can be accommodated in the system is given by

$$N + 1 = A_r \, \text{int}(2B), \qquad (2.79)$$

where A_r is the number of antenna elements and int(∘) denotes the integer part of ∘. For CDMA systems with processing gain G, and $A_r = 1$, the maximum number of possible users is then given by

$$N = \text{int}(G) - 1 \ . \qquad (2.80)$$

This result shows that the decision feedback multi-user receiver is capable of suppressing a number of interferers proportional to the bandwidth of the system; that result was foreseen by the results of Shnidman (1967). Indeed the conclusion that the

number of separable (orthogonal) signals is proportional to the bandwidth is a well-known result of signal theory and is the basis for CDMA, as well as FDMA and TDMA multiple access schemes. In wireless systems, however, the orthogonality of the signals is often lost because of the frequency selective fading characteristic of the channel. This result, therefore, shows that self and interuser interference, as well as multipath can be to a certain degree eliminated by equalization.

The above theoretical limit is attainable only if the zero-forcing solution exists. Practically, even if the zero-forcing solution exists, it may involve significant enhancement of additive thermal noise. Minimization of the total mean squared error (MSE) is usually a more useful criterion. Derivation of a practical decision feedback adaptive multi-user receiver based on transversal filters using the MSE criterion is shown in detail in Abdulrahman (1993), Abdulrahman et al. (1994) and Falconer et al. (1993) and will not be repeated here. The interested reader is encouraged to consult the review of the topic in Falconer et al. (1993). Klein et al. (1994) demonstrate that for MMSE designs, decision feedback multi-user receivers perform better than receivers without decision feedback.

Performance evaluation of a computer simulated system using the decision feedback multi-user receiver derived under the MSE criterion is presented in Abdulrahman (1993) and Abdulrahman et al. (1993; 1994). The analyzed system has a data rate of 9600 bps, spread bandwidth of 76.8 kHz, and a processing gain of 8. The intention is to divide the 1.25 MHz band of the IS-95 system into 16 sub-bands. The reason for splitting up the 1.25 MHz band is mainly to limit the size of the equalizer to 14 delay taps and two feedback taps. The results presented show that a maximum of four users can coexist in each of the sub-bands. Thus a total of 64 users can coexist in the 1.25 MHz band of the

IS-95 system. This represents an approximately 2.5 times improvement over the system without interference cancellation analyzed in Gilhousen *et al.* (1991). However, the improvement drops to 1.4 times when voice activity is considered for the two systems. Furthermore, if guard-bands for the sub-bands are taken into account, the performance advantage will be even smaller. Another disadvantage of this particular system is that it requires 16 different radios. Reduction of the number of required radios is one of the key advantages of CDMA systems. Other studies of the MMSE decision feedback equalizer can be found in Duel-Hallen (1995), Klein *et al.* (1996) and Jung and Blanz (1995).

Multivariable MMSE decision feedback equalizer for multi-user detection is introduced by Tidestav *et al.* (1995). This detector has the ability to operate even if numbers of transmit and received antenna are unequal. It is derived under the constraint of realizability and is calculated by solving a system of linear equations. Simulation results show that the performance is significantly better than that of the conventional matched filter receiver.

It is shown in Hafeez and Stark (1996) that convolutional coding with soft decision decoding can be used to improve the performance of decision feedback multi-user detectors. Their results show that the scheme works very well for weak users but strong users do not gain much over a linear decorrelation detector.

2.5.2.4.2 Neural network multi-user receiver

Since neural networks have, in the past few years, been applied to equalization for intersymbol interference, it is not too surprising to find that they also have a role in multiple access interference rejection. A review of recent developments can be found in

Howitt *et al.* (1994) and Verdu (1994). The earliest paper on applying adaptive neural networks to multi-user detection is by Aazhang *et al.* (1992). The neural network is a multilayer perceptron where each node in the first stage computes a nonlinear function of a linear transformation of the matched filter outputs. Training sequences are used to adapt the linear transformations. Depending on whether only the desired user's signature or the signature sequences of all users are known, the neural network converges onto two different configurations of the detector. The complexity of this detector grows exponentially as the number of users increases because the number of neurons needed for the network grows exponentially.

Neural networks that grow exponentially with the number of users are only practical for systems with a very limited number of users. A network that only grows linearly with the number of users, the Hopfield network, has been suggested for binary DS-CDMA (Miyajima *et al.*, 1993) and m-ary DS-CDMA (Nagaosa *et al.*, 1994) systems. The crosscorrelation of the spreading sequences and the signal amplitudes are assumed known. The weights of the network are not adaptive but are set equal to the crosscorrelation multiplied by the corresponding amplitude. The performance of the proposed detector is comparable to that of the optimum detector.

A detector employing the Kohonen's self organizing map has been suggested for synchronous CDMA systems (Hottinen, 1994). The detector assumes the knowledge of the signature sequences but it does not require the use of training sequences or the knowledge of signal amplitudes. The receiver combines channel estimation and data detection in a recursive structure. The performance is close to that of the 2 stage multi-stage detector with perfect channel estimates in Varanasi and Aazhang (1991a).

2.5.2.5 Subtractive multi-user receiver

Another slightly different approach is to consider what would be the simplest augmentation to the conventional matched filter detector capable of achieving some resistance to multiple access interference. Recall that the multiple access interference is deterministic. By that we mean determinism not in the Laplacian sense but in the sense that the multiple access interference (MAI) can be regenerated at the receiver. The least complex multi-user receiver is then one that regenerates the MAI and then removes it, by subtraction, from the received signal (Viterbi, 1990). This can be done either in parallel, where all of the users' signals are simultaneously subtracted from all of the others', or successively, where each user's signal is successively subtracted form the received composite signal. It is found in Petal and Holtzman (1994a) that the successive interference cancellation (SIC) scheme outperforms the parallel scheme when the received users signals have different powers. An interference scheme which is a compromise between parallel and successive interference cancellation, known as the groupwise successive interference cancellation, is suggested by van der Wijk et al. (1995). The groupwise SIC scheme separates the users into groups, and feedbacks and cancels the MAI in groups. Thus, the interference cancellation within a group is cancelled in parallel and the MAI from each group is cancelled successively. The hardware complexity of this scheme is reduced from that required by SIC schemes by a factor equal to the group size while retaining some of the advantages of SIC. The numerical results show that the performance approaches that of the purely SIC receiver when the group size is not too large.

The performance of the parallel interference cancelling receiver using orthogonal convolutional codes on multipath Rayleigh fading channel is analyzed by Sanada and Wang (1994; 1995). In this method, the received signals are both demodulated and decoded by a soft decision Viterbi decoder. Single cell results show that user capacity is between 1.5 to 3 times higher than that of the conventional decorrelating receiver.

A slightly different twist on SIC is developed by Dent *et al.* (1992). In their system, the data bits are first encoded and spread using Walsh-Hadamard codes and then scrambled with an access code which is unique to each user. Since the access codes do not increase the chip rate, all of the spectral spreading is a result of Walsh-Hadamard encoding. At the receiver, the composite received signal is descrambled with the access code of the strongest user. A Walsh-Hadamard transform is then applied. In the resulting spectrum, one component should be far greater than the other ones. The index of this component is the transmitted symbol of that user. The other users' power should be, on the average, evenly distributed over the entire spectrum. After extracting the index of the maximum spectral component, the component is removed by setting the bin to zero. An inverse Walsh-Hadamard transform is then used to convert back to the time domain. This new composite signal no longer contains the strongest user's signal. The process is now repeated using the second strongest user's access code for descrambling. The process iterates until all users are detected. The performance of this receiver is significantly better than that of the conventional matched filter. But in its present state, many issues, such as its performance relative to other SIC receivers, need further study.

SIC has been extended to the case of fading channels recently. A SIC receiver operating in a flat fading channel using coherent detection is analyzed by Yoon *et al.*

(1993). Channel estimates that are corrupted by additive white Gaussian noise are assumed known at the receiver. The results show that, in a single cell system, the capacity of a CDMA wireless system can be increased by an order of magnitude. However, no means of estimating the time varying channel characteristics, which is critical to a successful practical multiple access interference cancellation scheme and coherent detection, is given. Recent results have shown that interference cancellation schemes requiring hard decisions can be significantly compromised with inaccurate amplitude estimation (Gray *et al.*, 1995; Wu and Duel-Hallen, 1996). A system similar to the CDMA system proposed in IS-95, with the exception of the SIC receiver, is investigated by Patel and Holtzman (1994b) and is currently being realized via DSP's by Pedersen *et al.* (1996). The channel characteristics are estimated from the received signal. The results show that this receiver performs significantly better than the conventional one. Since this receiver does not attempt to estimate the phase of the carrier, it may be possible to improve the performance with accurate phase estimation. This receiver is an example of interference cancellation receiver using soft decisions. Other subtractive detectors using soft decisions have been analyzed by Buehrer and Woerner (1996).

The application of the SIC receiver to a multi-rate DS-CDMA system gives considerable improvement in performance and flexibility as compared to the conventional matched filter detector (Johansson and Svensson, 1995). A shortcoming in this study, however, is that it assumes perfect knowledge of the phase, time delay and channel gain for each signal. The performance with realistic estimation algorithms is still unknown.

Díaz and Agustí(1994a; b) analyzed the performance of a PIC receiver in a frequency selective fading channel. The data frame structure consists of a preamble of 10

bits followed by 90 information bits. A filter matched to the Gold sequences, which are used as spreading sequences, is used during the preamble to estimate the channel impulse response. The results show that some improvement over the conventional receiver is possible. The performance increase is not very substantial because the channel is significantly different at the end of the frame than at the preamble. Therefore the channel estimates are not quite sufficient to track the channel.

2.5.2.5.1 Multi-stage multi-user receiver

Multi-stage receiver takes advantage of the fact that with each additional stage, the decisions used for interference cancellation get progressively more reliable[1] and thus the performance gets progressively better. Multi-stage detection with the conventional matched filter as the first stage has been suggested by Varanasi and Aazhang for synchronous (1991a) and asynchronous (1990) CDMA systems. The performance of this receiver (which we will now call the Varanasi multi-stage receiver) with dual antenna diversity and fast closed loop power control (step size = 1.0 dB, 5% errors in power control bits) is studied by Holma et al. (1996). Single cell simulation shows that 60 to 70 % of the intracellular multiple access interference can be removed with 2 stages.

It is possible to view the multi-user receiver proposed by Xie et al. (1990) as a two stage multi-stage receiver. The major difference between the two receivers is that the Varanasi multi-stage receiver uses only first stage decision in its second stage multiple access interference estimates, while the Xie multi-stage receiver uses as many of the

---

[1] We have made an implicit assumption that the decisions at the first stage are sufficiently reliable so that MAI can be reduced by cancellation. If the first stage decisions are very unreliable, then the performance may be worse with multi-stage receivers.

second stage decisions, which are more reliable, as are available. The performance of this receiver is, however, only slightly better than the Varanasi multi-stage receiver (Giallorenzi and Wilson, 1996).

Multi-stage SIC is introduced by Grant *et al.* (1993), Kawabe *et al.* (1993), Mowbray *et al.* (1993) and Giallorenzi and Wilson (1996). The performance of the two stage SIC receiver is significantly better than either the Varanasi or Xie multi-stage receiver (Giallorenzi and Wilson, 1996). Kaul and Woerner (1994) derive the asymptotic limit on performance improvement as the number of stages approaches infinity. Li and Steele (1994) show that, at least for AWGN channels, that multi-stage SIC receiver performs better than the multi-stage parallel interference cancelling receiver. Kawabe *et al.* (1993) demonstrate that orthogonal convolutional coding can further improve the performance.

The performance of a multi-stage interference cancelling receiver can be improved by performing a partial interference cancellation at each stage (Divsalar and Simon, 1995). The reconstructed multiple access interference is first scaled by a fraction before cancellation. The fraction increases for each stage to account for the improved accuracy of the tentative decisions. The results show that substantial gain over a multi-stage parallel interference cancelling receiver is possible because the reliabilities of the decisions for interference cancellation are taken into account. This might be the most powerful of the subtractive interference cancellation detectors and warrants further study (Moshavi, 1996).

The decorrelating receiver has also been suggested as a receiver structure for the first stage of the multi-stage receiver (Varanasi and Aazhang, 1991a; Juntti, 1994) to

66

improve the performance of the Varanasi multi-stage receiver. An adaptive version of this detector that does not require amplitude estimates is proposed in Zhu *et al.* (1995). Another modification for asynchronous systems, is suggested by Sourour and Nakagawa (1994), and takes advantage of the fact that in an asynchronous system, a desired bit of any user is affected by the interference from two bits from each of the other users. After first stage decision estimates are obtained, at the end of the integration period of a desired bit the interference estimates form the earlier of the two interfering bits can be obtained and used in the second stage estimate. Also in the second stage, after waiting a period equal to a bit duration, the interference from the second bit can be estimated. Therefore interference from both bits can be cancelled in the second stage. The results show that, assuming perfect estimates of the received powers, delays and phases of all users are available, the performance is better than the Varanasi multi-stage receiver. Abrams *et al.* (1995) suggest a detector based entirely on feedback cancellation of the outputs of the correlator. The cancellation scheme is parallel with correlator output continuously fed back for cancellation.

A slightly different approach to multi-stage detection in AWGN channel is suggested by Siveski *et al.* (1994). Instead of using estimates of the received powers, delays and phases of all users in reconstructing the multiple access interference, it is constructed as a weighted sum of the decision estimates. The weights are determined by an adaptive structure that uses a stochastic version of the steepest decent method which minimizes the signal energy at the output with averaging of the error function computed over a number of iterations. The performance of this receiver is shown to be much better than that of the decorrelating receiver, particularly in the presence of strong interfering signals. A

recursive least squares algorithm can be used to increase the convergence speed of algorithm for updating the weights (Kamel and Siveski, 1995).

Multicellular performance of the Varanasi multi-stage receiver operating on a AWGN channel is investigated by Agashe and Woerner (1995). As expected, their results show that intercellular interference will severely limit the benefits of interference cancellation. The weakness of this study is that a circular cell geometry was assumed.

The performance of multi-stage receivers on fading channels has been of considerable interest in the literature. Soong (1994) shows that the performance of the multi-stage SIC receiver can be improved significantly over that of the conventional matched filter by using reference symbols for channel estimation (see Chapter 3 for more detail). Hottinen et al. (1995) apply joint estimation and multi-stage detection in a multipath fading environment with and without rate 1/2 convolutional coding. Simulation results demonstrate that significant increase in capacity over the conventional matched filter is possible. Jamal and Dahlman (1996) show that the multi-stage SIC receiver clearly outperforms the decorrelating receiver, especially in the frequency selective environment where the linear scheme loses much of its near-far resistance.

The combination of multi-stage SIC and forward error correction coding has also received some attention in the literature. In Shaheen and Gupta (1995a), error correction decoding is preceded by three stages of SIC using hard decisions on the coded symbols. The results show that substantial capacity improvement is possible if accurate estimation of the channel parameters (less than 1% error) can be guaranteed. Other work, such as Hoeher (1993) and Saifuddin et al. (1994) shows that performance is better when the decoded bits are used for interference cancellation instead of hard decisions on the coded

symbols.

In an attempt to reduce complexity of the multi-stage receiver operating on the fading channel with convolutional coding, Shaheen and Gupta (1995b) suggest that the second stage may be used only when it is needed (i.e. in cases where errors in the detected sequence are likely) and when sufficient time for the computations is available. The results show that significant computational savings can be obtained especially when there are mobiles subjected to large amount of interference. The applicability of multi-stage SIC receivers to multirate CDMA systems is studied by Johansson and Svensson (1996). Performance close to the single user bound is demonstrated in slow fading channel with known channel parameters.

2.5.2.6 Decorrelating decision-feedback multi-user receiver

A slightly different approach is proposed by Duel-Hallen (1993; 1995). Her detector, in addition to using a linear transformation, employs successive interference cancellation. The linear transformation partially decorrelates the users without noise enhancement and the SIC is used to subtract out the residual interference. This receiver is analogous to the zero forcing decision feedback equalizer for intersymbol interference and is thus similar to the decision feedback multi-user detectors. Its performance is similar to that of the decorrelating receiver for the strongest user and gradually approaches the single user bound as the user's power decreases relative to the powers of the interferers. Thus the performance advantage is greater for relatively weaker users. An improved zero forcing decision feedback multi-user detector is proposed in Wei and Schlegel (1994). Performance advantage is obtained because this detector feeds back more than one set of

69

likely decisions and their corresponding matrices.

2.5.2.7 MAI suppression with adaptive antennas

The above discussion of multi-user receivers has focused on temporal processing of the multiple access interference (MAI). A different approach is to process the multiple access interference in the spatial domain. This method is based upon the fact that in spread-spectrum radio communication, the received signals with different angles of arrival can be distinguished by beam-forming antennas (antenna arrays). If the desired signal's angle of arrival is unknown, an adaptive antenna can be useful in suppressing interfering signals (Compton, 1978; 1988). Such an antenna can be considered to be an adaptive spatial filter. The weights of the antenna elements can be updated by using a reference signal (training sequence) in a way similar to updating the tap coefficients of an adaptive equalizer. For example, Tsoulos et al. (1995) suggest the use of the RLS algorithm.

More recently, the research in adaptive antennas has been directed along the line of combining spatial processing with temporal processing. Since adaptive antenna cannot suppress interfering signal from an undesired user with the same angle of arrival as that of the desired user, temporal processing is also necessary. The optimal spatial and temporal filtering system, employing an adaptive antenna, a temporally whitening matched filter and a Viterbi algorithm to implement the optimal MLSE, is proposed by Kohno et al. (1995). Numerical results show that this receiver has the lowest bit error rate when compared with other schemes. The combination of adaptive antenna with a subtractive multi-user receiver is studied by Kohno et al. (1990) and Kohno (1994). The results show that joint spatial-temporal processing can achieve stable demodulation and improve error rate of decoded

70

data even in a heavily interfered channel where a conventional array antenna system cannot achieve acquisition. Hosur *et al.* (1995) introduce the combination of an adaptive antenna with a adaptive decorrelating receiver. The performance is significantly better than that of the decorrelating receiver. Ghazi-Moghadam and Kaveh (1995) investigate a combination of an adaptive antenna and a SIC receiver. Performance comparison with the single antenna interference canceller shows that using multiple antennas improves the performance of the interference canceller and compensates for nonzero crosscorrelations between the user' signature waveforms.

The above discussion of adaptive antennas has been cursory in nature. The interested reader is encouraged to consult the excellent reviews in Kohno (1991; 1995).

2.6 Conclusion

The above review of the literature shows that multi-user receivers have the potential to significantly increase the traffic capacity of CDMA systems. The least complex of the multi-user receivers discussed in Section 2.5 and, thus, the most practical multi-user receiver is the successive interference cancellation (SIC) receiver. Moreover, the SIC receiver, especially that of the multi-stage variety, performs better than parallel interference cancelling receivers and the decorrelating receiver, if perfect estimates of the channel are available. The performance, however, of multi-stage SIC receivers with practical channel estimation schemes has not received much attention in the literature. Therefore, the remainder of this thesis will focus on evaluating the performance of a multi-stage SIC receiver in flat and frequency selective Rayleigh fading channels with reference symbol assisted estimation of the channel parameters.

71

2.8 References

Aazhang, B., Paris, B.-P. and Orsak, G.C. (1992): Neural networks for multiuser detection in code-division multiple-access communications. *IEEE Trans. Commun.*, vol. 40, no. 7, pp. 1212-1222.

Abend, K. and Fritchman, B. (1970): Statistical detection for communication channels with intersymbol interference. *Proc. IEEE*, vol. 58, no. 5, pp. 779-785.

Abdulrahman, M. (1993): *Fractionally-Spaced DFE for Spread Spectrum Multiple Access System*, Ph.D. dissertation, Carleton University.

Abdulrahman, M., Falconer D.D., and Sheikh, A.U.H. (1992): Equalization for Interference Cancellation in Spread Spectrum Multiple Access Systems. *Proc. of IEEE VTC*, pp. 71-74.

Abdulrahman, M., Sheikh, A.U.H., and Falconer D.D. (1993): DFE Convergence for Interference Cancellation in Spread Spectrum Multiple Access Systems. *Proc. of IEEE VTC*, pp. 807-810.

Abdulrahman, M., Sheikh, A.U.H. and Falconer D.D. (1994): Decision Feedback Equalization for CDMA in Indoor Wireless Communications", *IEEE J. Select. Areas Commun.*, vol. 12, no. 4, pp. 698-706.

Abrams, B.S., Zeger, A.E. and Jones, T.E. (1995): Efficiently structured CDMA receiver with near-far immunity. *IEEE Trans. Veh. Technol.*, vol. 44, no. 1, pp. 1-13.

Agashe, P. and Woerner, B.D. (1995): Analysis of interference cancellation for a multicellular CDMA environment. *Proc. IEEE PIMRC*, pp. 747-752.

Agrell, E. and Ottoson, T. (1995): ML optimal CDMA multiuser receiver. *Elect. Lett.*, pp. 1554-1555.

Ariyavistakul, S. (1992): SIR-based power control in a CDMA system. *Proc. IEEE Globecom Conf.*, pp. 868-873.

Ariyavistakul, S. and Chang, L.F. (1991): Signal and interference statistics of a CDMA system with feedback power control. *Proc. IEEE Globecom Conf.*, pp. 1490-1495.

Bar-Ness, Y., Chen, D.W. and Siveski, Z. (1994a): Adaptive multiuser bootstrapped decorrelating CDMA detector in asynchronous unknown channels. *Proc. IEEE PIMRC*, pp. 533-537.

Bar-Ness, Y., Siveski, Z. and Chen, D.W. (1994b): Bootstrapped decorrelating algorithm for adaptive interference cancellation in synchronous CDMA communications systems. *Proc. IEEE ISSSTA*, pp. 162-166.

Bar-Ness, Y. and Punt, J.B. (1995): An improved multi-user CDMA decorrelating detector. *Proc. IEEE PIMRC*, pp. 975-979.

Batalama, S.N. and Pados, D.A. (1995): Blind real-time low-complexity receivers for DS-CDMA mobile users. *Proc. IEEE Globecom/CTMC*, pp. 122-125.

Bello, P. (1963): Characterization of random time-variant linear channels. *IEEE Trans. Commun.*, vol. 11, pp. 360-393.

Bello, P. (1964): Time-frequency duality. *IEEE Trans. Infrom. Theory*, vol. IT-9, pp. 18-33.

Black, D.M. and Reudink, D.O. (1972): Some characteristics of radio propagation at 800 MHz in the Philadelphia area. *IEEE Trans. Veh. Tech.*, vol. VT-21, pp. 45-51.

Buehrer, R.M. and Woerner, B.D. (1996): Analysis of adaptive multistage interference cancellation for CDMA using an improved Gaussian approximation. *Proc IEEE MILCOM*, pp. 1195-1199.

Chang, L.F. and Ariyavistakul, S. (1991): Performance of power control method for CDMA radio communications system. *Elect. Lett.*, vol. 27, no. 11, pp. 920-922.

Chen, D.S. and Roy S. (1994): An adaptive multiuser receiver for CDMA systems. *IEEE J. Select. Areas Commun.*, vol. 12, no. 5. pp. 808-816.

Clark, R.H. (1968): A statistical theory of mobile radio reception. *Bell Syst. Tech. J.*, vol.

47, pp. 957-1000.

Compton, R.T., Jr. (1978): An adaptive array in a spread-spectrum communication system. *Proc. IEEE*, vol. 66, no. 3, pp. 289-298.

Compton, R.T., Jr. (1988): *Adaptive antennas concepts and performance*. Englewood Cliffs: Prentice-Hall.

Dent, P., Gudmundson, B. and Ewerbring, M. (1992): CDMA-IC: A novel code division multiple access scheme based on interference cancellation. *Proc. IEEE PIMRC*, pp. 98-102.

Díaz, P. and Agustí, R. (1992): Analysis of a fast CDMA power control scheme in an indoor environment. *Proc. of IEEE VTC*, pp. 67-70.

Díaz, P. and Agustí, R. (1994a): Analysis of a linear interference canceller in cellular DS/CDMA systems. *Proc. of IEEE VTC*, pp. 785-788.

Díaz, P. and Agustí, R. (1994b): On the influence of the channel impulsional response estimation on the performance of a linear interference canceller for a DS/CDMA system. *Proc. of IEEE PIMRC*, pp. 529-532.

Divsalar, D. and Simon, M. (1995): Improved CDMA performance using parallel interference cancellation. *JPL Pub.*

Duel-Hallen, A. (1993): Decorrelating decision-feedback multiuser detector for synchronous code-division multiple-access channel. *IEEE Trans. Commun.*, vol. 41, no. 2, pp. 285-290.

Duel-Hallen, A. (1995): A family of multiuser decision-feedback detectors for asynchronous code-division multiple-access channels. *IEEE Trans. Commun.*, vol. 43, no. 2/3/4, pp. 421-434.

Duel-Hallen, A., Holtzman, J. and Zvonar, Z. (1995): Multiuser detection for CDMA systems. *IEEE Personal Communications*, vol. 2, no. 4, pp. 46-58.

Egli, J. (1957): Radio propagation above 40 MC over irregular terrain. *Proc. IRE*, pp. 1383-1391.

Esmailzadeh, R., Nakagawa, M. and Kajiwara, A. (1992): Power control in packet switched time division duplex direct sequence spread spectrum communications. *Proc. of IEEE VTC*, pp. 989-992.

Falconer D.D., Abdulrahman, M., Lo, N.W.K., Petersen, B.R. and Sheikh, A.U.H. (1993): Advances in Equalization and Diversity for Portable Wireless Systems. *Digital Signal Processing: A Review Journal*, vol. 3, no. 3, pp. 148-162.

Fawer, U. and Aazhang, B. (1995): A multiuser receiver for code division multiple access communications over multipath channels. *IEEE Trans. Commun.*, vol. 43, no. 2/3/4, pp. 1556-1565.

Fukawa, K. and Suzuki, H. (1991): Adaptive equalization with RLS-MLSE for frequency selective fast fading mobile radio channels. *Proc. IEEE GlobeCom Conf.*, pp. 548-552.

Gans, M.J. (1972): A power-spectral theory of propagation in the mobile-radio environment. *IEEE Trans. Veh. Tech.*, vol. VT-21, pp. 27-38.

Ge, H. and Bar-Ness, Y. (1996): Comparative study of the linear minimum mean squared error (LMMSE) and the adaptive bootstrap multiuser detectors for CDMA communications. *Proc. IEEE ICC*, pp. 78-82.

Ghazi-Moghadam, V. and Kaveh, M. (1995): Interference cancellation using antenna arrays. *Proc. IEEE PIMRC*, pp. 936-939.

Giallorenzi, T.R. and Wilson, S.G. (1993): Decision feedback multiuser receivers for asynchronous CDMA systems. *Proc. IEEE GlobeCom Conf.*, pp. 1677-1682.

Gilbert, E.N. (1965): Energy reception for mobile radio. *Bell Syst. Tech. J.*, vol. 44.

Gilhousen, K.S., Jacobs, I.M., Padovani, R., Viterbi, A.J., Weaver, L.A. and Wheatley III, C.E. (1991): On the capacity of cellular CDMA system. *IEEE Trans. Veh. Technol.*, vol. VT-27, pp 303-312.

Gray, S.D., Kocic, M. and Brady, D. (1995): Multi-user detection in mismatched multiple-access channels. *IEEE Trans. Commun.*, vol. 43, no. 12, pp. 3080-3089.

Golub, G.H. and Van Loan, C.F. (1985): *Matrix Computations*. Baltimore: The John Hopkins University Press.

Hafeez, A. and Stark, W.E. (1996): Combined decision-feedback multiuser detection/soft-decision decoding for CDMA channels. *Proc. IEEE VTC*, pp. 382-386.

Hashemi, H. (1993a): The Indoor Radio Propagation Channel. *Proc. IEEE*, vol. 81, no. 7, pp 943-968.

Hashemi, H. (1993b): Impulse Response Modeling of Indoor Radio Propagation Channels. *IEEE J. Select. Areas Commun.*, vol. 11, no. 7, pp. 967-978.

Helstrom, C.W. (1995): *Elements of Signal Detection and Estimation*. Englewood Cliffs: Prentice Hall.

Hizlan, M. and Hughes, B. (1991): On the optimality of direct sequence for arbitrary interference rejection. *IEEE Trans. Commun.*, vol.39, no.8, pp. 1193-1196.

Hoeher, P. (1993): On channel coding and multiuser detection for DS-CDMA. *Proc. IEEE ICUPC*, pp. 641-646.

Holma, H,, Toskala, A. and Hottinen, A. (1996): Performance of CDMA multiuser detection with antenna diversity and closed loop power control. *Proc. IEEE VTC*, pp. 362-366.

Honig, M.L., Madhow, U. and Verdú, S. (1994): Blind adaptive interference suppression for near-far resistant CDMA. *Proc. Globecom Conf.*, pp. 379-384.

Honig, M.L. and Veerakachen, W. (1996): Performance variability of linear multiuser detection for DS-CDMA. *Proc. IEEE VTC*, pp. 372-376.

Hottinen, A. (1994): Self-organizing multiuser detection. *Proc. IEEE ISSSTA*, pg. 152-156.

Hottinen, A., Holma, H. and Toskala, A. (1995): Performance of multistage multiuser detection in a fading multipath channel. *Proc. IEEE PIMRC*, pp. 960-964.

Hosur, S., Tewfik, A.H. and Ghazi-Moghadam, V. (1995): Adaptive multiuser receiver schemes for antenna arrays. *Proc. IEEE PIMRC*, pp. 940-944.

Howitt, L., Reed, J.H., Venuri, V. and Hsia, T.C. (1994): Recent developments in applying neural nets to equalization and interference rejection. In Rappaport, T.S., Woerner, B.D., and Reed, J.H. (eds.): *Wireless Personal Communications: Trends and Challenges*. Boston: Kluwer academic publishers.

Huang, H.C. and Schwartz, S.C. (1994): A comparative analysis of linear multi-user detectors for fading multipath channels. *Proc. IEEE Globecom*, pp. 11-15.

Iltis, R.A. and Mailaender, L. (1994): An adaptive multiuser detector with joint amplitude and delay estimation. *IEEE J. Select. Areas Commun.*, vol. 12, no. 5, pp. 774-785.

Jakes, W.C. (1974): *Microwave Mobile Communications*. New York: John Wiley, 1974.

Jalali, A. and Mermelstein, P. (1994): Effects of diversity, power control and bandwidth on the capacity of microcellular CDMA systems. *IEEE J. Select. Areas Commun.*, vol. 12, no. 9, pp. 952-961.

Jamal, K. and Dahlman, E. (1996): Multi-stage serial interference cancellation for DS-CDMA. *Proc IEEE VTC*, pp. 671-675.

Jung, P. and Blanz, J. (1995): Join detection with coherent receiver antenna diversity in CDMA mobile radio systems. *IEEE Trans. Veh. Tech.*, vol. 44, no. 1, pp. 76-88.

Jung, P., Naßhan, M. and Blanz, J. (1994): Application of turbo-codes to a CDMA mobile radio system using joint detection and antenna diversity. *Proc. IEEE VTC*, pp. 770-774.

Johansson, A.-L. and Svensson, A. (1995): Successive interference cancellation schemes in multi-rate DS/CDMA systems. *Proc. WINLAB Conf.*, pp. 155-174.

Johansson, A.-L. and Svensson, A. (1996): Multistage interference cancellation in multirate DS/CDMA on a mobile radio channel. *Proc. IEEE VTC*, pp. 666-670.

Joseph, K. and Raychaudhuri, D. (1991): Performance evaluation of cellular packet CDMA networks with transmit power constraints. *Proc. IEEE ICC*, pp. 1614-1620.

Jung, P. and Blanz, J. (1995): Joint detection with coherent receiver antenna diversity in CDMA mobile radio systems. *IEEE Trans. Veh. Technol.*, vol. 44, no. 1, pp. 76-88.

Juntti, M.J. (1994): Performance of multistage detector with one-shot decorrelating type first stage in an asynchronous DS/CDMA system. *Proc. IEEE ISSSTA*, pp. 157-161.

Juntti, M.J. (1995): Linear multiuser detector update in synchronous dynamic CDMA systems. *Proc. IEEE PIMRC*, pp. 980-984.

Juntti M.J. and Aazhang, B. (1995): Linear finite memory-length multiuser detectors. *Proc. IEEE Globecom/CTMC*, pp. 126-130.

Kamel, R.E. and Siveski, Z. (1995): Rapidly converging multiuser CDMA detector for an synchronous AWGN channel. *Elect. Lett.*, vol. 31, no. 12, pp. 951-952.

Kajiwara, A., Falconer, D.D. and Sheikh, A.U.H. (1993): On a linear interference canceller in cellular CDMA systems. *Proc. Wireless 93*, pp. 245-256.

Kajiwara, A. and Nakagawa, M. (1991): Crosscorrelation cancellation in SS/DS block demodulator. *IEICE Trans.*, vol. E74, no. 9, pp. 2596-2601.

Kajiwara, A. and Nakagawa, M. (1994): Microcellular CDMA system with a linear multiuser interference canceller. *IEEE J. Select. Areas Commun.*, vol. 12, no. 4, pp. 605-611.

Kaul, A. and Woerner, B.D. (1994): Analytic limits on performance of adaptive multistage interference cancellation for CDMA. *Elect. Lett.*, vol. 30, no. 25, pp. 2093-2095.

Kawabe, M., Kato, T., Kawahashi, A., Sato, T. and Fukasawa, A. (1993): Advanced CDMA scheme based on interference cancellation. *Proc. IEEE VTC*, pp 448-451.

Kawabe, M., Kato, T., Sato, T., Kawahashi, A. and Fukasawa, A. (1993): Advanced CDMA scheme for PCS based on interference cancellation. *Proc. IEEE ICUPC*, pp. 1000-1003.

Kawahara, T. and Matsumoto, T. (1995): Join decorrelating multiuser detection and channel estimation in asynchronous CDMA mobile communications channels. *IEEE Trans. Veh. Technol.*, vol. 44, pp. 506-515.

Klein, A., Kaleh, G.K. and Baier, P.W. (1994): Equalizers for multi-user detection in code division multiple access mobile radio systems. *Proc. IEEE VTC*, pp. 762-766.

Kohno, R. (1991): Pseudo-noise sequences and interference cancellation techniques for spread spectrum systems - spread spectrum theory and techniques in Japan. *IEICE Trans. Commun.*, vol. J74-B-I, no. 5, pp. 1083-1092.

Kohno, R. (1994): Spatial and temporal filtering for co-channel interference in CDMA. *Proc. IEEE ISSSTA*, pp. 51-60.

Kohno, R. (1995): Spatial and temporal filtering for co-channel interference in CDMA. In Glisic, S.G. and Lappänen, P.A. (eds.): *Code Division Multiple Access Communications*, Boston: Kluwer Academic Publishers.

Kohno, R., Hatori, M., and Imai H. (1983): Cancellation techniques of co-channel interference in asynchronous spread spectrum multiple access systems. *Elect. and Commun. in Japan*, vol. 66-A, no. 5, pp. 20-29.

Kohno, R., Imai, H., Hatori, M. and Pasupathy, S. (1990): Combination of an adaptive array antenna and a canceller of interference for direct-sequence spread spectrum multiple access system. *IEEE J. Select. Areas Commun.*, vol. 8, no. 4, pp. 675-682.

Kohno, R., Ishii, N. and Nagatsuka, M. (1995): A spatially and temporally optimal multi-

user receiver using an array antenna for DS/CDMA. *Proc. IEEE PIMRC*, pp. 950-954.

Lee E.K.B. (1993): Rapid converging adaptive interference suppression for direct sequence code-division multiple-access systems. *Proc. Globecom Conf.*, pp 1683-1687

Lee, W.C.Y. (1991): Power control in CDMA. *Proc. of IEEE VTC*, pp. 77-80.

Li, Y. and Steel, R. (1994): Serial interference cancellation method for CDMA. *Elect. Lett.*, vol. 30, no. 19, pp. 1581-1583.

Lupas, R. and Verdu, S.(1989): Linear multiuser detectors for synchronous code-division multiple-access channels. *IEEE Trans. on Inform. Theory*, vol. 35, no. 1, pp. 123-136.

Lupas, R. and Verdu, S. (1990): Near-far resistance of multiuser detectors in asynchronous channels. *IEEE Trans. Commun.*, vol. 38, no. 4, pp. 496-508.

Madhow, U. and Honig, M.L. (1994): MMSE interference suppression for direct-sequence spread-spectrum CDMA. *IEEE Trans. Commun.*, vol. 42, no. 12, pp. 3178-3188.

Maric, S.V. and Titlebaum, E.L. (1992): A class of frequency hop codes with nearly ideal characteristics for use in multiple-access spread-spectrum communications and radar and sonar systems. *IEEE Trans. Commun.*, vol. 40, no. 9, pp. 1442-1447.

Miki, Y. and Sawahashi, M. (1995a): Combination performance of truncated decorrelator and coherent RAKE receiver for DS-CDMA. *Elect. Lett.*, vol. 31, no. 19, pp. 1628-1630.

Miki, Y. and Sawahashi, M. (1995b): Preselection-type coherent decorrelating detector for asynchronous DS-CDMA. *Elect. Lett.*, vol. 31, no. 19, pp. 1636-1637.

Milstein, L.B., Rappaport ,T.S. and Barghouti, R. (1992): Performance evaluation for cellular CDMA. *IEEE J. Select. Areas Commun.*, vol. 10, no. 4.

Mitra, U. and Poor, H.V. (1996a): Adaptive decorrelating detectors for CDMA systems. *Wireless Personal Commun.*, vol. 2, pp. 415-440.

Mitra, U. and Poor, H.V. (1996b): Analysis of an adaptive decorrelating detector for synchronous CDMA channels. *IEEE Trans. Commun.*, vol. 44, no. 2, pp. 257-268.

Miyajima, T., Hasegawa, T. and Haneisi, M. (1993): On the multiuser detection using a Hopfield network in code-division multiple-access communications. *IEICE Trans. Commun.*, vol. E76-B, no. 8.

Moshavi, S. (1996): Multi-user detection for DS-CDMA communications. *IEEE Communications Magazine*, vol. 34, no. 10, pp. 124-136.

Moshavi, S., Kanterakis, E.G. and Schilling, D.L. (1996): Multistage linear receiver for DS-CDMA systems. *Int'l J. Wireless Info. Networks*, vol. 3, no. 1.

Monk, A.M., Davis, M., Milstein, L.B. and Helstrom, C.W. (1994): A noise-whitening approach to multiple access noise rejection-part I: Theory and background. *IEEE J. Select. Areas Commun.*, vol. 12, no. 5, pp. 817-827.

Mokhtar, M.A. and Gupta, S.C. (1992): Power control considerations for DS/CDMA personal communication systems. *IEEE Trans. Veh. Tech.*, vol. 41, no. 4, pp. 479-487.

Mowbray, R.S., Pringle, R.D. and Grant, P.M. (1993): Increased CDMA system capacity through adaptive cochannel interference regeneration and cancellation. *IEE Proceedings-I*, Vol. 139, no. 5, pp 515-524.

Nagaosa, T., Miyajima, T. and Hasegawa, T. (1994): On the multiuser detection using a Hopfield network in m-ary/ SSMA communications. *Proc. IEEE PIMRC*, pp. 420-424.

Nemsick, L.W. and Geraniotis, E. (1992): Adaptive multichannel detection of frequency-hopping signals. *IEEE Trans. Commun.*, vol. 40, no. 9, pp. 1502-1511.

Okumura, Y.E., Ohmori, T., Kawano T. and Fukuda, K. (1964): Field strength and its

variability in VHF and UHF land mobile radio service. *Rev. Elec. Commun. Lab.*, vol. 16, pp. 825-873.

Ossana, J.F. (1964): A model for mobile radio fading due to building reflections: theoretical and experimental fading waveform power spectra. *Bell Syst. Tech. J.*, vol. 43, pp. 2935-2971.

Parkvall, S., Ottersten, B. and Ström, E.G. (1995): Sensitivity analysis of linear DS-CDMA detectors to propagation delay estimation errors. *Proc. IEEE Globecom Conf.*, pp. 1872-1876.

Parsons, J.D. (1992): *The Mobile Radio Propagation Channel.* New York: John Wiley and Sons.

Patel, P. and Holtzman, J. (1994a): Performance comparison of a DS/CDMA system using a successive interference cancellation (IC) scheme and a parallel IC scheme under fading. *Proc. IEEE ICC*, pp. 510-515.

Patel, P. and Holtzman, J. (1994b): Analysis of a simple successive interference cancellation scheme in a DS/CDMA system. *IEEE J. Select. Areas Commun.*, vol. 12, no. 5, pp 796-807.

Pedersen, K.I., Kolding, T.E., Seskar, I. and Holtzman, J.M. (1996): Practical implementation of successive interference cancellation in DS/CDMA systems. *Proc. IEEE ICUPC*, pp. 321-325.

Poor, H.V. and Verdu, S.(1988): Single-User Detectors for Multiuser Channels. *IEEE Trans. Commun.*, vol. 36, no. 1, pp. 50-60.

Prasad, R. Kegel, A. and Jansen, M.G. (1992): Effect of imperfect power control on cellular code division multiple access system. *Elect. Lett.*, vol. 28, no. 9, pp. 848-849.

Proakis, J.G. (1995): *Digital Communications 3rd ed.* N.Y.: McGraw-Hill Inc..

Rapajic, P. and Vucetic, B. (1994): Linear adaptive transmitter-receiver structures for asynchronous CDMA systems. *Proc. IEEE ISSSTA*, pp. 181-185.

Rappaport, T.S. and Milstein, L.B. (1992): Effects of radio propagation path loss on DS-CDMA cellular frequency reuse efficiency for the reverse channel. *IEEE Trans. Veh. Tech.*, vol. VT-41, no. 3, pp. 231-241.

Robertson, R.C. and Ha, T.T. (1992): Error probabilities of fast frequency-hopped MFSK with noise-normalization combining in a fading channel with partial-band interference. *IEEE Trans. Commun.*, vol. 40, no. 2, pp. 404-412.

Roy, S., Chen, D.S. and Mau, S.C. (1994): An adaptive multi-user decorrelating receiver for CDMA systems. In: Holtzman, J.M. and Goodman, D.J. (eds): *Wireless and Mobile Communications.* Boston: Kluwer Academic Publishers.

Saifuddin, A., Kohno, R. and Imai, H. (1994): Cascaded combination of cancelling co-channel interference and decoding of error-correcting codes for CDMA. *Proc. IEEE ISSSTA*, pp. 171-175.

Sanada, Y. and Wang Q. (1994): Co-channel interference cancellation technique using orthogonal convolutional codes. *Proc IEEE ISSSTA*, pp. 176-180.

Sanada, Y. and Wang Q. (1995): A co-channel interference cancellation technique using orthogonal convolutional codes on multipath Rayleigh fading channel. *Proc. IEEE ICC*, pp. 858-862.

Saquib, M., Yates, R. and Mandayam, N. (1996): Decorrelating detectors for a dual rate synchronous DS/CDMA system. *Proc. IEEE VTC*, pp. 377-381.

Schlegel, C.B., Xiang, Z-J and Roy, S. (1995): Projection receiver: a new efficient multi-user detector. *Proc. IEEE Globecom/CTMC*, pp. 142-146.

Schneider, K.S. (1979): Optimum detection of code division multiplexed signals. *IEEE Trans. Aerospace Elect. Sys.*, vol. AES-15, no. 1, pp. 181-185.

Schodorf, J.B. and Williams, D.B. (1996): Partially adaptive multiuser detection. *Proc. VTC*, pp. 367-371.

Sezgin, N. and Bar-Ness, Y. (1996): Adaptive soft limiter bootstrap separator for one-shot asynchronous CDMA channel with singular partial cross-correlation

77

matrix. *Proc. IEEE ICC*, pp. 73-77.

Shaheen, K.M. and Gupta, S. (1995a): Cascaded CCI cancellation and error-correcting codes for DS-SS CDMA mobile communication system. *Proc. IEEE GlobeCom Conf.*, pp. 2177-2181.

Shaheen, K.M. and Gupta, S. (1995b): Adaptive combination of cancelling co-channel interference and decoding of error-correcting codes for DS-SS CDMA mobile communication system. *Proc. IEEE PIMRC*, pp. 737-741.

Simon, M.K., Omura, J.K., Scholtz, R.A. and Levitt, B.K. (1985): *Spread Spectrum Communications*. Maryland: Computer Science Press.

Shi, Z-L, Driessen, P.F. and Du, W. (1993): One shot signal detection in asynchronous CDMA systems. *Proc. IEEE Pac. Rim Conf.*, pp. 690-693.

Siveski, Z., Zhong, L. and Bar-Ness, Y. (1994): Adaptive multiuser CDMA detector for asynchronous AWGN channels. *Proc. IEEE PIMRC*, pp. 416-419.

Soong, A.C.K. (1994): A Multi-Stage Interference Cancellation Scheme for CDMA Wireless Systems. *Proc. Wireless94 Conf.*, pp.

Sourour, E. and Nakagawa, M. (1994): A modified multi-stage co-channel interference cancellation in asynchronous CDMA systems. *Proc. IEEE PIMRC*, pp. 425-429.

Steele, R. (1992): *Mobile Radio communications*. N.Y.: IEEE Press.

Ström, E.G, Parkvall, S., Miller, S.L. and Ottersten, B.E. (1994): Sensitivity analysis of near-far resistant DS-CDMA receivers to propagation delay estimation errors. *Proc. IEEE VTC*, pp. 757-761.

Stüber, G.L. (1996): *Principles of Mobile Communication*. Boston: Kluwer Academic Press.

Stüber, G.L. and Kchao, C. (1992): Analysis of a multiple-cell direct-sequence CDMA cellular mobile radio system. *IEEE J. Select. Areas Commun.*, vol. 10, no. 4, pp. 669-679.

Tang, Z. and Cheng, S. (1994a): Pre-decorrelating single user detection for CDMA systems. *Proc. IEEE VTC*, pp. 767-769.

Tang, Z. and Cheng, S. (1994b): Interference cancellation for DS-CDMA systems over flat fading channels through pre-decorrelating. *Proc. IEEE PIMRC*, pp. 435-438.

TIA/EIA/IS-95 (1993): *Mobile station-base station compatibility standard for dual-mode wideband spread spectrum cellular system*. Telecommunications Industry Association.

Tidestav, C. Ahlén, A. and Sternad, M. (1995): Narrowband and broadband multiuser detection using a multivariable DFE. *Proc. IEEE PIMRC*, pp. 732-736.

Tse, R.T.S. (1992): *Spread spectrum multiple access with orthogonal convolutional codes for indoor digital radio*. M.Sc. dissertation, University of Alberta.

Tsoulos, G.V., Beach, M.A. and Swales, S.C. (1995): DS-CDMA capacity enhancement with adaptive antennas. *Elect. Lett.*, vol. 31, no. 16, pp. 1319-1320.

van der Wijk, F., Janssen, G.M.J. and Prasad, R. (1995): Groupwise successive interference cancellation in a DS/CDMA system. *Proc. IEEE PIMRC*, pp. 742-746.

Varanasi, M.K. (1993): Noncoherent detection in asynchronous multi-user channels. *IEEE Trans. Info. Theory*, vol. 39, no. 1, pp. 157-176.

Varanasi, M.K. (1995): Group detection for synchronous Gaussian code division multiple access channels. *IEEE Trans. Info. Theory*, vol. 41, no. 4, pp. 1083-1096.

Varanasi, M.K. (1996): Parallel group detection for synchronous CDMA communication over frequency selective Rayleigh fading channels. *IEEE Trans. Info. Theory*, vol. 42, no. 1, pp. 116-128.

Varanasi, M.K. and Aazhang, B. (1990): Multistage detection in asynchronous code-division multiple-access communications. *IEEE Trans. Commun.*, vol. 38, no. 4, pp. 509-519.

Varanasi, M.K. and Aazhang, B. (1991a): Near-optimum detection in synchronous code-division multiple-access systems. *IEEE Trans. Commun.*, vol. 39, no. 5, pp. 725-736.

Varanasi, M.K. and Aazhang, B. (1991b): Optimally near-far resistant multi-user detection in differentially coherent synchronous channels. *IEEE Trans. Info. Theory*, vol. 37, no. 4, pp. 1006-1018.

Varanasi, M.K. and Vasudevan, S. (1994): Multi-user detectors for synchronous CDMA communications over non-selective Rician fading channels. *IEEE Trans. Commun.*, vol. 42, no. 2/3/4, pp. 711-722.

Vasudevan, S. and Varanasi, M.K. (1994): Optimum diversity combiner based multi-user detection for time dispersive Rician fading CDMA channels. *IEEE J. Select. Areas Commun.*, vol. 12, no. 4, pp. 580-593.

Vembu, S. and Viterbi, A.J. (1996): Two different philosophies in CDMA - a comparison. *Proc. IEEE VTC*, pp. 869-873.

Verdu, S. (1986): Minimum probability of error for asynchronous Gaussian multiple-access channels. *IEEE Trans. Infrom. Theory*, vol. IT-32, no. 1, pp. 85-96.

Verdu, S. (1995): Adaptive multiuser detection. In *Code Division Multiple Access Communications* (Glisic, S.G. and Lappanen, P.A., eds.). Kluwer: The Netherlands, pp. 43-50.

Vijayan, R. and Poor, H.V. (1990): Nonlinear techniques for interference suppression in spread-spectrum systems. *IEEE Trans. Commun.*, vol. 38, no. 7, pp. 1060-1065.

Viterbi, A.J. (1990): Very low rate convolutional codes for maximum theoretical performance of spread spectrum multiple access channels. *IEEE J. Select. Areas Commun.*, vol. 8, no. 4, pp. 641-649.

Wang, Y.C. and Milstein, L.B. (1988): Rejection of multiple narrow-band interference in both BPSK and QPSK DS spread spectrum systems. *IEEE Trans. Commun.*, vol. 36, no. 2, pp. 195-204.

Wei, L. and Schlegel, C. (1994): Synchronous DS-SSMA system with improved decorrelating decision feedback multi-user detection. *IEEE Trans. Veh. Technol.*, vol. 43, no. 3, pp. 767-772.

Wijayasuriya, S.S.H., McGeehan, J.P. and Norton, G.H. (1992a): A near-far resistant sliding window decorrelating algorithm for multi-user detectors in DS-CDMA systems. *Proc. IEEE Globecom*, pp. 1331-1338.

Wijayasuriya, S.S.H., McGeehan, J.P. and Norton, G.H. (1993a): RAKE decorrelating receiver for DS-CDMA mobile radio networks. *Elect. Lett.*, vol. 29, No. 4, pp. 395-396.

Wijayasuriya, S.S.H., Norton, G.H. and McGeehan, J.P. (1992b): Sliding window decorrelating algorithm for DS-CDMA receivers. *Elect. Lett.*, vol. 28, No. 17, pp. 1596-1598.

Wijayasuriya, S.S.H., Norton, G.H. and McGeehan, J.P. (1993b): A novel algorithm for dynamic updating of decorrelator coefficients in mobile DS-CDMA. *Proc. IEEE PRMIC*, pp. 292-296.

Wu, H.Y. and Duel-Hallen, A. (in press): Performance comparison of multi-user detectors with channel estimation for flat Rayleigh fading CDMA channels. *Wireless Personal Communications*.

Xie, Z., Rushforth, C.K. and Short, R.T. (1990): Multiuser signal detection using sequential decoding. *IEEE Trans. Commun.*, vol. 38, no. 5, pp. 578-583.

Xie, Z., Rushforth, C.K., Short, R.T. and Moon, T. (1993): Joint signal detection and parameter estimation in multiuser communications. *IEEE Trans. Commun.*, vol. 41, no.8, pp. 1208-1216.

Xie, Z., Short, R.T. and Rushforth, C.K. (1990): A family of suboptimum detectors for coherent multiuser communications. *IEEE J. Select. Areas Commun.*, vol. 8, no. 4, pp. 683-690.

Yokota, J., Horikoshi, J. and Suzuki, H. (1995): MLSE multiple co-channel interference cancelling with channel estimation for future mobile radios. *Proc. IEEE PIMRC*, pp. 753-757.

Yoon, S.Y., Hong, S.E., Ahn, J. and Lee, H.S. (1994): Pilot symbol aided coherent decorrelating detector for up-link CDMA mobile radio communication. *Elect. Lett.*, vol. 30, no. 12, pp. 929-930.

Yoon, Y.C., Kohno, R. and Imai, H. (1993): A spread-spectrum multiaccess system with cochannel interference cancellation for multipath fading channels. *IEEE J. Select. Areas Commun.*, vol. 11, no. 7, pp. 1067-1075.

Yoon, Y.C. and Leib, H. (1996): Matched filters with interference suppression capabilities for DS-CDMA. *IEEE J. Select. Areas Commun.*, vol. 14, no. 8, pp. 1510-1521.

Young, W.R. (1972): Comparison of mobile radio transmission of 150, 450, 900, and 3700 MC", *Bell Syst. Tech. J.*, vol. 31, pp. 1-14.

Ziemer, R.E. and Peterson, R.L. (1985): *Digital Communications and Spread Spectrum Systems*. New York: MacMillan Publising Company.

Zheng, F.C. and Barton, S.K. (1994): A new signalling scheme for one-shot near-far resistant detection in DS/CDMA. *Proc. IEEE PIMRC*, pp. 194-198.

Zheng, F.C. and Barton, S.K. (1995): Near-far resistant detection of CDMA signals via isolation bit insertion. *IEEE Trans. Commun.*, vol. 43, no. 2/3/4, pp. 1313-1317.

Zhu, B., Ansari, N. and Siveski, Z. (1995): Convergence and stability analysis of a synchronous adaptive CDMA receiver. *IEEE Trans. Commun.*, vol. 43, no. 12, pp. 3073-3079.

Zvonar, Z. (1994): Multiuser detection and diversity combining for wireless CDMA systems. In: Holtzman, J.M. and Goodman, D.J. (eds): *Wireless and Mobile Communications*. Boston: Kluwer Academic Publishers.

Zvonar, Z. (1996a): Multiuser detection in asynchronous CDMA frequency selective fading channels. *Wireless Personal Commun.*, vol. 2, pp. 373-392.

Zvonar, Z. (1996b): Combined multiuser detection and diversity reception for wireless CDMA systems. *IEEE Trans. Veh. Technol.*, vol. 45, pp 205-211.

Zvonar, Z. and Brady, D. (1996): Linear multipath-decorrelating receivers for CDMA frequency-selective fading channels. *IEEE Trans. Commun.*, vol. 44, no. 6, pp. 650-653.

Zvonar, Z. and Brady, D. (1995): Suboptimal multi-user detector for frequency-selective Rayleigh fading synchronous CDMA channels. *IEEE Trans. Commun.*, vol. 43, no. 2/3/4, pp. 154-157.

Zvonar, Z. and Brady, D. (1994): Multi-user detection in single-path fading channels. *IEEE Trans. Commun.*, vol. 42, no. 2/3/4, pp. 1729-1739.

Chapter 3: Reference symbol assisted multistage successive interference cancelling receiver for CDMA wireless communication systems*

3.1 Introduction

The desire to increase the capacity of cellular radio systems has resulted in growing interest in direct sequence code division multiple access (DS-CDMA). As is well known, the capacity of DS-CDMA wireless systems is directly limited by multi-user interference. Therefore, much attention has been devoted to receiver structures that are capable of cancelling multi-user interference (see Section 2.5).

Successive interference cancellation (SIC), first suggested by Viterbi (1990), has been the topic of many studies in the last few years because it is, arguably, the least complex of all interference cancelling schemes. It takes advantage of the fact that multiple access interference is deterministic and can be regenerated at the receiver. Consequently, it can be removed from the received signal. This approach was combined with the multistage approach in Varanasi and Aazhang (1990) to form the multi-stage successive interference cancelling (MSIC) receiver (Kawabe et al., 1993 and Mowbray et al., 1993). However, the analyses in Kawabe et al. (1993) and Mowbray et al. (1993) assumed a stationary channel. The performance of MSIC on a flat fading channel was considered in Yoon et al. (1993) and analysis with noncoherent M-ary orthogonal modulation and power control in frequency selective fading channel with power control was presented in Patel and

Holtzman (1994). Estimation of the channel parameters which is critical to a successful and practical successive interference cancellation scheme is only addressed in Patel and Holtzman (1994) which uses data based channel estimation. Unfortunately, at low SIR's and fast fading, data based estimates are not sufficiently reliable (Ling, 1993).

An analysis of a MSIC receiver with reference symbol assisted channel estimation for direct sequence CDMA communications is presented here. The availability of reliable channel estimates makes coherent detection possible. A brief description and analysis of the system are given in Section 3.2. Single cell analysis in Section 3.3 will show that although the transmission of reference symbols by itself causes a loss of traffic capacity, multi-user interference cancellation using channel estimates obtained from the received reference symbols more than compensates for that loss and results in the overall traffic capacity gain. We will also answer several optimization questions arising in the context of the system's implementation. An improved transmitted signal structure and its effect on traffic capacity will be discussed in Section 3.4. Multi-cell performance is considered in Section 3.5. Section 3.6 will conclude the chapter.

3.2 System description and analysis

The block diagram of the transmitter and receiver is given in Figure 3.1. The multi-user interference cancellation algorithm is shown in Figure 3.2. After the detection of each users' signal, the algorithm reconstructs multi-user interference given the following: (a) incoming signal and its timing, (b) signal modulation scheme, (c) channel transfer function, and (d) spreading sequence. The reconstructed signal is then subtracted from the
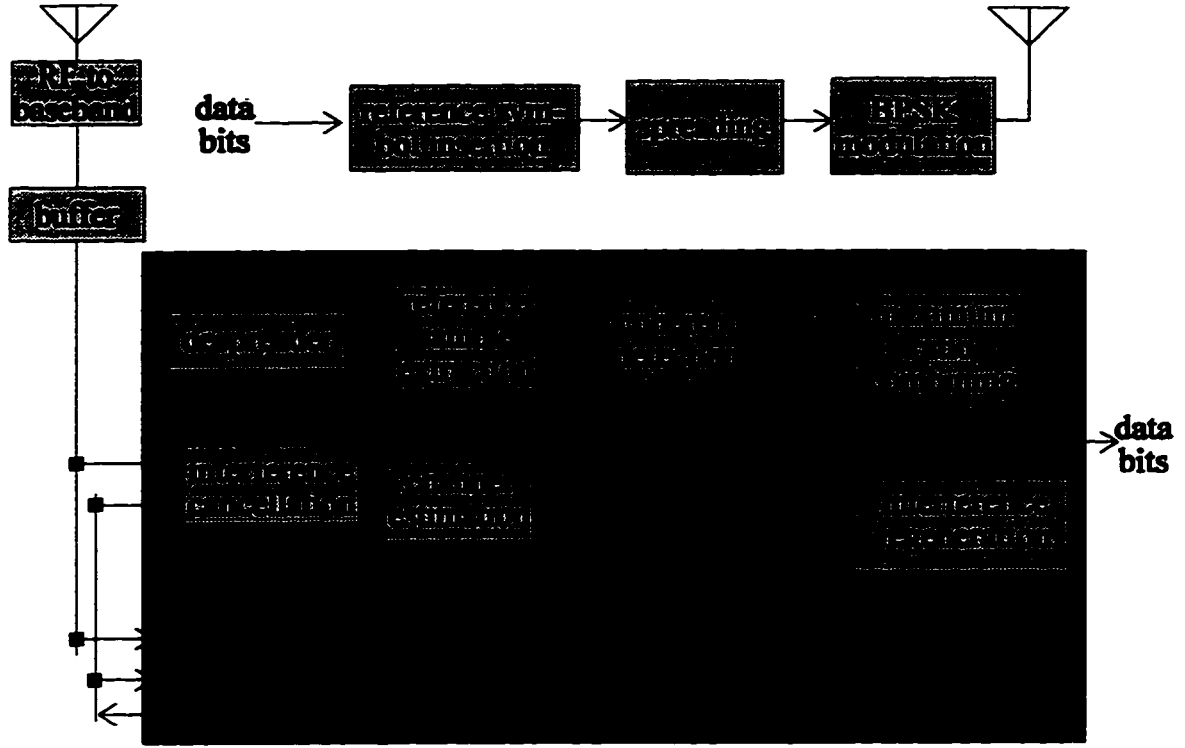
Fig. 3.1. A block diagram of the transmitter and receiver.

composite received signal to remove the multi-user interference caused by this user. The algorithm then continues to detect the next user's signal. Each user's signal is thus detected sequentually and each user's multi-user interference is cancelled successively.

Consider a system containing M mobile users in a cell. The signal transmitted by each user propagates through a frequency selective multipath Rayleigh fading channel. The baseband equivalent representation of the signal transmitted by the m-th user is

$$s_m(t) = \sqrt{2P_m}\; d_m(t)c_m(t)\exp[j\theta_m] \qquad (3.1)$$

where $d_m(t)$ is the data waveform with reference symbols inserted, $c_m(t)$ is the spreading waveform and θ_m is the phase of the carrier. Each pulse of $d_m(t)$ has a duration of T_s, the symbol duration. The spreading waveform is of the form
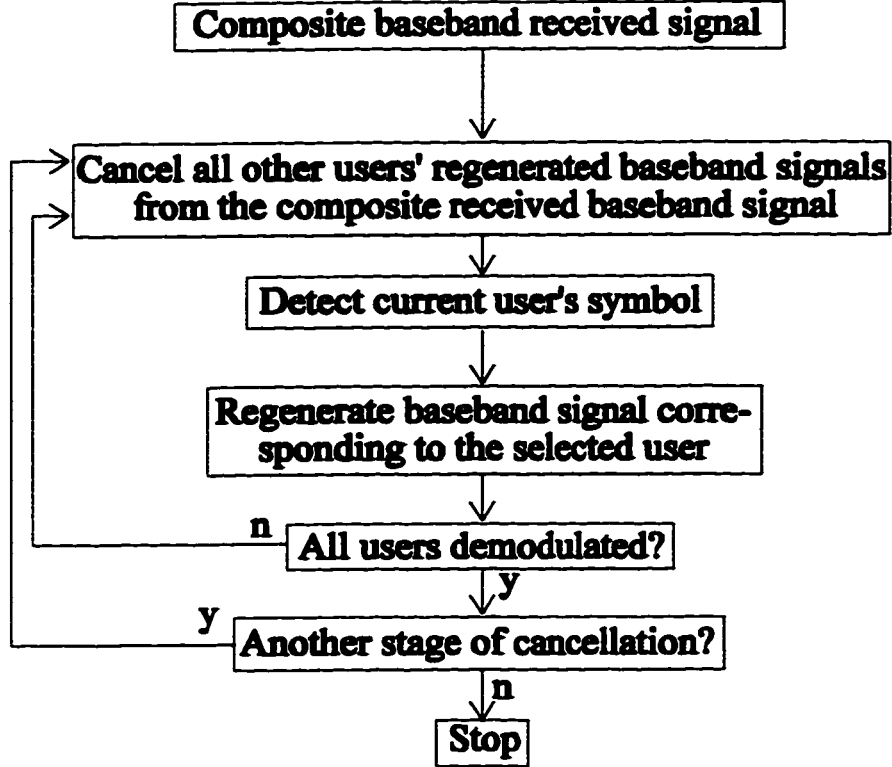
Fig. 3.2. Signal flow diagram of the interference cancellation scheme.

$$c_m(t) = \sum_{i=-\infty}^{\infty} c_{m,i} \, \psi(t - iT_c) \tag{3.2}$$

where $c_{m,i}$ is a member of the binary pseudorandom sequence $\{c_{m,i}\}$ which can take on values of ± 1; $\psi(t)$ is the chip pulse of duration T_c ($T_c \ll T_s$). Without loss of generality we will assume that the energy of the chip waveform is normalized as follows:

$$\int_0^{T_c} \psi^2(t) \, dt = T_c \quad . \tag{3.3}$$

The baseband equivalent representation of the composite received signal at the base station is:

$$r(t) = \sum_{m=1}^{M} \sum_{l=1}^{L} a_{m,l}(t) \, s_m(t - \tau_{m,l}) + n(t) \tag{3.4}$$

which is the sum of the signals transmitted by all users convolved with the channel transfer function and corrupted by Gaussian noise. The function $a_{m,l}(t)$ is the complex channel gain and $\tau_{m,l}$ is the propagation delay for the l-th path of the m-th user's received signal. We have assumed here that the total number of significant paths, L, is the same for all users. The background noise $n(t)$ is modelled as a zero mean complex white Gaussian noise with two-sided power spectral density $N_0/2$. A RAKE structure is employed at the receiver for time diversity combining and to facilitate the reconstruction of multipath signals received from all users.

The novel approach being investigated in this paper is multi-stage successive interference cancellation (MSIC) using reference symbol assisted channel estimates. The use of reference (or pilot) symbol based channel estimation for coherent detection has been previously proposed for direct sequence CDMA systems operating in frequency selective multipath fading environment (Ling, 1993) and (D'Amours et al., 1993). These two contributions demonstrated that channel estimation for a frequency selective fading environment was possible and hinted at the possibility of its application in successive interference cancellation receivers.

Reference symbols may be inserted in blocks or be uniformly distributed in the data stream. Block insertion is not suitable for time-variant channels because effective tracking of the channel parameters over long interval between reference blocks may not be possible. It is better to insert reference symbols periodically throughout the data stream because that approach allows for better tracking (Ling, 1993).

Reference symbol based channel estimation can be described as follows. A reference

symbol that is known to the receiver is inserted into a sequence of information bearing data symbols after every Q data symbols. The received signal samples corresponding to the reference symbols are then correlated with the known reference symbol to obtain unbiased but noisy channel estimates. These channel estimates do not have a phase ambiguity because no detection errors are made. The variance of the noise contaminating the estimates can be reduced somewhat by passing the noisy estimates through a properly designed filter. It is well known that an optimal unbiased channel estimate in the least-squared-error sense is obtained by passing the noisy estimates through a Wiener filter whose transfer function is equal to the Doppler spectrum of the channel divided by the sum of the Doppler spectrum of the channel and the spectrum of the noise contaminating the channel estimate (Papoulis, 1965). Since it may often be difficult to implement the Wiener filter, a suboptimum but practical solution is to use a fixed, linear phase, digital low pass filter whose cutoff frequency is greater than or equal to the maximum possible Doppler frequency (Ling, 1993). This process removes the high frequency noise components and the resulting channel estimates are relatively noise free and may be used for coherent detection.

The above estimation process, however, only produces a channel estimate at every t = $(Q+1)T_s$, and interpolation is necessary to obtain channel estimates for every symbol if coherent detection is to be used. Many interpolation methods exist in the literature. However, when $(Q+1)T_s$ is short relative to the channel coherence time, a simple but effective approach is linear interpolation (Ling, 1993).

Any practical low pass filter used to improve channel estimates will have a finite

delay. This delay will most likely be the dominant delay in the system. For example, with an information bit rate of 9600 bits/s, Q = 12 and a 25 tap FIR filter, the delay will be a little less than 15 ms. Therefore, enough memory must be present in the system to buffer 15 ms of the received signal.

Insertion of reference symbols separates the data stream into blocks. In a quasi-synchronous system, where the reference symbols from each user arrive within one symbol time of each other, a receiver that detects an entire block of data before interference regeneration performs better than a receiver (e.g. that considered in Yoon *et al.* (1993)) that regenerates interference after the detection of each data symbol. This is because in the latter case, multi-user interference from the next data symbol cannot be regenerated, since it has not yet been detected. In the former case, the next symbol is a reference symbol which is known to the receiver.

After n-1 stages of cancellation of all interfering multipath signals, and after cancelling the multipath signal of the j-th user in the n-th stage, the decision variable in the k-th demodulator of the RAKE receiver, detecting the k-th path of the j+1 user, can be expressed as follows:

$$D_{j+1,k}^{(n)} = \frac{1}{T_s} \int_{\tau_{j+1,k}}^{\tau_{j+1,k}+T_s} \hat{A}_{j+1,k}^*(t) \hat{r}_{j+1}^{(n)}(t) c_{j+1}(t - \tau_{j+1,k}) \, dt$$

$$\approx \left| A_{j+1,k} \right|^2 d_m + N_{j+1,k}^{(n)} A_{j+1,k}^* \tag{3.5}$$

where

$$\hat{r}_{j+1}^{(n)}(t) = r(t) - \sum_{m=1}^{j} \hat{s}_m^{(n)}(t) - \sum_{m=j+2}^{M} \hat{s}_m^{(n-1)}(t) \quad ,$$

$$\hat{A}_{m,l}(t) = A_{m,l}(t) + n_{a,m,l}(t) \quad ,$$

$$A_{m,l}(t) = a_{m,l}(t)\sqrt{2P_m}\exp\left[j\theta_{m,l}\right] \quad,$$

$\hat{s}_m^{(n)}(t)$ is the baseband regenerated signal for the m-th user after n stages of cancellation, P_m is the average power of the m-th user, $\theta_{m,l}$ is the carrier phase and $n_{a,m,l}$ is the noise corrupting the channel estimate $\hat{A}_{m,l}$. Equation (3.5) is approximate because we assumed that the second order noise terms are negligible and that the channel parameters are constant over one symbol interval. Furthermore, since we can, without lost of generality, analyze the symbol transmitted at $t = 0$, the dependency on time has been dropped in equation (3.5) for notational simplicity. The noise term $N_{j+1,k}^{(n)}$ contaminating the decision variable, is given by:

$$N_{j+1,k}^{(n)} = \left[\left(1+\frac{1}{Q}\right)\left(1+\frac{2f_{cutoff}}{f_r}\right)\right]^{\frac{1}{2}} \times$$

$$\left\{\sum_{m=j+2}^{M}\sum_{l=1}^{L} N_{m,l}^{(n-1)}\frac{I_{m,l;j+1,k}}{T_s} + \sum_{\substack{l=1\\l\neq k}}^{L} A_{j+1,l}\frac{I_{j+1,l;j+1,k}}{T_s} - \sum_{m=1}^{j}\sum_{l=1}^{L} N_{m,l}^{(n)}\frac{I_{m,l;j+1,k}}{T_s} + N\right\} \quad (3.6)$$

where

$$I_{m,l;j,k} = \int_{\tau_{j,k}}^{T_s+\tau_{j,k}} d_{m,l}(t-\tau_{m,l})c_{m,l}(t-\tau_{m,l})c_{j,k}(t-\tau_{j,k})\,dt \quad,$$

f_r is the reference symbol insertion frequency, $f_{cut\text{-}off}$ is the cut off frequency of the low pass filter used to reduce the noise corrupting the channel estimate, Q is the number of data symbols after which a reference symbol is inserted and N represents the effect of the background noise on the decision variable. The first term in equation (3.6) is the noise enhancement factor due to channel estimation (Ling, 1993), and the other terms represent residual interference from the users that have not yet been cancelled in this stage, self

88

interference and residual interference from users that have been cancelled in this stage, respectively. It can be shown (see Appendix) that variance of $I_{m,l;j,k}$ is given by:

$$\text{VAR}(I_{m,l;j,k}) = G\left[R_{\psi}^2(\tilde{\tau}_{m,l;j,k}) + R_{\psi}^2(T_c - \tilde{\tau}_{m,l;j,k})\right] \qquad (3.7)$$

where,

$$\tilde{\tau}_{m,l;j,k} = (\tau_{m,l} - \tau_{j,k}) \bmod T_c,$$

and following (Pursley, 1981), the partial autocorrelation function for the chip waveform is defined as

$$R_{\psi}(s) = \int_0^s \psi(t)\psi(t - T_c - s)dt \quad 0 \le s < T_c \quad .$$

The variance of $N_{j+1,k}^{(n)}$, denoted by $\eta_{j+1,k}^{(n)}$, can then be written as:

$$\eta_{j+1,k}^{(n)} \approx \left[\left(1 + \frac{1}{Q}\right)\left(1 + \frac{2f_{cutoff}}{f_r}\right)\right]\left\{\sum_{m=j+2}^{M}\sum_{l=1}^{L}\frac{\eta_{m,l}^{(n-1)}}{2}\frac{\text{VAR}(I_{m,l;j,k})}{T_s^2} + \right.$$
$$\left. \sum_{\substack{l=1 \\ l \ne k}}^{L}\frac{|A_{j+1,l}|^2}{2}\frac{\text{VAR}(I_{j+1,l;j,k})}{T_s^2} + \sum_{m=1}^{j}\sum_{l=1}^{L}\frac{\eta_{m,l}^{(n)}}{2}\frac{\text{VAR}(I_{m,l;j,k})}{T_s^2} + \frac{N_0}{T_s}\right\} \quad . \qquad (3.8)$$

The signal to noise ratio, $\gamma_{j+1}^{(n)}$, after maximum ratio combining (Proakis, 1989) is

$$\gamma_{j+1}^{(n)} = \frac{\left|\sum_{k=1}^{L}|A_{j+1,k}|^2\right|^2}{\sum_{k=1}^{L}|A_{j+1,k}|^2\eta_{j+1,k}^{(n)}} \quad , \qquad (3.9)$$

and, for antipodal signals, the probability of a bit error becomes:

$$P_{j+1}^{(n)} = \frac{1}{2}\text{erfc}\left[\sqrt{\frac{1}{2}\gamma_{j+1}^{(n)}}\right] \quad . \qquad (3.10)$$

It should be noted that $P_{j+1}^{(n)}$ is a conditional probability conditioned on the path gains and

the partial autocorrelation function of the chip waveform. We will first remove the condition on the partial autocorrelation. This is usually done by integration. However, because of the complexity of the erfc function closed form solution of the intergral is not known and, therefore, numerical integration is necessary. A good approximate closed form solution, on the other hand, can be obtained by deriving an upper and lower bound on the error probability conditioned on the path gains and then approximating the conditional error probability with a function in between the bounds (Torrieri, 1992).

To obtain an upper bound on the error probability $P_{j+1}^{(n)}$ conditioned on the path gains, the following inequality (Torrieri, 1992) can be used

$$R_\psi^2(\tilde{\tau}_{m,l;j,k}) + R_\psi^2(T_c - \tilde{\tau}_{m,l;j,k}) \le T_c^2 \quad . \tag{3.11}$$

Therefore, the upper bound of conditional error probability can be obtained by substituting equations (3.11), (3.7), (3.8) and (3.9) into equation (3.10) to obtain

$$P_{j+1}^{(n)} < \frac{1}{2}\mathrm{erfc}\left[\frac{\sum_{k=1}^{L}|A_{j+1,k}|^2}{\left[2\sum_{k=1}^{L}|A_{j+1,k}|^2 \eta_{ub,j+1,k}^{(n)}\right]^{\frac{1}{2}}}\right] \quad , \tag{3.12}$$

where

$$\eta_{ub,j+1,k}^{(n)} = \left[\left(1+\frac{1}{Q}\right)\left(1+\frac{2f_{cutoff}}{f_r}\right)\right]\left\{\sum_{m=j+2}^{M}\sum_{l=1}^{L}\frac{\eta_{m,l}^{(n-1)}}{2G} + \sum_{\substack{l=1 \\ l\ne k}}^{L}\frac{|A_{j+1,l}|^2}{2G} + \sum_{m=1}^{j}\sum_{l=1}^{L}\frac{\eta_{m,l}^{(n)}}{2G} + \frac{N_0}{T_s}\right\}. \tag{3.13}$$

A lower bound on the error probability $P_{j+1}^{(n)}$ conditioned on the path gains is obtained by noting that the expectation of the even and odd correlation is (Torrieri, 1992)

$$\left\langle R_{\psi}^2(\tilde{\tau}_{m,l;j,k}) + R_{\psi}^2(T_c - \tilde{\tau}_{m,l;j,k}) \right\rangle = \frac{2}{3}T_c^2 \qquad (3.14)$$

for rectangular chip pulses, where $\langle x \rangle$ denotes expectation of x. Since Jensen's inequality (Royden, 1988) can be used to show that

$$\langle \mathrm{erfc}(x) \rangle \geq \mathrm{erfc}(\langle x \rangle) \quad ,$$

the lower bound can be expressed as

$$P_{j+1}^{(n)} \geq \frac{1}{2}\mathrm{erfc}\left[\frac{\sum_{k=1}^{L}\left|A_{j+1,k}\right|^2}{\left[2\sum_{k=1}^{L}\left|A_{j+1,k}\right|^2 \left\langle \eta_{j+1,k}^{(n)} \right\rangle \right]^{\frac{1}{2}}} \right] , \qquad (3.15)$$

where

$$\left\langle \eta_{j+1,k}^{(n)} \right\rangle = \left[\left(1+\frac{1}{Q}\right)\left(1+\frac{2f_{cutoff}}{f_r}\right) \right]\left\{ \sum_{m=j+2}^{M}\sum_{l=1}^{L}\frac{\eta_{m,l}^{(n-1)}}{3G} + \sum_{\substack{l=1 \\ l \neq k}}^{L}\frac{\left|A_{j+1,l}\right|^2}{3G} + \sum_{m=1}^{j}\sum_{l=1}^{L}\frac{\eta_{m,l}^{(n)}}{3G} + \frac{N_0}{T_s} \right\} ,(3.16)$$

by substituting equation (3.14), (3.7), (3.8) and (3.9) into equation (3.10).

A better approximation of the conditional error probability $P_{j+1}^{(n)}$ can be obtained by noting that the difference between the upper and lower bound is in the interference terms of η. Therefore a reasonable approximation is obtained by substituting into equation (3.8) the geometric average of the interference terms in equation (3.13) and (3.16) to obtain

$$P_{j+1}^{(n)} \approx \frac{1}{2}\mathrm{erfc}\left[\frac{\sum_{k=1}^{L}\left|A_{j+1,k}\right|^2}{\left[2\sum_{k=1}^{L}\left|A_{j+1,k}\right|^2 \eta_{a,j+1,k}^{(n)} \right]^{\frac{1}{2}}} \right] , \qquad (3.17)$$

where

$$\eta^{(n)}_{a,j+1,k} = \left[\left(1+\frac{1}{Q}\right)\left(1+\frac{2f_{cutoff}}{f_r}\right)\right]\left\{\sum_{m=j+2}^{M}\sum_{l=1}^{L}\frac{\eta^{(n-1)}_{m,l}}{\sqrt{6}G} + \sum_{\substack{l=1 \\ l\neq k}}^{L}\frac{|A_{j+1,l}|^2}{\sqrt{6}G} + \sum_{m=1}^{j}\sum_{l=1}^{L}\frac{\eta^{(n)}_{m,l}}{\sqrt{6}G} + \frac{N_0}{T_s}\right\} \quad .(3.18)$$

The condition on the path gains can now be removed by taking the expectation of the conditional error probability over the path gains. An estimate of the average error probability can then be obtained by averaging the unconditional error probability over all users:

$$P^{(n)} = \left\langle P^{(n)}_{j+1}\right\rangle \approx \frac{1}{2}\left\langle \mathrm{erfc}\left[\frac{\sum_{k=1}^{L}|A_{j+1,k}|^2}{\left[2\sum_{k=1}^{L}|A_{j+1,k}|^2\eta^{(n)}_{a,j+1,k}\right]^{\frac{1}{2}}}\right]\right\rangle \quad . \tag{3.19}$$

3.3 Single cell performance

The above analysis gives an approximate measure of the receiver's performance. Extensive computer simulations have been carried out to obtain more accurate performance results, not burdened by simplifying assumptions which were necessary to obtain the analytical expressions of the previous section and to verify the accuracy of equation (3.19). In particular, instead of describing multi-user interference statistically, all other users' signals and hence residual interferences were simulated. The assumed information bit rate was 9600 bits/s, the chip rate of the system was 1.23 Mchips/s, the effect of shadowing and path loss was mitigated by open loop power control and the maximum Doppler frequency for each user was 100 Hz for all simulation results presented

in this paper. The Rayleigh fader used in these simulations is described in (Jakes, 1981). In order to account for the reduction in capacity due to the transmission of the reference symbol, the chip rate of the system was kept constant and the processing gain was changed accordingly for different values of Q. Figure 3.3 shows the performance of a reference symbol assisted coherent (RSAC) receiver on a flat fading channel with the particular low pass filter used. The reference symbol insertion parameter Q=7 was chosen from the design equation of (Ling, 1993) and was verified with simulations from Q = 2 to Q = 15. Computer simulation results showed that the performance of the receiver using unfiltered channel estimates was 5 dB worse than that using perfect channel estimates. This performance improved when filtering was applied to the estimates, except at high SNR's. Low pass filters were used to approximate the optimal Wiener filter. They were implemented as digital FIR filters with a Hamming window because of its favourable sidelobe response; however, computer simulation with other windowing functions resulted in very small differences in performance. Although not clearly evident in Figure 3.3, examination of the raw simulation results shows that as the SNR increases, the low-pass digital FIR filter approximates the optimal Wiener filter better and better, until it reaches a point of optimal approximation. Any increase in SNR after that point results in gradually deteriorating performance. This is because under high SNR conditions there is very little noise in the unfiltered channel estimate and the estimation errors due to ripples in the pass band of the low pass filter more than offset the gain of noise suppression in the stop band of the filter. The point where the digital FIR filter optimally approximates the Wiener filter can be adjusted by changing the cutoff frequency of the filter. We have simulated the

93
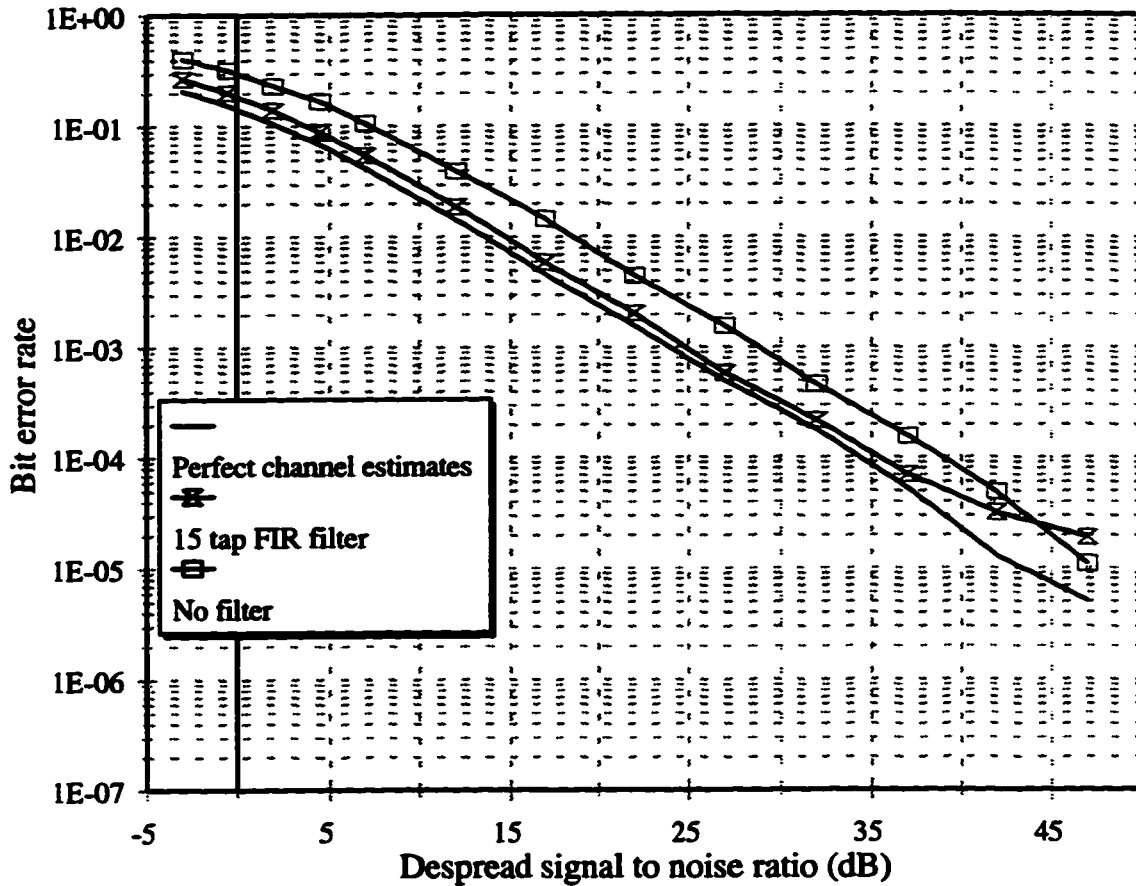
Fig. 3.3. Performance of a reference symbol assisted coherent detector with and without low pass filtering operating in a flat Rayleigh fading environment. The filter has f_{cutoff} = 225 Hz and was designed with the Hamming window.

performance of the receiver with many cutoff frequencies and have chosen the one with the best performance. Nevertheless we can conclude that, in general, the reference assisted coherent receiver with low pass filtering performed approximately only 1.5 dB worse than the ideal coherent detector.

The performance of the RSAC receiver on a frequency selective fading channel is shown in Figure 3.4. A three path channel model is used where the energy of successive paths decays exponentially (0, -2, -4 dB), and all three paths are perfectly tracked by the RAKE receiver. The performance of the receiver, using the low pass filter of Figure 3.3, is
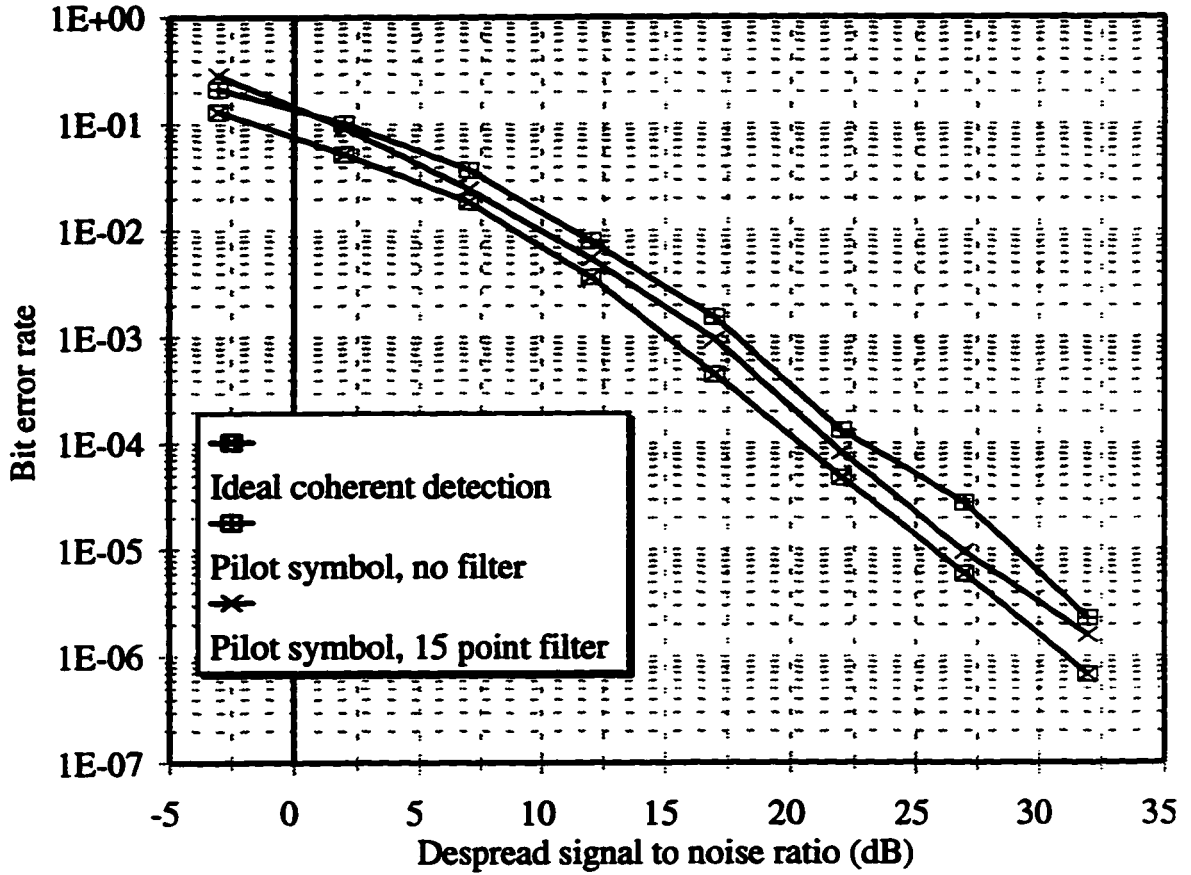
Fig. 3.4. The performance of pilot symbol assisted coherent detector with and without low pass filtering and an ideal coherent receiver in frequency selective Rayleigh fading environment.

approximately 1.5 dB worse, while that with no low pass filtering is approximately 2.5 dB worse than that of the coherent receiver using perfect channel estimates.

The single cell multi-user performance of RSAC receiver and that of a coherent receiver using perfect channel information (which we call an ideal coherent receiver) on a flat fading channel with no AWGN is shown in Figure 3.5. The low pass filter of Figure 3.3 is used to reduce noise in the channel estimates. The performance decrease due to reference symbol assisted channel estimation is evident. The number of simultaneous users decreases from 4 to 3 for a BER of 10^{-3}.
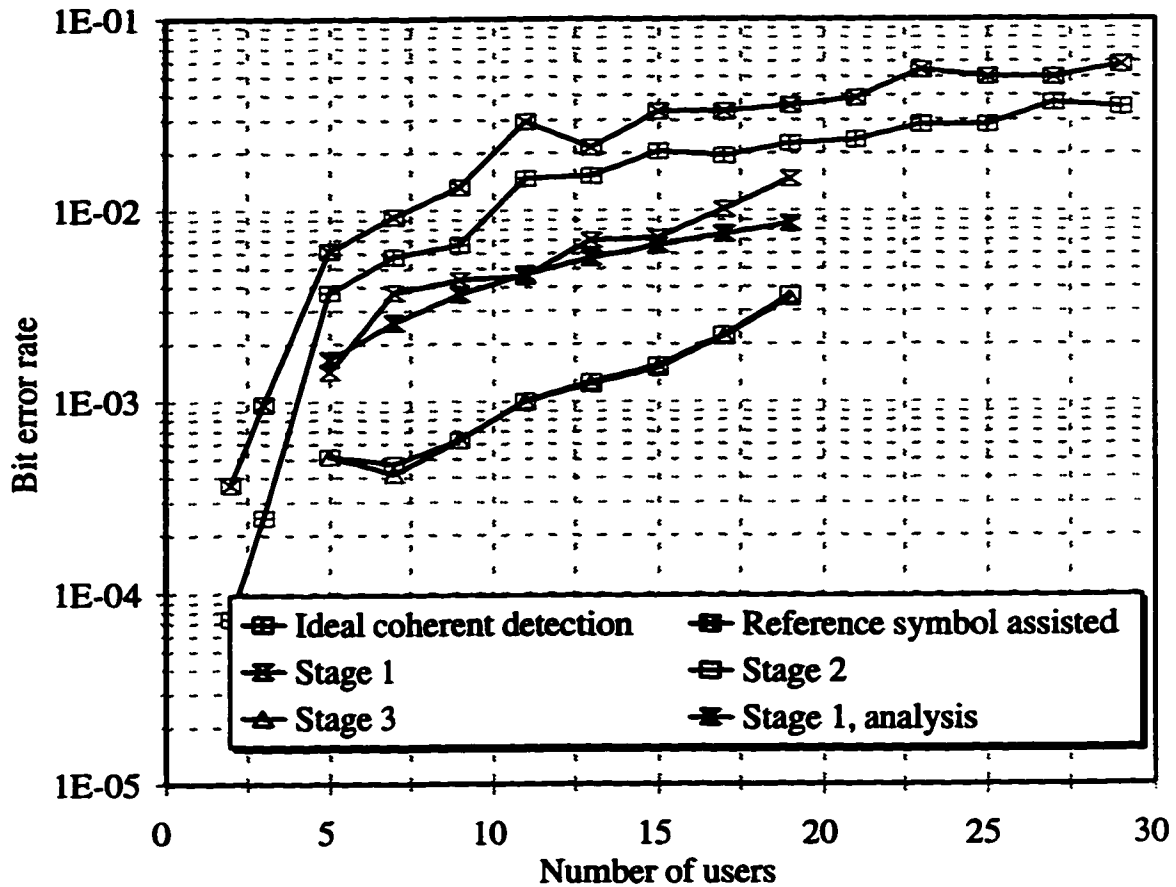
Fig 3.5. The multiuser performance of an ideal coherent matched filter receiver, a RSAC receiver and a RAMSIC receiver in flat Rayleigh fading environment. The results from analysis as well as simulations are presented.

Figure 3.5 also shows the performance of the reference symbol assisted multistage successive interference cancelling (RAMSIC) receiver on a flat fading channel operating in a single cell environment. For a BER of 10^{-3}, the number of simultaneous users is 11. This represents a substantial improvement over the non-interference cancelling receiver which is not capable of supporting more than 3 users at a BER of 10^{-3}. It can also be seen from the figure that there is very little to be gained with more than two stages of successive interference cancellation.

Performance of the receiver determined from (3.19) is likewise shown in Figure 3.5.

It can be seen that the simulation and analytical results agree very closely after one stage of cancellation. After more than one stage of cancellation, however, the results of the analytical performance evaluation are much too optimistic. This is because in the derivation of the closed form expression for the error probability, the effect of detection errors on interference cancellation was not taken into account. If the detection errors are taken into account, the distribution of $N_{j+1,t}^{(n)}$ is no longer Gaussian, but rather asymmetrically contaminated Gaussian. It, therefore, must be analyzed using methods of
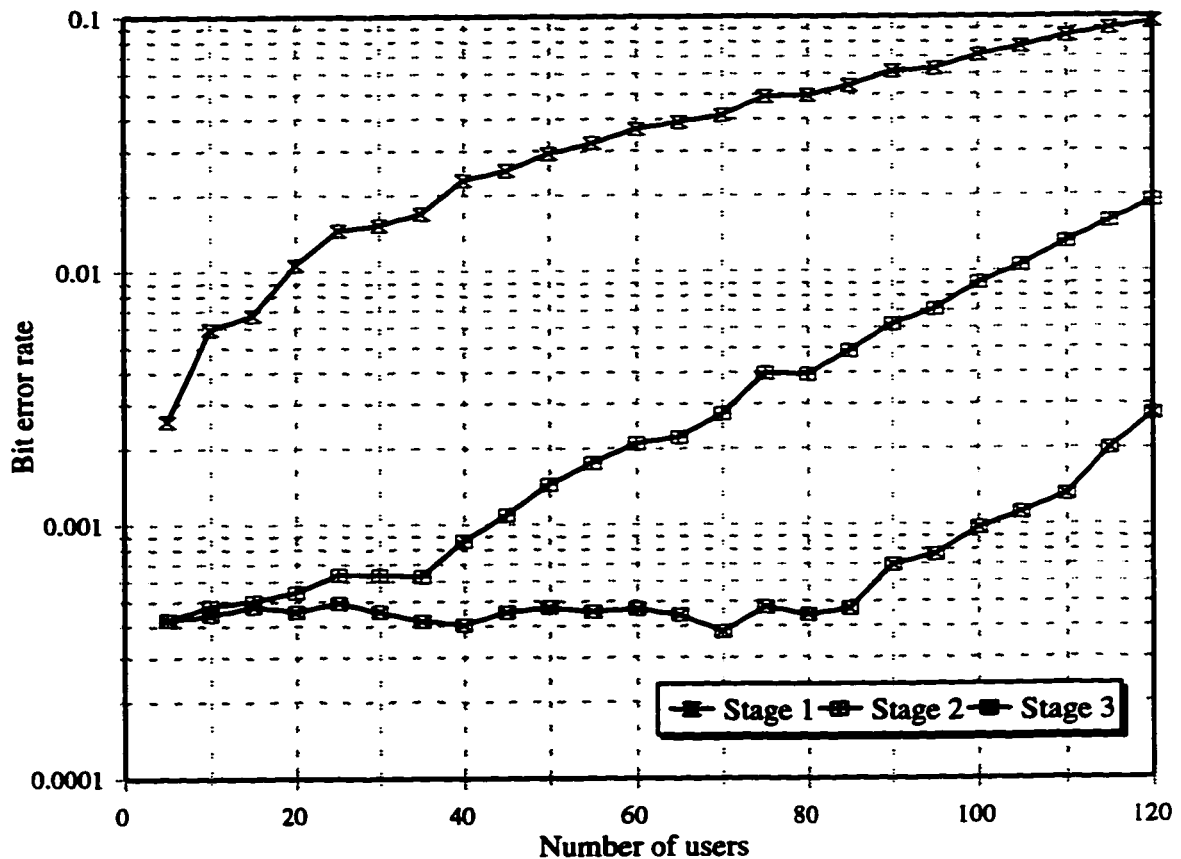

Fig. 3.6. The performance of an ideal coherent SIC receiver. The spreading gain is 128.

robust statistics (Huber, 1981), which involve quite unwieldy mathematics. Moreover, since the run time of the program to evaluate (3.19) is about the same as that of the simulation, further investigation will be made purely by simulations.

Figure 3.6 shows the performance of a coherent successive interference cancelling (SIC) receiver on a flat Rayleigh fading channel using perfect channel information. It can be seen from the figure that the capacity of the system increases with the number of cancellation stages. At the bit error rate (BER) of 10^{-3}, the maximum number of users of the system with 3 stages of cancellation is 100. This is approximately 7.7 times the maximum number of users with the RAMSIC receiver.

3.4 Performance with improved channel estimates

The results in Figures 3.5 and 3.6 demonstrated that the performance of a RAMSIC receiver is less than satisfactory. The poor performance is due to the channel estimates being significantly corrupted by interference from symbols that have not yet been demodulated and cancelled by the receiver. We propose, in this section, some modifications to the transmitted signal structure that will decrease the noise contaminating the channel estimates. In particular, instead of transmitting information symbols immediately before and after the transmission of the reference symbol, we propose to turn the transmitter off during the respective intervals. In other words, the transmitter will turn itself off (or reduce its power below the background noise) for one symbol interval immediately before and immediately after the transmission of a reference symbol. Consequently, in a quasi-synchronous system in which the reference symbols from all

users arrive within one symbol interval of each other, the channel estimates will no longer be corrupted by interference from the information bearing symbols. Interference from other users' reference symbols, on the other hand, is minimized by the interference cancellation scheme. The transmitter gating mechanism employed in the scheme is in itself identical to the one used in the IS-95 system to reduce transmitted power whenever the output bit rate of the variable bit rate voice encoder is reduced.

The performance of a RAMSIC receiver with the improved transmitted signal structure is shown in Figure 3.7. The reference symbol insertion parameter, Q, is 12. This
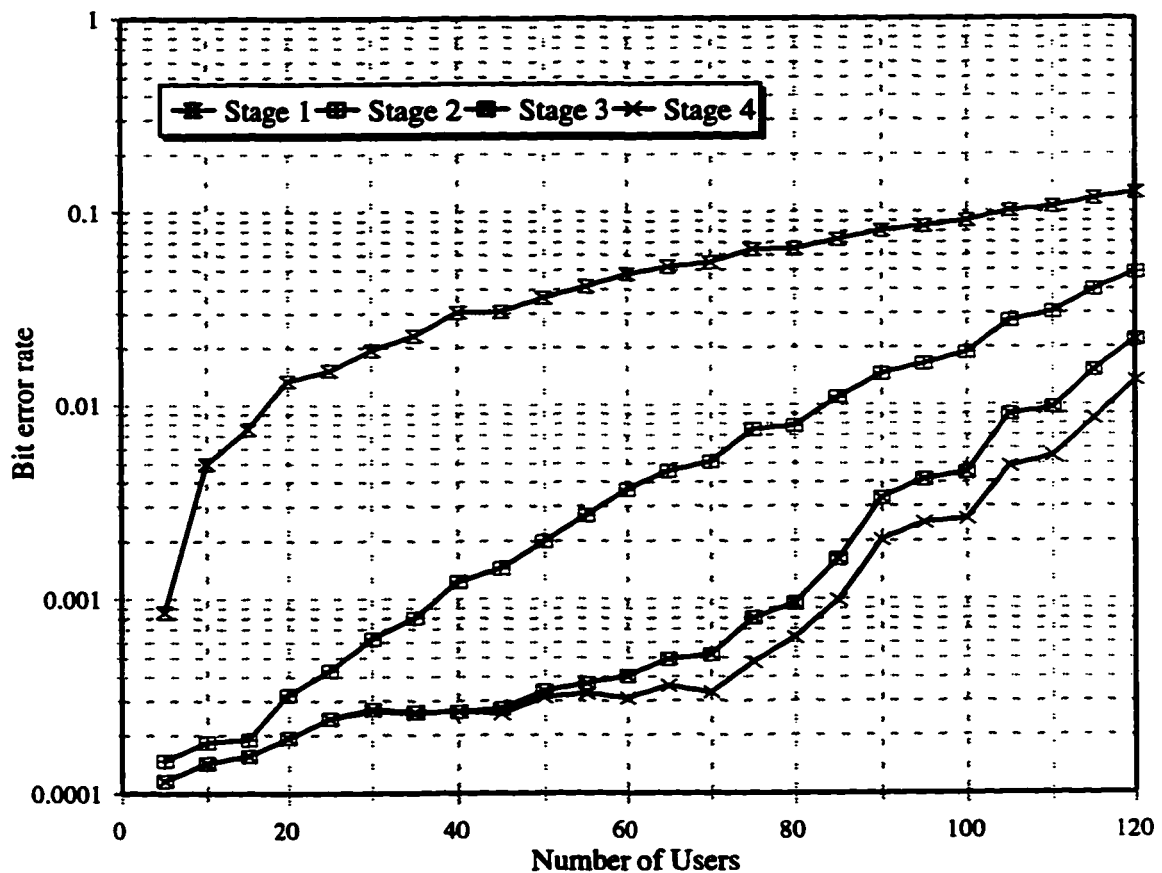

Fig. 3.7. The performance of a RAMSIC receiver on a flat Rayleigh fading channel with no AWGN. The transmitter is turned off for one symbol interval before and after the transmission of the reference symbol.

rate was chosen because it was predicted to give the best performance by the design equation in (Ling, 1993) and was verified by simulation. The capacity of the system increases when the number of the cancellation stages is increased. It should be noted, however, that increasing the number of cancellation stages from 3 to 4 results in marginal capacity increase. We can, therefore, conclude that increasing the number of stages of cancellation beyond 3 is not necessary. It can also be seen from the figure that for a BER of 10^{-3}, the maximum number of users in the system is approximately 80. Comparing this result with that from Figure 3.6, we see that it represents approximately 80% of the capacity of the ideal coherent SIC receiver (using perfect channel parameters). Comparison with the results from Figure 3.5, in which the maximum number of simultaneous users is 11, reveals that the RAMSIC receiver with the proposed transmitted signal structure increases the capacity of the system 7.27 times.

The performance of the ideal coherent SIC receiver on a frequency selective Rayleigh fading channel is shown in Figure 3.8. A channel model consisting of three independent Rayleigh fading paths of exponentially decaying average powers (0, -2, -4 dB) is used. All three paths are assumed to be perfectly tracked by the RAKE receiver. The maximum number of users with 3 stages of cancellation for a BER of 10^{-3} is 53. This is less than that for the flat Rayleigh fading channel because the additional paths introduce more residual cancellation noise on the decision variable.

Figure 3.8 also illustrates performance of the RAMSIC receiver with the improved transmitted signal structure on a frequency selective fading channel. Because self interference is now contributing significantly to the noise contaminating the channel

100

estimate, a 25 tap Hamming windowed low pass filter is used to reduce the noise of the channel estimates. Figure 3.8 shows that performance of the system improves with the addition of each stage of interference cancellation. However, it is also evident that very little capacity gain is obtained by increasing the number of cancellation stages from 3 to 4. The maximum number of simultaneous users for a bit error rate of 10^{-3} is approximately 41 with 3 stages, and 43 with 4 stages of interference cancellation, which represents approximately 80% of the capacity of the ideal coherent SIC receiver. These results can be compared to the results in Patel and Holtzman (1994) where the capacity was 29 simultaneous users with imperfect fast power control using 64-ary orthogonal modulation. It should be noted that the results in Patel and Holtzman (1994) were obtained with a spreading gain of 42.66 in order for the results to be applicable to the DS-CDMA system of Gilhousen *et al.* (1991) which uses a 1/3 rate convolutional encoder. In order to directly compare with the results presented here, the spreading gain must be increased by a factor of three. Assuming that increasing the spreading gain by a factor of three results in a three fold increase in capacity, the equivalent number of simultaneous users in Patel and Holtzman (1994) is 87. This would at first seem to be much better than the capacity reported here. However, the capacity of the system investigated here can be increased if QPSK modulation is used (see Chapter 4). Moreover, because Patel and Holtzman (1994) considered a power controlled system, its channel is effectively lognormal, and therefore it is much more benign than the frequency selective Rayleigh fading channel considered here.
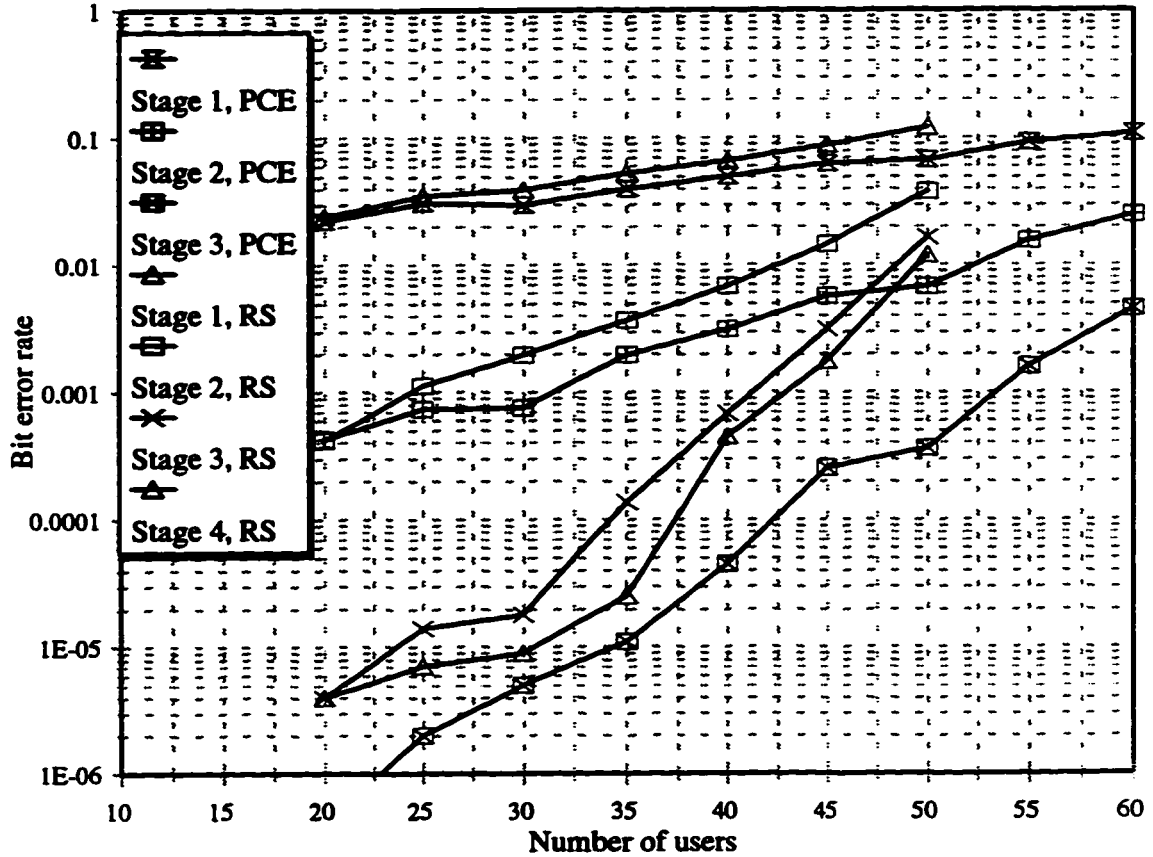
Fig. 3.8. The performance of a coherent SIC receiver using perfect channel estimates (PCE) and a RAMSIC receiver (RS) on a frequency selective fading channel. The spreading gain is 128 for the receiver using PCE and 114 for the RAMSIC receiver. The reference insertion parameter Q = 12 was used and the transmitter was turned off for one symbol interval immediately before and after the reference symbol to improve the performance of the RAMSIC receiver.

3.5 Multi-cell Simulations

The foregoing analysis gives the receiver's performance in a single cell environment. Multi-cell performance of the receiver will be determined in this section. We have assumed that the noise term is dominated by intercellular interference and that the background thermal noise is negligible. Furthermore, the intercellular interference will be modelled as a zero mean complex white Gaussian noise process with power spectral density $N_0/2$. We

have chosen to approximate the intercellular interference as a Gaussian process on the basis of a central limit theorem argument. This argument is valid for intercell interference because, unlike for intracell interference, a large number of users is involved. Equation (3.19) may still be used to give an approximation to the bit error rate if the noise enhancement factor due to channel estimation in equation (3.18) is modified to

$$\left[\left(1+\frac{3}{Q}\right)\left(1+\frac{2f_{cutoff}}{f_r}\right)\right]$$ (3.20)

in order to account for the decrease in capacity due to the modified transmitted signal structure. The term N_0/T_s in (3.18) now represents the intercellular interference which can be expressed as a function of intracellular interference as follows:

$$\frac{N_0}{T_s} = f\left\{(M-1)\sum_{l=1}^{L}\frac{A_l^2}{\sqrt{6G}} + \sum_{\substack{l=1\\l\neq k}}^{L}\frac{A_l^2}{\sqrt{6G}}\right\}$$ (3.21)

where A_l^2 is the expected value of $\langle|A_{m,l}|^2\rangle$ over all possible M users, f is the intercellular to intracellular interference ratio. The terms within the braces represent the average intracellular interference without interference cancellation which can be obtained from the first two terms within the braces of equation (3.18) before interference cancellation. The first term in the braces represents multi-user interference and the second term represents self interference. However, because of the approximate nature of equation (3.19), investigation of multi-cell performance will involve only computer simulations. Imperfect closed loop power control will be modelled as a lognormal variable (Viterbi et al., 1993) in these simulations.

103

Figure 3.9 shows the performance of the RAMSIC receiver with perfect power control on a Rayleigh flat fading channel. The intercellular to intracellular interference ratio, $f = 0.55$ has been assumed, which corresponds to the value given in Milstein and Rappaport (1992) for hexagonal cell geometry with radius of 2 miles and path loss exponent of 4. The pilot insertion parameter $Q = 4$ has been chosen, because after simulation with various rates it gives the best performance. This value is not predicted by the design equations in (Ling, 1993), because error in the interpolation, which was not
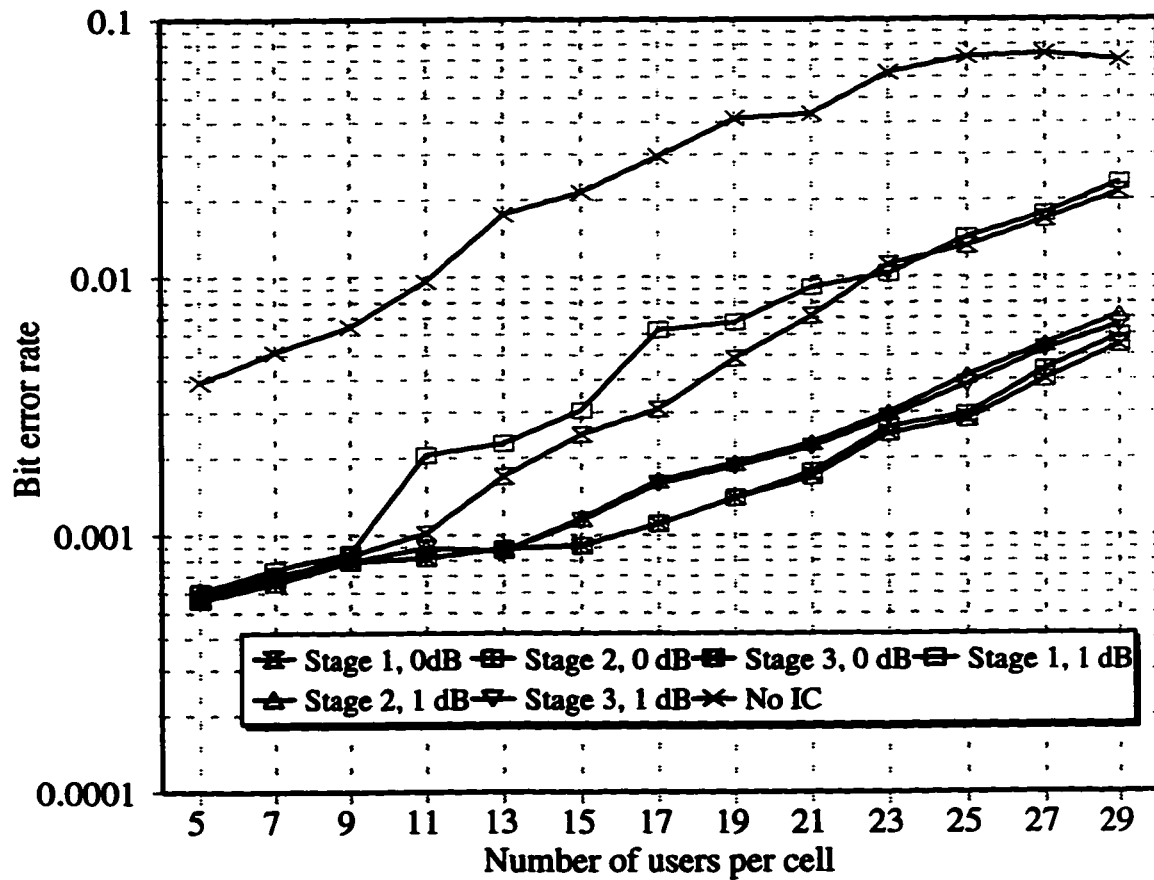

Fig. 3.9. Multi-cell performance of a RAMSIC receiver with perfect power control and imperfect power control with 1 dB standard deviation on a flat Rayleigh fading channel; hexagonal cells, f=0.55.

104

accounted for in the design equations, now causes significant errors in the channel estimates. A 31 tap FIR filter is used to reduce noise in the channel estimates. It can be seen from the figure that increasing the number of cancellation stages beyond 2 will not result in any increase in capacity. At the bit error rate (BER) of 10^{-3} the maximum number of users per cell is 16. Performance with imperfect power control with standard deviation of 1dB is also shown in Figure 3.9. The capacity of the system is reduced and the maximum number of users for a BER of 10^{-3} is now 14 per cell. This compares very favourably with the capacity of 18 users per cell in the system described in Gilhousen *et al.* (1991), when voice activity is not accounted for. Therefore, we can conclude that capacity of the DS-CDMA system with a RAMSIC receiver, biphase spreading and without any forward error correction coding is 0.78 times that in Gilhousen *et al.* (1991).

The performance of the RAMSIC receiver with perfect power control, hexagonal cell geometry and path loss exponent of 4 on a frequency selective Rayleigh fading channel is shown in Figure 3.10. A channel model consisting of three independent paths, where the energy of successive paths decays exponentially (0, -2, -4 dB), is used. All 3 paths are assumed to be perfectly tracked by a RAKE receiver. The optimal reference symbol insertion parameter $Q = 12$, as determined in the previous section, is used. The effective spreading gain is 102 which results in a chip rate of 1.23 Mchips/s. A 25 tap FIR filter is used to reduce the noise on the channel estimates. It can be seen from the figure that increasing the number of cancellation stages beyond 2 does not increase the capacity of the system. For a BER of 10^{-3}, the maximum number of users is 23 per cell. The performance of the same system using imperfect power control with standard deviation of
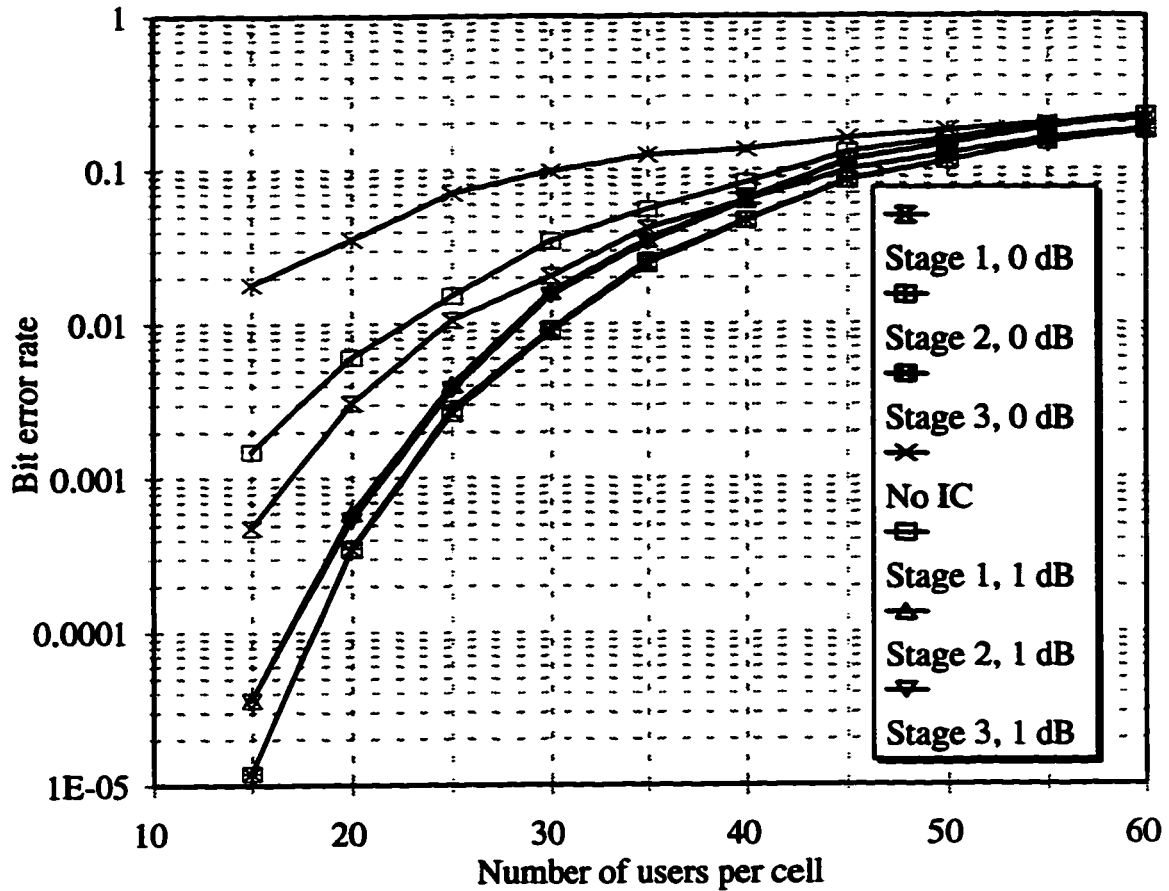
Fig. 3.10. Multi-cell performance of a RAMSIC receiver with perfect power control and imperfect power control of 1 dB standard deviation on a frequency selective Rayleigh fading channel; hexagonal cells, f=0.55.

1 dB is also shown in Figure 3.10. For BER of 10^{-3}, the capacity of the system drops to 22 users per cell. Hence, even without powerful forward error correction coding, capacity 1.22 times that of the system in Gilhousen *et al.* (1991) can be achieved.

The multi-cell capacity of the system, unlike that for a single cell, is greater with the frequency selective Rayleigh fading channel than with the flat Rayleigh fading channel. This is because, in the flat fading case, power control causes rapid changes in the real and imaginary part of the complex channel gain. This rate of change is very difficult for the

linear interpolator to track. As a result, interpolation error in the flat fading case is larger than the additional error caused by multiple paths in the frequency selective fading case.

Since the assumption of hexagonal cell configuration and path loss exponent of 4 may not be realistic, Figures 3.11, 3.12 and 3.13 demonstrate the performance of the
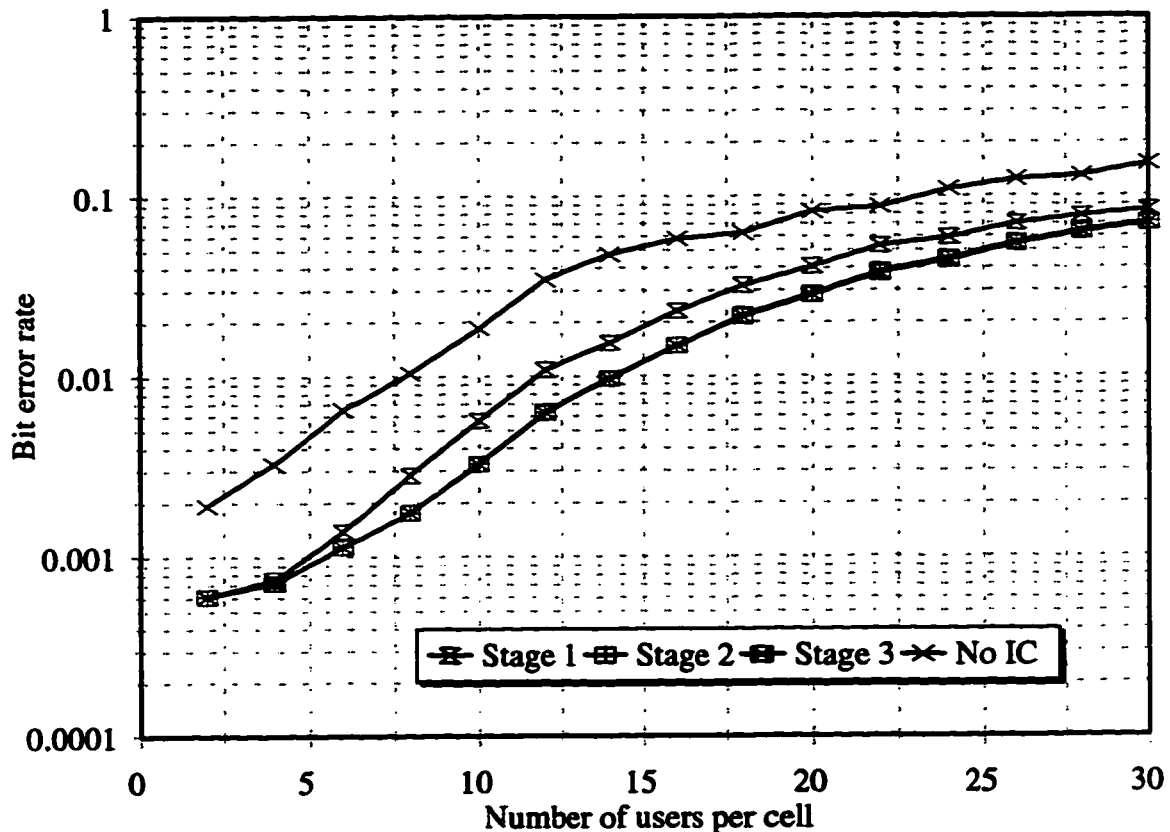

Fig. 3.11. Multi-cell performance of a RAMSIC receiver on a flat Rayleigh fading channel; nonideal cells, f=1.57, imperfect power control with 1dB standard deviation.

RAMSIC receiver on a Rayleigh flat fading channel with frequency reuse factors half way between the upper and lower bound in Milstein and Rappaport (1992), path loss exponents of 2, 3 and 4 (f = 1.57, 0.959 and 0.686) and power control error standard deviation of 1 dB. All other system parameters are as in Figure 3.9. The capacity of the

system decreases with the path loss exponent. For a BER of 10^{-3}, the maximum number of users per cell is 5, 8 and 11 for path loss exponent of 2, 3 and 4 respectively. This compares very favourably with the capacity of less than 1 user per cell without interference cancellation. The performance without cancellation is very poor because the channel estimates are highly corrupted by multi-user interference. Multistage cancellation only marginally increases capacity when the path loss exponent is 2 (Figure 3.11), but the increase is significant when the path loss exponent is greater than 2 (Figures 3.12 and 3.13). However, in all cases no capacity increase is obtained by increasing the number of cancellation stages beyond 2.
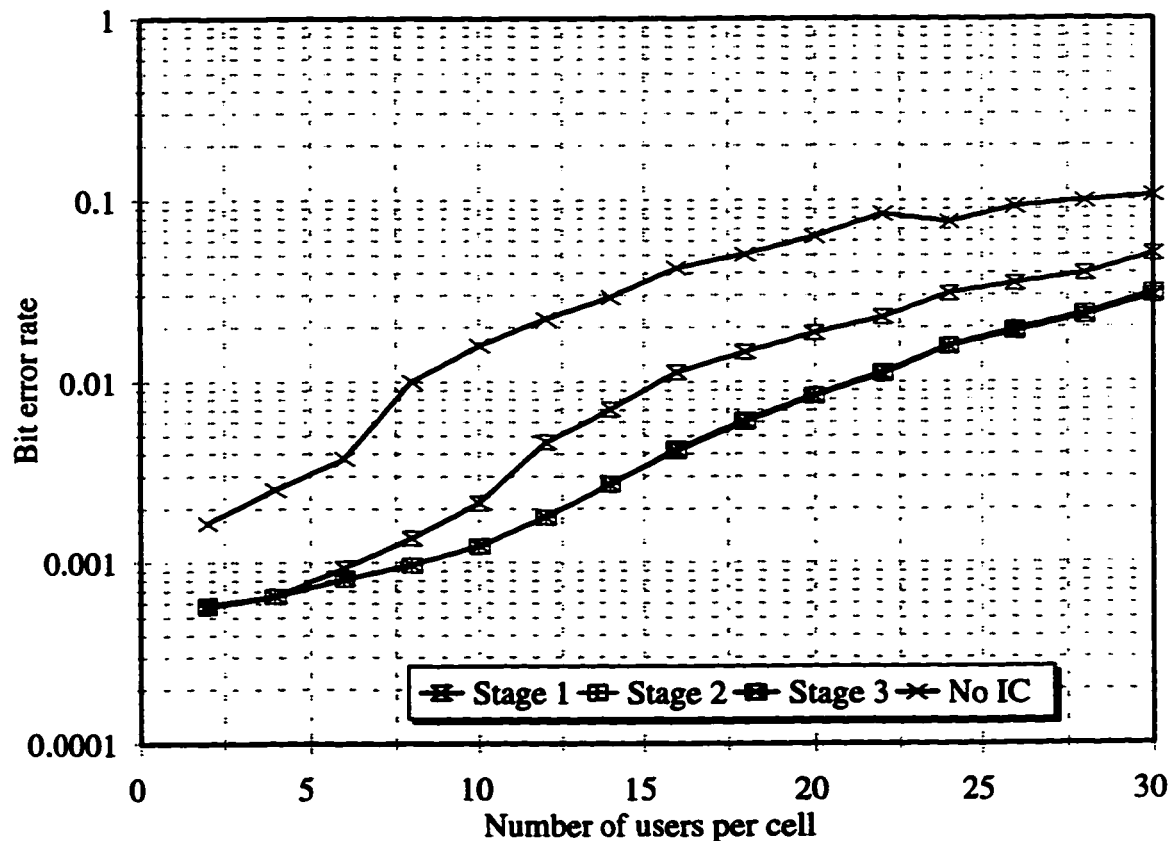

Fig. 3.12. Multi-cell performance of a RAMSIC receiver on a flat Rayleigh fading channel; nonideal cells, f=0.959, imperfect power control with 1dB standard deviation.
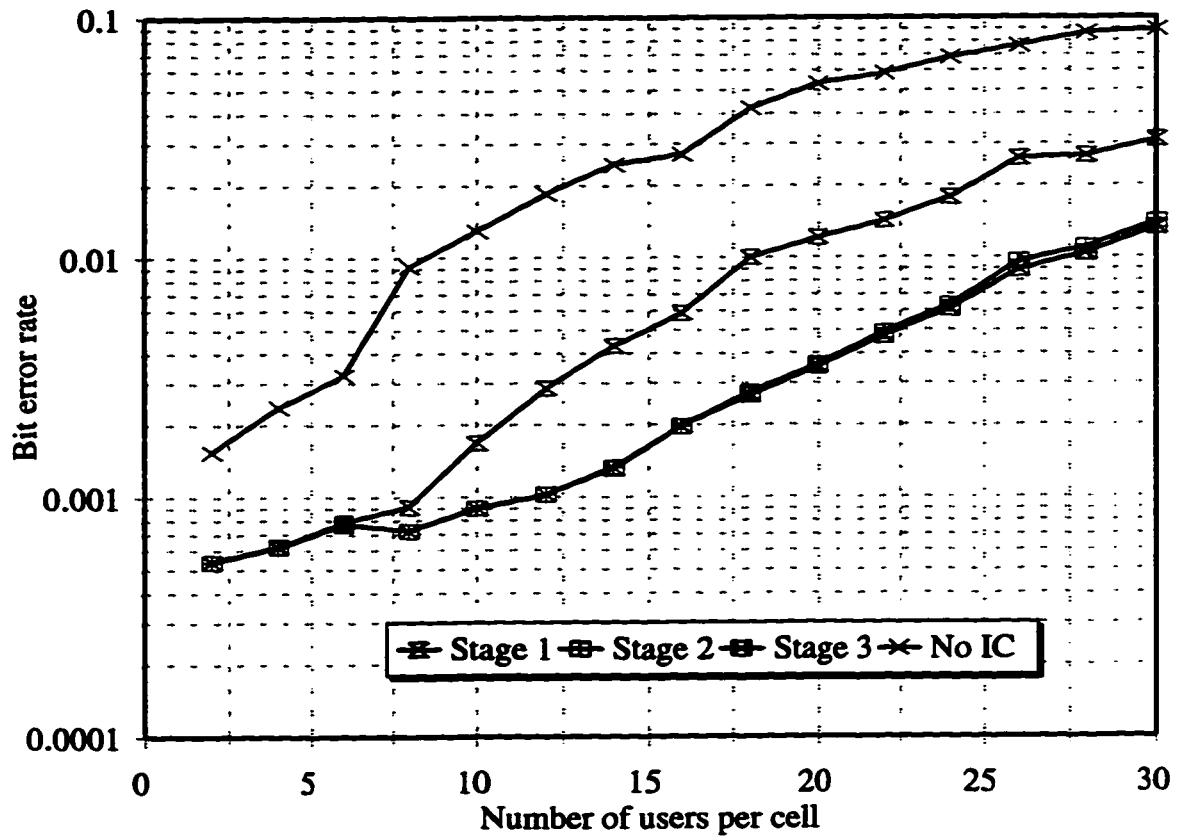
Fig. 3.13. Multi-cell performance of a RAMSIC receiver on a flat Rayleigh fading channel; nonideal cells, f=0.686, imperfect power control with 1dB standard deviation.

The performance of the RAMSIC receiver on a frequency selective Rayleigh fading channel with frequency reuse factor half way between the upper and lower bound in Milstein and Rappaport (1992), path loss exponents of 2, 3 and 4, non-ideal cells with 2 mile radius and power control error standard deviation of 1 dB, is reported in Figures 3.14, 3.15 and 3.16, respectively. All other system parameters are as in Figure 3.10. For a BER of 10^{-3} the maximum number of users per cell is 10, 14 and 18 for path loss exponent of 2, 3 and 4, respectively. It can also be seen from the figures that there is very little increase in capacity when the number of cancellation stages is increased beyond two.
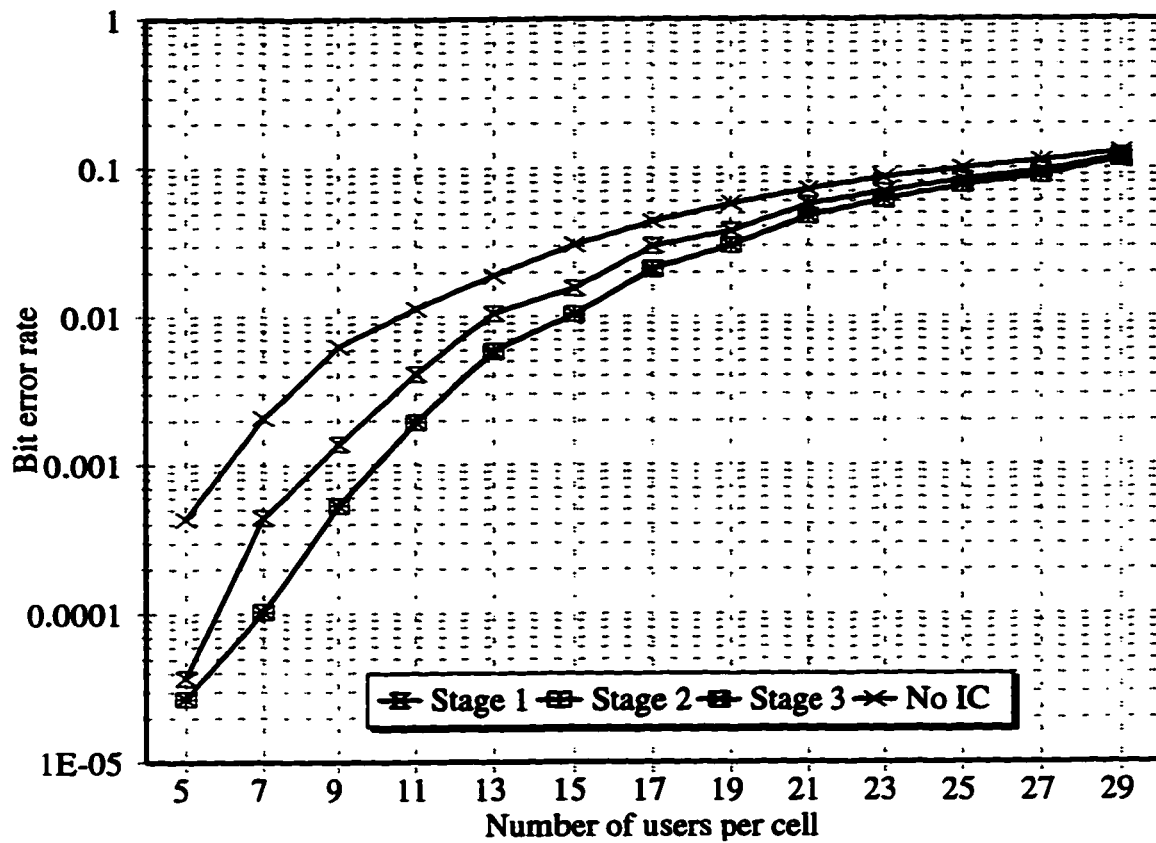
Fig. 3.14. Multi-cell performance of a RAMSIC receiver on a frequency selective Rayleigh fading channel; nonideal cells, f=1.57, imperfect power control with 1dB standard deviation.
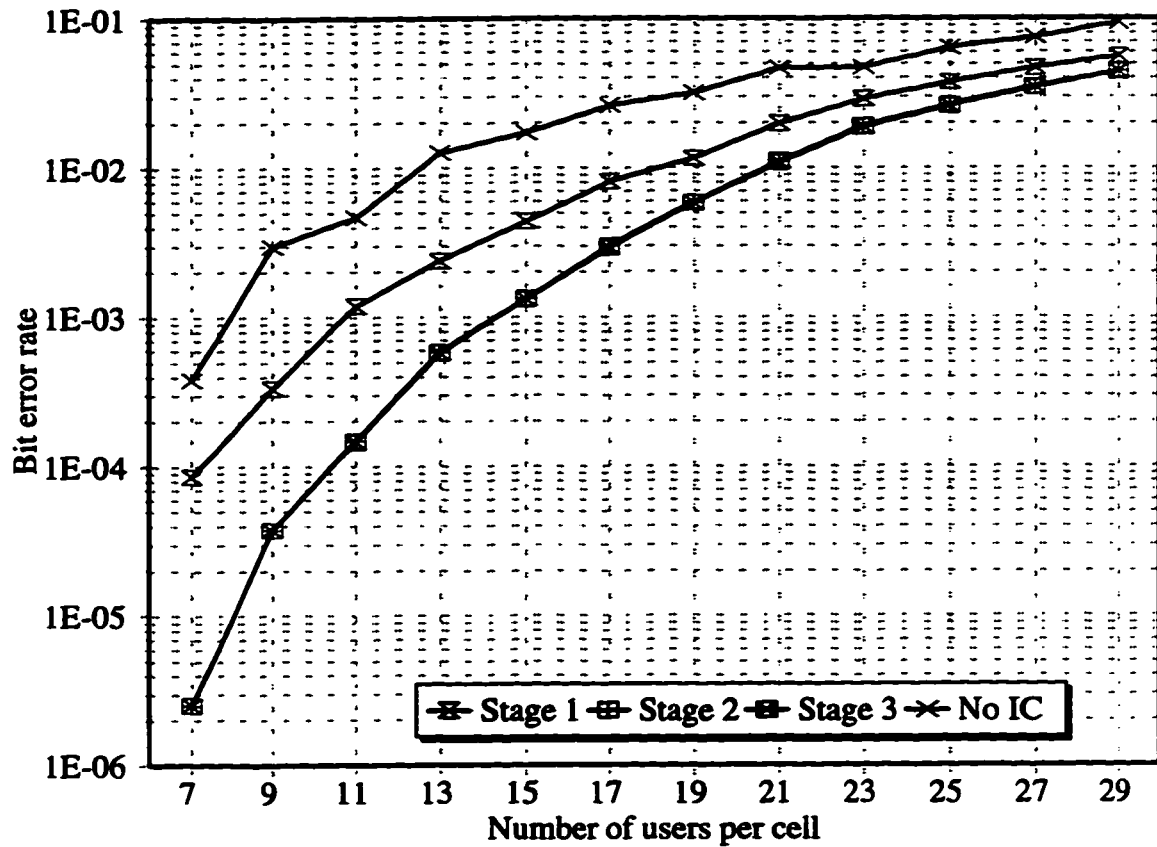
Fig. 3.15. Multi-cell performance of a RAMSIC receiver on a frequency selective Rayleigh fading channel; nonideal cells, f=0.959, imperfect power control with 1dB standard deviation.
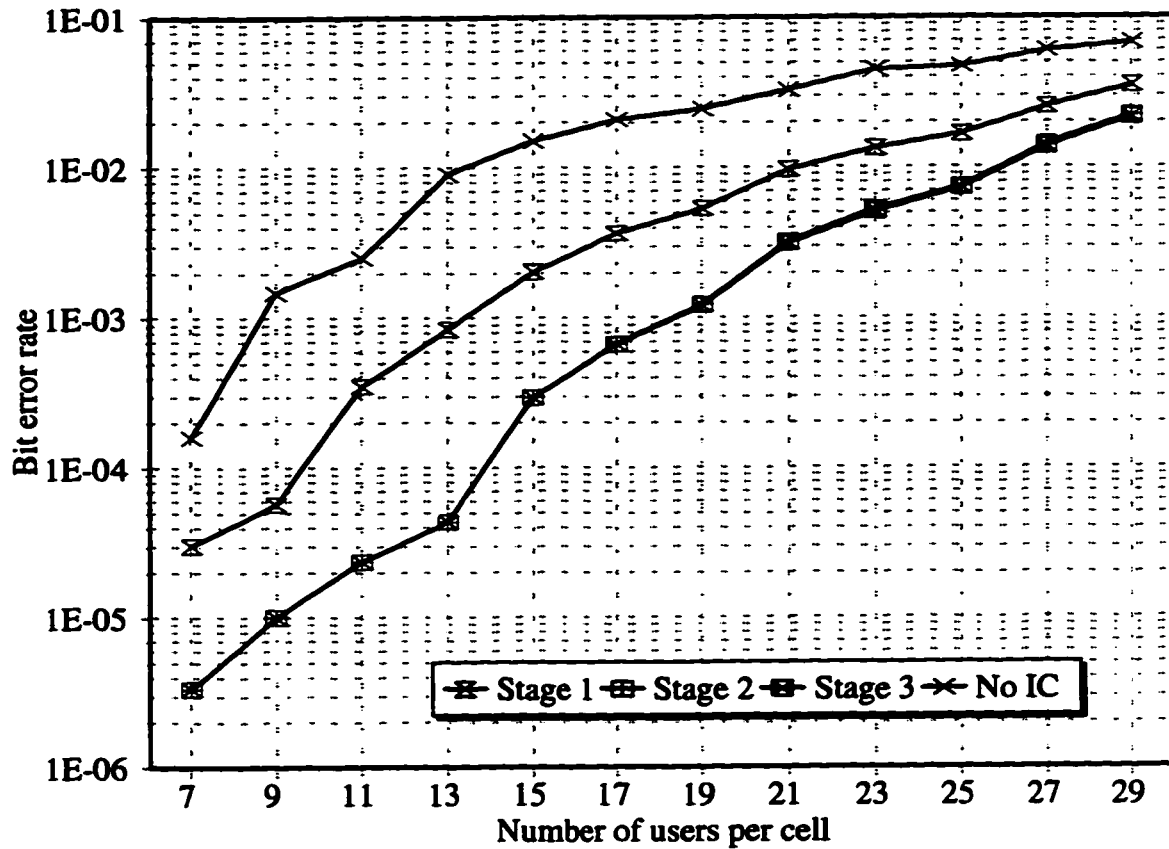
111

Fig. 3.16. Multi-cell performance of a RAMSIC receiver on a frequency selective Rayleigh fading channel; nonideal cells, f=0.686, imperfect power control with 1dB standard deviation.

3.6 Conclusion

The use of reference symbols for coherent detection as well as interference cancellation was analyzed in this chapter. It was shown in Section 3.3 that the reference symbol assisted coherent receiver performed approximately 1.5 dB worse than the coherent receiver using perfect channel estimates (ideal coherent receiver), and that substantial capacity gain could be obtained with a reference symbol assisted multi-stage successive interference cancelling (RAMSIC) receiver. At the first glance the capacity of the system with RAMSIC receivers may appear relatively small. It should, however, be

noted that forward error correction coding has not been considered and that coding will significantly improve the capacity. Moreover, since successive interference cancellation only reconstructs the multi-user interference from the symbols that have already been demodulated, multi-user interference from symbols that have not yet been demodulated may be significant. Even higher capacity is, therefore, possible if the channel estimates can be improved.

Section 3.4 investigated the capacity of a DS-CDMA system with a RAMSIC receiver operating on improved channel estimates. It was shown that the proposed gating technique resulted in a system with capacity approaching 80% that of the system with successive interference cancellation operating with perfect channel estimates.

The multi-cell performance of the RAMSIC receiver with biphase spreading was considered in Section 3.5. It was shown that without any forward error correction coding, the capacity is between 0.77 and 1.22 times that in Gilhousen *et al.* (1991). It was also shown that the RAMSIC receiver provided significant capacity even when the path loss exponent was 2.

It is, however, worth noting that because of the intercellular interference, the estimates of the channel parameters are quite noisy. The potential for higher capacity exists, if the channel estimates can be improved. One method for improving the channel estimates in flat fading is antenna diversity. The reason for this is that without some form of diversity, power control causes rapid changes in the real and imaginary part of the complex channel gain. With this high rate of change, it is difficult for the linear interpolator to track the changes in the channel gain. This is one reason for better

performance in the frequency selective fading channel, when a RAKE receiver is used to combine multiple paths, than in the flat fading channel. Antenna diversity will slow down the rapid changes in the channel gain and result in more accurate channel estimates.

3.7 Appendix

We will derive the variance of $I_{m,l;j,k}$ which is necessary in the expression (3.8) for variance of the interference term $N_{j+1,k}^{(n)}$ in the decision variable give by (3.5).

Lemma 1: If

$$I_{m,l;j,k} = \int_{\tau_{j,k}}^{T_r + \tau_{j,k}} d_{m,l}(t - \tau_{m,l}) c_{m,l}(t - \tau_{m,l}) c_{j,k}(t - \tau_{j,k}) \, dt \quad ,$$

then

$$\mathrm{VAR}(I_{m,l;j,k}) = G \left[R_\psi^2 (\tilde{\tau}_{m,l;j,k}) + R_\psi^2 (T_c - \tilde{\tau}_{m,l;j,k}) \right]$$

where $\mathrm{VAR}(x)$ denotes the variance of x, and

$$\tilde{\tau}_{m,l;j,k} = (\tau_{m,l} - \tau_{j,k}) \bmod T_c \, ,$$

and, following Pursley (1981), the partial autocorrelation function for the chip waveform is defined as

$$R_\psi (s) = \int_0^s \psi(t) \psi(t - T_c - s) \, dt \quad 0 \le s < T_c \quad .$$

Proof:

We can rewrite $I_{m,l;j,k}$ as

$$I_{m,l;j,k} = \int_0^{T_r} d_m(t - \tau_{m,l} + \tau_{j,k}) c_m(t - \tau_{m,l} + \tau_{j,k}) c_j(t) \, dt \quad ,$$

Recall that the spreading waveform was defined as

114

$$c_m(t) = \sum_{i=-\infty}^{\infty} c_{m,i} \, \psi(t - iT_c) \, .$$

Therefore

$$I_{m,l;j,k} = \sum_{\upsilon=0}^{G-1} c_{j\upsilon} \int_0^{T_c} \psi(t - \upsilon T_c) d_m(t - \tau_{m,l} + \tau_{j,k}) c_m(t - \tau_{m,l} + \tau_{j,k}) \, dt \quad , \quad (3.1.1)$$

where G denotes the processing gain. Assuming that the pulse shape of the data waveform $d_m(t)$ is rectangular, define

$$q_m(t) \equiv d_m(t) c_m(t)$$

$$= \sum_{i=-\infty}^{\infty} \sum_{j=0}^{G-1} d_{m,i} c_{m,j} \psi(t - iT_s - jT_c)$$

$$= \sum_{\upsilon=-\infty}^{\infty} q_{m,\upsilon} \psi(t - \upsilon T_c) \quad ,$$

where

$$q_{m,\upsilon} = d_{m,\left\lfloor \frac{\upsilon}{G} \right\rfloor} c_{m,\upsilon \bmod G} \quad ,$$

and $\lfloor x \rfloor$ denotes the largest integer smaller than or equal to x. For notational ease later in the proof, we define

$$\mu = \left\lfloor \frac{\tau_{m,l} - \tau_{j,k}}{T_c} \right\rfloor$$

and let

$$p_m(t) = q_m(t - \mu T_c)$$

$$= \sum_{i=-\infty}^{\infty} p_{m,i} \psi(t - iT_c)$$

where $p_{m,i} = q_{m,i+\mu}$. With the set $\{p_{m,i}\}$ so defined, $q(t - \tau_{m,l} + \tau_{j,k})$ can now be written as

$$q(t - \tau_{m,l} + \tau_{j,k}) = \sum_{i=-\infty}^{\infty} p_{m,i} \psi(t - iT_c - \widetilde{\tau}_{j,k;m,l}) \quad . \tag{3.1.2}$$

Putting Equation (3.1.2) into Equation (3.1.1) gives

$$
\begin{aligned}
I_{m,l;j,k} &= \sum_{\upsilon=0}^{G-1} c_{j,\upsilon} \Bigg\{ p_{m,\upsilon-1} \int_{\upsilon T_c}^{\upsilon T_c + \widetilde{\tau}_{j,k;m,l}} \psi(t - \upsilon T_c) \psi\Big[t - (\upsilon-1)T_c - \widetilde{\tau}_{j,k;m,l}\Big] dt \quad + \\
&\qquad p_{m,\upsilon} \int_{\upsilon T_c + \widetilde{\tau}_{j,k;m,l}}^{(\upsilon+1)T_c} \psi(t - \upsilon T_c) \psi(t - \upsilon T_c - \widetilde{\tau}_{j,k;m,l}) dt \Bigg\} \\
&= \sum_{\upsilon=0}^{G-1} c_{j,\upsilon} J_{m,\upsilon} \quad ,
\end{aligned}
$$

where

$$J_{m,\upsilon} = p_{m,\upsilon-1} R_\psi(\widetilde{\tau}_{j,k;m,l}) + p_{m,\upsilon} R_\psi(T_c - \widetilde{\tau}_{j,k;m,l}) \quad .$$

Since both $J_{m,\upsilon}$ and $J_{m,\upsilon+1}$ contain the same random variable $q_{m,\upsilon}$, it does not appear at first that the members of the set $\{J_{m,\upsilon}\}$ are independent even when $\widetilde{\tau}_{j,k;m,l}$ are given. Direct application of Lemma in Torrieri (1992), however, indicates that the members of the set $\{J_{m,\upsilon}\}$ are independent. Therefore,

$$\mathrm{VAR}(I_{m,l;j,k}) = \sum_{\upsilon=0}^{G-1} \mathrm{VAR}(J_{m,\upsilon}) \tag{3.1.3}$$

where

$$\mathrm{VAR}(J_{m,\upsilon}) = R_\psi^2(\widetilde{\tau}_{j,k;m,l}) + R_\psi^2(T_c - \widetilde{\tau}_{j,k;m,l}) \tag{3.1.4}$$

because the cross terms in the $\mathrm{VAR}(J_{m,\upsilon})$ are zero since the members of the set $\{p_{m,\upsilon}\}$ are orthogonal. Equation (3.1.3) shows that $\mathrm{VAR}(J_{m,\upsilon})$ is independent of υ. Hence, putting equation (3.1.4) into equation (3.1.3) gives

$$\mathrm{VAR}(I_{m,l;j,k}) = G\Big\{ R_\psi^2(\widetilde{\tau}_{j,k;m,l}) + R_\psi^2(T_c - \widetilde{\tau}_{j,k;m,l}) \Big\} \quad .$$

116

3.8 References

D'Amours, C., Moher, M., Yongacoglu, A. and Wang, J. (1993): RAKE receiver structures for differential and pilot symbol-assisted detection of DS-CDMA signals in frequency-selective Rayleigh fading channels, *Proc. IEEE GLOBECOM'93*, pp. 1798-1802.

Gilhousen, K.S., Jacobs, I.M., Padovani, R., Viterbi, A.J., Weaver, L.A. and Wheatley III, C.E. (1991): On the capacity of cellular CDMA system. *IEEE Trans. Veh. Technol.*, vol. VT-27, pp 303-312.

Huber, P.J. (1981): *Robust Statistics*, John Wiley & Sons Pub.: N.Y..

Jakes, W.C. (1974): *Microwave Mobile Communications*, John Wiley: N.Y..

Kawabe, M., Kato, T., Kawahashi, A., Sato, T. and Fukasawa, A. (1993): Advanced CDMA scheme based on interference cancellation. *Proc. IEEE VTC*, pp 448-451.

Ling, F. (1993): Coherent detection with reference-symbol based channel estimation for direct sequence CDMA uplink communications, *Proc. IEEE Vehicular Technology Conf.*, pp. 400-403.

Milstein, L.B. and Rappaport, T.S. (1992): Effects of radio propagation path loss on DS-CDMA cellular frequency reuse efficiency for the reverse channel. *IEEE Trans. Vehicular Technology*, vol. 41, no. 3, pp. 231-241.

Mowbray, R.S., Pringle, R.D. and Grant, P.M. (1993): Increased CDMA system capacity through adaptive cochannel interference regeneration and cancellation. *IEE Proceedings-I*, Vol. 139, no. 5, pp 515-524.

Papoulis, A. (1965): *Probability, Random Variables, and Stochastic Processes*, McGraw-Hill: N.Y..

Patel, P. and Holtzman, J. (1994b): Analysis of a simple successive interference cancellation scheme in a DS/CDMA system. *IEEE J. Select. Areas Commun.*, vol. 12, no. 5, pp 796-807.

Proakis, J.G. (1989): *Digital Communications*, 2-nd ed., McGraw-Hill: N.Y..

Pursley, M.B. (1981): Spread-spectrum multiple-access communications. In Longo, G. (eds): *Multi-User Communication Systems*, New York: Springer-Verlag.

Royden, H.L. (1988): *Real Analysis*, 3rd ed., MacMillan: N.Y..

Torrieri, D.J. (1992): Performance of direct-sequence systems with long pseudonoise sequences, *IEEE J. Select. Areas Commun.*, vol. 10, no. 4, pp. 770-781.

Varanasi, M.K. and Aazhang, B. (1990): Multistage detection in asynchronous code-division multiple-access communications. *IEEE Trans. Commun.*, vol. 38, no. 4, pp. 509-519.

Viterbi, A.J. (1990): Very low rate convolutional codes for maximum theoretical performance of spread spectrum multiple access channels. *IEEE J. Select. Areas Commun.*, vol. 8, no. 4, pp. 641-649.

Viterbi, A.J., Viterbi, A.M., and Zehavi, E. (1993): Performance of power-controlled wideband terrestrial digital communication, *IEEE Trans. Commun.*, vol. 41, no. 4, pp. 559-569.

Yoon, Y.C., Kohno, R. and Imai, H. (1993): A spread-spectrum multiaccess system with cochannel interference cancellation for multipath fading channels. *IEEE J.*

Chapter 4: Robustness to parameter imperfections with biphase and quadriphase spreading*

4.1 Introduction

It can be argued that the RAMSIC receiver introduced in the last chapter is one of the most attractive multi-user receivers currently under investigation because of its simplicity and thus implementability. Single cell analysis have shown that it has the capability of increasing the traffic capacity (see Chapter 3). However, the achievable traffic capacity is still very modest when the channel estimates are significantly corrupted by interference from symbols not yet demodulated and cancelled by the receiver. A modification of the transmitted signal structure to decrease that interference has been proposed. The results of a single cell analysis of the modified cancellation scheme demonstrated that the system's traffic capacity could reach approximately 80% of that of a multistage successive interference cancelling receiver operating on perfect channel parameters. Multi-cell analysis showed that significant traffic capacity increase over the conventional matched filter receiver was possible even when the path loss exponent was 2. Although Chapter 3 has demonstrated the potential of the RAMSIC receiver, the sensitivity of its performance to system imperfections, which is the focus of this chapter, has not been considered there.

The chapter is organized as follows. A brief description of the system is given in Section 4.2. The sensitivity of the receiver with biphase spreading to system imperfections

---

is investigated in Section 4.3. In Section 4.4, the performance differences between the biphase and quadriphase spread system in an AWGN channel will be demonstrated. Section 4.5 will detail the performance of the RAMSIC receiver with quadriphase spreading as well as its sensitivity to system imperfections. Finally some general conclusions will be given in Section 4.6.

4.2 System description and analysis

The analysis in this chapter is restricted to the reverse link of a mobile CDMA cellular system. Block diagram of the transmitter and the receiver is given in Fig. 4.1. The transmitter first inserts reference symbols into a stream of data symbols. The reference symbols are inserted after every Q symbols. Periodic insertion of the reference symbols is
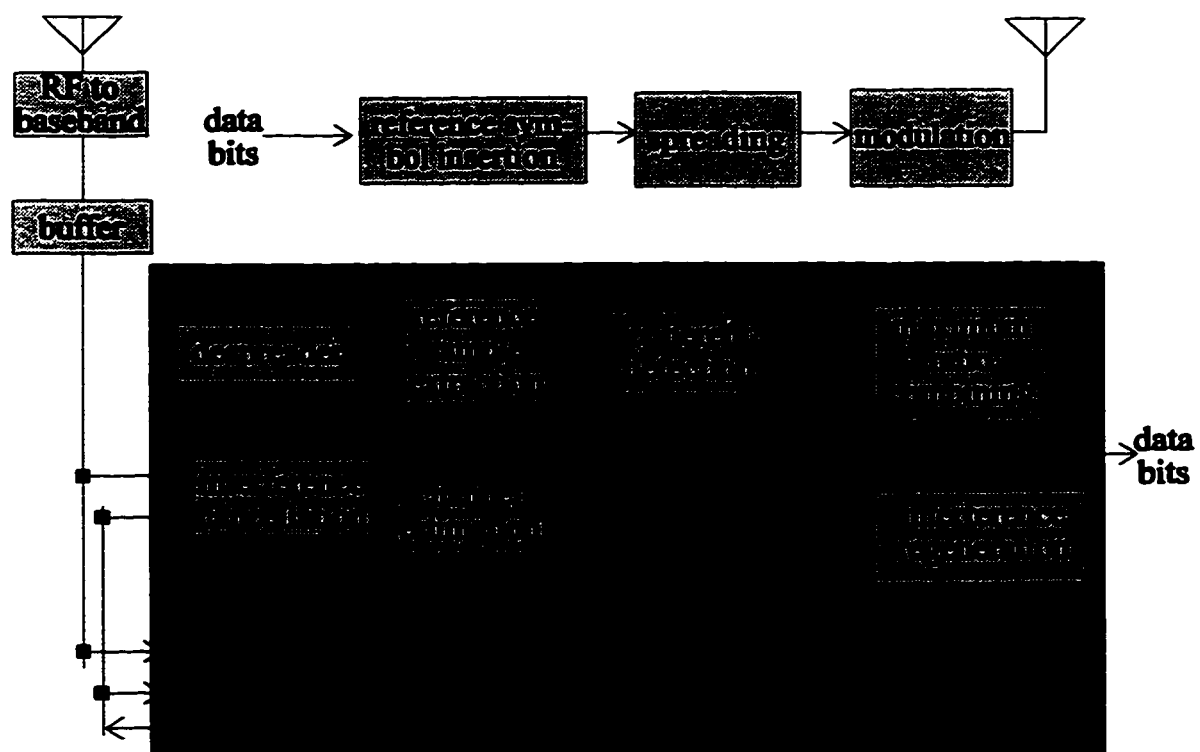
Fig. 4.1. A block diagram of the transmitter and receiver.

chosen because, for the case of non stationary channels, block insertion is less effective. Insertion of reference symbols periodically throughout the data stream allows for the better tracking of changing channel parameters (Ling, 1993). Corruption of the channel estimate by interference can be reduced significantly if the transmitter is gated off for one symbol (null symbol) before and after the transmission of the reference symbol (see Chapter 3). This gating can be realized in a similar fashion to that employed in the IS-95 standard where the transmitted power is reduced whenever the output bit rate of the variable bit rate voice encoder is reduced. The data stream with reference and null symbols inserted is then spread in the usual manner, modulated and transmitted. Both biphase and quadriphase spreading will be considered in this chapter. In quadriphase spreading the same data symbol is spread in the in-phase and quadrature branch with different PN sequences.

Flat and frequency selective Rayleigh fading channels are considered. A wideband tapped delay line model of the channel is used:

$$h(t,\tau) = \sum_{i=1}^{N(t)} a_i(t)\delta[\tau - \tau_i]e^{j\theta_i(t)} \quad , \tag{4.1}$$

where δ is the delta function, t and τ are the observation time and application time of the impulse respectively, $N(t)$ is the number of multipath components, $a_i(t)$ is the attenuation coefficient which is a random variable with a Rayleigh distribution, $\tau_i(t)$ is the delay time, and $\theta_i(t)$ is the phase delay for each path. The Rayleigh fader is simulated in a similar fashion as that described in Jakes (1974).

The RAMSIC receiver performs baseband interference cancellation. The

cancellation algorithm is described by Fig. 4.2. The first step is to cancel all the regenerated baseband signals from other users that have been detected from the composite baseband received signal. The current user's symbol is then detected and the baseband received signal corresponding to that symbol is regenerated. Interference cancellation, detection and regeneration continue in this fashion for the next user. Thus each user's signal is detected and cancelled successively. Note that in the case of a frequency selective Rayleigh fading channel, a RAKE receiver is used for time diversity combining and to facilitate the regeneration of the baseband received signal from all significant paths.

The channel estimation algorithm is described in Ling (1993) and in Chapter 3, and only the important steps will be briefly highlighted here. An unbiased but noisy estimate of
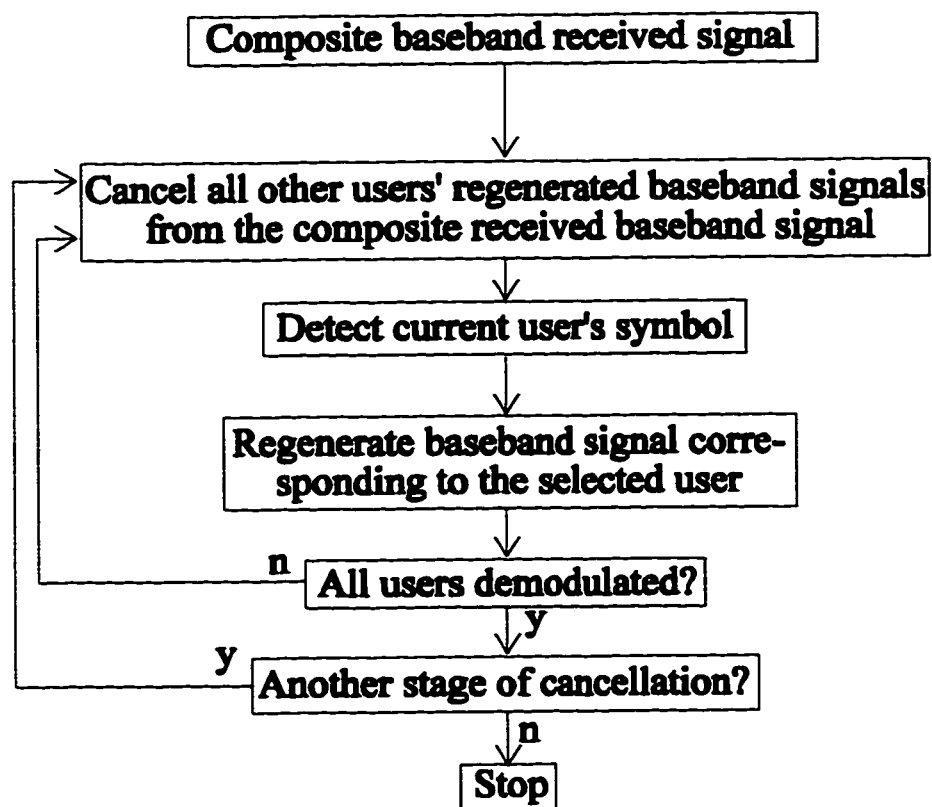
Fig. 4.2. Signal flow diagram of the interference cancellation scheme.

the channel is obtained by correlating the received signal samples corresponding to the reference symbols with the known reference symbol. The noise contaminating the estimate is then reduced by passing the noisy channel estimates through a low pass smoothing filter that has a cutoff frequency greater than or equal to the maximum possible Doppler frequency. Successive interference cancellation is also employed in the channel estimation algorithm to lessen the effect of multiple access interference on the channel estimates. Estimates of the channel are thus obtained at instants where reference symbols were transmitted. Linear interpolation is used to obtain channel estimates at instants corresponding to data symbols for coherent detection and interference cancellation.

Any practical low pass filter used to improve channel estimates will have a finite delay. This delay will most likely be the dominant delay in the system. For example, with an information bit rate of 9600 bits/s, $Q = 12$ and a 25 tap FIR filter, the delay will be about 15 ms. Therefore, enough memory must be present in the system to buffer 15 ms of the received signal.

Insertion of reference symbols partitions the data stream into blocks. In a quasi-synchronous system, where the reference symbols from each user arrive within one symbol time of each other, a receiver that detects an entire block of data before interference regeneration performs better than a receiver (e.g. that considered in Yoon *et al.*, 1993) that regenerates interference after the detection of each data symbol. This is because in the latter case, multi-user interference from the next data symbol cannot be regenerated, since it has not yet been detected. In the former case, the next symbol is a reference symbol which is known to the receiver.

It is worth noting that the system considered here does not contain any forward error correction coding. Further increases in capacity are possible when coding is employed.

4.3 Sensitivity of biphase spread system to parameter estimation errors

The sensitivity of the RAMSIC receiver to parameter estimation errors in a biphase spread system will be investigated by computer simulations. Computer simulation is used because of the limitations of analytical techniques as discussed in Chapter 3. The assumed information bit rate is 9600 bits/s, the chip rate of the system is 1.23 Mchips/s, and the maximum Doppler frequency for each user is 100Hz for all simulation results presented here. The pilot insertion parameter Q is set to 4 for the system operating in a flat Rayleigh fading channel, and 12 for the frequency selective fading channel. These insertion rates were determined to be optimal in Chapter 3. The low pass filters are the optimal low pass filters as used in Chapter 3. The intercellular interference is modelled as a zero mean complex white Gaussian noise process, the variance of which is related to the intracellular interference by the intercell to intracell interference ratio f. The intercellular interference is approximated as a Gaussian process because it originates from the signals of a large number of relatively distant users in surrounding cells, and hence approximately satisfies the assumptions of the central limit theorem. Frequency reuse factors half way between the upper and lower bounds given in Milstein and Rappaport (1992) for path loss exponent of 4 with hexagonal cell geometry of 2 miles radius ($f=0.55$), and nonidealized cell geometries with path loss exponents of 2, 3, 4 ($f = 1.57$, 0.959 and 0.686,

respectively) are considered. Imperfect power control is modelled as a lognormal variable (Viterbi, 1993). Capacity of the system is obtained by first determining the bit error rate (BER) for various numbers of users per cell, ranging from three to 30 in steps of two. The capacity of the system is then taken to be the number of users per cell at a BER of 10^{-3}.

4.3.1 Effects of non idealized transmitter gating

In order to improve the estimate of the channel parameter, the transmitter is gated off for one period before and after the transmission of the reference symbol. Consequently, it is necessary to study the performance degradation due to non idealized transmitter gating. Table 4.1 gives the capacity values for a system with power control standard deviation of 1 dB and non idealized transmitter gating operating on either flat or frequency selective Rayleigh fading channel. The channel model contains three independent Rayleigh fading paths of exponentially decaying average powers (0, -2, -4 dB). All three paths are assumed to be perfectly tracked by the RAKE receiver. Two different transmitter gating masks are considered: IS-95 and a more relaxed transmitter gating (RTG) mask. For the IS-95 mask, during gated-off periods, one symbol interval before and after the transmission of the pilot symbol, the mobile transmitters reduce their mean output power

Table 4.1: Sensitivity of the RAMSIC receiver with power control standard deviation of 1.0 dB operating in either flat or frequency selective Rayleigh fading channel to the shape of transmitter gating mask.

	Number of users per cell at BER = 10^{-3}			
	Flat Rayleigh fading channel		Frequency selective Rayleigh fading channel	
f	IS-95 mask	RTG mask	IS-95 mask	RTG mask
0.55	13	11	20	19
0.686	11	10	18	17
0.959	8	8	14	14
1.57	5	5	10	10

either by 20 dB or to the transmitter noise floor, whichever is higher. The transition is no longer than 6 μs.

Analysis of the performance curves (see Appendix 4A) demonstrates that the performance of the system improves with increasing number of stages. However, increasing the number of stages beyond two only results in very minor performance gains. Comparison of the results in Table 4.1 with those in Chapter 3 shows that non-ideal transmitter gating reduces the capacity by 1 user for the case where $f = 0.55$, but has no effect for other intercell to intracell interference ratios. This is because with higher intercell to intracell interference ratios, the error in the channel estimation is mainly due to intercellular interference and an error due to non ideal transmitter mask is comparatively insignificant. Capacity of the system with a more relaxed transmitter gating (RTG), where the transmitter only reduces its power by 10 dB instead of 20 dB, is also shown in Table 4.1. For $f = 0.55$ and 0.686 (path loss exponent of 4 for idealized and non idealized cells), there is a small reduction in the capacity of the system, while the capacity was not affected for other intercellular to intracellular interference ratios for both flat and frequency selective Rayleigh fading channels. Hence, the transmitter gating specification may be relaxed with a minor reduction in capacity.

4.3.2 Effects of power control errors

Capacity of the system for different values of standard deviation, σ_p, of power controlled signal with the IS-95 transmitter gating mask in both flat and frequency selective Rayleigh fading channels is shown in Table 4.2. Similarly to the results in

Table 4.2: Sensitivity to power control errors of the RAMSIC receiver with the IS-95 transmitter gating mask operating on flat or frequency selective Rayleigh fading channel.

	Number of users per cell at BER = 10^{-3}									
	Flat Rayleigh fading channel					Frequency selective Rayleigh fading channel				
f	$\sigma_p = 0.7$	1.0	1.6	2.2	2.9	$\sigma_p = 0.7$	1.0	1.6	2.2	2.9
0.55	14	13	10	7	2	22	20	18	15	12
0.686	13	11	9	6	2	19	18	16	13	10
0.959	10	8	6	4	2	15	14	12	10	8
1.57	6	5	5	3	2	10	10	8	7	6

Subsection 4.3.1, the performance curves (see Appendix 4B) demonstrate that increasing the number of stages beyond two does not improve the performance of the system. It can be seen from the table that decreasing the accuracy of power control reduces capacity of the system. This is because with larger standard deviation of power controlled signal, the signal to noise ratio necessary to maintain a BER of 10^{-3} increases. Therefore the amount of interference that the system can withstand decreases and that results in decreased capacity. Hence, a system designer can trade off complexity of the power control algorithm for capacity. It should, however, be noted that for the case of path loss exponent of 2 and power control standard deviation of 2.9 dB, capacity of the system is relatively small on a flat fading channel. This implies that diversity should be exploited on a flat fading channel to minimize the power control variance; especially if the path loss exponent is 2.

4.3.3 Effects of synchronization error

Sensitivity of the RAMSIC receiver to chip synchronization errors is shown in Table 4.3. The performance curves (see Appendix 4C) demonstrate that the performance does not improve when the number of cancellation stages is increased beyond two. The results

in Table 4.3 show that sensitivity of the system to synchronization errors is similar for both frequency selective and flat Rayleigh fading channels. It can also be seen from the table that the effect of increasing synchronization error on the capacity of the system is not linear. Synchronization error in the range acceptable for effective spread spectrum communication (less than $0.1T_c$) does not have any significant effect on capacity. Larger synchronization errors, however, decrease the capacity (at least for path loss exponents of 3 and 4). Comparing our results with those given in Sunay and McLane (1995a) for a BPSK CDMA system operating on an additive white Gaussian noise channel, we conclude that the RAMSIC receiver seems to be more robust. This is because imperfect estimation of channel parameters exerts dominant influence on capacity. In the multi-cell system considered here, intercell interference which is not cancelled by the inference cancelling algorithm significantly corrupts channel estimates. The resultant error in detection and interference cancellation is much more significant than that caused by synchronization errors of reasonable magnitude. This also accounts for the fact that synchronization errors have more effect on the capacity as intercell to intracell interference ratio decreases, because the channel parameter estimation error becomes less dominant over synchronization errors.

The results here can also be compared with those from Cheng and Holtzman (1994) which analyzed a coherent binary single stage successive interference cancellation receiver with perfect channel estimates in a single cell DS/CDMA system operating on a flat Rayleigh fading channel. It should be noted that the assumptions in that work was slightly different then those here. Synchronization error was modelled as a zero mean white

Table 4.3: Sensitivity of the RAMSIC receiver with the IS-95 transmitter gating mask and power control standard deviation of 1.0 dB operating on flat or frequency selective Rayleigh fading channel to synchronization error (ϵ).

f	Number of users per cell at BER = 10^{-3}									
	Flat Rayleigh fading channel					Frequency selective Rayleigh fading channel				
	$\epsilon = 0.0T_c$	$0.05T_c$	$0.10T_c$	$0.15T_c$	$0.20T_c$	$\epsilon = 0.0T_c$	$0.05T_c$	$0.10T_c$	$0.15T_c$	$0.20T_c$
0.55	13	13	13	11	10	20	20	20	19	18
0.686	11	11	11	10	9	18	18	18	17	17
0.959	8	8	8	8	7	14	14	14	13	13
1.57	5	5	5	5	5	10	9	9	9	9

Gaussian process, received powers were assumed equal for all users in the system, and only the noiseless case and the case where the signal to noise ratio was 10 dB were considered. Nevertheless, the performance losses reported there are very similar to those reported here for path loss exponent of 4. However, for path loss exponent of 2 and 3, the RAMSIC receiver appears to be more robust. Once again, this is because imperfect channel estimation has a dominant influence on capacity.

4.4 Biphase versus Quadriphase spreading in AWGN channel

Before going on to discuss the effect of quadriphase spreading with the RAMSIC receiver, we will try to obtain some insights into the problem by first considering the effect of biphase and quadriphase spreading on the conventional matched filter receiver operating in an AWGN channel. Consider first a biphase spread system with K users. The received signal is

$$r(t) = \sum_{k=1}^{K} \sqrt{2P_k} c_k(t - \tau_k) d_k(t - \tau_k) \cos(\omega t + \phi_k) + n(t) \tag{4.2}$$

where P_k is the received power, $c_k(t)$ is the spreading waveform, $d_k(t)$ is the antipodal binary data waveform, ω is the carrier frequency, τ_k is the delay (modelled as a random

variable uniformly distributed from 0 to T_s) and ϕ_k is the carrier phase (modelled as a uniformly distributed random variable from 0 to 2π) of the kth user. The thermal noise, $n(t)$, is modelled as zero mean white Gaussian noise with two sided spectral density of $N_0/2$. Each pulse of $d_k(t)$ has a duration of T_s, the symbol duration. The spreading waveform is of the form

$$c_k(t) = \sum_{i=-\infty}^{\infty} c_{k,i} \, \psi(t - iT_c) \tag{4.3}$$

where $c_{k,i}$ is a member of the binary pseudorandom sequence $\{c_{k,i}\}$ which can take on values of ± 1; $\psi(t)$ is the chip pulse of duration T_c ($T_c \ll T_s$). Without loss of generality we will assume that the energy of the chip waveform is normalized as follows:

$$\int_0^{T_c} \psi^2(t) \, dt = T_c \quad . \tag{4.4}$$

For convenience, we will assume that $\tau_l = \phi_l = 0$ and confine our analysis to the interval from 0 to T_s. The decision variable for user one, the desired user, is

$$D_1 = \frac{2}{T_s} \int_0^{T_s} r(t) c_1(t) \cos \omega t \, dt$$

$$= \sqrt{2P_1} d_1 + \frac{1}{T_s} \sum_{k=2}^{K} \int_0^{T_s} \sqrt{2P_k} c_1(t) c_k(t - \tau_k) d_k(t - \tau_k) \cos \phi_k \, dt \tag{4.5}$$

$$+ \frac{2}{T_s} \int_0^{T_s} n(t) c_1(t) \cos \omega t \, dt \quad .$$

The first term of (4.5) is the desired signal, the second term is the multiple access interference (MAI), and the third term is the additive Gaussian noise. We will assume that the MAI is much larger than the Gaussian noise term and the latter may be ignored. The decision variable may then be rewritten as

$$D_1 = \sqrt{2P_1} d_1 + \sum_{k=2}^{K} \left\{ \frac{\sqrt{2P_k} \cos \phi_k}{T_s} \sum_{v=0}^{G-1} J_{v,k} \right\} \tag{4.6}$$

where G is the processing gain and

$$J_{\upsilon,k} = \int_{\upsilon T_c}^{(\upsilon+1)T_c} c_1(t)c_k(t-\tau_k)d_k(t-\tau_k)\,dt \ . \tag{4.7}$$

Since $J_{\upsilon,k}$ and $J_{\upsilon+1,k}$ contain some common random variables, it does not appear that the members of the set $\{J_{\upsilon,k}\}$ for a given k are statistically independent. However, application of the lemma in Torrieri (1992) demonstrates their independence. The random variable

$$L_k = \sum_{\upsilon=0}^{G-1} J_{\upsilon,k} \tag{4.8}$$

is thus a sum of independent random variables. Moreover, since $G \gg 1$ (often $G > 100$), L_k can be considered Gaussian based upon central limit theorem arguments. The MAI for a given set of ϕ_k's is, therefore, a weighted sum of Gaussian random variables which is also a Gaussian random variable.

In order to determine the bit error rate (BER), it is necessary to determine the variance of the MAI conditioned upon $\{\phi_k\}$. It was shown in Section 3.7 that the variance of L_k is

$$\text{VAR}(L_k) = G\left[R_\psi^2(\tilde{\tau}_k) + R_\psi^2(T_c - \tilde{\tau}_k)\right] \tag{4.9}$$

where

$$\tilde{\tau}_k = \tau_k \quad \text{mod} \, T_c \tag{4.10}$$

and following Pursley (1981)

$$R_\psi(s) = \int_0^s \psi(t)\psi(t - T_c - s)\,dt \qquad 0 \le s \le T_c \ . \tag{4.11}$$

The variance of the MAI assuming perfect power control ($P_1 = P_2 = ... = P_K = P$) is then given by

$$\text{VAR}(\text{MAII}\phi_2,\phi_3,....,\phi_K,\tilde{\tau}_2,\tilde{\tau}_3,....,\tilde{\tau}_K) = \frac{2PG}{T_s^2} \sum_{k=2}^{K} \cos^2 \phi_k \left[R_\psi^2 (\tilde{\tau}_k) + R_\psi^2 (T_c - \tilde{\tau}_k) \right] . \qquad (4.12)$$

The conditions on the delays can be removed by following the approximation given in Torrieri (1992). The result is

$$\text{VAR}(\text{MAII}\phi_2,\phi_3,....,\phi_K) = \frac{\sigma_I^2}{T_s} \sum_{k=2}^{K} \cos^2 \phi_k , \qquad (4.13)$$

where for rectangular pulses

$$\sigma_I^2 \approx \sqrt{\frac{8}{3}} \frac{PT_s}{G} . \qquad (4.14)$$

The quantity σ_I^2 can be interpreted as the interference energy per symbol per interferer when the phases are aligned. The probability of a bit error conditioned upon $\{\phi_k\}$ becomes then

$$P_{e,1}(\phi_2,\phi_3,....,\phi_K) = \frac{1}{2} \text{erfc} \left\{ \left[\frac{PT_s}{\sigma_I^2 \sum_{k=2}^{K} \cos^2 \phi_k} \right]^{\frac{1}{2}} \right\} \qquad (4.15)$$

The condition upon the $\{\phi_k\}$ can be removed by ensemble averaging to obtain

$$P_{e,1} = \frac{1}{2} \left\langle \text{erfc} \left\{ \left[\frac{PT_s}{\sigma_I^2 \sum_{k=2}^{K} \cos^2 \phi_k} \right]^{\frac{1}{2}} \right\} \right\rangle , \qquad (4.16)$$

where $\langle \circ \rangle$ denotes expectation.

Consider now the same system as before but with quadriphase spreading. With

quadriphase spreading, different spreading sequences are used in the in-phase and quadrature branches but the same signal is being spread in both branches. The received signal is

$$r(t) = \sum_{k=1}^{K} \sqrt{2P_k} d_k(t-\tau_k)\{c_{I,k}(t-\tau_k)\cos(\omega t+\phi_k)+c_{Q,k}(t-\tau_k)\sin(\omega t+\phi_k)\} \tag{4.17}$$
$$+ n(t)$$

where $c_{I,k}$ is the in-phase and $c_{Q,k}$ is the quadrature spreading waveform. The form of the spreading waveform is given by (4.3) and is normalized according to (4.4). As before, we will assume that $\tau_I = \phi_I = 0$, the Gaussian noise term is much smaller than the MAI term and so may be ignored and confine our analysis to the interval from 0 to T_s.

The correlator output for the in-phase branch of the receiver for the first user is

$$D_{I,1} = \frac{2}{T_s} \int_0^{T_s} r(t)c_{I,1}(t)\cos\omega t \; dt = \sqrt{2P_1}d_1 + I_{I,1} + I_{I,2} \tag{4.18}$$

where

$$I_{I,1} = \frac{1}{T_s} \sum_{k=2}^{K} \int_0^{T_s} \sqrt{2P_k} d_k(t-\tau_k)c_{I,k}(t-\tau_k)c_{I,1}(t)\cos\phi_k \; dt \tag{4.19}$$

and

$$I_{I,2} = \frac{1}{T_s} \sum_{k=2}^{K} \int_0^{T_s} \sqrt{2P_k} d_k(t-\tau_k)c_{Q,k}(t-\tau_k)c_{I,1}(t)\sin\phi_k \; dt \; . \tag{4.20}$$

Note the similarity between (4.19), (4.20) and the MAI term of (4.5). Therefore, for a given set of ϕ_k's, the random variables $I_{I,1}$ and $I_{I,2}$ are both Gaussian. The variance of $I_{I,1}$ conditioned upon $\{\phi_k\}$ is given by

$$\text{VAR}(I_{I,1}|\phi_2,\phi_3,....,\phi_K) = \frac{\sigma_I^2}{T_s} \sum_{k=2}^{K} \cos^2\phi_k \; , \tag{4.21}$$

133

while that of $I_{I,2}$ is given by

$$\text{VAR}(I_{I,1}|\phi_2,\phi_3,....,\phi_K) = \frac{\sigma_I^2}{T_s}\sum_{k=2}^{K}\sin^2\phi_k \, , \qquad (4.22)$$

if perfect power control is assumed. For a given set of ϕ_k's, $D_{I,I}$ is Gaussian and due to the independence of $I_{I,1}$ and $I_{I,2}$, its variance is:

$$\text{VAR}(D_{I,1}|\phi_2,\phi_3,....,\phi_K) = \text{VAR}(I_{I,1}|\phi_2,\phi_3,....,\phi_K) + \text{VAR}(I_{I,2}|\phi_2,\phi_3,....,\phi_K)$$

$$= \frac{\sigma_I^2}{T_s}\sum_{k=2}^{K}\cos^2\phi_k + \frac{\sigma_I^2}{T_s}\sum_{k=2}^{K}\sin^2\phi_k = \frac{\sigma_I^2(K-1)}{T_s} \qquad (4.23)$$

The correlator output for the quadrature branch of the receiver for the first user is

$$D_{Q,1} = \frac{2}{T_s}\int_0^{T_s} r(t)c_{Q,1}(t)\sin\omega t\, dt = \sqrt{2P_1}d_1 + I_{Q,1} + I_{Q,2} \qquad (4.24)$$

where

$$I_{Q,1} = \frac{-1}{T_s}\sum_{k=2}^{K}\int_0^{T_s}\sqrt{2P_k}d_k(t-\tau_k)c_{I,k}(t-\tau_k)c_{Q,1}(t)\sin\phi_k\, dt \qquad (4.25)$$

and

$$I_{Q,2} = \frac{1}{T_s}\sum_{k=2}^{K}\int_0^{T_s}\sqrt{2P_k}d_k(t-\tau_k)c_{Q,k}(t-\tau_k)c_{Q,1}(t)\cos\phi_k\, dt \, . \qquad (4.26)$$

Note that (4.25) is similar to (4.20) while (4.26) is similar to (4.19). Therefore, for given $\{\phi_k\}$, $D_{Q,1}$ is a Gaussian random variable with variance

$$\text{VAR}(D_{Q,1}|\phi_2,\phi_3,....,\phi_K) = \frac{\sigma_I^2(K-1)}{T_s} \, . \qquad (4.27)$$

The overall decision variable for the receiver is

$$D_2 = D_{I,1} + D_{Q,1} \, . \qquad (4.28)$$

When $\{\phi_k\}$ is given, $D_{I,I}$ and $D_{Q,I}$ are independent Gaussian random variables, and hence

D_2 is also Gaussian with variance

$$\text{VAR}(D_2|\phi_2,\phi_3,....,\phi_K) = \frac{2\sigma_I^2(K-1)}{T_s} .$$ (4.29)

The conditional error probability then becomes

$$P_{e,2}(\phi_2,\phi_3,....,\phi_K) = \frac{1}{2}\text{erfc}\left\{\left[\frac{2PT_s}{(K-1)\sigma_I^2}\right]^{\frac{1}{2}}\right\} .$$ (4.30)

Note that the right hand side of (4.30) is not dependent upon $\{\phi_k\}$ and so it is also the unconditional error probability.

The performance difference between biphase and quadriphase spreading can be determined by comparison of (4.16) with (4.30). Because of the averaging over the $\{\phi_k\}$ necessary in (4.16), the differences are not immediately obvious. Further insight can be obtained if two special cases are considered. Firstly, let us restrict ourselves to the case where K = 2. The performance advantage of quadriphase over biphase spreading is shown in Fig. 4.3. The curve for biphase spreading was obtained via numerical integration. From the figure, we see that the performance advantage of quadriphase spreading over biphase spreading is 2 dB and that the advantage is independent of the ratio $\frac{E_b}{\sigma_I^2}$.

Now consider the case when K is large enough (i.e. K > 30 (Sunay and McLane, 1995a)) so that the MAI in (4.5) (with random ϕ_k's) may be considered Gaussian. In this case we can use the Gaussian approximation to obtain the BER for biphase spreading. To do so, we need to calculate the unconditional variance of the MAI which can be obtained by averaging (4.13) over uniformly distributed ϕ_k's:
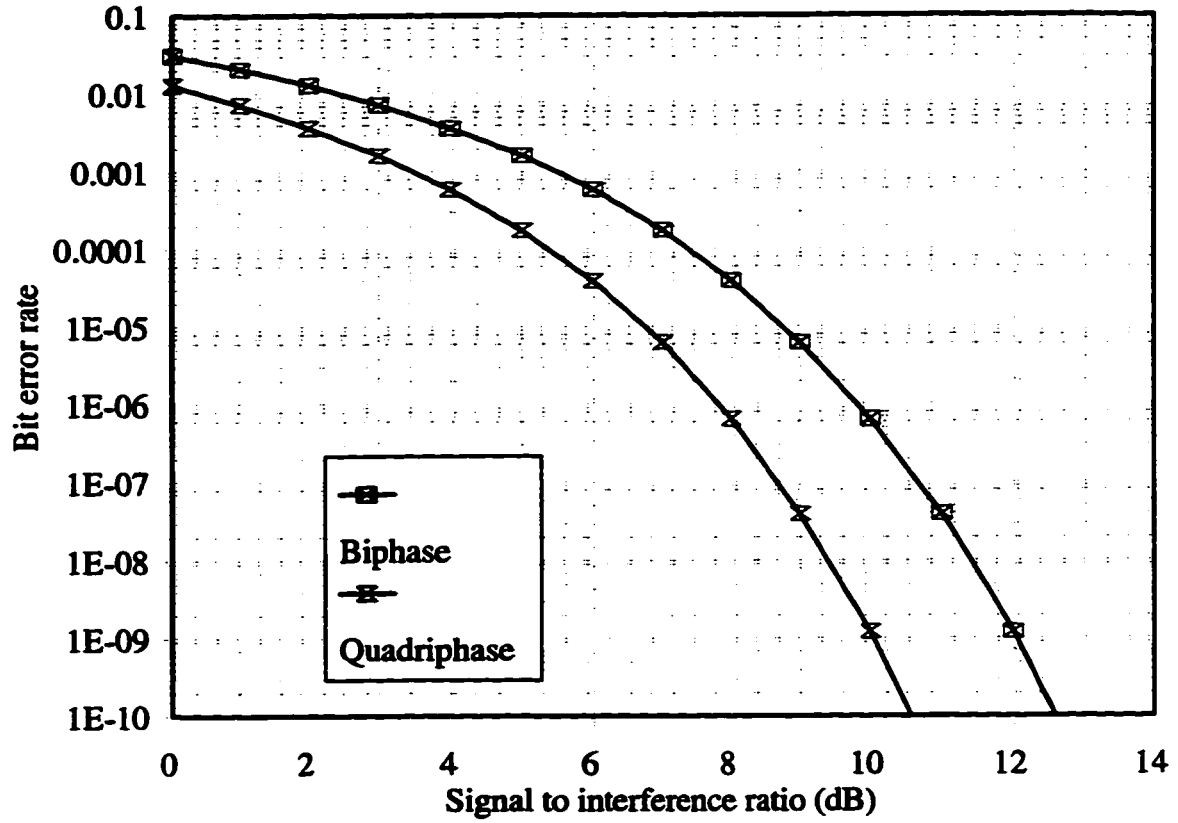
Fig. 4.3. The performance of the conventional matched filter receiver for various signal to interference ratios ($\frac{PT_s}{\sigma_I^2}$) for a two user system.

$$VAR(MAI) = \langle VAR(MAI|\phi_2,\phi_3,....,\phi_K)\rangle = \frac{(K-1)\sigma_I^2}{2T_s} .$$ \hfill (4.31)

The probability of error is then

$$P_{e,1} = \frac{1}{2}\text{erfc}\left\{\left[\frac{2PT_s}{(K-1)\sigma_I^2}\right]^{\frac{1}{2}}\right\} \qquad K > 30.$$ \hfill (4.32)

This is the same expression as that in (4.30). We thus conclude that when the number of users per cell is large so that the Gaussian approximation is valid, there is no capacity advantage with quadriphase spreading over biphase spreading, which is consistent with the

findings of Sunay and McLane (1995b). But when the number of users per cell is small, there is a distinct capacity advantage with quadriphase spreading.

4.5 Biphase vs quadriphase spreading with the RAMSIC receiver

The analysis in the preceding section showed that when the number of users is small, such that the MAI cannot be accurately modelled as a Gaussian random variable, quadriphase spreading has a significant advantage over biphase spreading. Since the capacity of the RAMSIC receiver with biphase spreading is not sufficient to enable the MAI to be accurately modelled as a   Gaussian random variable (Chapter 3), it is
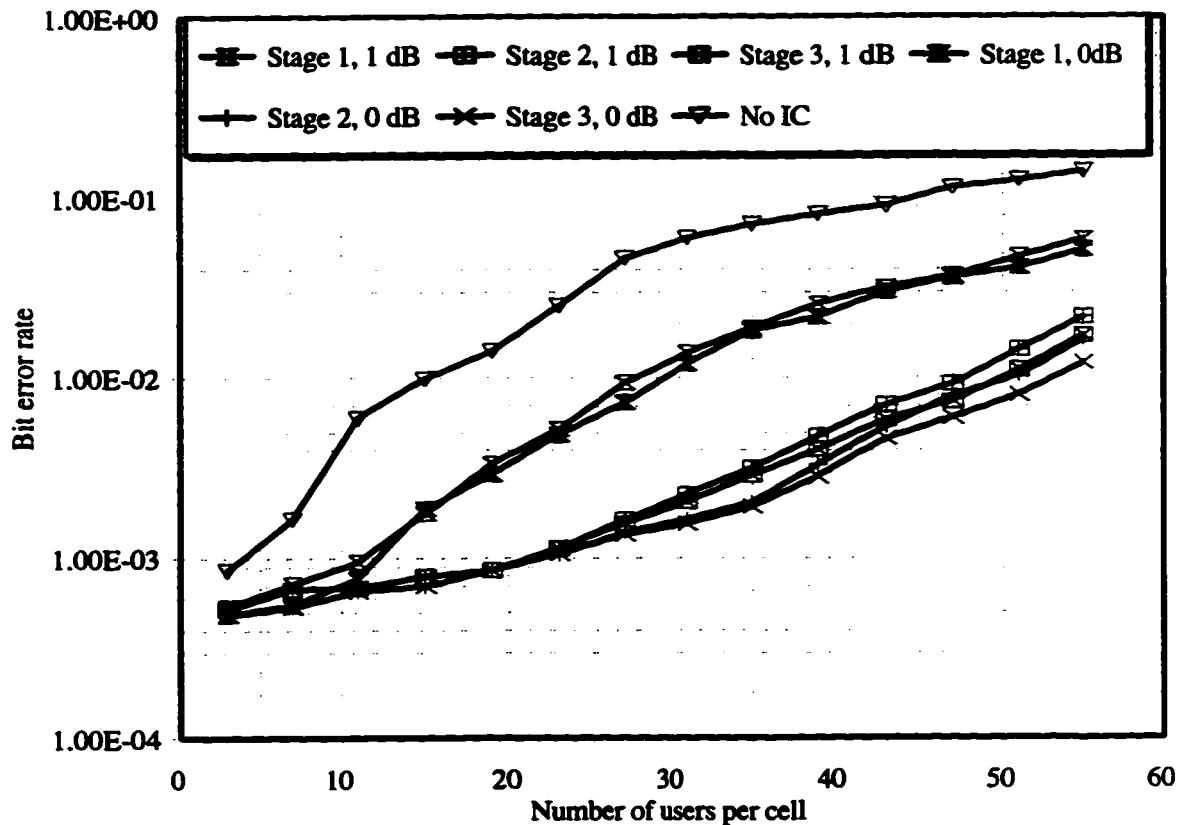
Fig. 4.4. Multi-cell (f = 0.55) performance of the RAMSIC receiver with quadriphase spreading under perfect and imperfect (σ_p = 1 dB) power control on a flat Rayleigh fading channel.

reasonable to expect that the capacity may be improved with quadriphase spreading. Moreover, channel estimation is also improved with quadriphase spreading because in the case of a large processing gain (as in the system considered here) the two sequences of samples of the channel provided to the estimation algorithm are nearly independent. Therefore, this section will investigate (by computer simulations) the performance of the RAMSIC receiver in a quadriphase spread BPSK modulated system. The specifics of the system simulated are the same as that specified in Section 3. The IS-95 transmitter gating mask is used for all results presented in this section.

The multi-cell performance of the RAMSIC receiver with quadriphase spreading and $f = 0.55$ under perfect and imperfect power control (with standard deviation of 1 dB) on a
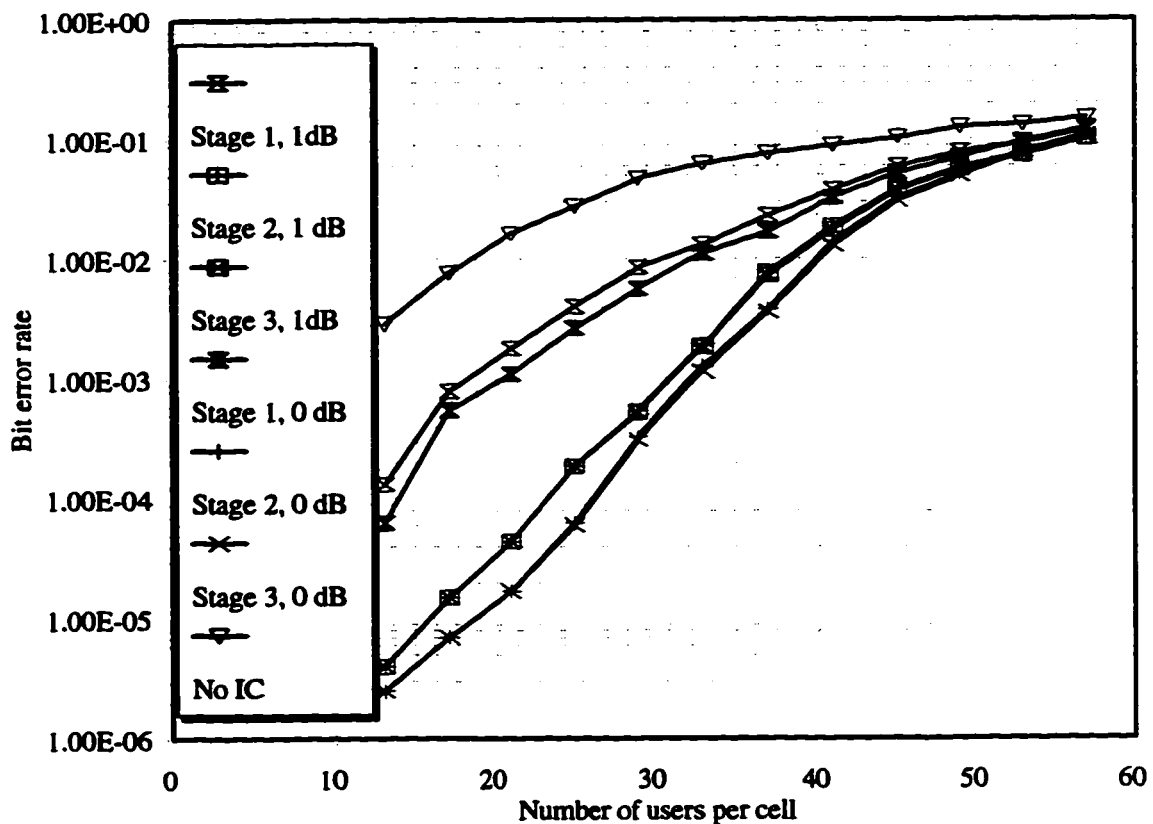
Fig. 4.5. Multi-cell performance of the RAMSIC receiver with quadriphase spreading for perfect and imperfect ($\sigma_p = 1$ dB) power control on a frequency selective Rayleigh fading channel with $f = 0.55$.

138

flat Rayleigh fading channel is shown in Fig. 4.4. It can be seen from the figure that increasing the number of cancellation stages beyond 2 results in a negligible increase in capacity. A similar observation was reported for biphase spread system in Chapter 3. At the bit error rate (BER) of 10^{-3}, the maximum number of users per cell is 23. Comparison with the results in Chapter 3 demonstrates a 1.4 fold increase in capacity. Imperfect power control decreases the capacity slightly to 21 users per cell. The performance improvement factor over biphase spreading, however, is increased to 1.6. This performance also compares very favourably with the capacity of 18 users per cell in the system described in Gilhousen et al. (1991). The capacity of a quadriphase DS-CDMA system with a RAMSIC receiver without any forward error correction coding is 1.17 times that reported there.
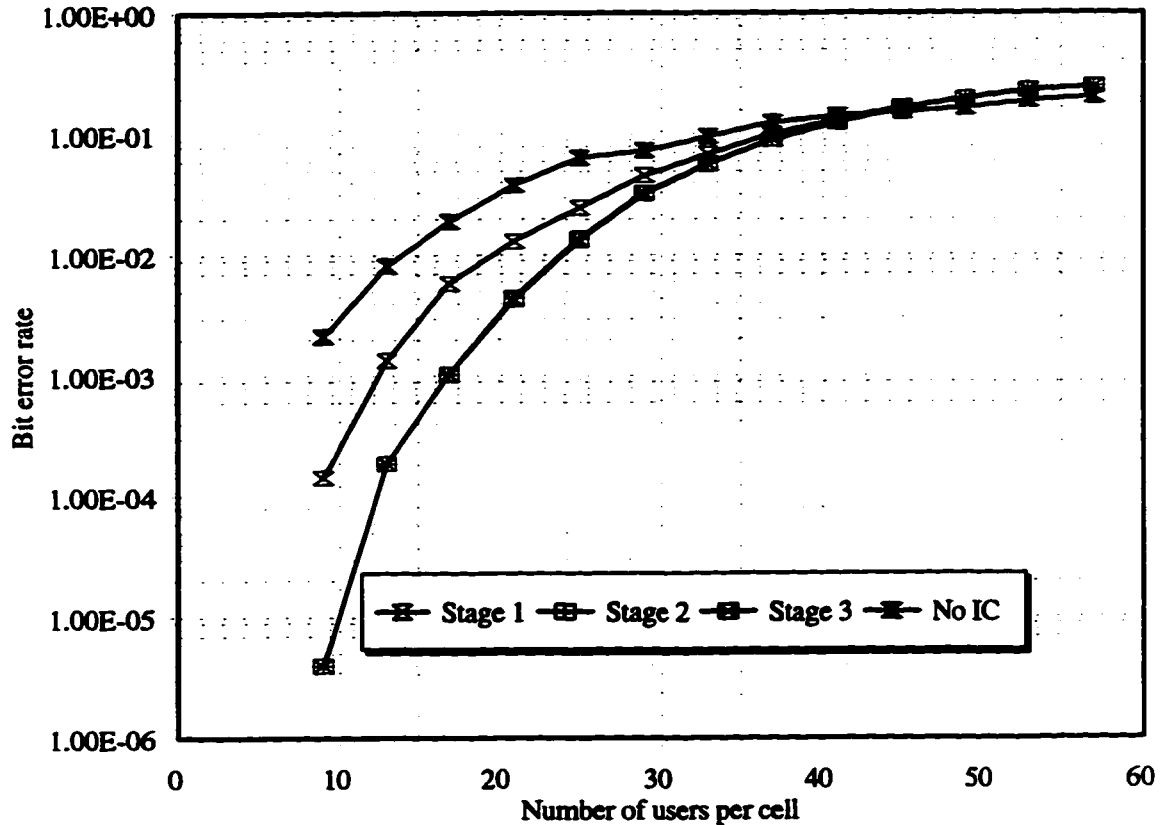
The performance of the RAMSIC receiver with quadriphase spreading on a frequency selective Rayleigh fading channel with perfect power control and $f = 0.55$ is shown in Fig. 4.5. The channel model consists of three independent Rayleigh fading paths of exponentially decaying average powers (0, -2, -4 dB). All three paths are assumed to be perfectly tracked by the RAKE receiver. It can be seen from the figure that increasing the number of cancellation stages beyond 2 does not increase the capacity. For a BER of 10^{-3}, the maximum number of users is 32 per cell. This represents a 1.4 fold increase in capacity over the biphase spreading system reported in Chapter 3. Performance of the same system using imperfect power control with standard deviation of 1 dB is also shown in the figure. For BER of 10^{-3}, the capacity drops to 31 users per cell which is a 1.6 fold increase over that reported in Chapter 3. Also, if we compare this number with 18 users per cell

reported in Gilhousen *et al.* (1991), we observe a 1.67 fold capacity increase without the use of forward error control coding.

Since the assumption of hexagonal cell configurations and path loss exponent of 4 may not be realistic, Fig. 4.6, 4.7 and 4.8 demonstrate the performance of the RAMSIC receiver on a flat Rayleigh fading channel for non-hexagonal cell shapes, quadriphase spreading, power control error standard deviation of 1 dB and path loss exponents of 4, 3 and 2 (or $f = 0.55$, 0.686 and 1.57 respectively). All other system parameters are as in Fig. 4.4. For a BER of 10^{-3}, the number of users per cell is 19, 13 and 10 respectively for path loss exponent of 4, 3 and 2. This compares very favourably with the capacity of at most 3 users per cell without interference cancellation. Performance without interference
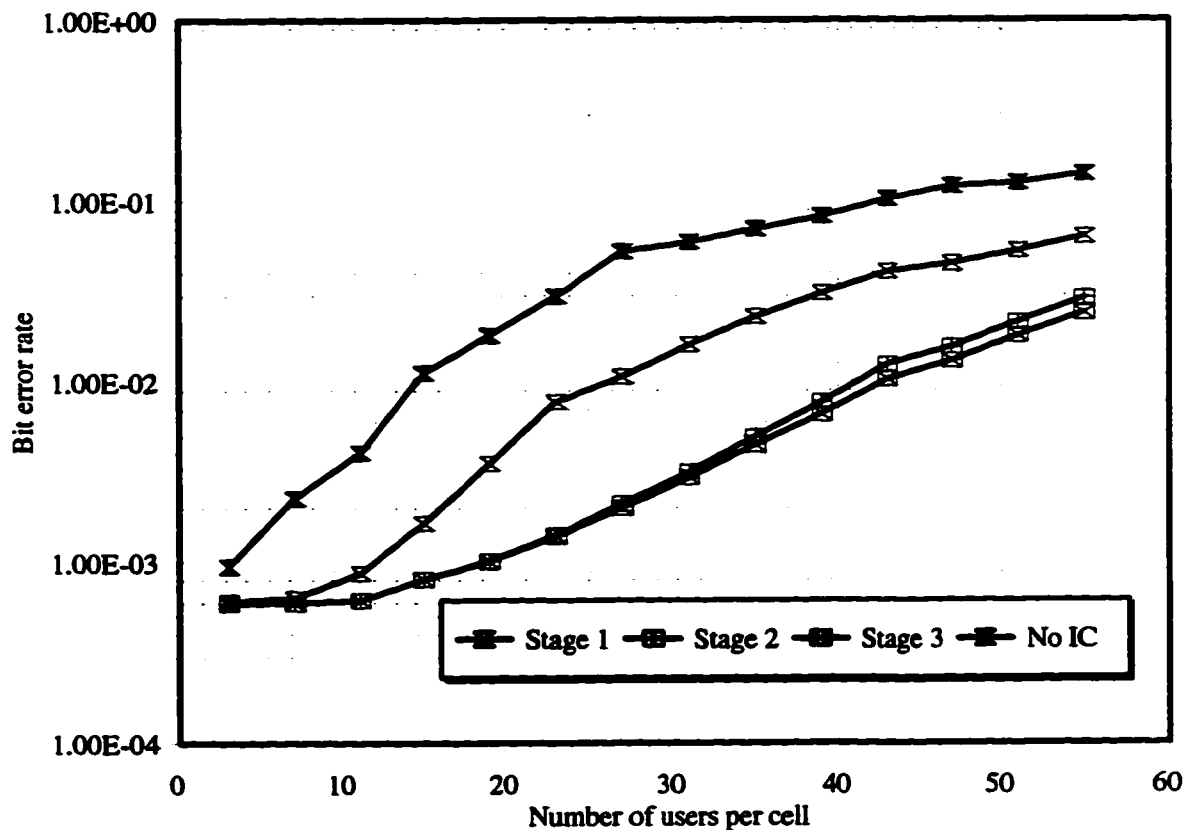
Fig. 4.6. Multi-cell performance of a RAMSIC receiver with quadriphase spreading on a flat Rayleigh fading channel with f = 0.686. Power control is non ideal with σ_p = 1.0 dB.

140

cancellation is very poor because channel estimates are severely corrupted by multi-user interference. As can be seen in the figures, system capacity does not increase when the number of interference cancellation stages is increased beyond two. The capacity improvements over the RAMSIC receiver with biphase spreading are shown in Table 4.4.

Performance of the RAMSIC receiver on a frequency selective Rayleigh fading channel for nonhexagonal cells, quadriphase spreading, power control error standard deviation of 1 dB and path loss exponents of 4, 3 and 2 (or $f = 0.55$, 0.686, and 1.57 respectively) is given in Fig. 4.9, 4.10 and 4.11, respectively. All other system parameters are as in Fig. 4.4. The maximum number of users per cell for a BER of 10^{-3}, is 27, 23 and
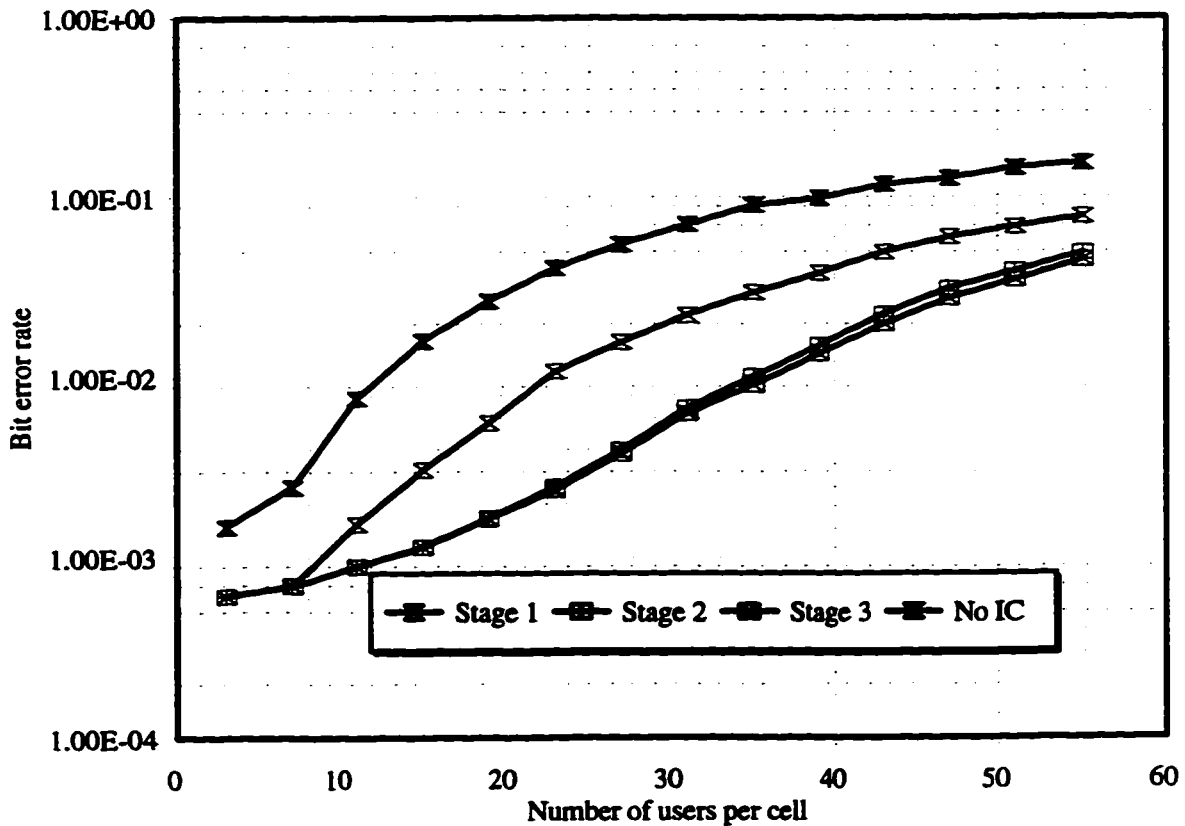
Fig. 4.7. Multi-cell performance of a RAMSIC receiver with quadriphase spreading on a flat Rayleigh fading channel with f = 0.959. Power control is non ideal with $\sigma_p = 1.0$ dB.

17. It can also be seen that there is no increase in capacity when the number of cancellation stages is increased beyond two. The capacity improvements over the RAMSIC receiver with biphase spreading can be found in Table 4.4.

Sensitivity of the system with quadriphase spreading to power control error of

Table 4.4: Performance improvement factor of the RAMSIC receiver with quadriphase spreading over that with biphase spreading for various power control errors. Both flat and frequency selective Rayleigh fading channel results are shown.

	Capacity increase factor at BER $= 10^{-3}$									
	Flat Rayleigh fading channel					Frequency selective Rayleigh fading channel				
f	$\sigma_p = 0.7$	1.0	1.6	2.2	2.9	$\sigma_p = 0.7$	1.0	1.6	2.2	2.9
0.55	1.5	1.6	1.5	1.7	1.5	1.4	1.5	1.5	1.5	1.4
0.686	1.5	1.7	1.6	1.7	1.5	1.5	1.6	1.5	1.5	1.6
0.959	1.6	1.6	2.0	2.0	1.5	1.6	1.6	1.7	1.7	1.6
1.57	1.8	2.0	1.6	2.0*	1.5	1.7	1.6	1.8	1.7	1.5

This factor is really 1.6 if the capacity is allowed to be a real number.
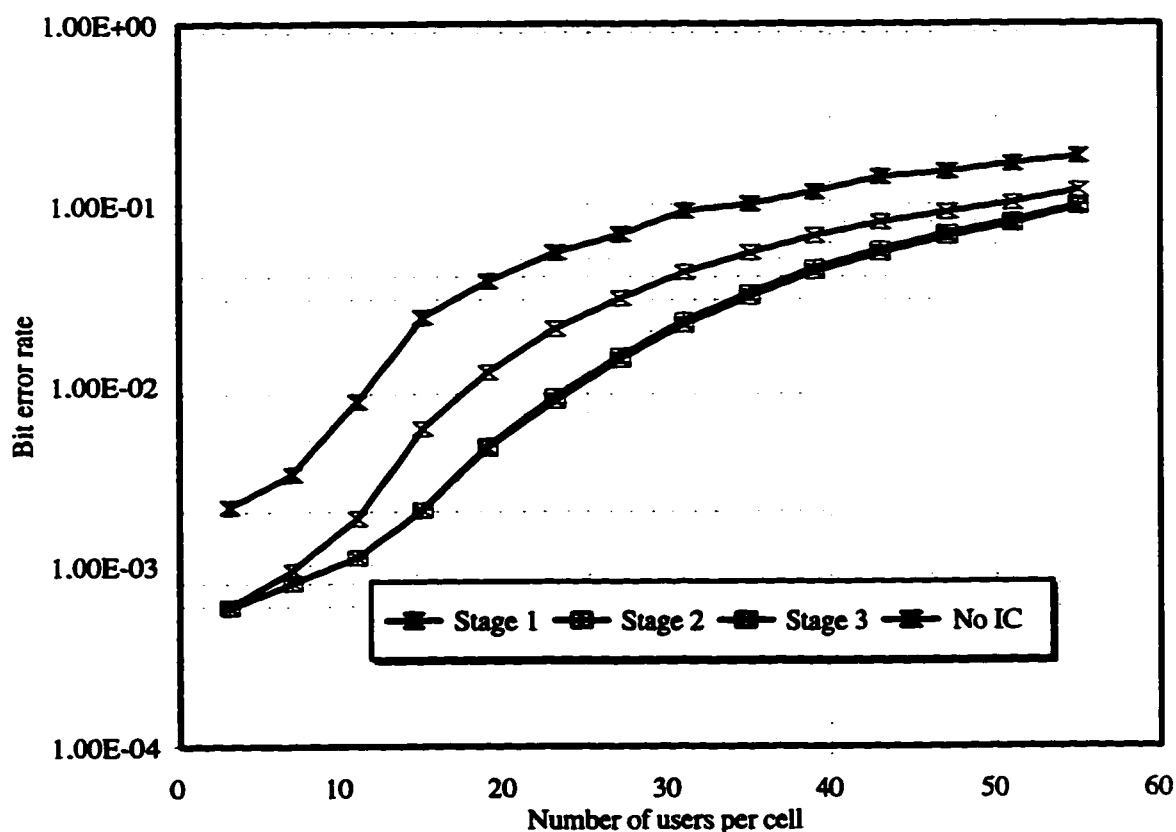
Fig. 4.8. Multi-cell performance of a RAMSIC receiver with quadriphase spreading on a flat Rayleigh fading channel with f = 1.57. Power control is non ideal with σ_p = 1.0 dB.

various standard deviations, σ_p, operating on both flat and frequency selective Rayleigh fading channel is shown in Table 4.5. The performance curves used for the construction of the table can be found in Appendix 4D. Clearly, the capacity of the system decreases with increasing σ_p. The capacity improvement factor over that of systems with biphase spreading is shown in Table 4.4. It can be seen from the table that the capacity improvement factor in most cases increases somewhat with increasing f and increasing σ_p. This is because transmission of a reference symbol in both the in-phase and quadrature channel provides the channel estimation algorithm with two sequences of channel samples. This allows for better estimation and thus better detection and cancellation. It should be noted that when both multiple access noise and power control variance are large, even this improved estimation mechanism of the channel parameters is not quite able to track the channel accurately and the performance increase factor decreases.

Sensitivity of the system with quadriphase spreading to synchronization errors is shown in Table 4.6. The performance curves can be found in Appendix 4E. It can be seen from the table that increasing synchronization error decreases the capacity of the system in a nonlinear fashion, and that the performance loss is similar for both the flat and frequency selective Rayleigh fading channels. An understanding of the differences in sensitivity of the

Table 4.5: System capacity with the RAMSIC receiver and quadriphase spreading for various power control errors. Both flat and frequency selective Rayleigh fading channel results are shown. The IS95 mask is used and ideal synchronization is assumed.

| | Number of users per cell at BER $= 10^{-3}$ | | | | | | | | | | |
| | Flat Rayleigh fading channel | | | | | Frequency selective Rayleigh fading channel | | | | | |
f	$\sigma_p = 0.0$	0.7	1.0	1.6	2.2	2.9	$\sigma_p = 0.0$	0.7	1.0	1.6	2.2	2.9
0.55	22	21	21	15	12	3	32	31	31	27	23	17
0.686	20	19	19	14	10	3	29	28	27	24	20	16
0.959	16	15	13	12	8	3	25	24	23	20	17	13
1.57	11	11	10	8	6	3	18	17	17	14	12	9

biphase and quadriphase spread systems to synchronization, the results of Table 4.6 can be compared with those of Table 4.3. It can be readily seen that the performance loss as measured by the decrease in capacity is greater with quadriphase spreading. However, when the capacity decrease is normalized by the capacity of the system without any synchronization error, the sensitivity of biphase and quadriphase spreading systems to synchronization error is approximately the same. Therefore, it can be concluded that the synchronization error has the same effect in both systems. Moreover, Table 4.6 also shows that synchronization errors in the range acceptable for effective spread spectrum communication have no significant effect on capacity.
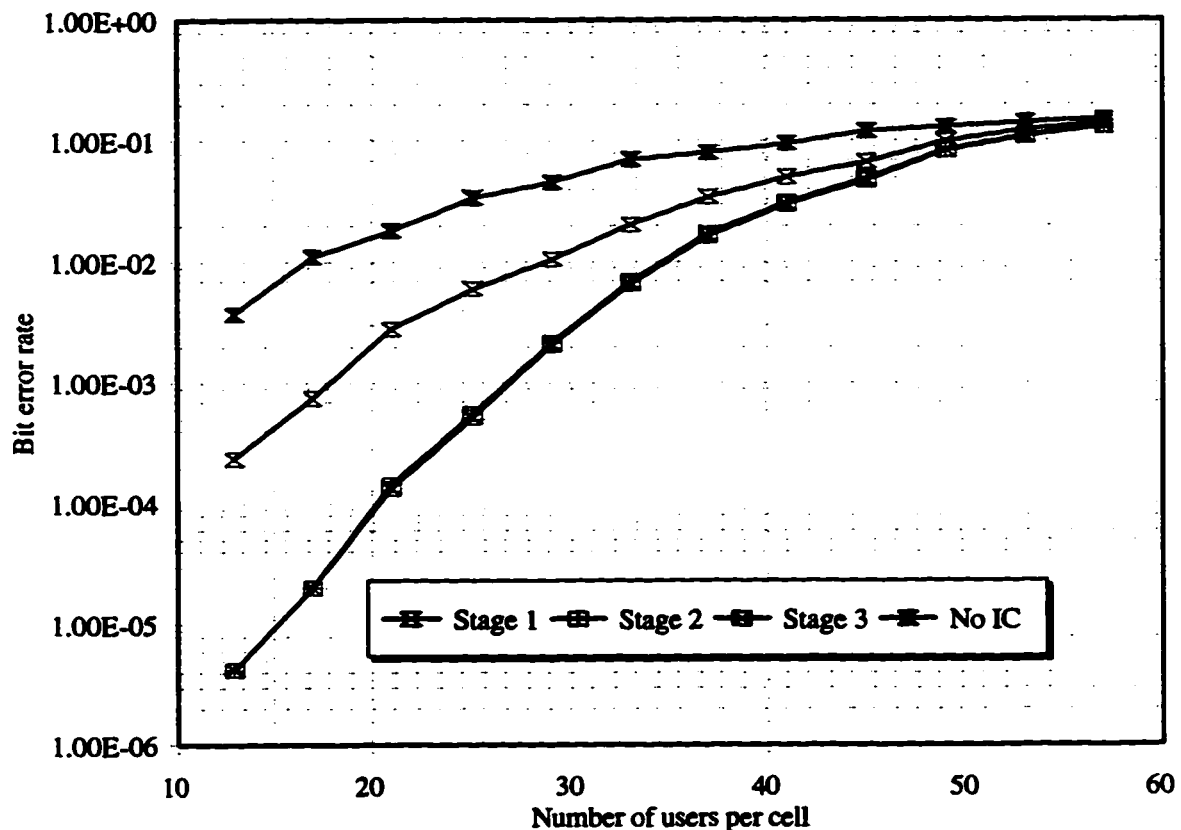
Fig. 4.9. Multi-cell performance of a RAMSIC receiver with quadriphase spreading on a frequency selective Rayleigh fading channel with f = 0.686. Power control is non ideal with σ_p = 1.0 dB.
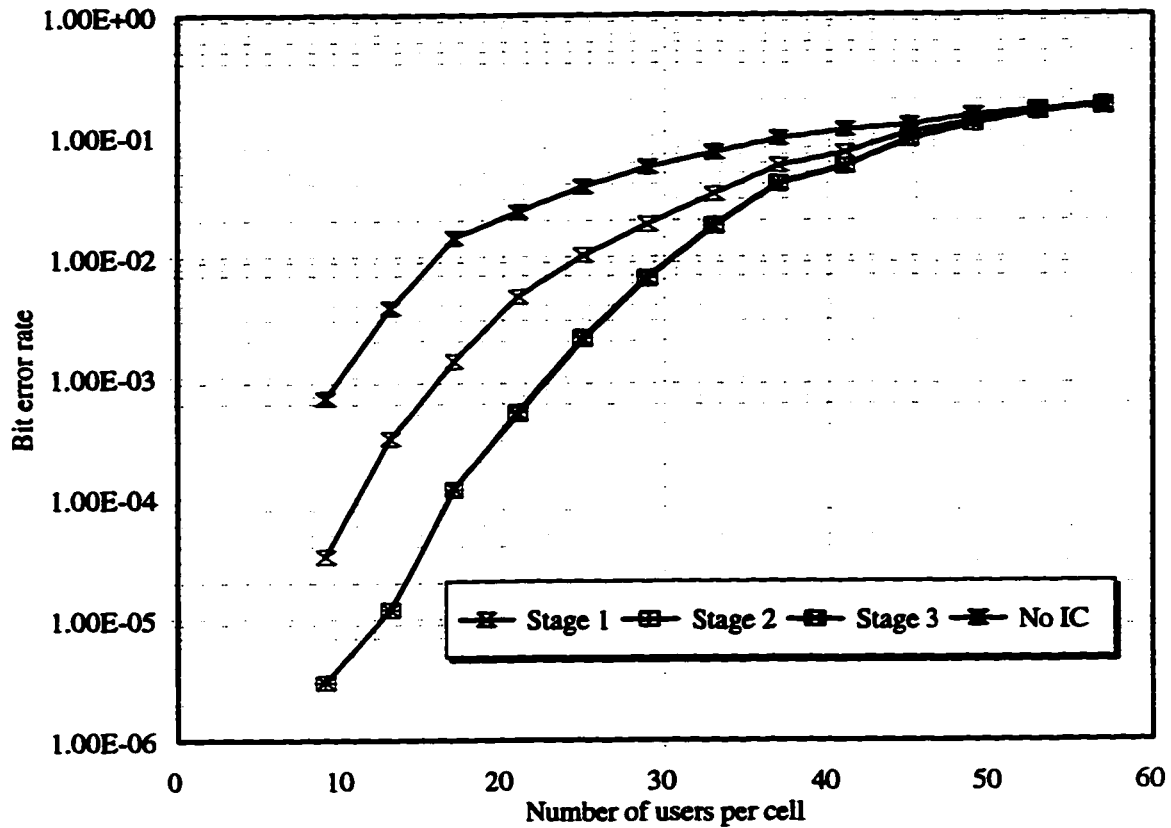
Fig. 4.10. The multi-cell performance of a RAMSIC receiver with quadriphase spreading on a frequency selective Rayleigh fading channel with f = 0.959. Power control is non ideal with σ_p = 1.0 dB.

Table 4.6: System capacity with the RAMSIC receiver and quadriphase spreading for various synchronization errors (ϵ). Both flat and frequency selective Rayleigh fading channel results are shown. The standard deviation of the power control error is 1.0 dB and the IS95 mask is used.

	Number of users per cell at BER = 10^{-3}									
	Flat Rayleigh fading channel					Frequency selective Rayleigh fading channel				
f	$\epsilon{=}0.0T_c$	$0.05\ T_c$	$0.1\ T_c$	$0.15\ T_c$	$0.2\ T_c$	$\epsilon{=}0.0\ T_c$	$0.05\ T_c$	$0.1\ T_c$	$0.15\ T_c$	$0.2\ T_c$
0.55	21	20	18	16	15	31	31	30	29	27
0.686	19	17	15	15	13	27	27	26	25	24
0.959	13	13	12	12	11	23	22	22	21	20
1.57	10	9	9	8	8	17	17	16	16	15

145

Fig. 4.11. The multi-cell performance of a RAMSIC receiver with quadriphase spreading on a frequency selective Rayleigh fading channel with f = 1.57. Power control is non ideal with σ_p = 1.0 dB.

4.6 Discussion and conclusion

Sensitivity of the reference symbol assisted multistage successive interference cancelling receiver (RAMSIC) with biphase as well as quadriphase spreading to various system imperfections has been investigated in this Chapter. For a biphase spread system, the results show that capacity with the transmitter gating as specified in the IS-95 standard is almost the same as that with idealized gating. Moreover, the capacity with a even more relaxed transmitter gating specification is decreased only slightly for path loss exponent 4, while there is no capacity reduction for other path loss exponents. Results concerning the sensitivity of the system to power control errors show that the capacity decreases with

increasing power control error and that the system cannot support more than 2 users on a flat fading channel with power control error standard deviation of 2.9 dB. This result strongly suggests that, for flat fading channels, some form of diversity (e.g. antenna diversity) should be employed to decrease the power control error in a practical system. Investigation into the sensitivity of the system to synchronization errors shows that there is no significant effect on the capacity, if the errors are of reasonable magnitude. This implies that conventional chip synchronization algorithms will perform adequately with successive interference cancelling receivers.

A significant increase in capacity is demonstrated for the case of quadriphase spread system. The traffic capacity without any forward error correction coding is between 1.17 and 1.67 times that in Gilhousen *et al.* (1991). It has also been shown that the RAMSIC receiver provides significant capacity even when the path loss exponent is 2. In the presence of synchronization errors, the performance loss is similar to that for the biphase spread system. Investigation into the sensitivity of the system to imperfect power control shows that the system capacity decreases with increasing power control error and that the performance improvement factor over biphase spreading is between 1.4 and 2.0. For power control error standard deviation of 2.9 dB on a flat fading channel, the system cannot support more than 3 users per cell. This suggest that although quadriphase spreading improves channel estimation, it is not sufficient, in this case, to offset the poor power control. Additional diversity should be introduced to decrease the power control error for the flat fading channel. Antenna diversity, or even better, adaptive beamforming, are prime candidates to be exploited because of their additional advantage over time

diversity of not introducing self interference. This should allow for much better channel

estimates for interference cancellation and hence result in even higher capacity.

4.7 Appendix 4A

This appendix presents the performance curves for the RAMSIC receiver on flat and frequency selective fading channels with different amplifier masks.
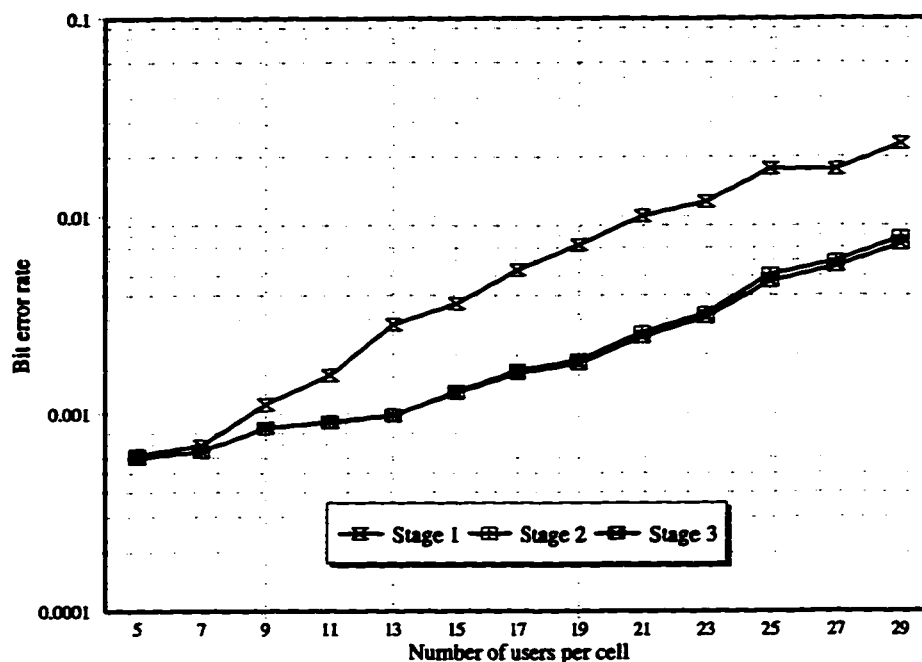
Fig. 4.A.1. The multi-cell performance of a RAMSIC receiver on a flat fading channel with f = 0.55. The transmitter power amplifier is gated according to the IS-95 mask.
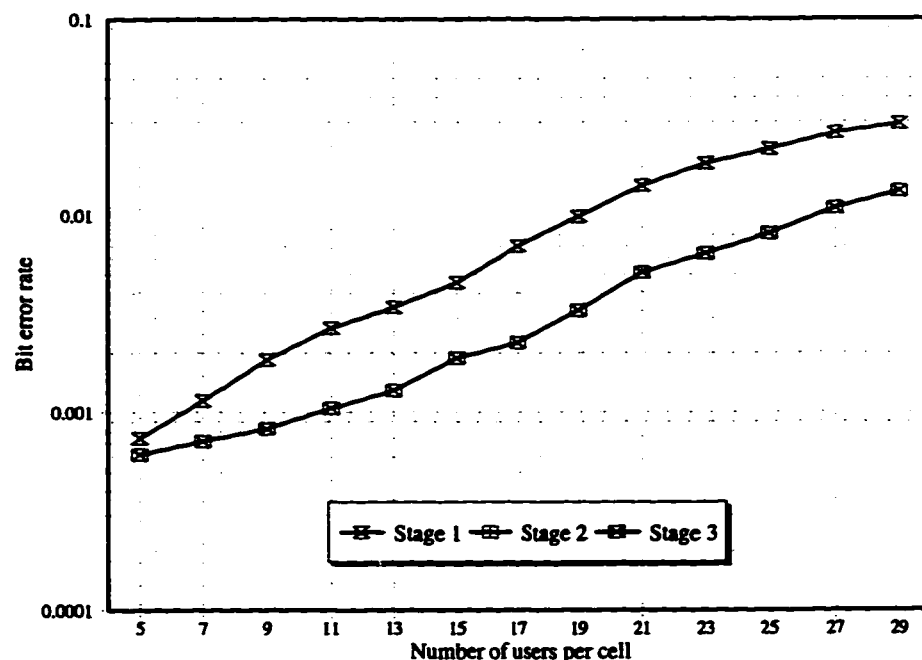
Fig. 4.A.2. The multi-cell performance of a RAMSIC receiver on a flat fading channel with f = 0.686. The transmitter power amplifier is gated according to the IS-95 mask.

149
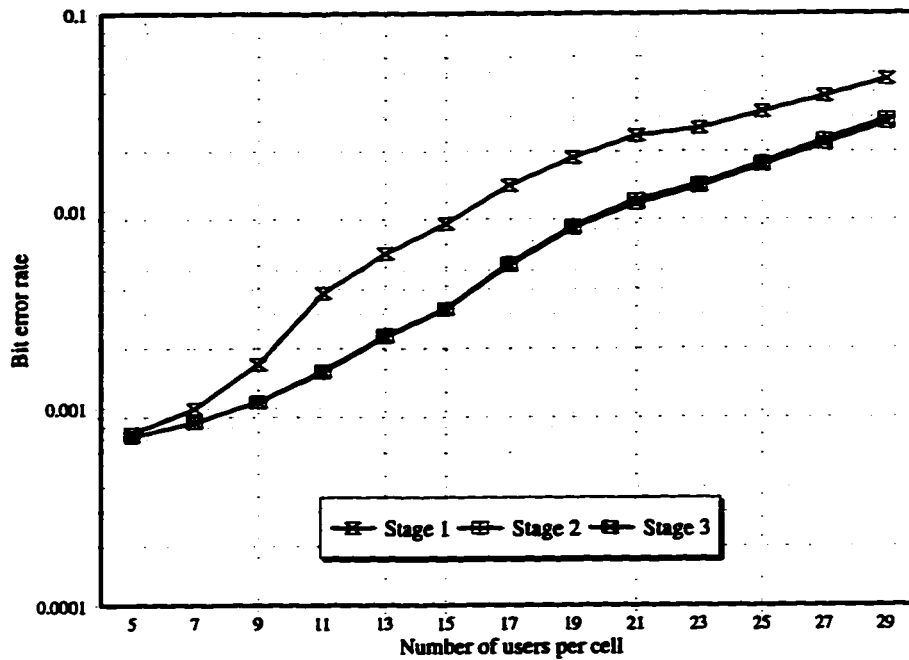
Fig. 4.A.3. The multi-cell performance of a RAMSIC receiver on a flat fading channel with f = 0.959. The transmitter power amplifier is gated according to the IS-95 mask.
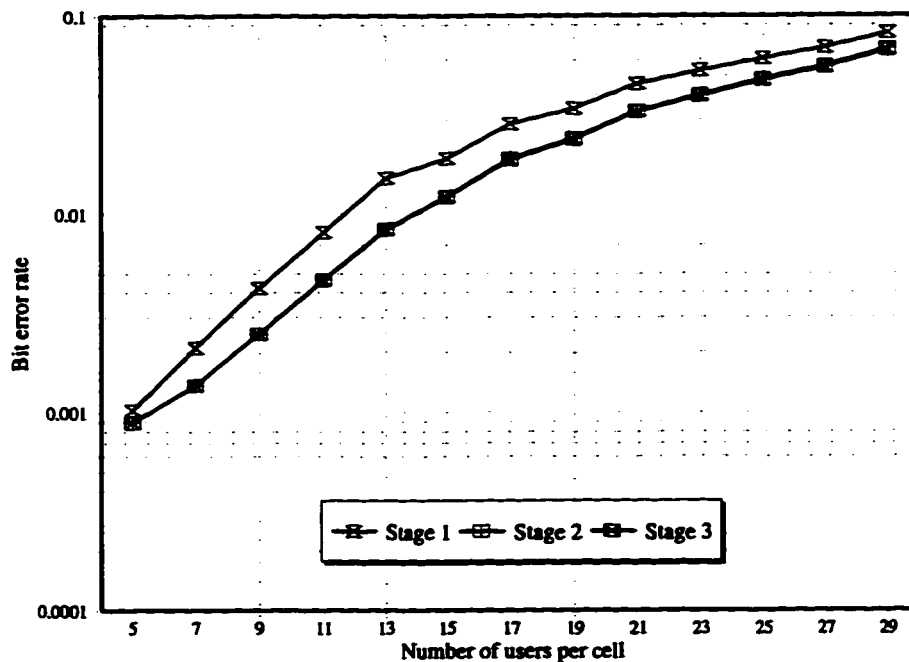
Fig. 4.A.4. The multi-cell performance of a RAMSIC receiver on a flat fading channel with f = 1.57. The transmitter power amplifier is gated according to the IS-95 mask.

150
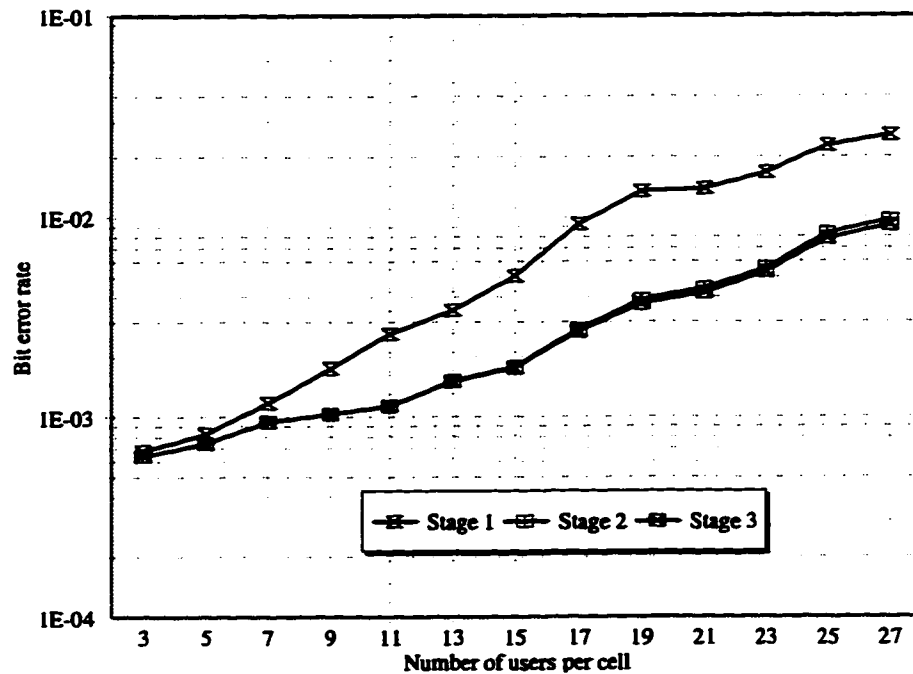
Fig. 4.A.5. The multi-cell performance of a RAMSIC receiver on a flat fading channel with f = 0.55. The transmitter power amplifier is gated according to the RTG mask.
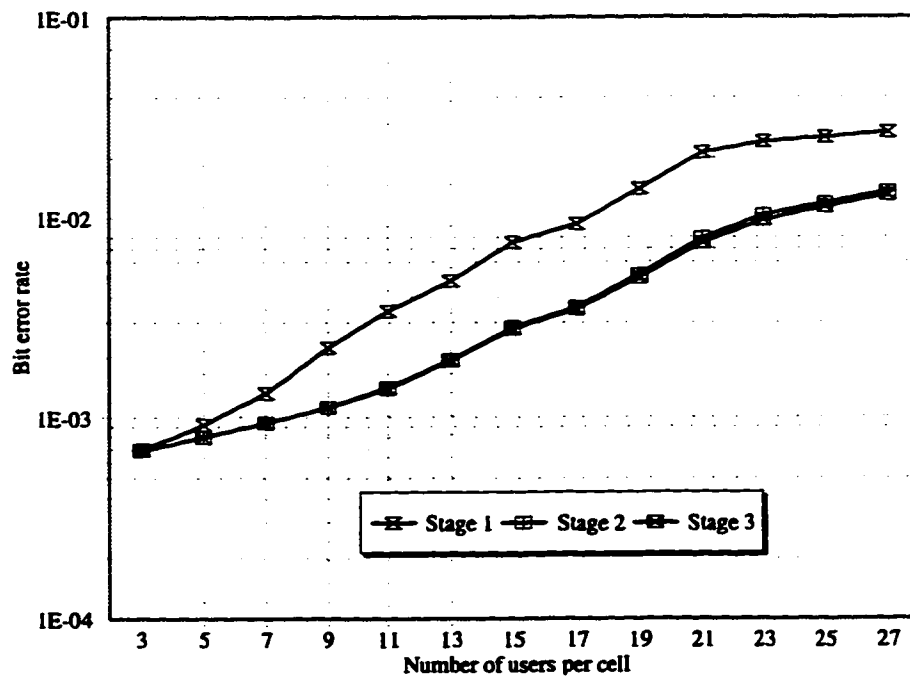
Fig. 4.A.6. The multi-cell performance of a RAMSIC receiver on a flat fading channel with f = 0.686. The transmitter power amplifier is gated according to the RTG mask.
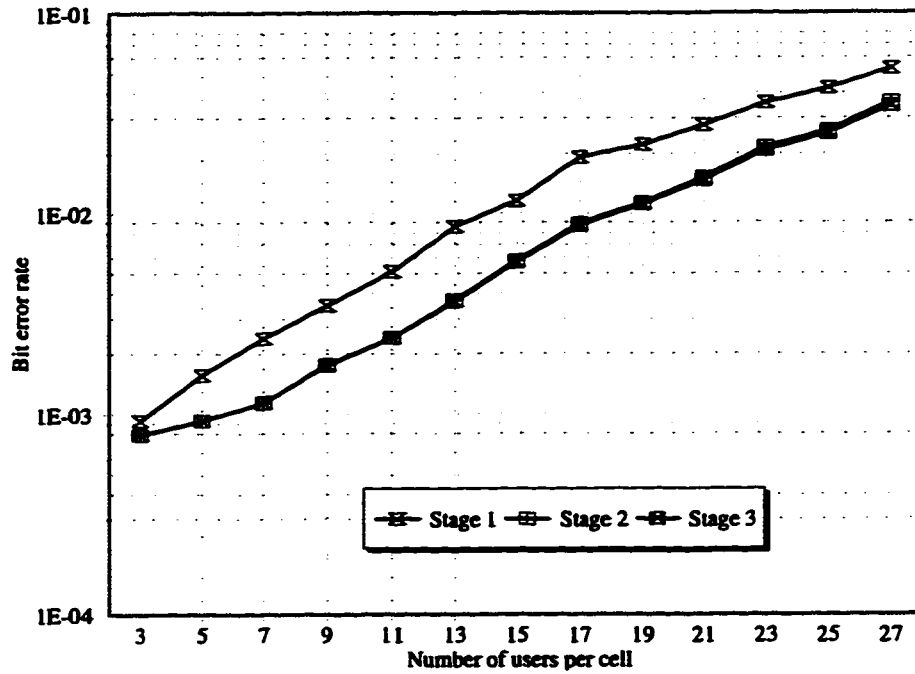
Fig. 4.A.7. The multi-cell performance of a RAMSIC receiver on a flat fading channel with f — 0.959. The transmitter power amplifier is gated according to the RTG mask.
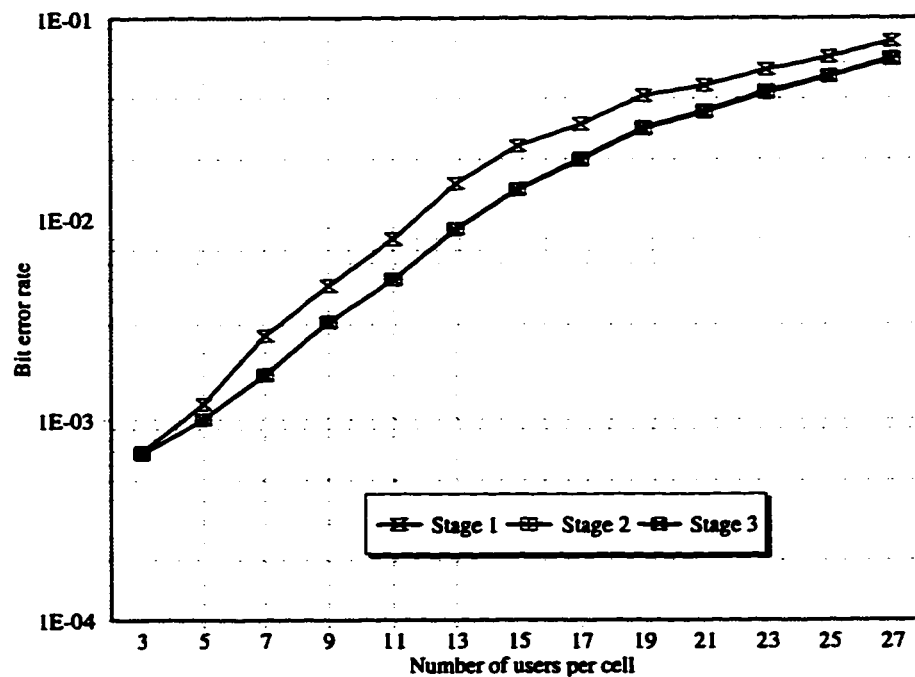
Fig. 4.A.8. The multi-cell performance of a RAMSIC receiver on a flat fading channel with f — 1.57. The transmitter power amplifier is gated according to the RTG mask.
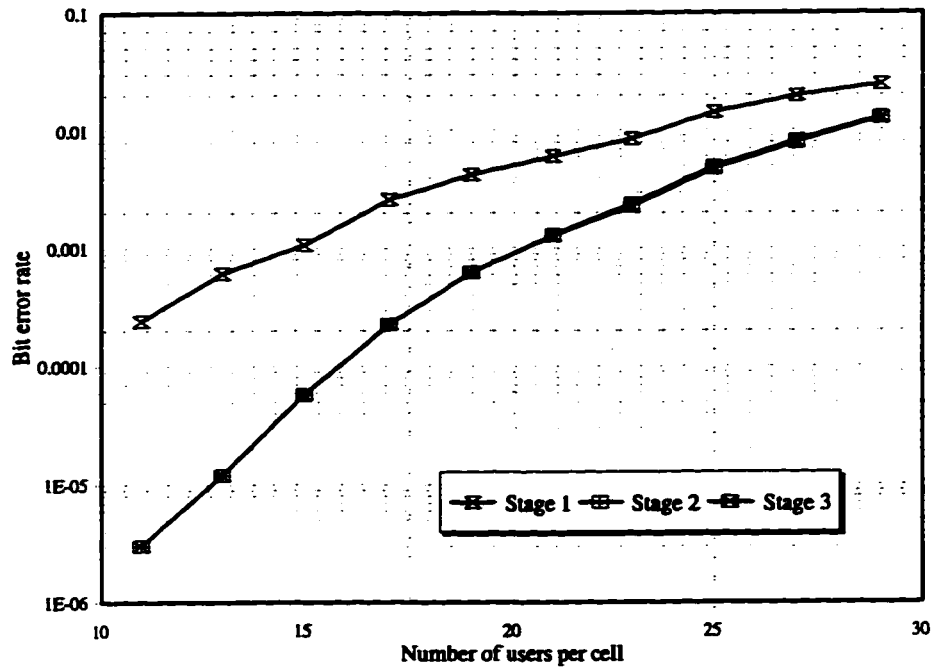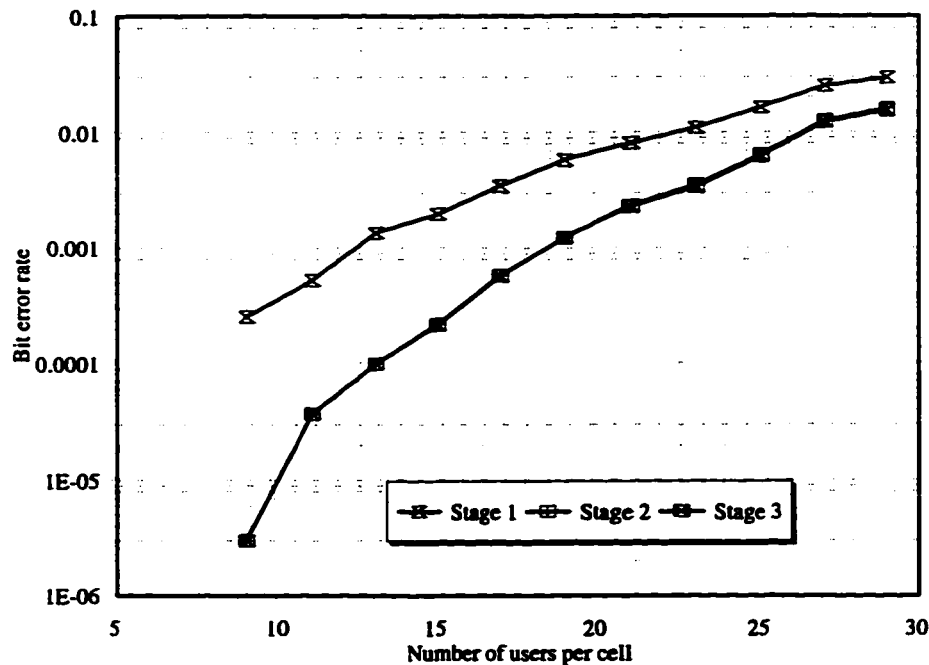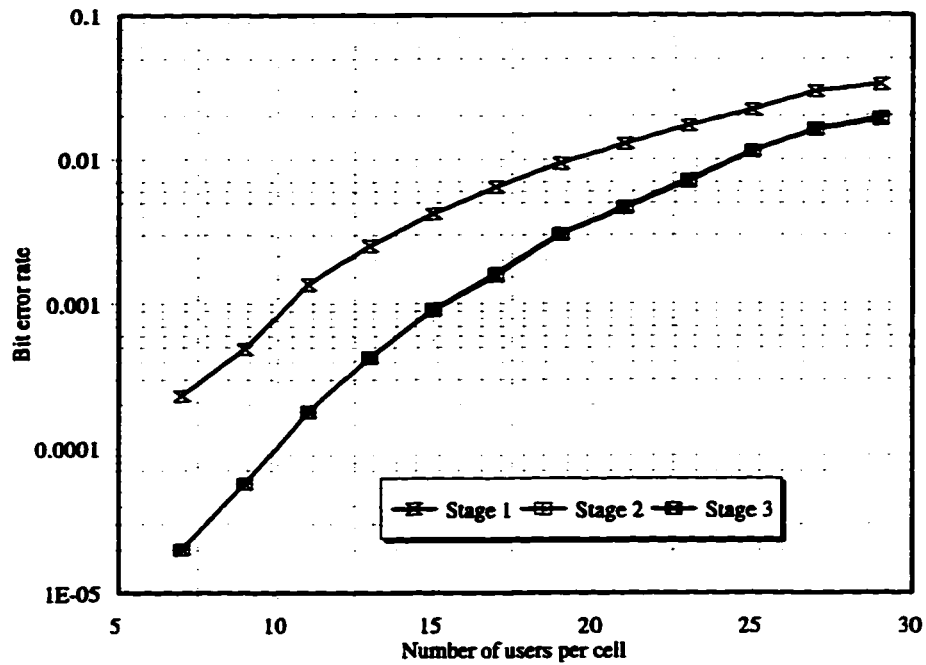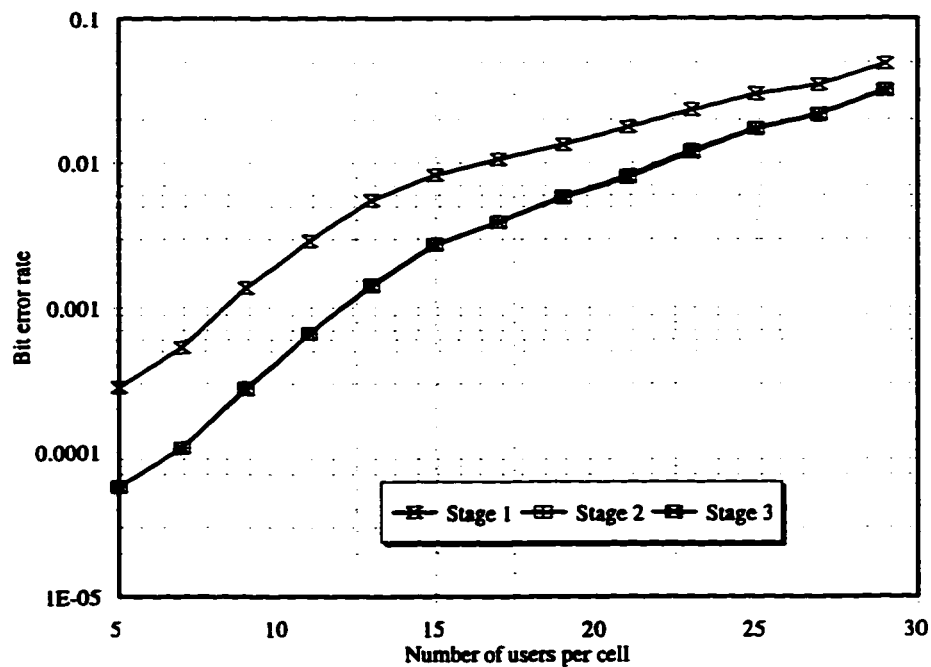
Fig. 4.A.9. The multi-cell performance of a RAMSIC receiver on a frequency selative Rayleigh fading channel with f = 0.55. The transmitter power amplifier is gated according to the IS-95 mask.
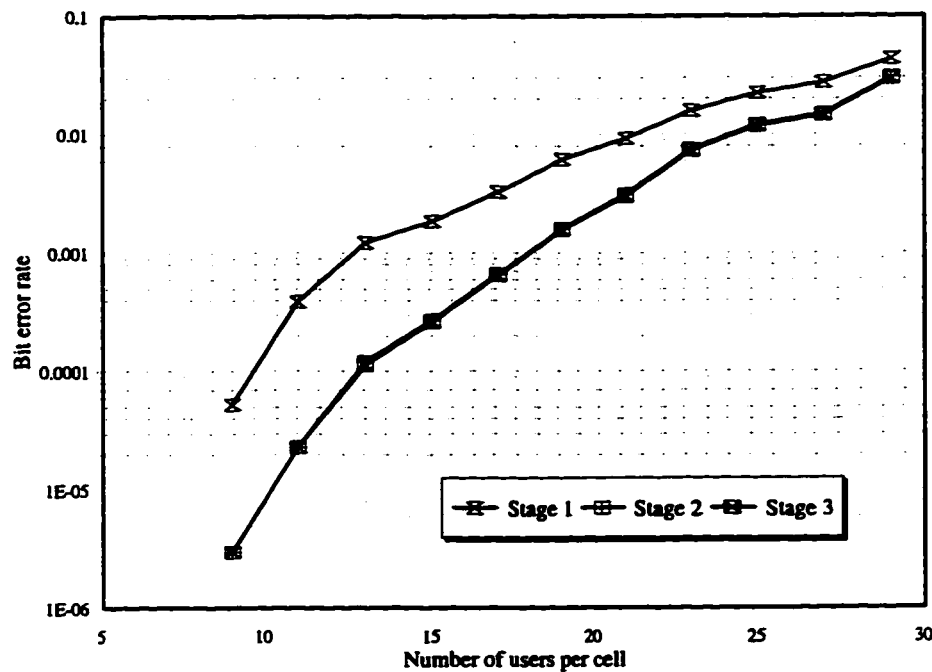
Fig. 4.A10. The multi-cell performance of a RAMSIC receiver on a frequency selative Rayleigh fading channel with f = 0.686. The transmitter power amplifier is gated according to the IS-95 mask.
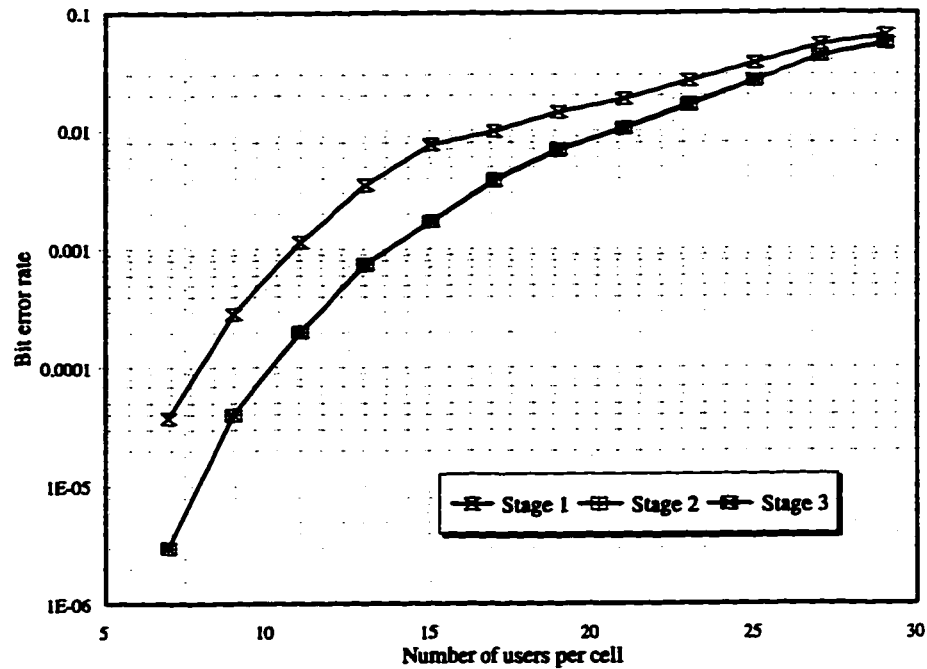
Fig. 4.A.11. The multi-cell performance of a RAMSIC receiver on a frequency selative Rayleigh fading channel with f = 0.959. The transmitter power amplifier is gated according to the IS-95 mask.
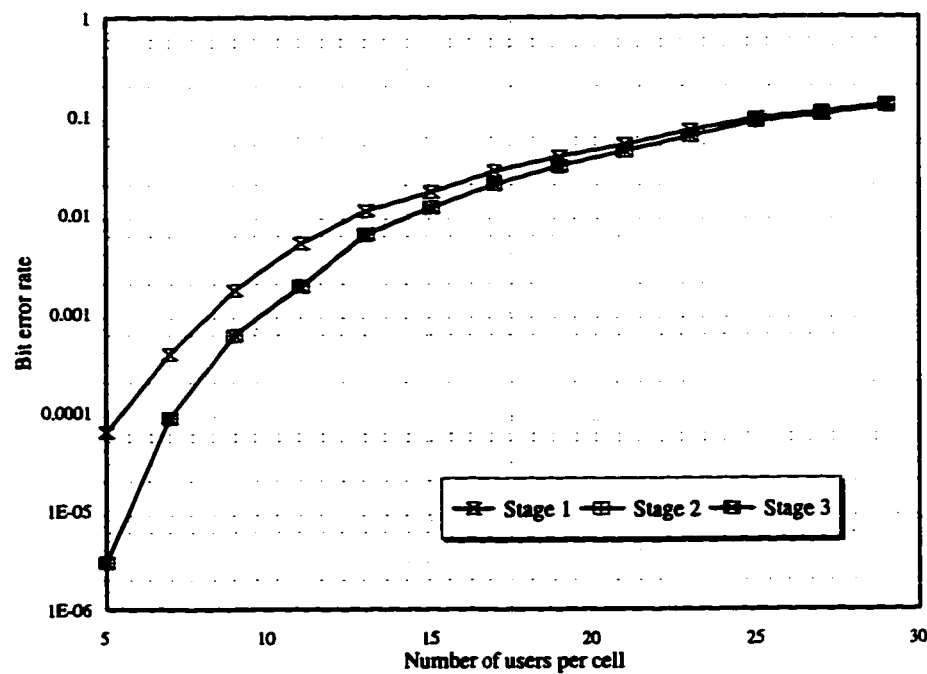
Fig. 4.A.12. The multi-cell performance of a RAMSIC receiver on a frequency selative Rayleigh fading channel with f = 1.57. The transmitter power amplifier is gated according to the IS-95 mask.
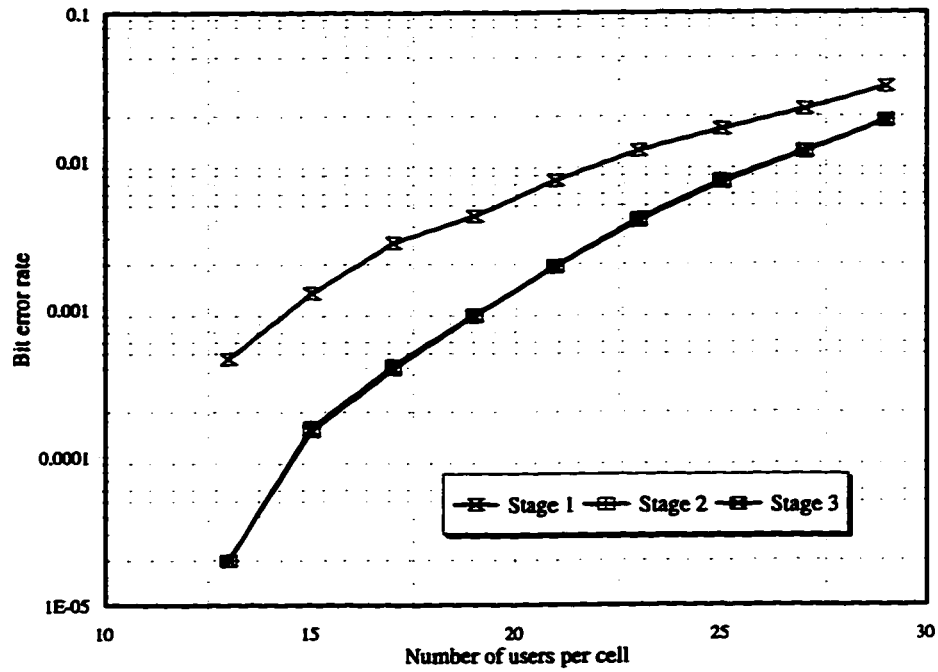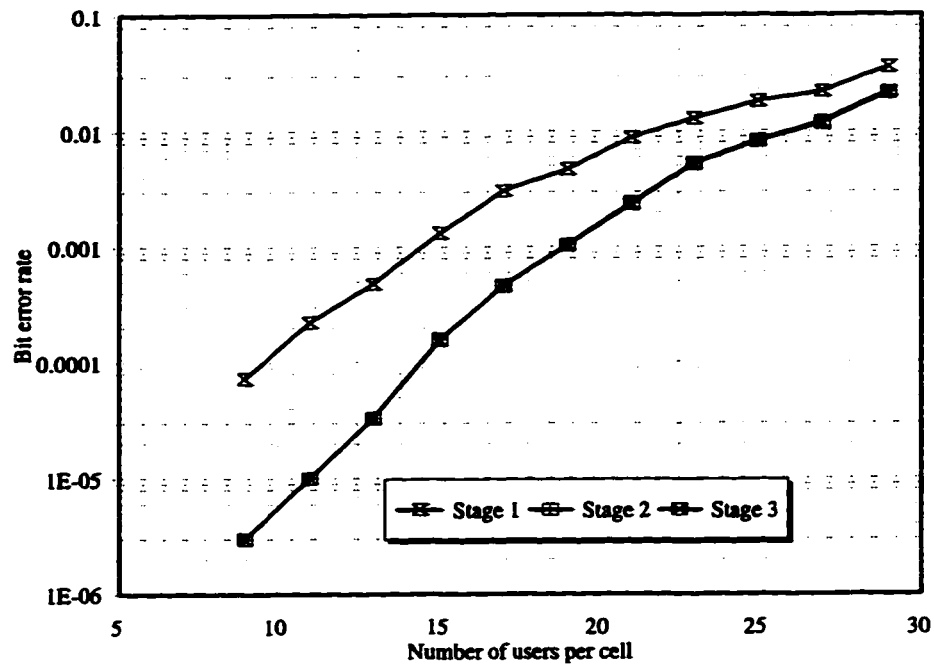
Fig. 4.A.13. The multi-cell performance of a RAMSIC receiver on a frequency selative Rayleigh fading channel with f = 0.55. The transmitter power amplifier is gated according to the RTG mask.
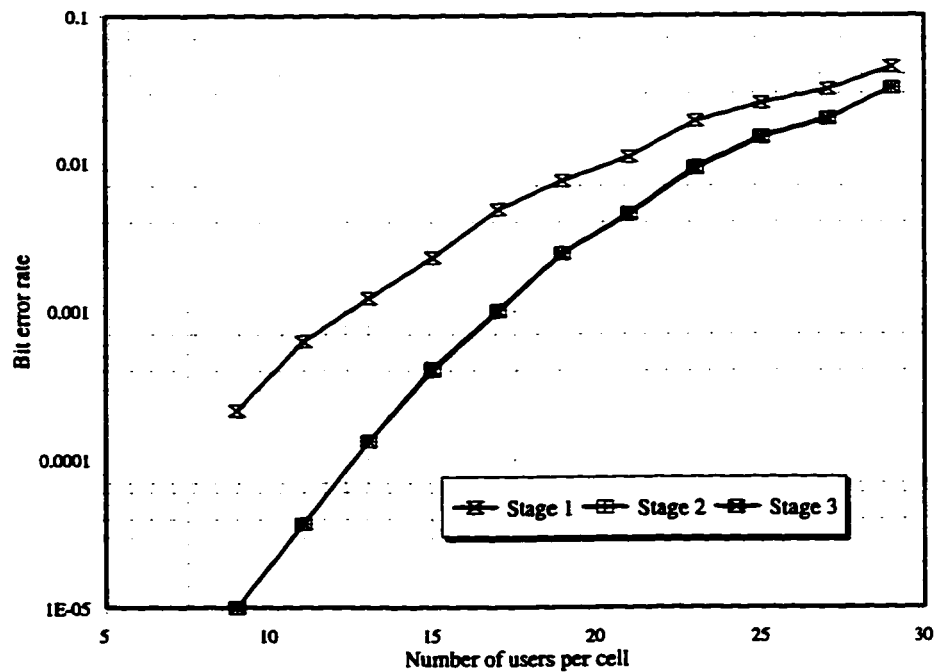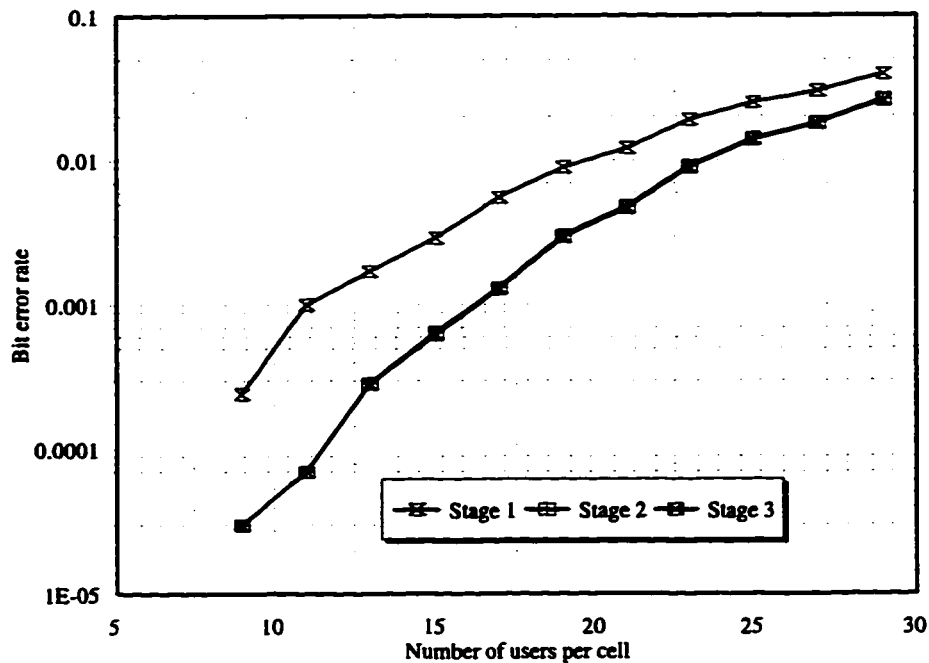

Fig. 4.A.14. The multi-cell performance of a RAMSIC receiver on a frequency selative Rayleigh fading channel with f = 0.686. The transmitter power amplifier is gated according to the RTG mask.
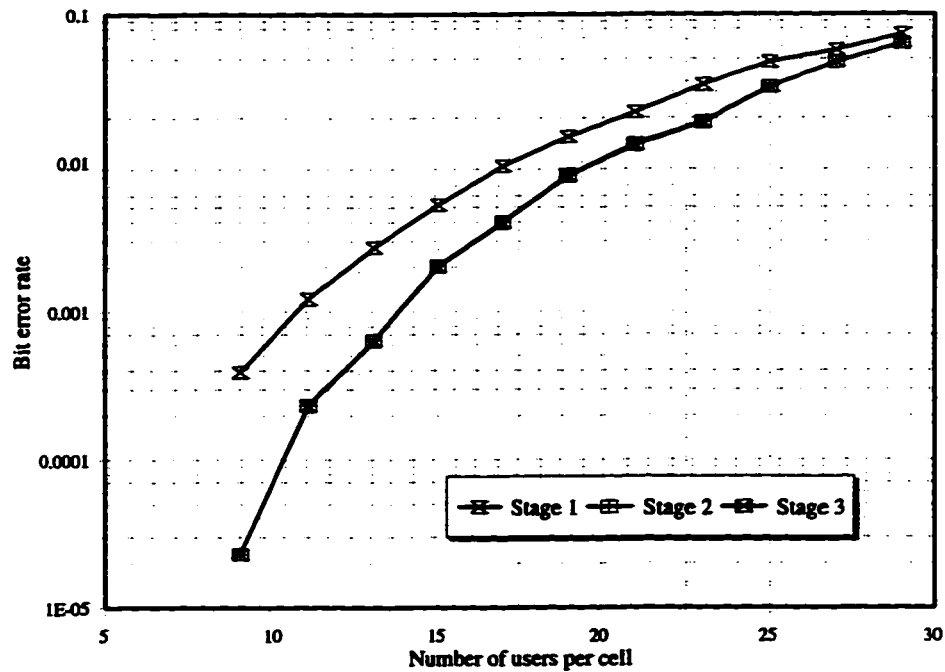
Fig. 4.A.15. The multi-cell performance of a RAMSIC receiver on a frequency selative Rayleigh fading channel with f = 0.959. The transmitter power amplifier is gated according to the RTG mask.
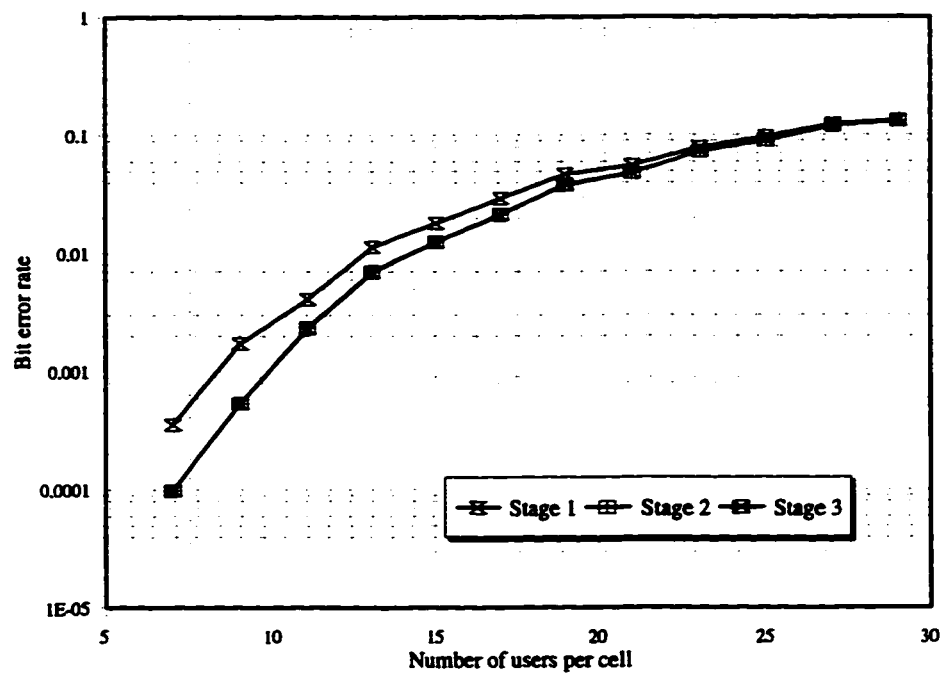
Fig. 4.A.16. The multi-cell performance of a RAMSIC receiver on a frequency selative Rayleigh fading channel with f = 1.57. The transmitter power amplifier is gated according to the RTG mask.

156

4.8 Appendix 4B

The performance curves illustrating the sensitivity of the RAMSIC receiver to power control error are presented.
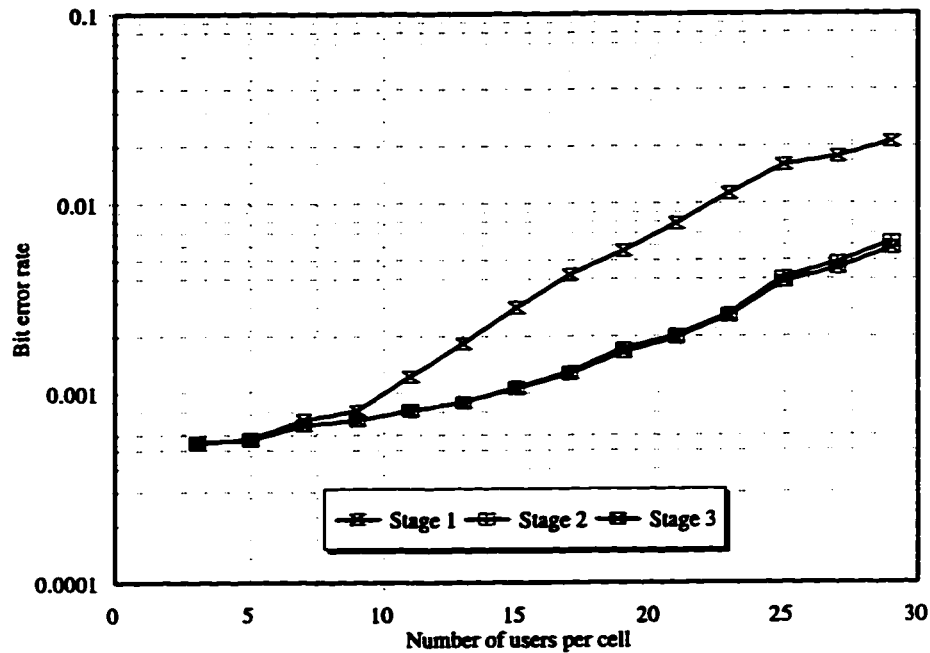
Fig. 4.B.1. The multi-cell performance of a RAMSIC receiver on a flat Rayleigh fading channel with f = 0.55. The power control is non-ideal with standard deviation of 0.7 dB and the transmitter power amplifier is gated according to the IS-95 mask.
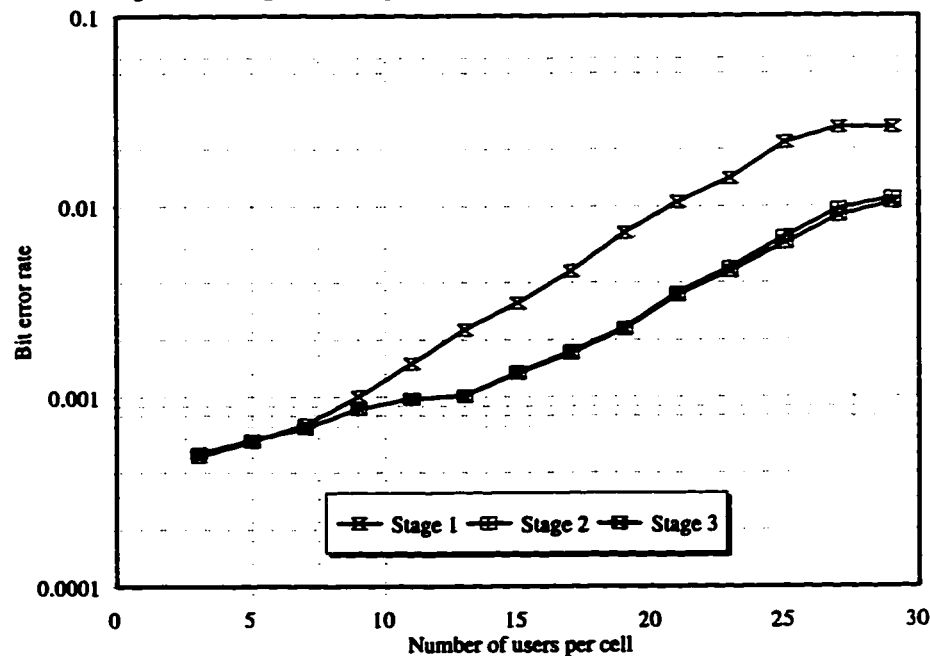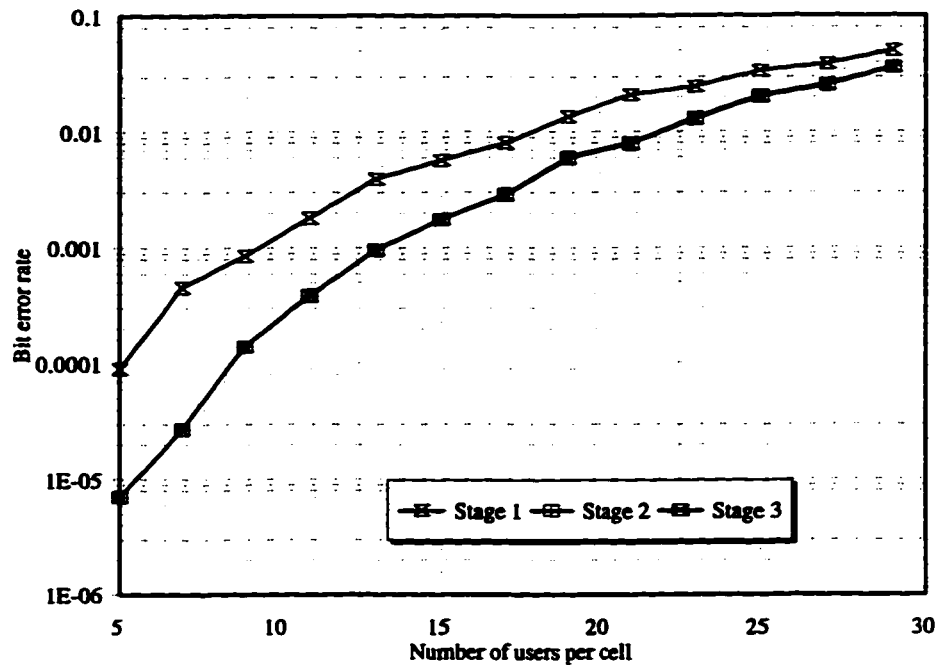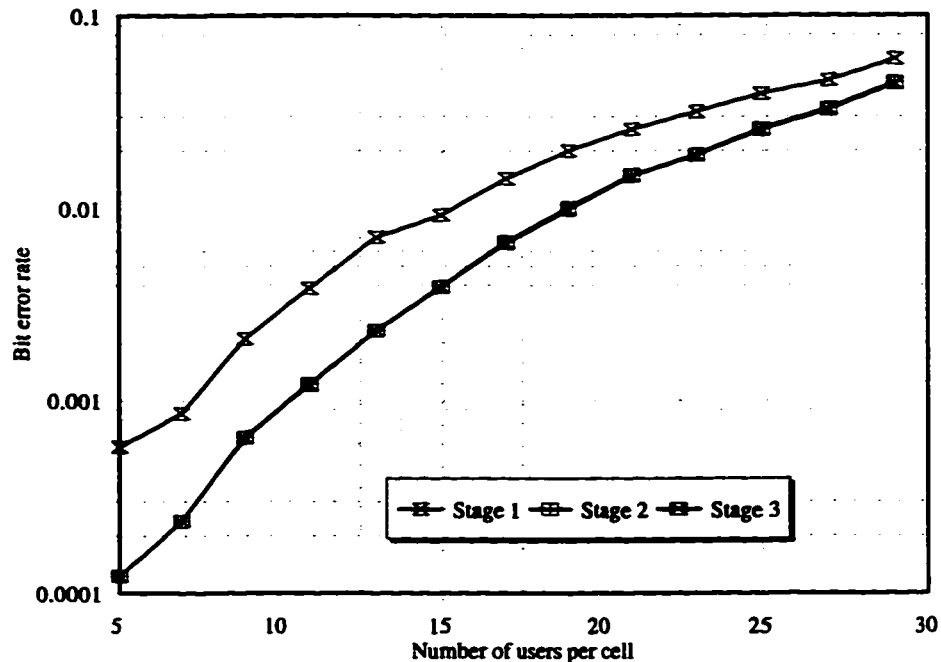

Fig. 4.B.2. The multi-cell performance of a RAMSIC receiver on a flat Rayleigh fading channel with f = 0.686. The power control is non-ideal with standard deviation of 0.7 dB and the transmitter power amplifier is gated according to the IS-95 mask.
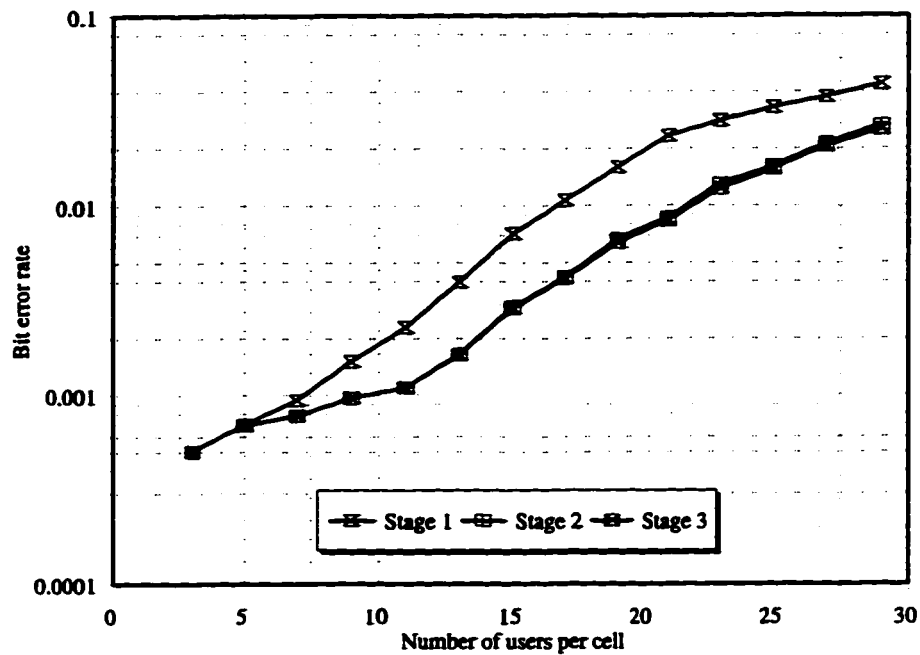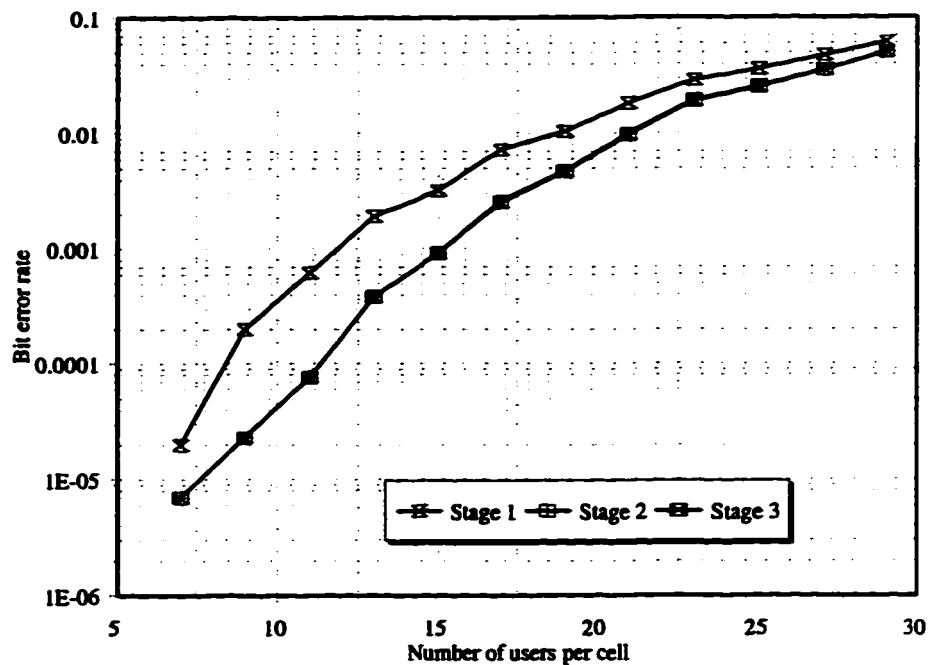
Fig. 4.B.3. The multi-cell performance of a RAMSIC receiver on a flat Rayleigh fading channel with f = 0.959. The power control is non-ideal with standard deviation of 0.7 dB and the transmitter power amplifier is gated according to the IS-95 mask.
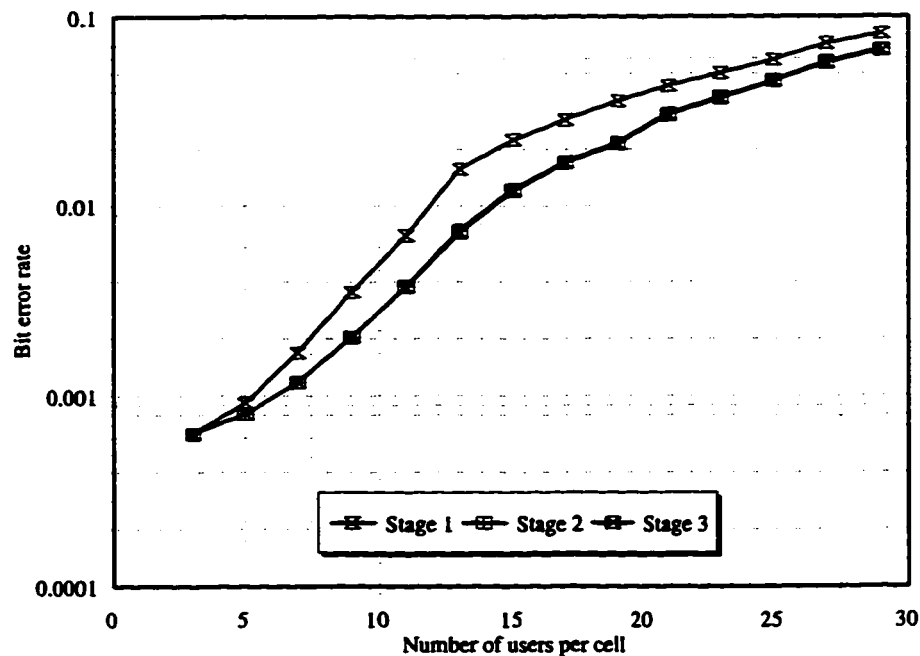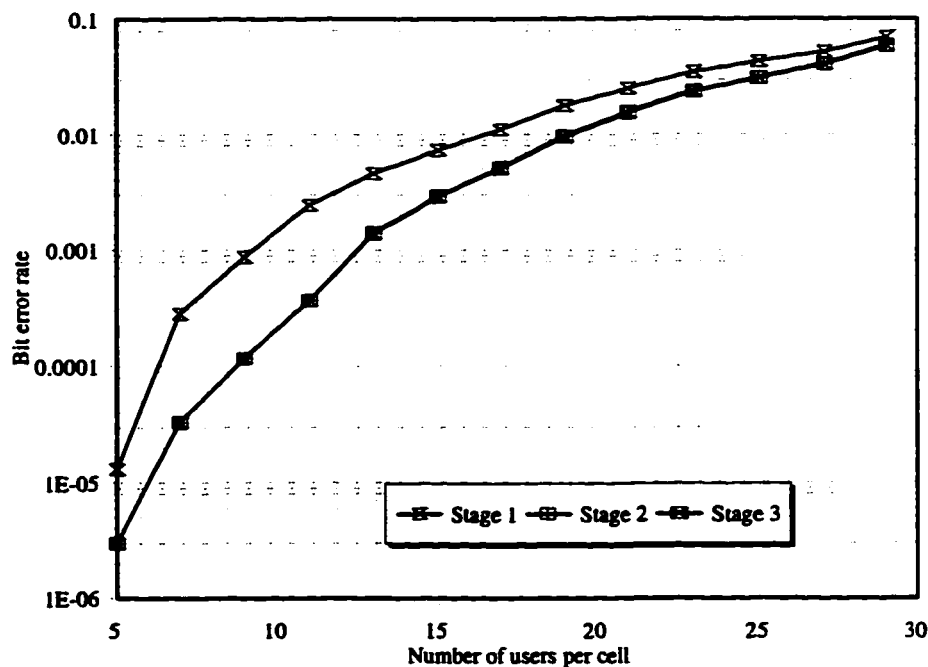

Fig. 4.B.4. The multi-cell performance of a RAMSIC receiver on a flat Rayleigh fading channel with f = 1.57. The power control is non-ideal with standard deviation of 0.7 dB and the transmitter power amplifier is gated according to the IS-95 mask.
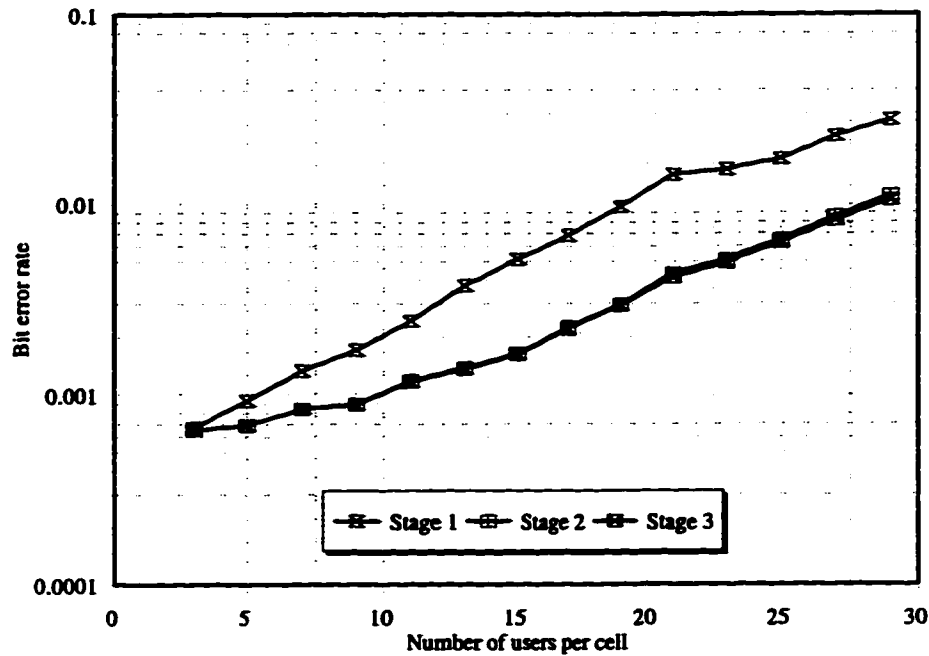
Fig. 4.B.5. The multi-cell performance of a RAMSIC receiver on a flat Rayleigh fading channel with f = 0.55. The power control is non-ideal with standard deviation of 1.6 dB and the transmitter power amplifier is gated according to the IS-95 mask.
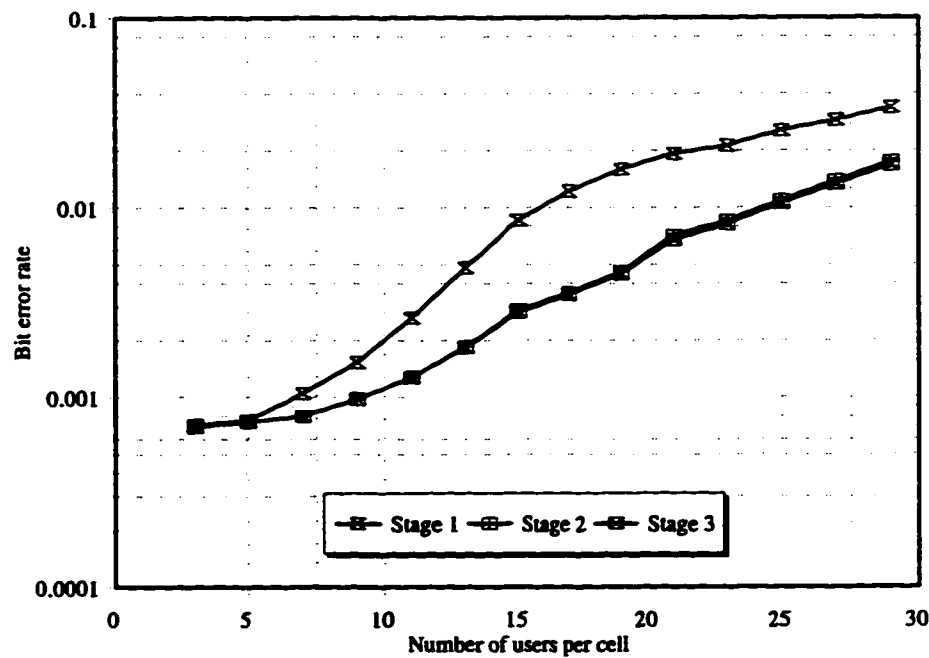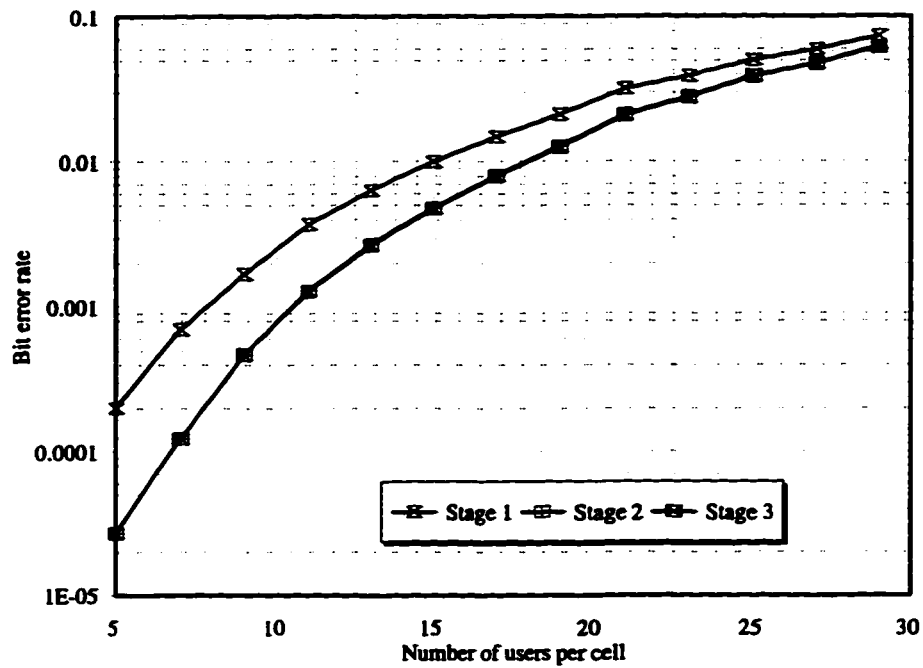

Fig. 4.B.6. The multi-cell performance of a RAMSIC receiver on a flat Rayleigh fading channel with f = 0.686. The power control is non-ideal with standard deviation of 1.6 dB and the transmitter power amplifier is gated according to the IS-95 mask.
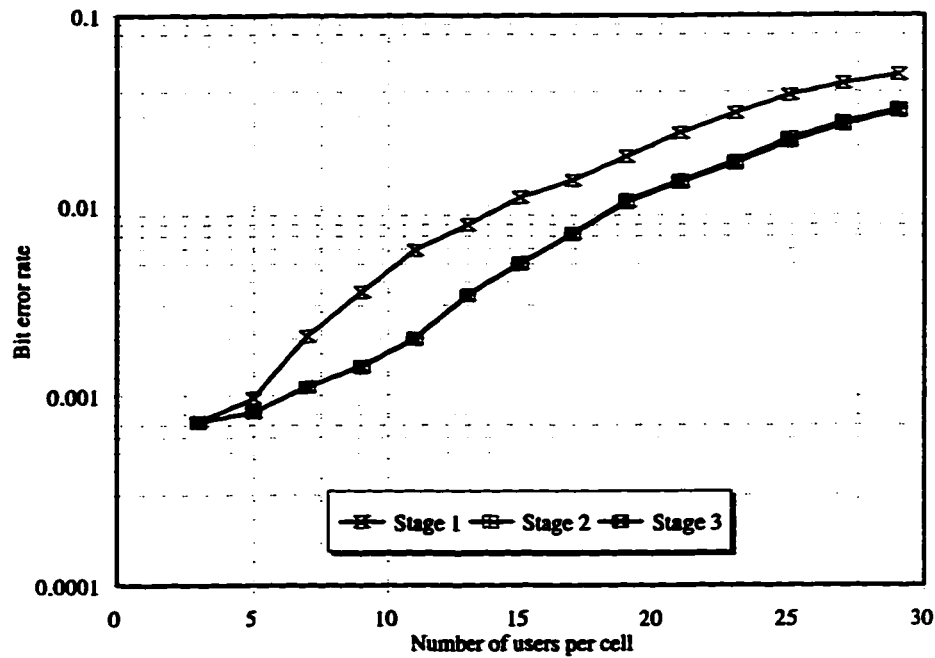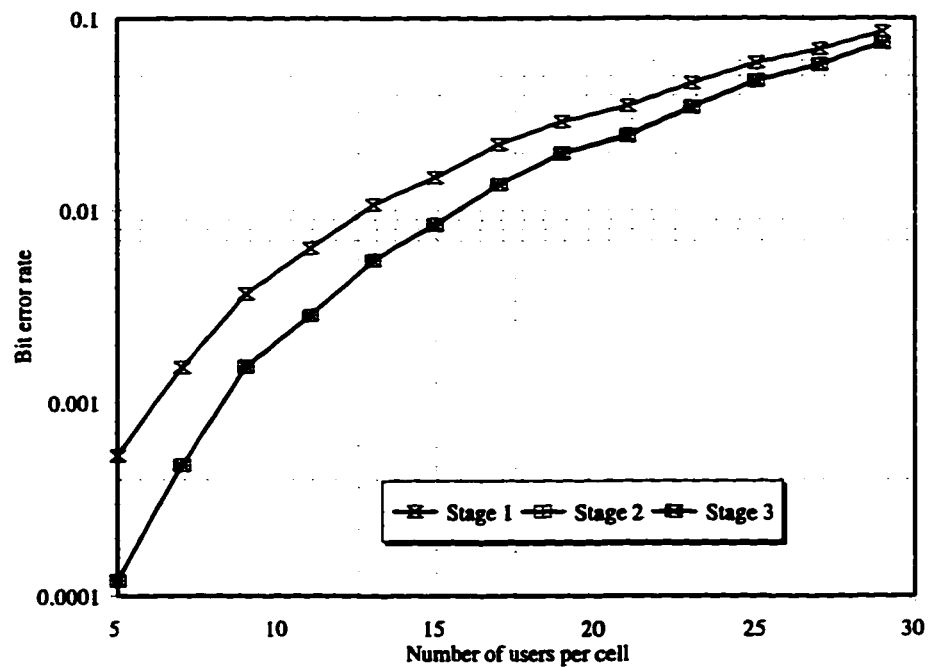
Fig. 4.B.7. The multi-cell performance of a RAMSIC receiver on a flat Rayleigh fading channel with f = 0.959. The power control is non-ideal with standard deviation of 1.6 dB and the transmitter power amplifier is gated according to the IS-95 mask.
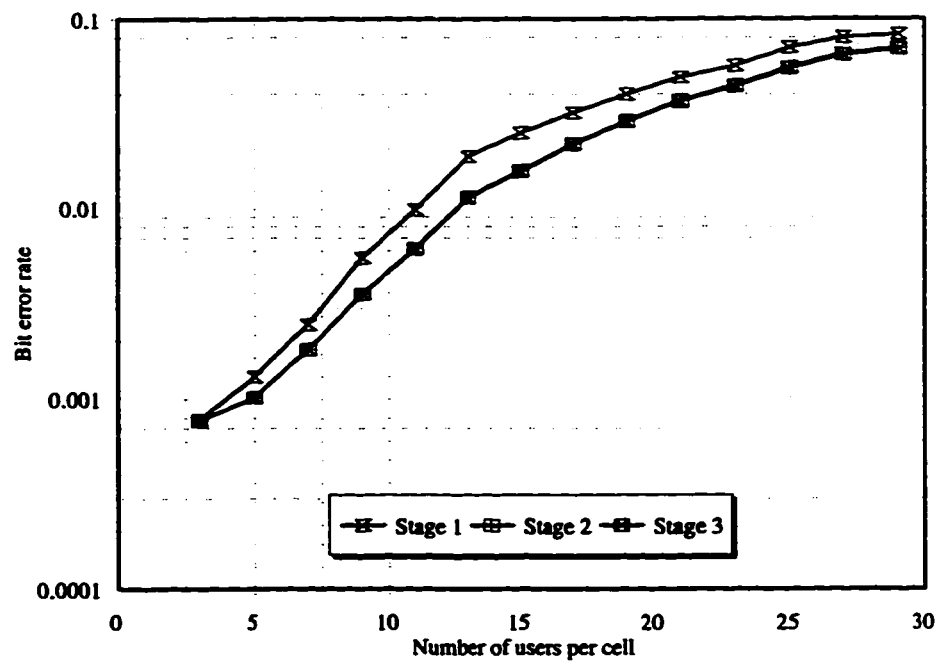
Fig. 4.B.8. The multi-cell performance of a RAMSIC receiver on a flat Rayleigh fading channel with f = 1.57. The power control is non-ideal with standard deviation of 1.6 dB and the transmitter power amplifier is gated according to the IS-95 mask.
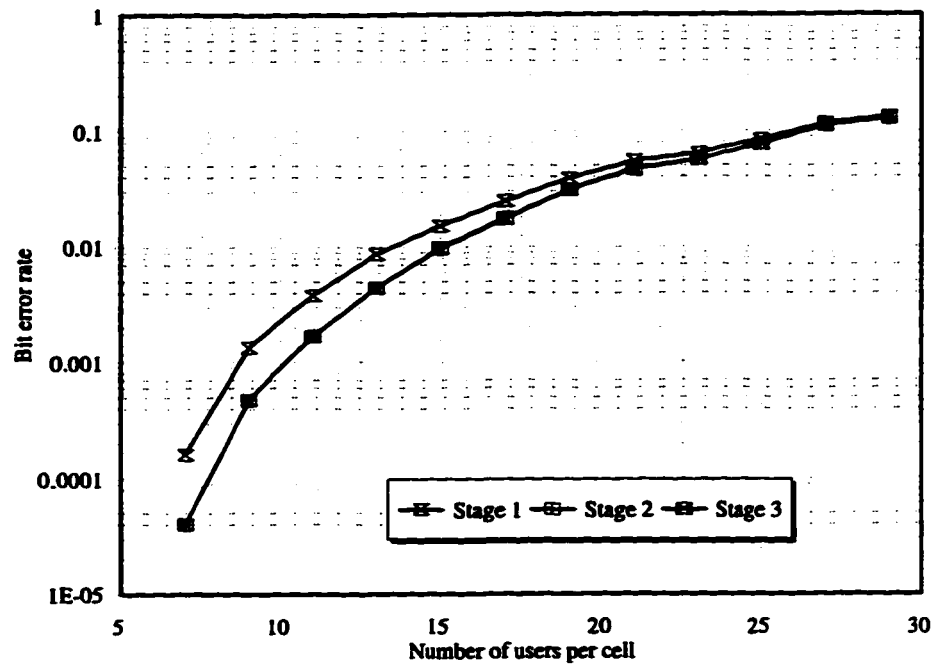
160
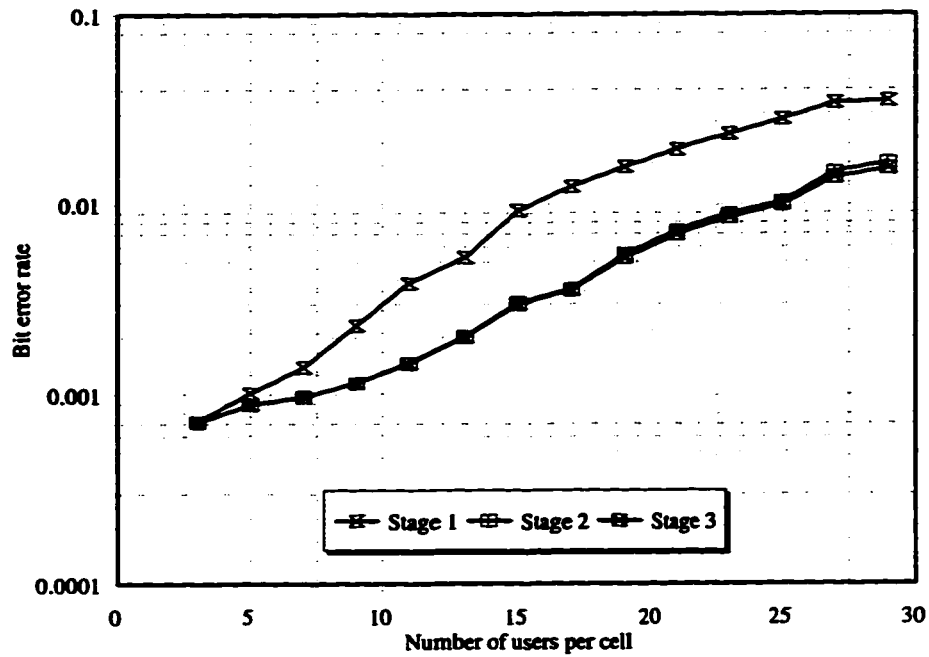
Fig. 4.B.9. The multi-cell performance of a RAMSIC receiver on a flat Rayleigh fading channel with f = 0.55. The power control is non-ideal with standard deviation of 2.2 dB and the transmitter power amplifier is gated according to the IS-95 mask.
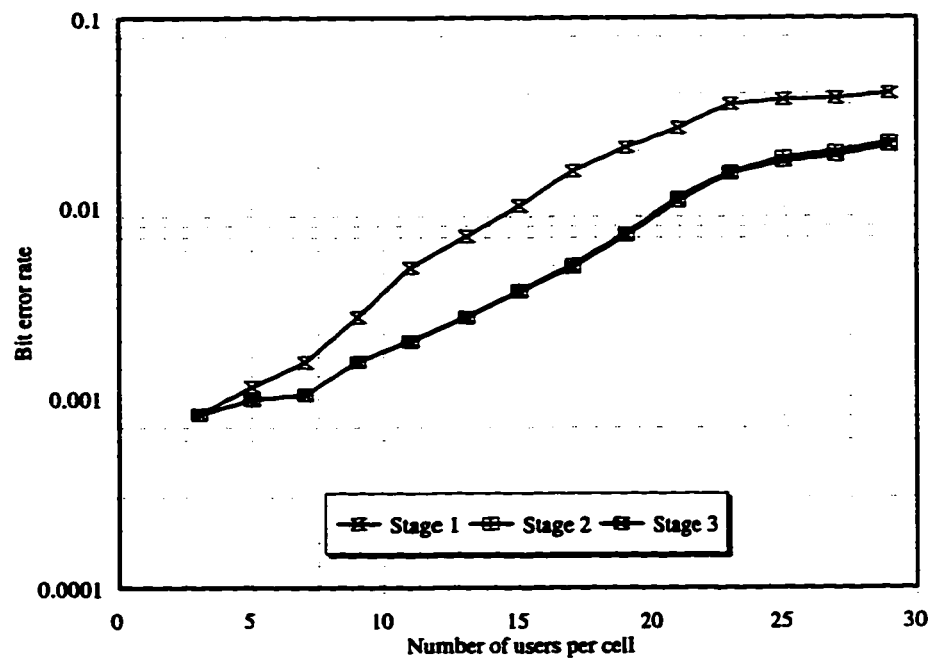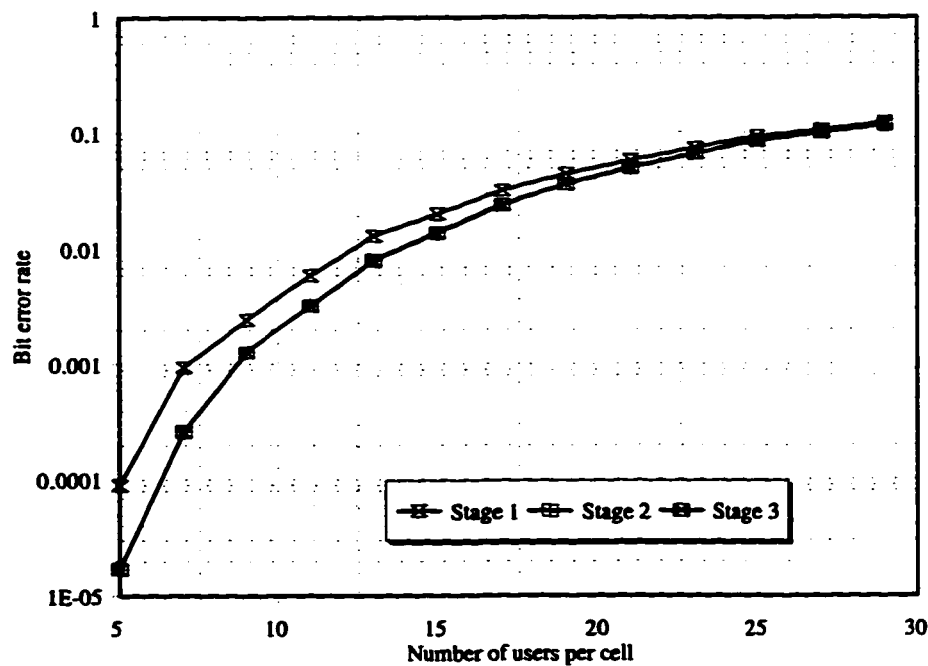

Fig. 4.B.10. The multi-cell performance of a RAMSIC receiver on a flat Rayleigh fading channel with f = 0.686. The power control is non-ideal with standard deviation of 2.2 dB and the transmitter power amplifier is gated according to the IS-95 mask.
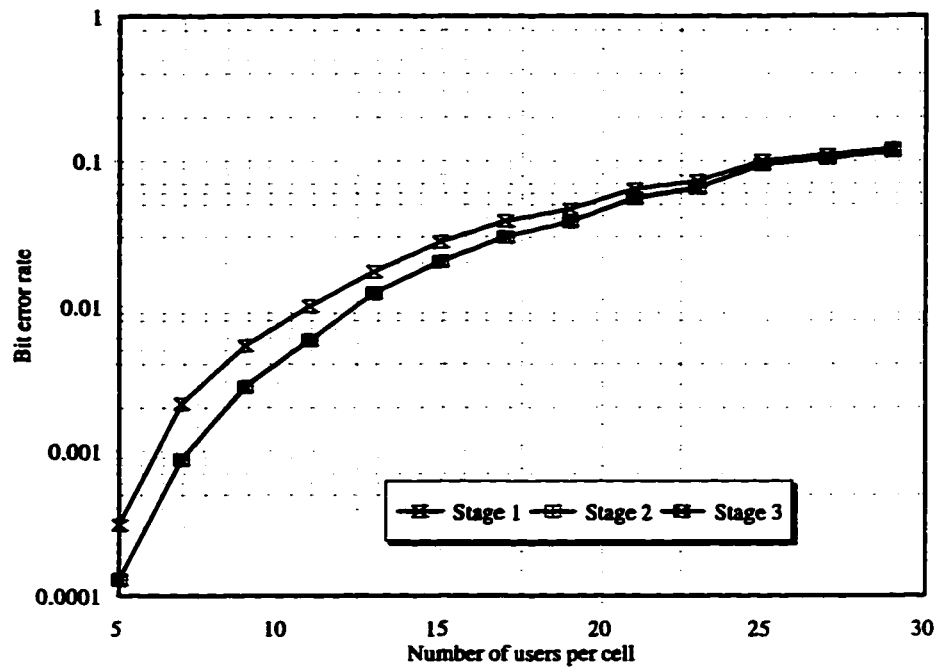
161
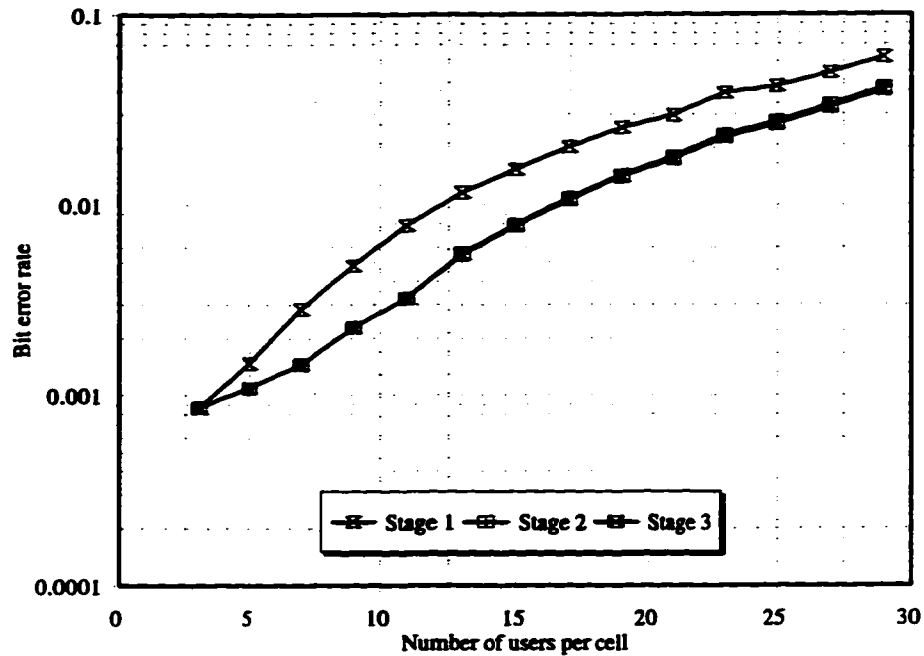
Fig. 4.B.11. The multi-cell performance of a RAMSIC receiver on a flat Rayleigh fading channel with f − 0.959. The power control is non-ideal with standard deviation of 2.2 dB and the transmitter power amplifier is gated according to the IS-95 mask.
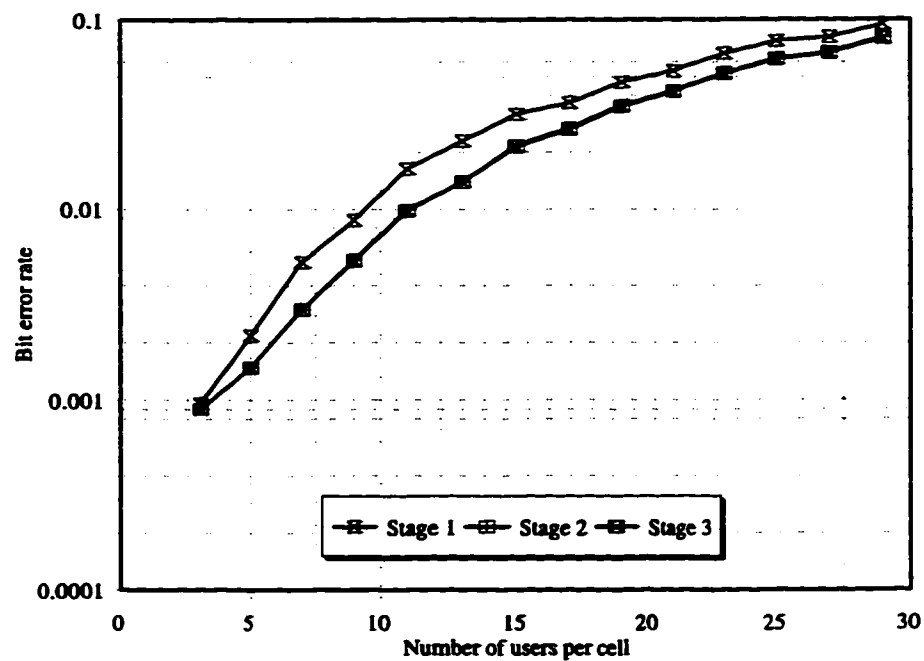
Fig. 4.B.12. The multi-cell performance of a RAMSIC receiver on a flat Rayleigh fading channel with f − 1.57. The power control is non-ideal with standard deviation of 2.2 dB and the transmitter power amplifier is gated according to the IS-95 mask.
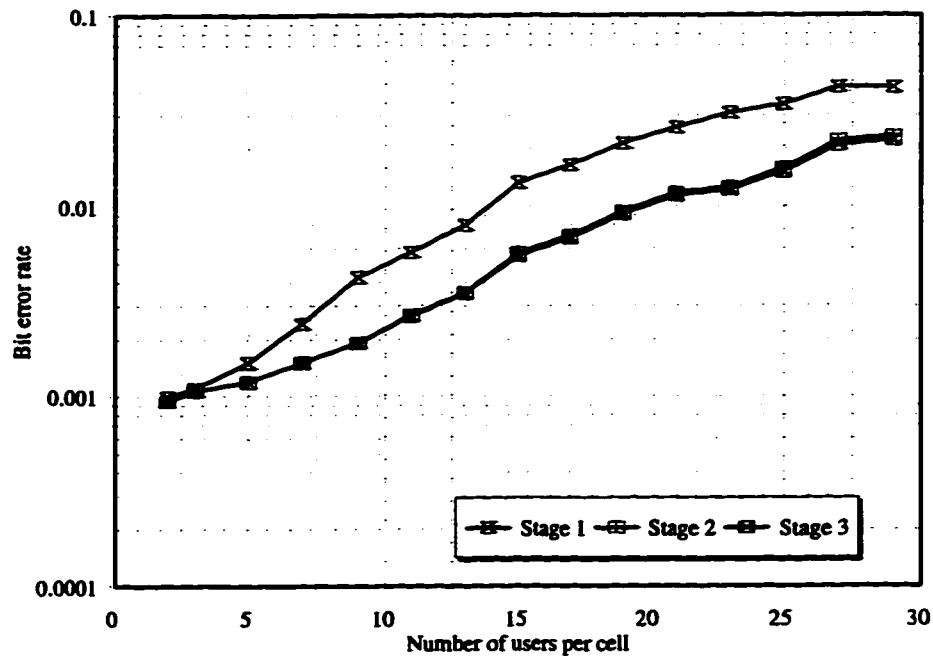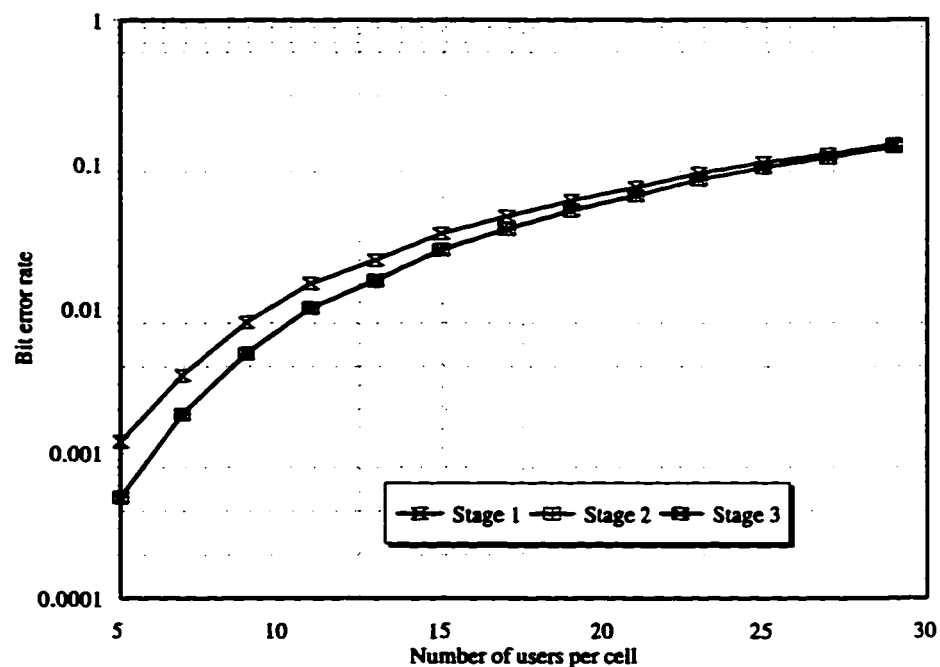
Fig. 4.B.13. The multi-cell performance of a RAMSIC receiver on a flat Rayleigh fading channel with f = 0.55. The power control is non-ideal with standard deviation of 2.9 dB and the transmitter power amplifier is gated according to the IS-95 mask.
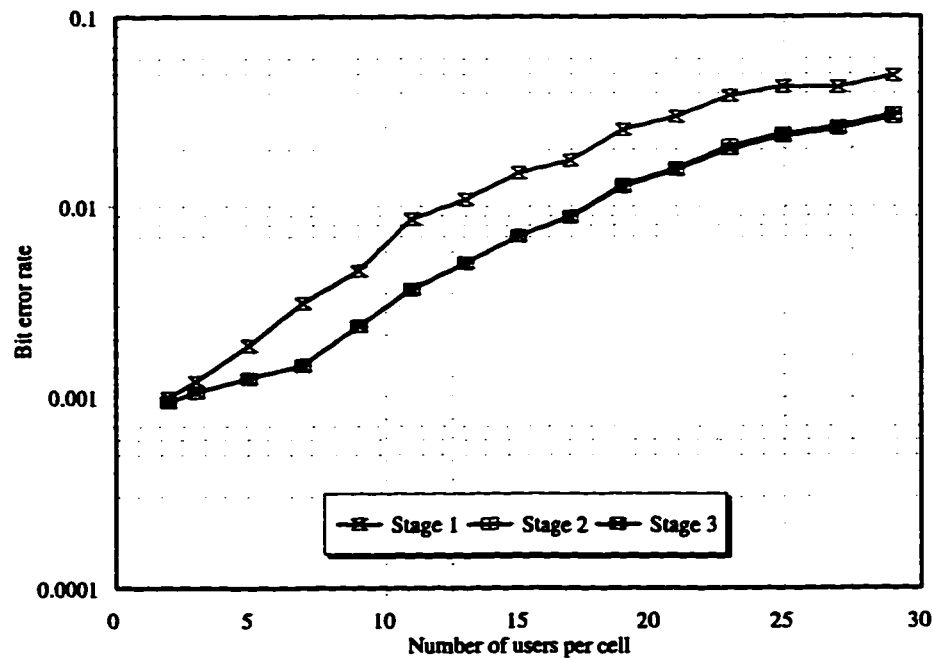
Fig. 4.B.14. The multi-cell performance of a RAMSIC receiver on a flat Rayleigh fading channel with f = 0.686. The power control is non-ideal with standard deviation of 2.9 dB and the transmitter power amplifier is gated according to the IS-95 mask.
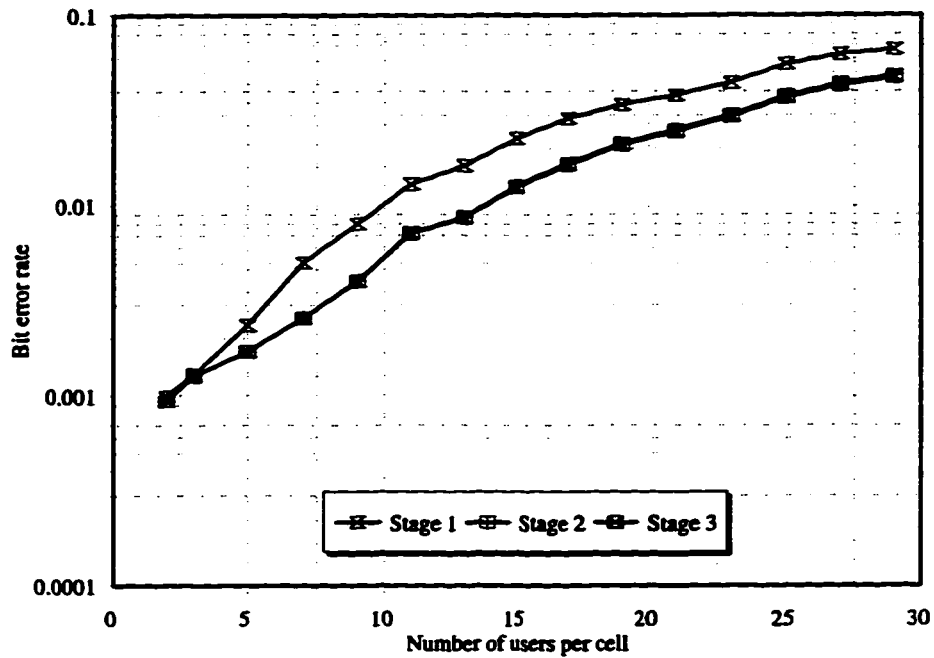
Fig. 4.B.15. The multi-cell performance of a RAMSIC receiver on a flat Rayleigh fading channel with f = 0.959. The power control is non-ideal with standard deviation of 2.9 dB and the transmitter power amplifier is gated according to the IS-95 mask.
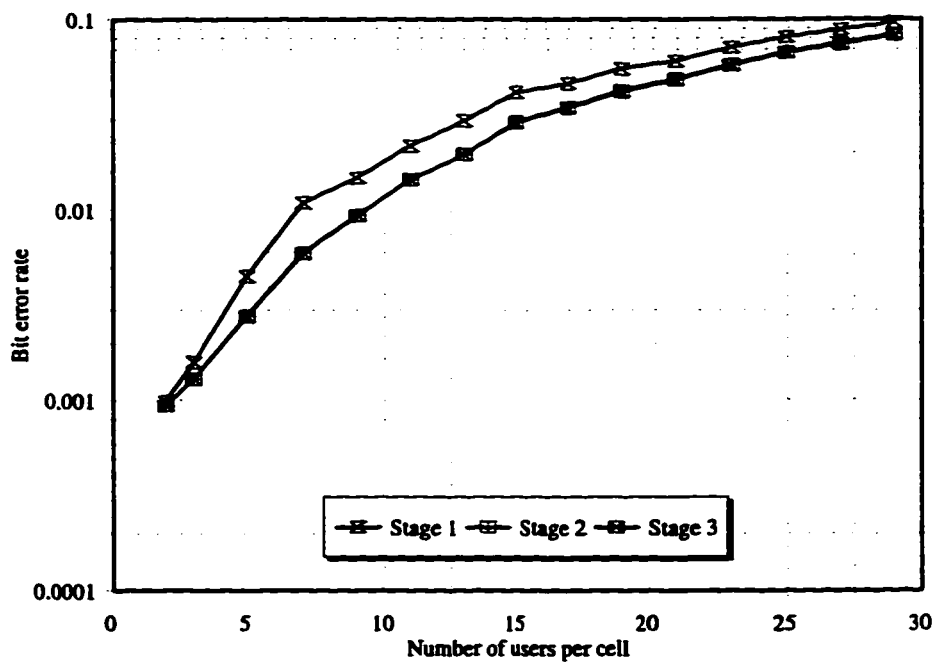
Fig. 4.B.16. The multi-cell performance of a RAMSIC receiver on a flat Rayleigh fading channel with f = 1.57. The power control is non-ideal with standard deviation of 2.9 dB and the transmitter power amplifier is gated according to the IS-95 mask.
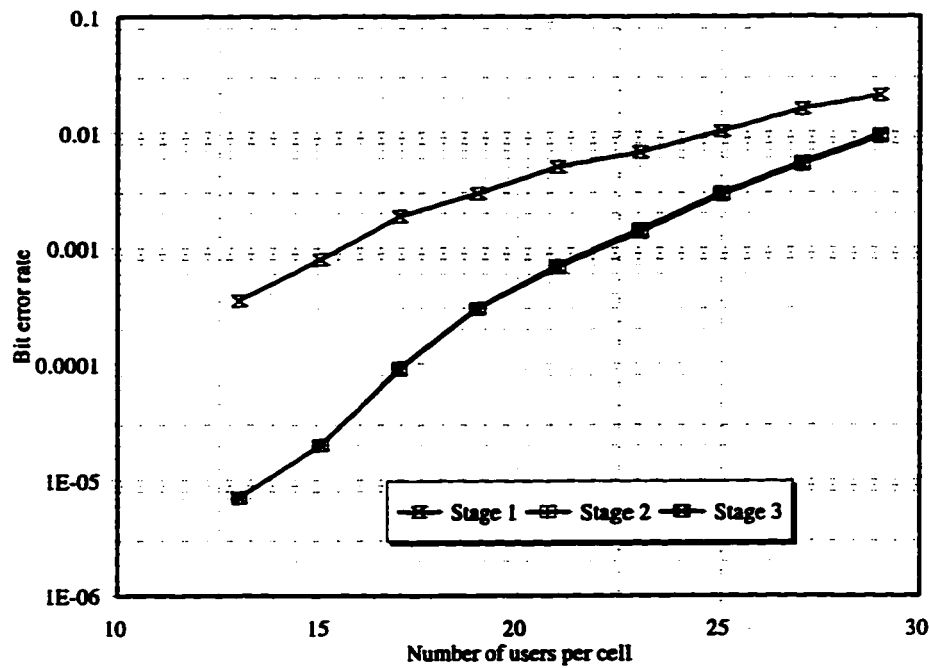
Fig. 4.B.17. The multi-cell performance of a RAMSIC receiver on a frequency selective Rayleigh fading channel with f = 0.55. The power control is non-ideal with standard deviation of 0.7 dB and the transmitter power amplifier is gated according to the IS-95 mask.

Fig. 4.B.18. The multi-cell performance of a RAMSIC receiver on a frequency selective Rayleigh fading channel with f = 0.686. The power control is non-ideal with standard deviation of 0.7 dB and the transmitter power amplifier is gated according to the IS-95 mask.

Fig. 4.B.19. The multi-cell performance of a RAMSIC receiver on a frequency selective Rayleigh fading channel with f = 0.959. The power control is non-ideal with standard deviation of 0.7 dB and the transmitter power amplifier is gated according to the IS-95 mask.

Fig. 4.B.20. The multi-cell performance of a RAMSIC receiver on a frequency selective Rayleigh fading channel with f = 1.57. The power control is non-ideal with standard deviation of 0.7 dB and the transmitter power amplifier is gated according to the IS-95 mask.

Fig. 4.B.21. The multi-cell performance of a RAMSIC receiver on a frequency selective Rayleigh fading channel with f = 0.55. The power control is non-ideal with standard deviation of 1.6 dB and the transmitter power amplifier is gated according to the IS-95 mask.

Fig. 4.B.22. The multi-cell performance of a RAMSIC receiver on a frequency selective Rayleigh fading channel with f = 0.686. The power control is non-ideal with standard deviation of 1.6 dB and the transmitter power amplifier is gated according to the IS-95 mask.

Fig. 4.B.23. The multi-cell performance of a RAMSIC receiver on a frequency selective Rayleigh fading channel with f = 0.959. The power control is non-ideal with standard deviation of 1.6 dB and the transmitter power amplifier is gated according to the IS-95 mask.

Fig. 4.B.24. The multi-cell performance of a RAMSIC receiver on a frequency selective Rayleigh fading channel with f = 1.57. The power control is non-ideal with standard deviation of 1.6 dB and the transmitter power amplifier is gated according to the IS-95 mask.

168

Fig. 4.B.25. The multi-cell performance of a RAMSIC receiver on a frequency selective Rayleigh fading channel with f = 0.55. The power control is non-ideal with standard deviation of 2.2 dB and the transmitter power amplifier is gated according to the IS-95 mask.

Fig. 4.B.26. The multi-cell performance of a RAMSIC receiver on a frequency selective Rayleigh fading channel with f = 0.686. The power control is non-ideal with standard deviation of 2.2 dB and the transmitter power amplifier is gated according to the IS-95 mask.

Fig. 4.B.27. The multi-cell performance of a RAMSIC receiver on a frequency selective Rayleigh fading channel with f = 0.959. The power control is non-ideal with standard deviation of 2.2 dB and the transmitter power amplifier is gated according to the IS-95 mask.

Fig. 4.B.28. The multi-cell performance of a RAMSIC receiver on a frequency selective Rayleigh fading channel with f = 1.57. The power control is non-ideal with standard deviation of 2.2 dB and the transmitter power amplifier is gated according to the IS-95 mask.

Fig. 4.B.29. The multi-cell performance of a RAMSIC receiver on a frequency selective Rayleigh fading channel with f = 0.55. The power control is non-ideal with standard deviation of 2.9 dB and the transmitter power amplifier is gated according to the IS-95 mask.
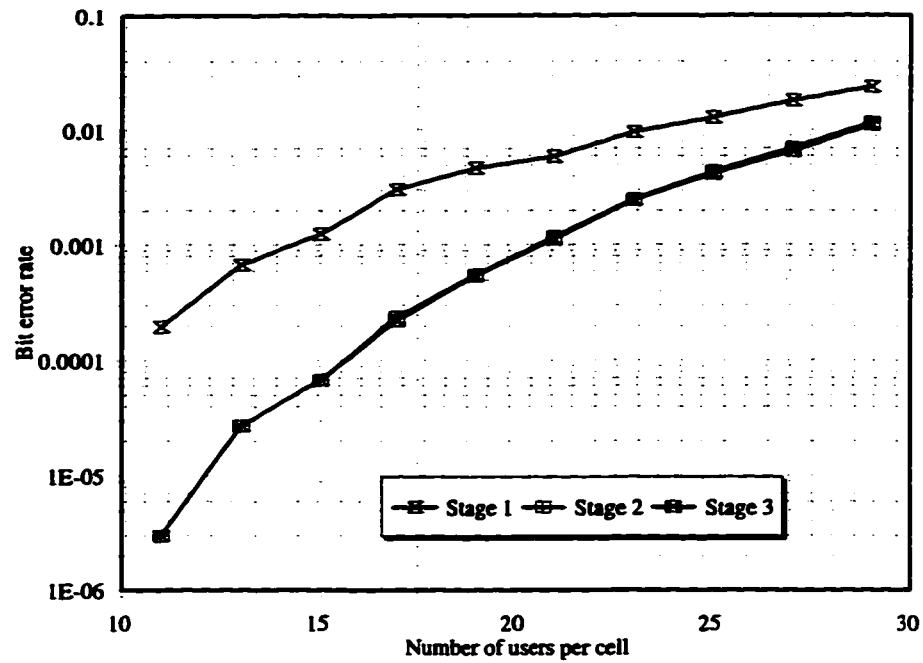

Fig. 4.B.30. The multi-cell performance of a RAMSIC receiver on a frequency selective Rayleigh fading channel with f = 0.686. The power control is non-ideal with standard deviation of 2.9 dB and the transmitter power amplifier is gated according to the IS-95 mask.
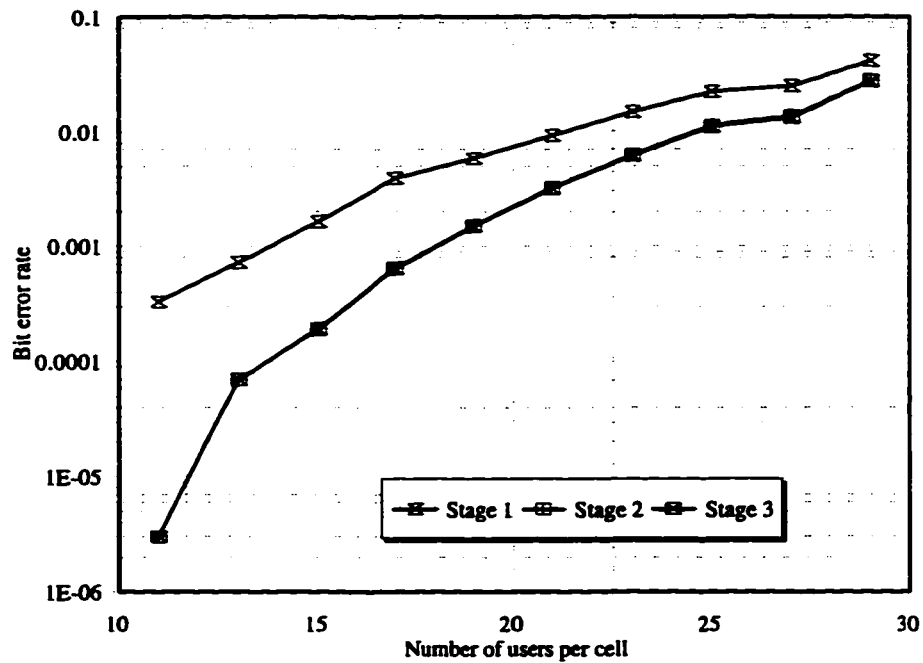
Fig. 4.B.31. The multi-cell performance of a RAMSIC receiver on a frequency selective Rayleigh fading channel with f = 0.959. The power control is non-ideal with standard deviation of 2.9 dB and the transmitter power amplifier is gated according to the IS-95 mask.
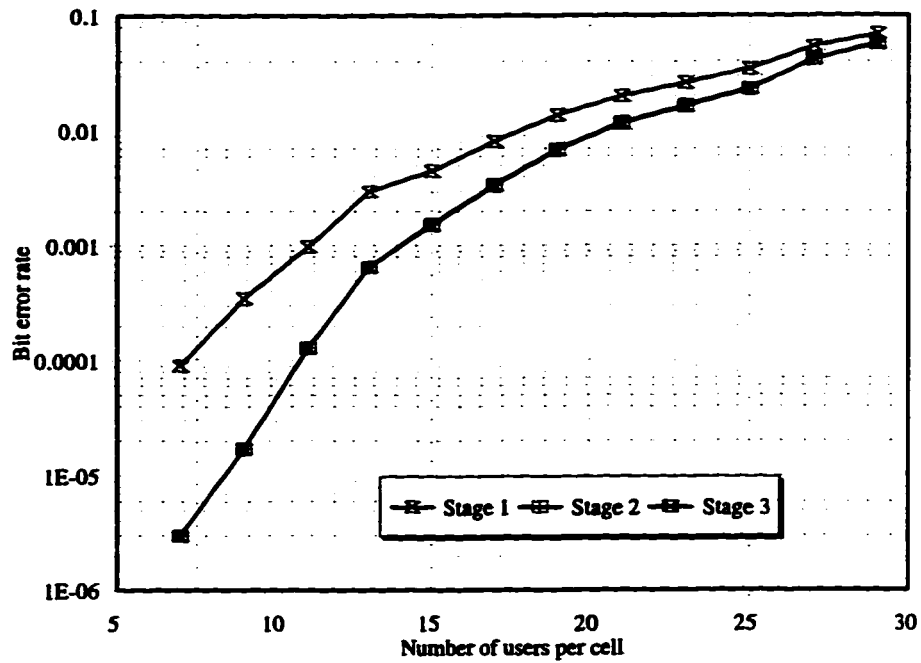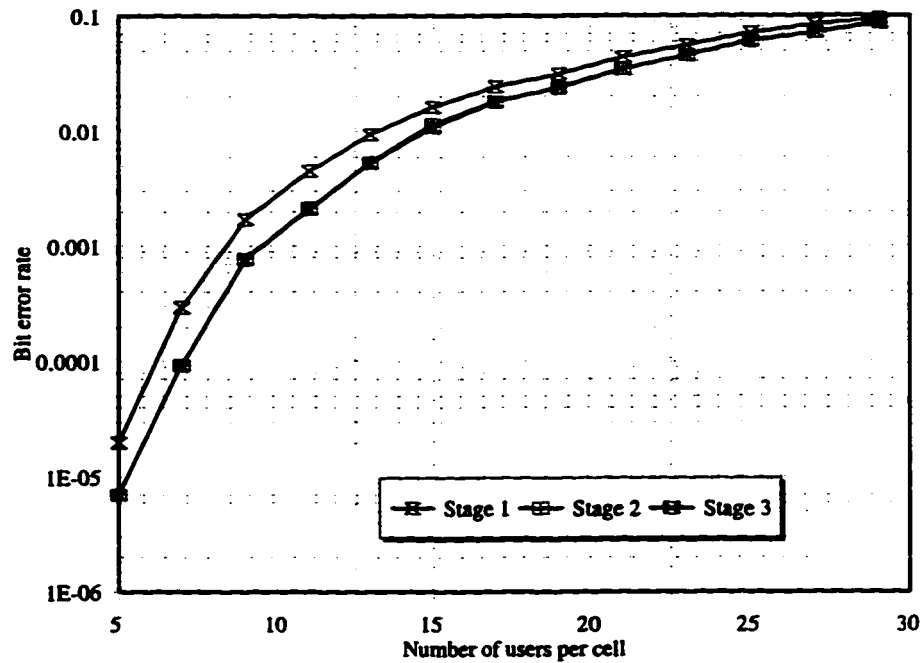

Fig. 4.B.32. The multi-cell performance of a RAMSIC receiver on a frequency selective Rayleigh fading channel with f = 1.57. The power control is non-ideal with standard deviation of 2.9 dB and the transmitter power amplifier is gated according to the IS-95 mask.

4.9 Appendix 4C

The performance curves illustrating the sensitivity of the RAMSIC receiver to synchronization error are presented here. The transmitter power amplifier is gated according to the IS-95 mask and the power control is nonideal with standard deviation of 1 dB for all Figures.
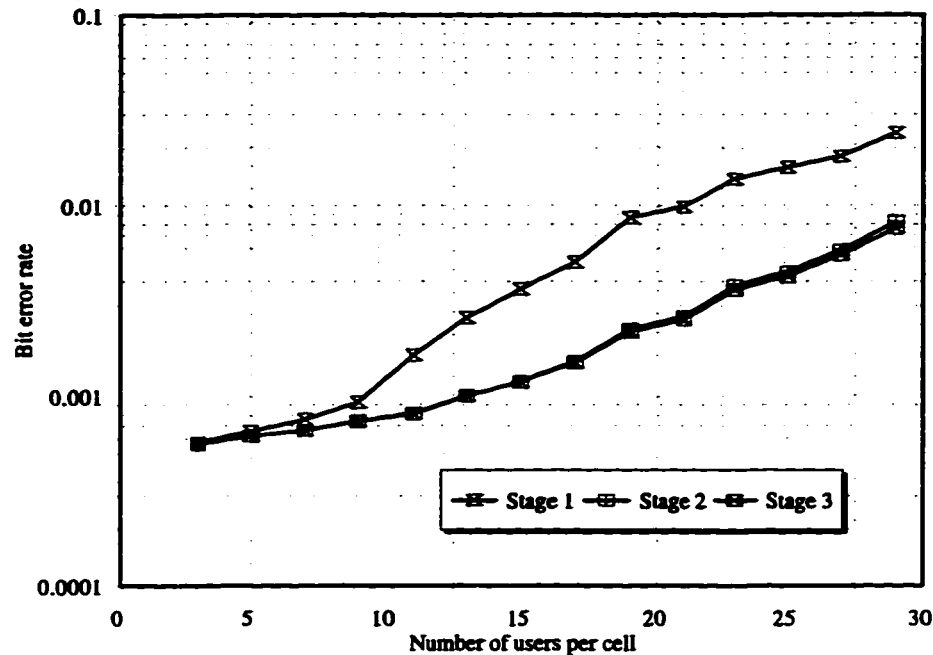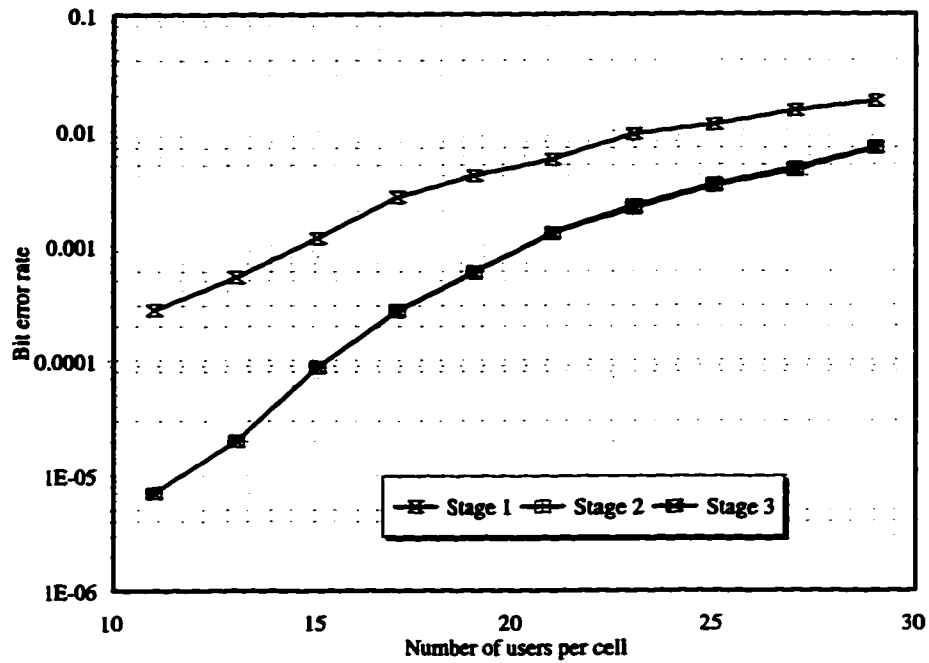

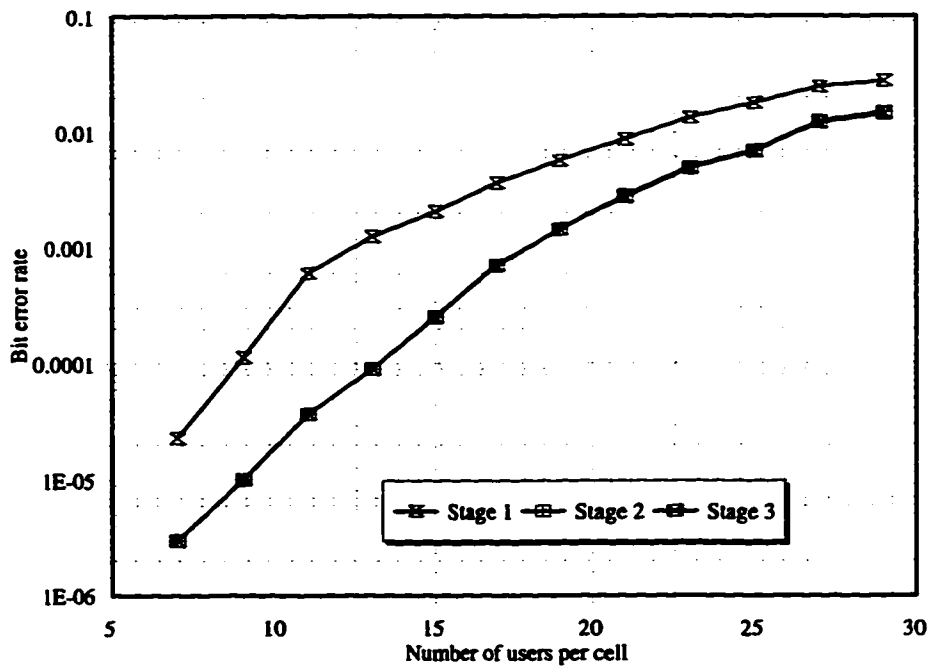Fig. 4.C.1. The multi-cell performance of a RAMSIC receiver on a flat fading channel with f = 0.55 and synchronization error of $0.05T_c$.
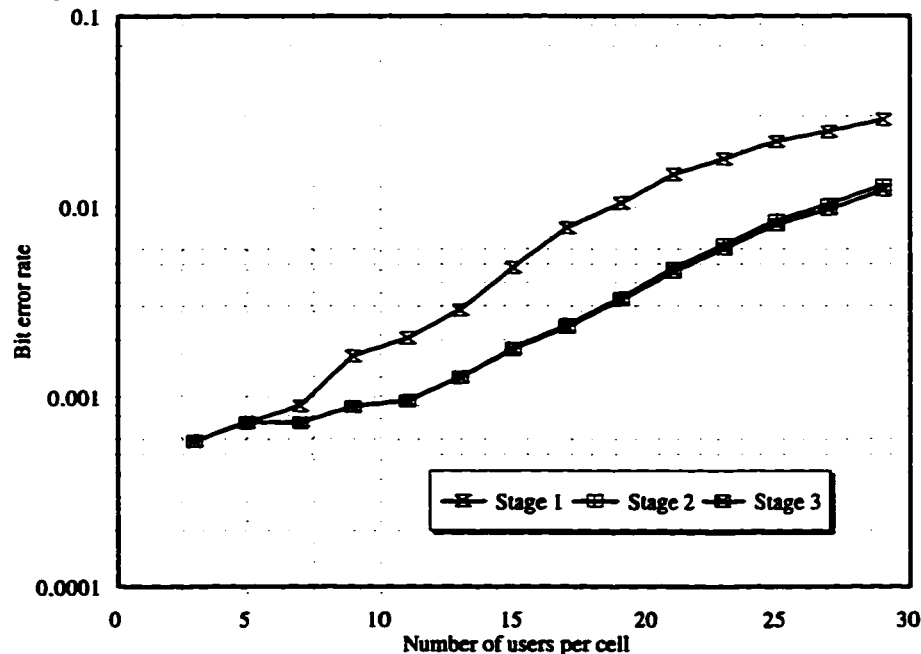
Fig. 4.C.2. The multi-cell performance of a RAMSIC receiver on a flat fading channel with f = 0.686 and synchronization error of $0.05T_c$.
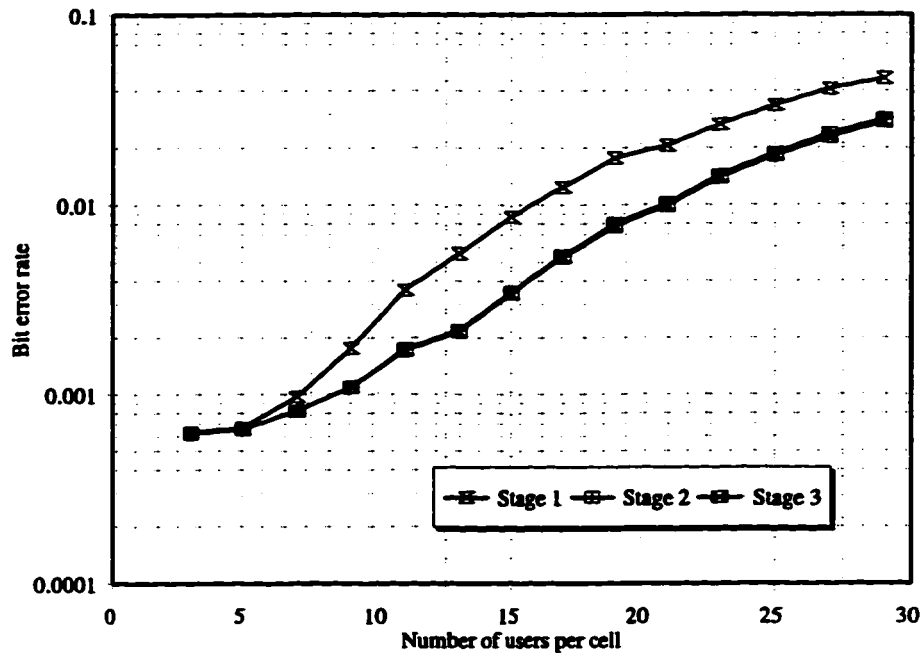
Fig. 4.C.3. The multi-cell performance of a RAMSIC receiver on a flat fading channel with
f = 0.959 and synchronization error of 0.05T_c.
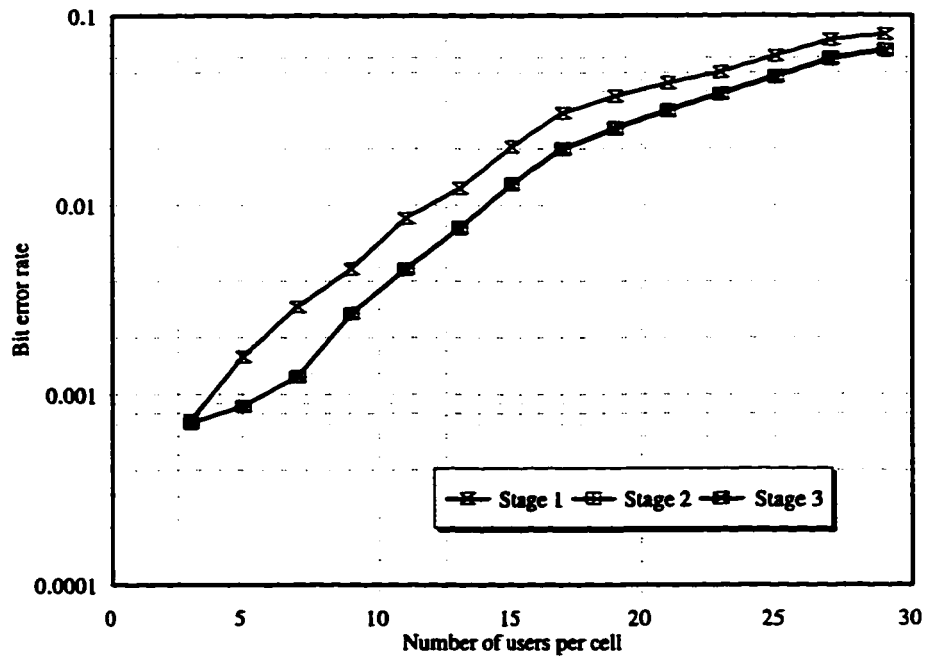
Fig. 4.C.4. The multi-cell performance of a RAMSIC receiver on a flat fading channel with
f = 1.57 and synchronization error of 0.05T_c.
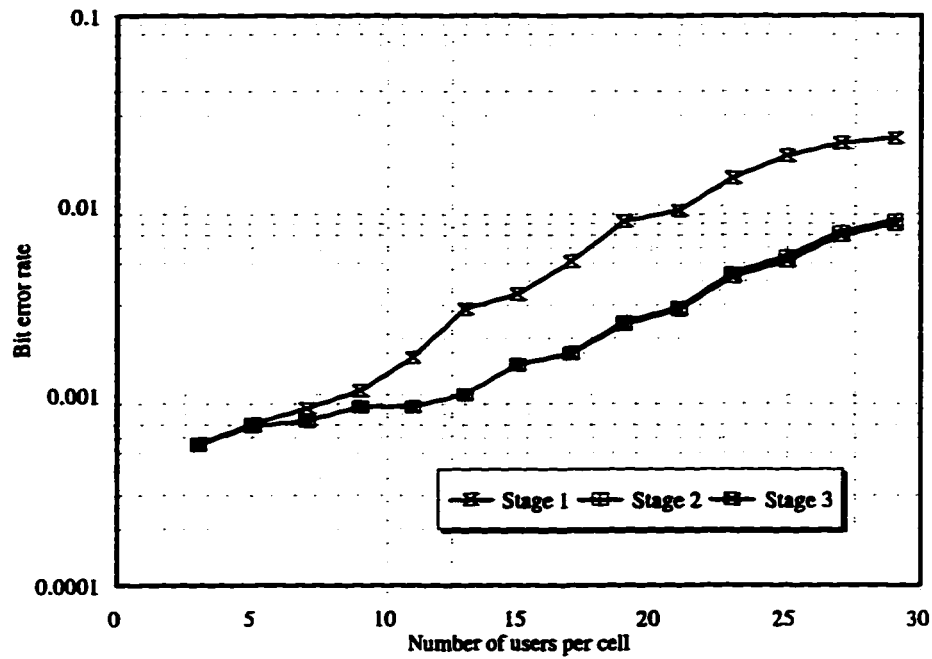
Fig. 4.C.5. The multi-cell performance of a RAMSIC receiver on a flat fading channel with f = 0.55 and synchronization error of $0.1T_c$.
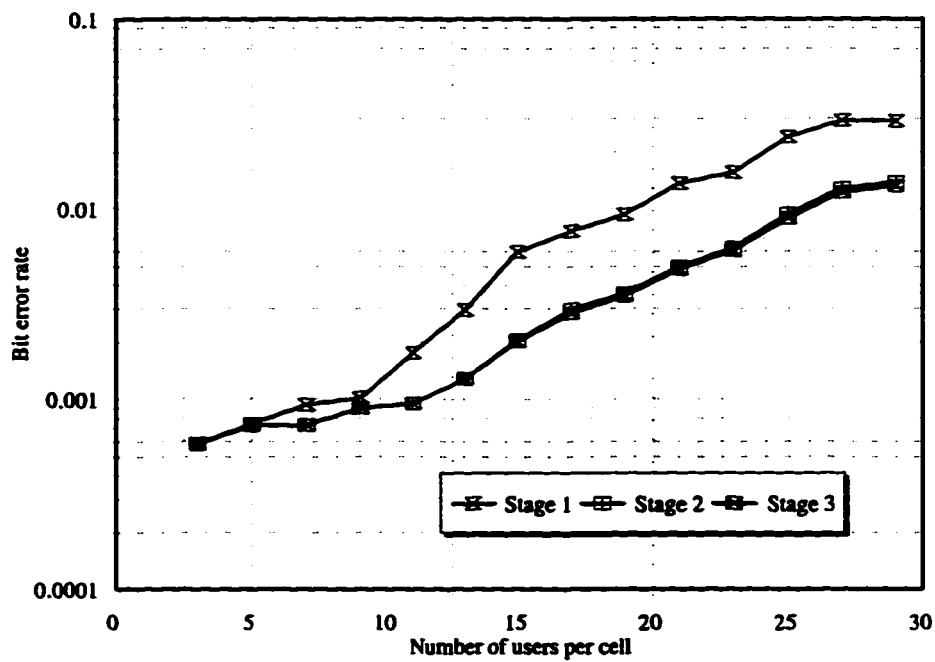
Fig. 4.C.6. The multi-cell performance of a RAMSIC receiver on a flat fading channel with f = 0.686 and synchronization error of $0.1T_c$.
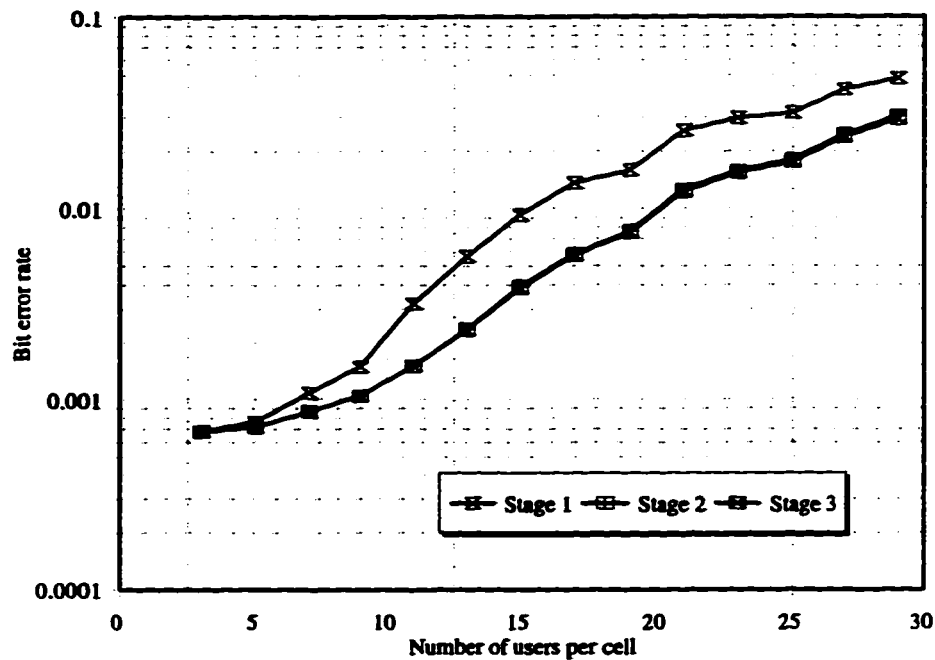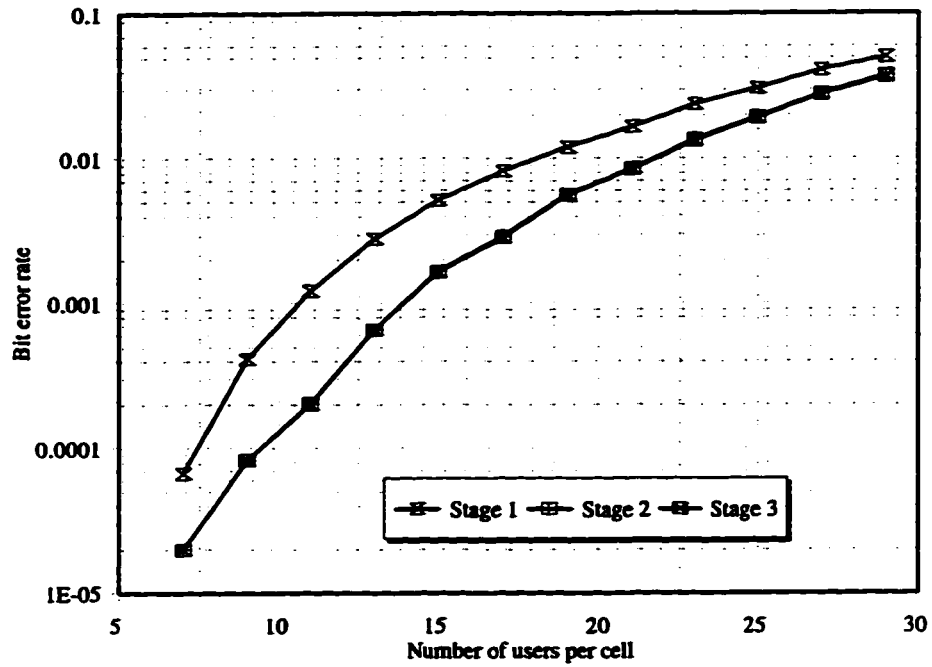
Fig. 4.C.7. The multi-cell performance of a RAMSIC receiver on a flat fading channel with f = 0.959 and synchronization error of $0.1T_c$.
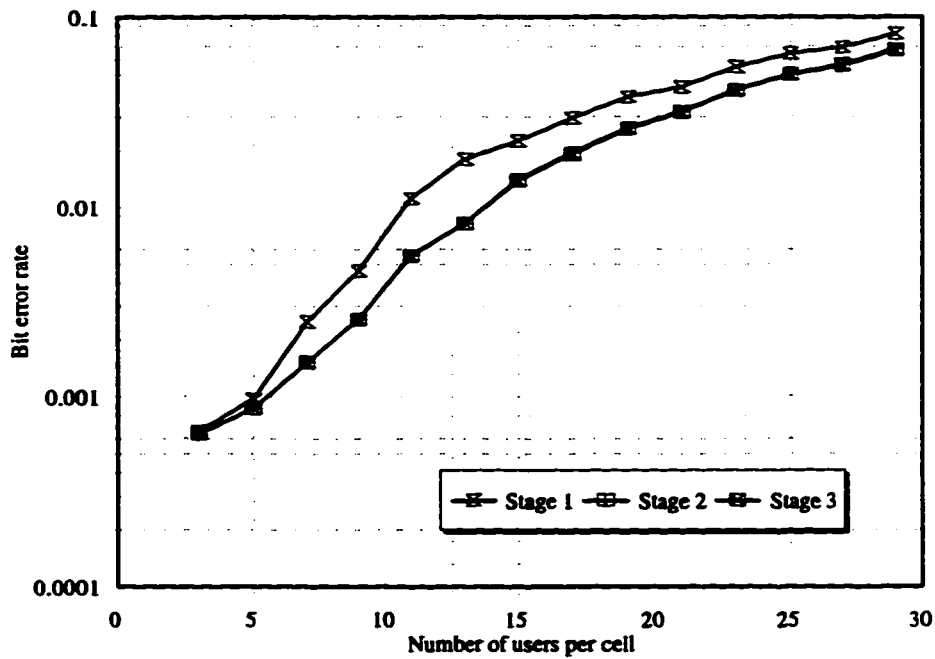
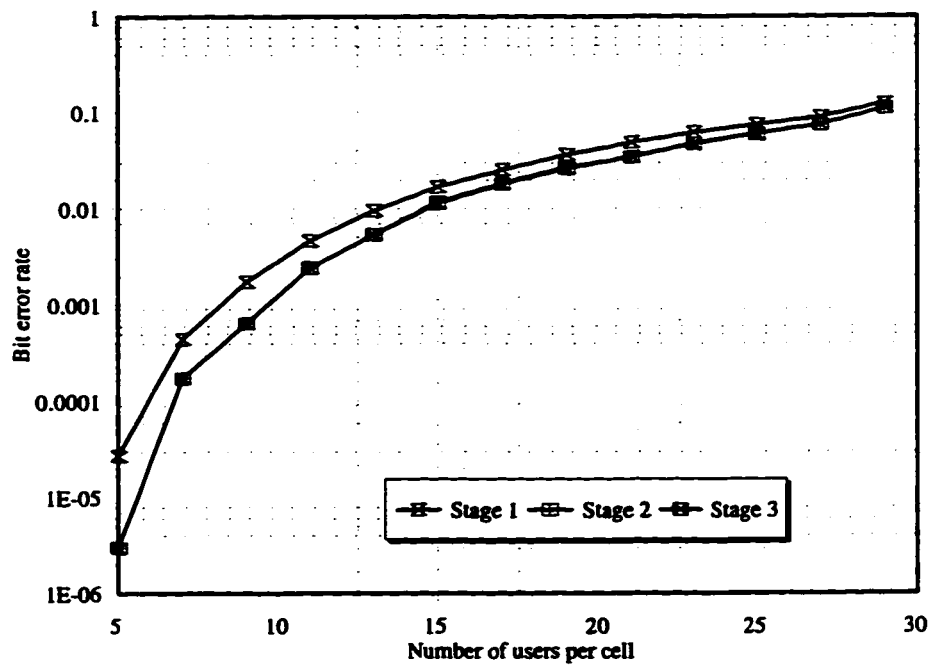Fig. 4.C.8. The multi-cell performance of a RAMSIC receiver on a flat fading channel with f = 1.57 and synchronization error of $0.1T_c$.
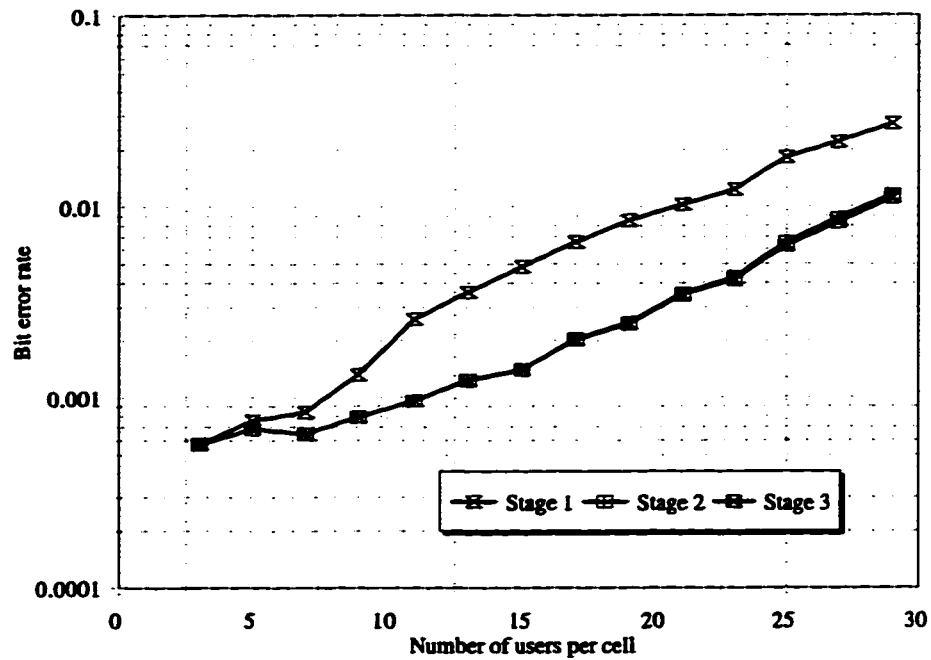
Fig. 4.C.9. The multi-cell performance of a RAMSIC receiver on a flat fading channel with f = 0.55 and synchronization error of $0.15T_c$.
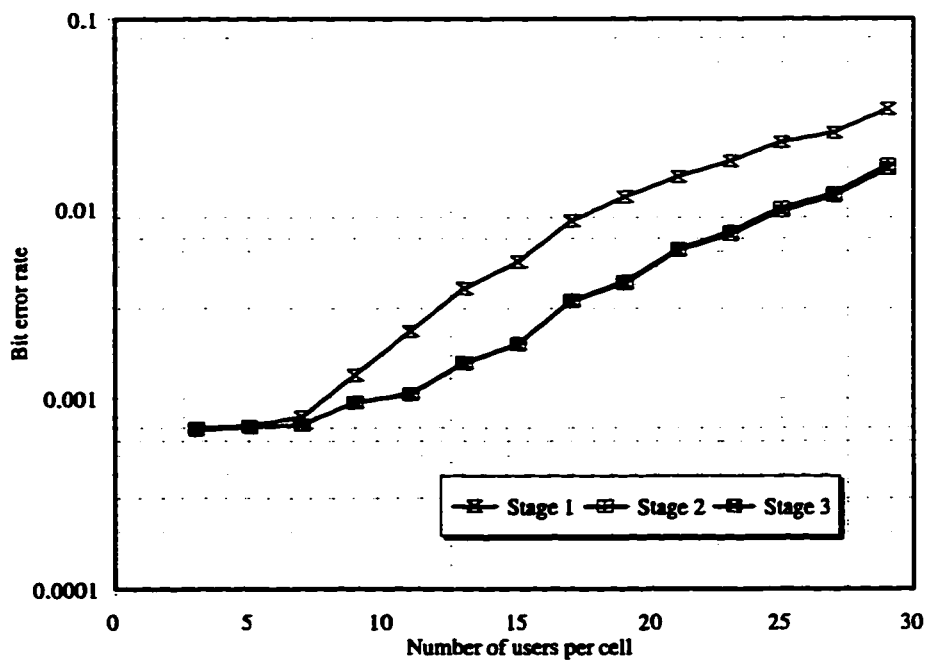
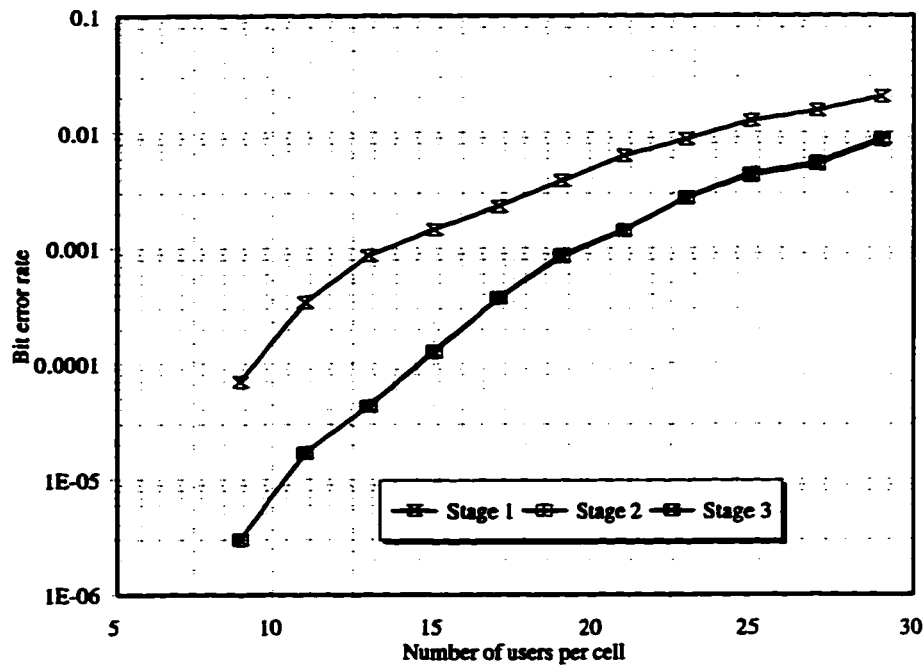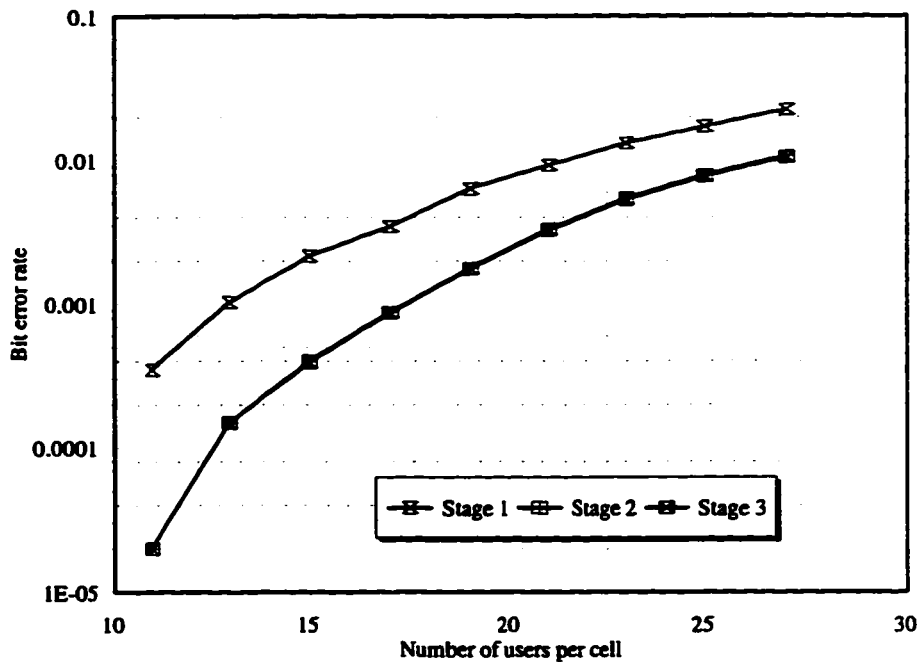Fig. 4.C.10. The multi-cell performance of a RAMSIC receiver on a flat fading channel with f = 0.686 and synchronization error of $0.15T_c$.
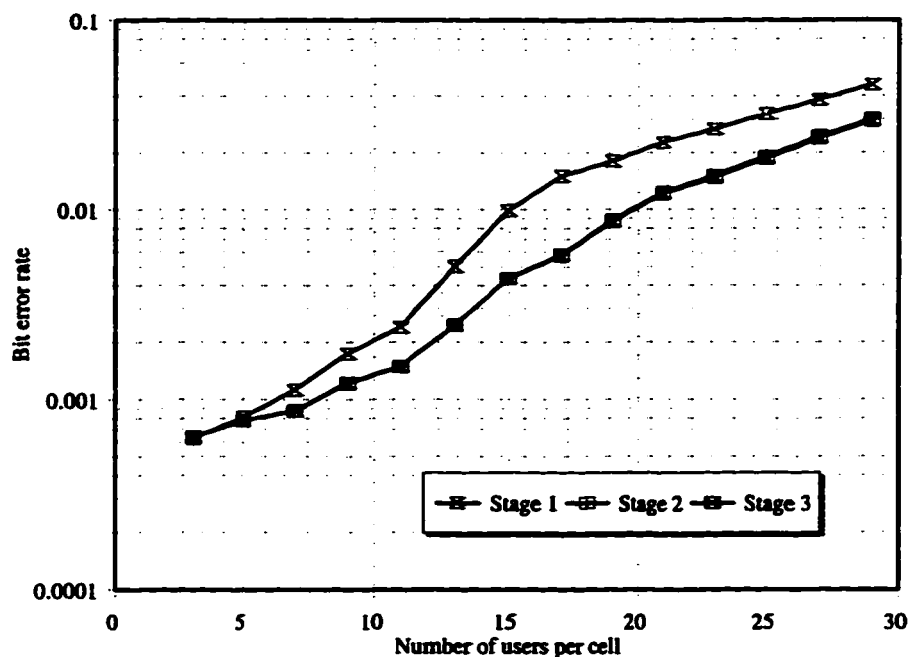
Fig. 4.C.11. The multi-cell performance of a RAMSIC receiver on a flat fading channel with f = 0.959 and synchronization error of $0.15T_c$.
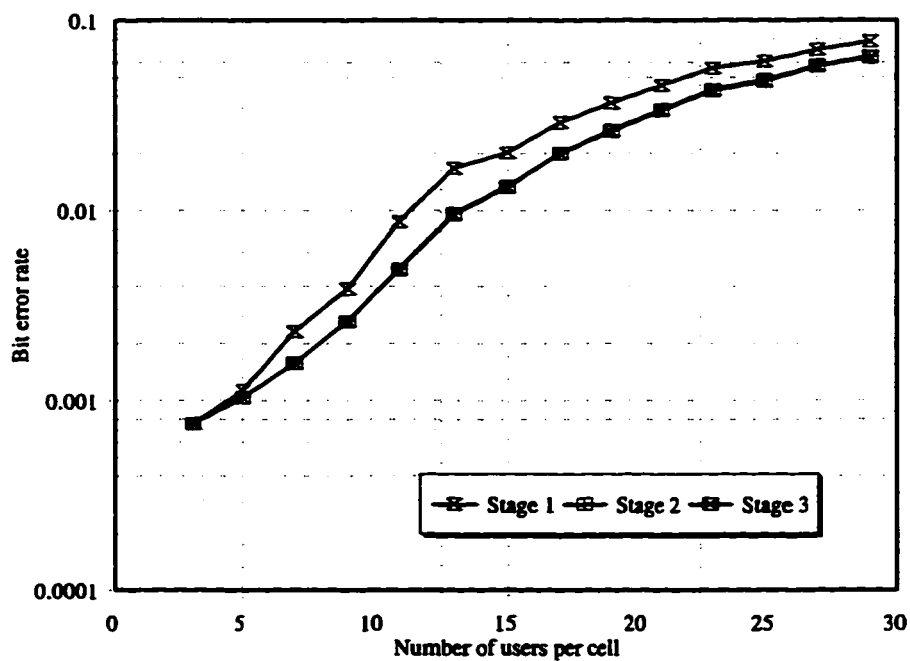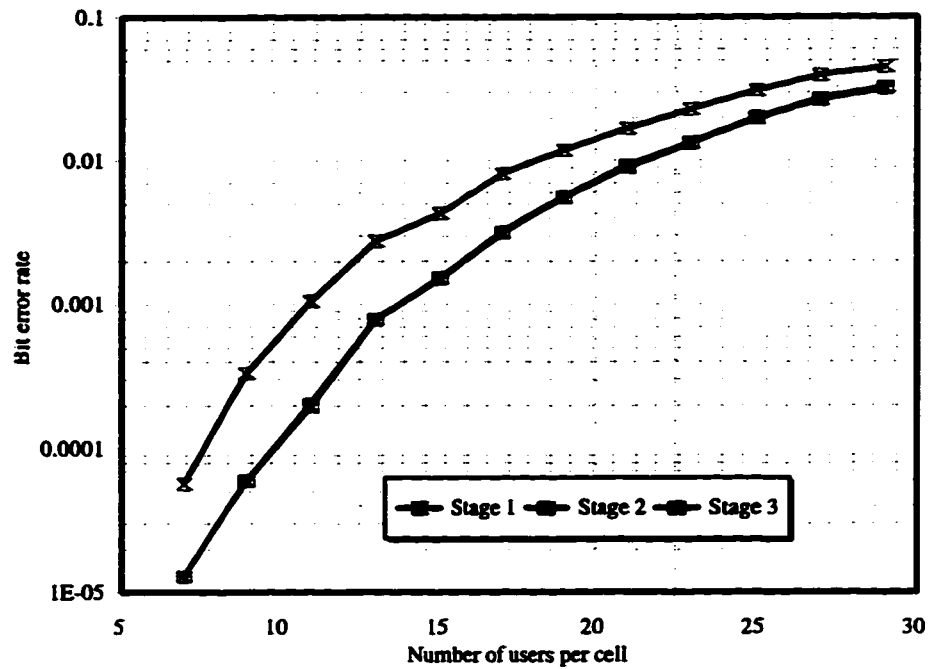

Fig. 4.C.12. The multi-cell performance of a RAMSIC receiver on a flat fading channel with f = 1.57 and synchronization error of $0.15T_c$.
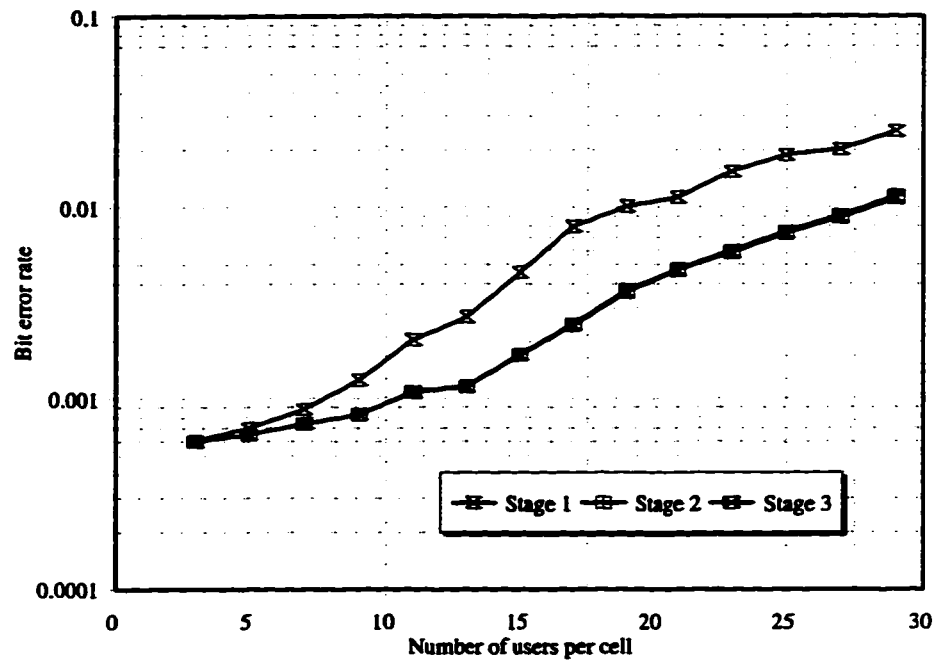
Fig. 4.C.13. The multi-cell performance of a RAMSIC receiver on a flat fading channel with f = 0.55 and synchronization error of $0.2T_c$.
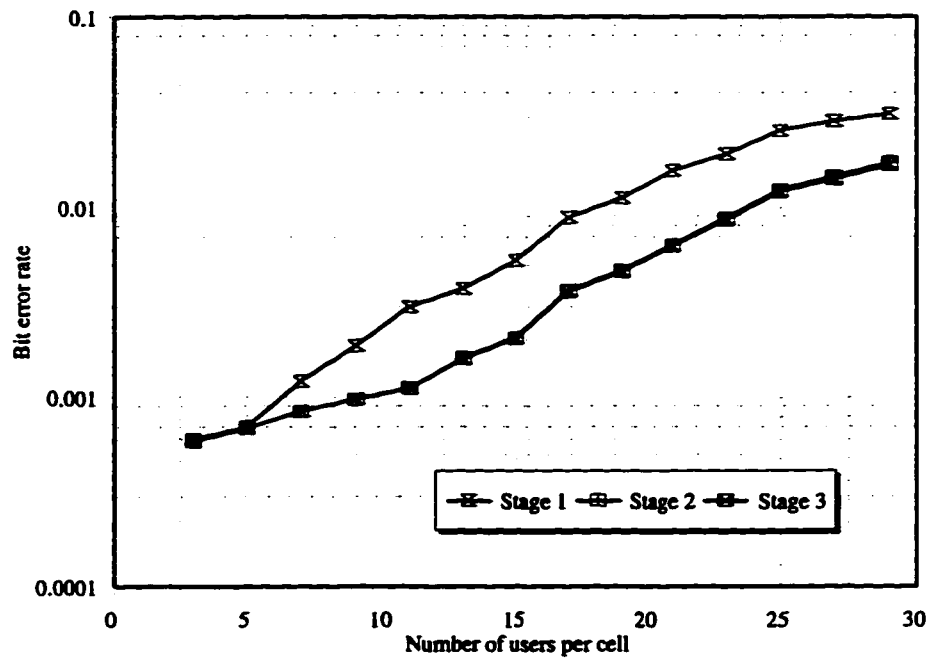
Fig. 4.C.14. The multi-cell performance of a RAMSIC receiver on a flat fading channel with f = 0.686 and synchronization error of $0.2T_c$.
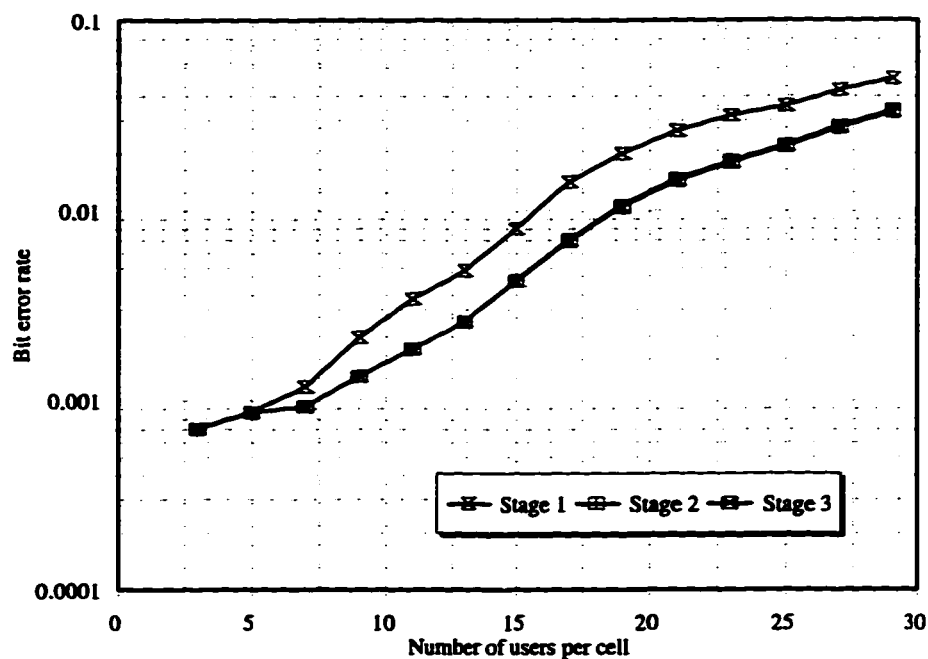
Fig. 4.C.15. The multi-cell performance of a RAMSIC receiver on a flat fading channel with f = 0.959 and synchronization error of $0.2T_c$.
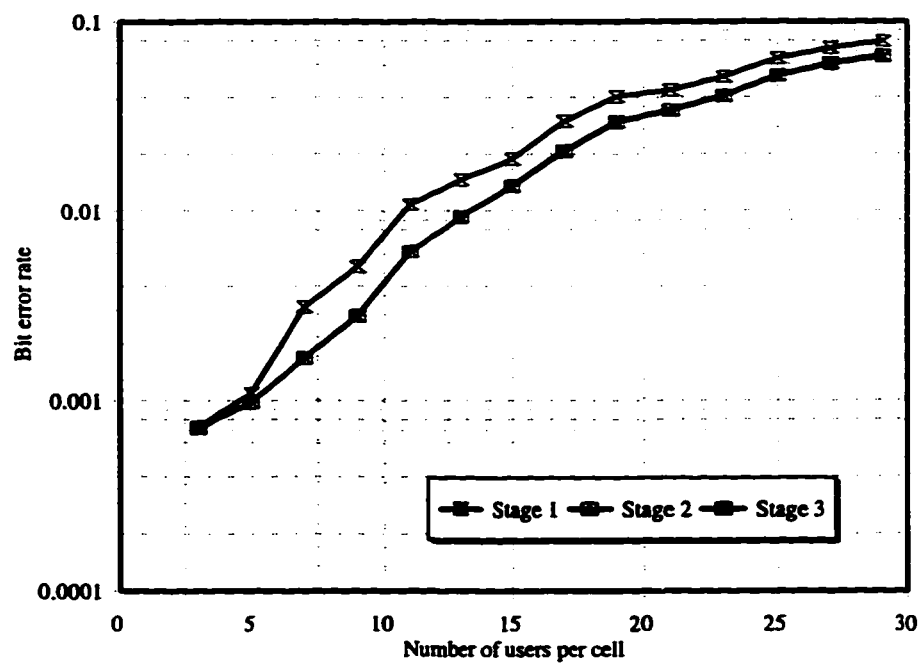
Fig. 4.C.16. The multi-cell performance of a RAMSIC receiver on a flat fading channel with f = 1.57 and synchronization error of $0.2T_c$.

Fig. 4.C.17. The multi-cell performance of a RAMSIC receiver on a frequency selective Rayleigh fading channel with f = 0.55 and synchronization error of $0.05T_c$.
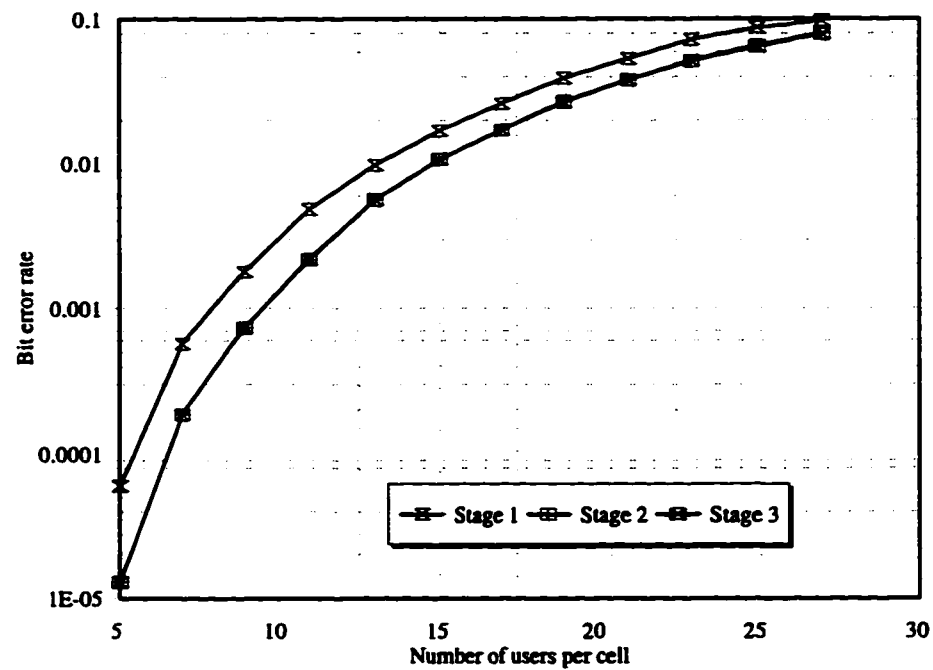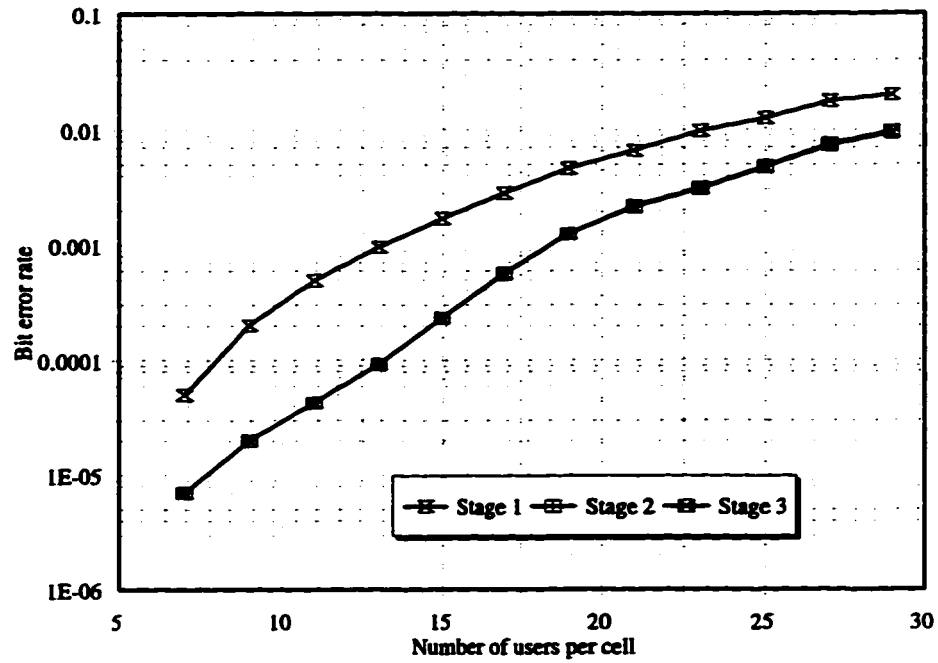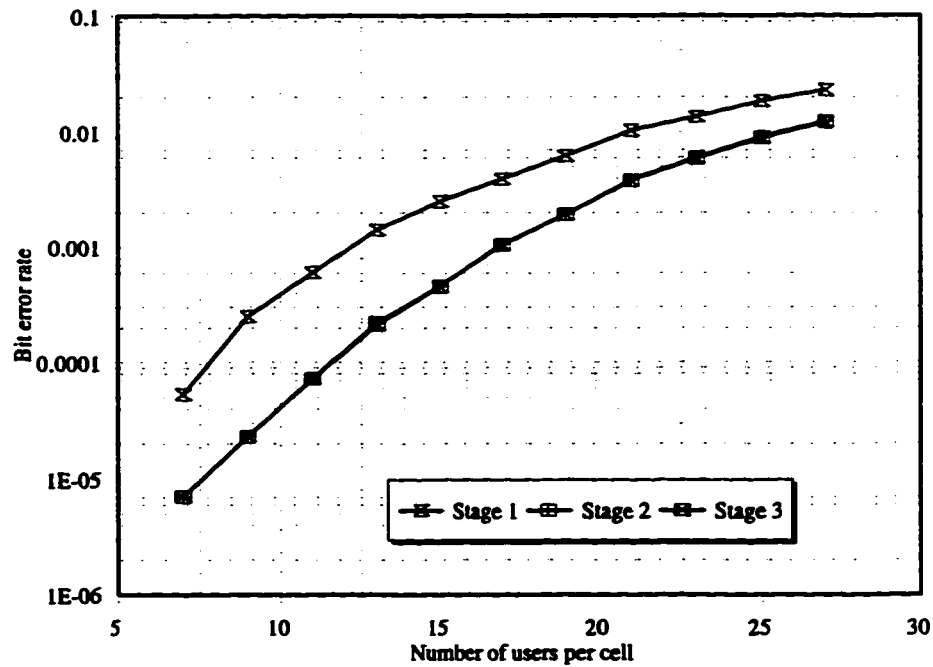

Fig. 4.C.18. The multi-cell performance of a RAMSIC receiver on a frequency selective Rayleigh fading channel with f = 0.686 and synchronization error of $0.05T_c$.
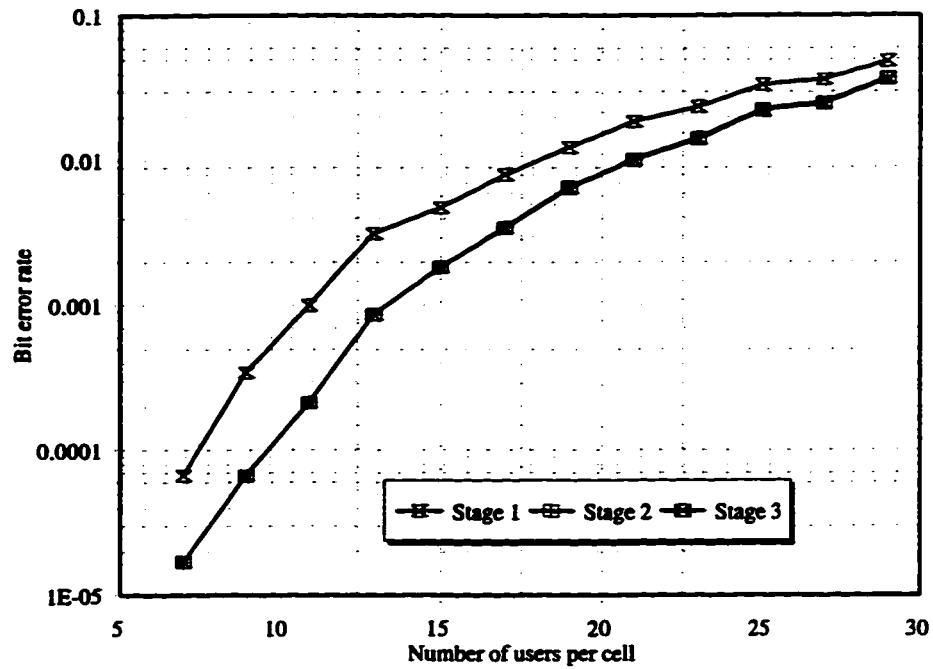
Fig.4.C.19. The multi-cell performance of a RAMSIC receiver on a frequency selective Rayleigh fading channel with f = 0.959 and synchronization error of $0.05T_c$.

Fig. 4.C.20. The multi-cell performance of a RAMSIC receiver on a frequency selective Rayleigh fading channel with f = 1.57 and synchronization error of $0.05T_c$.

Fig. 4.C.21. The multi-cell performance of a RAMSIC receiver on a frequency selective Rayleigh fading channel with f = 0.55 and synchronization error of $0.1T_c$.
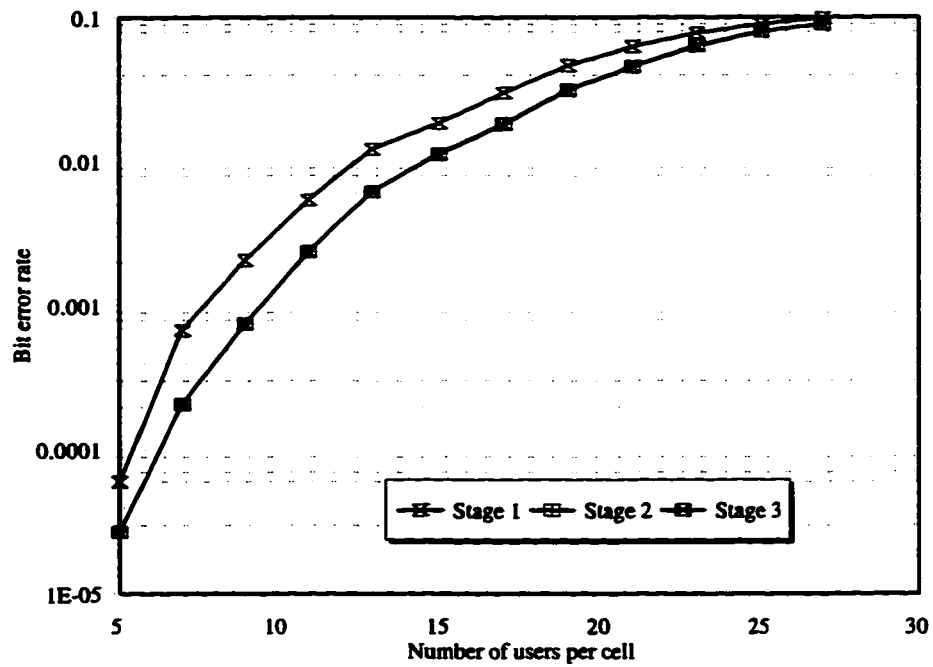

Fig.4.C.22. The multi-cell performance of a RAMSIC receiver on a frequency selective Rayleigh fading channel with f = 0.686 and synchronization error of $0.1T_c$.

Fig. 4.C.23. The multi-cell performance of a RAMSIC receiver on a frequency selective Rayleigh fading channel with f = 0.959 and synchronization error of $0.1T_c$.

Fig. 4.C.24. The multi-cell performance of a RAMSIC receiver on a frequency selective Rayleigh fading channel with f = 1.57 and synchronization error of $0.1T_c$.

Fig. 4.C.25. The multi-cell performance of a RAMSIC receiver on a frequency selective Rayleigh fading channel with f = 0.55 and synchronization error of $0.15T_c$.

Fig. 4.C.26. The multi-cell performance of a RAMSIC receiver on a frequency selective Rayleigh fading channel with f = 0.686 and synchronization error of $0.15T_c$.

Fig. 4.C.27. The multi-cell performance of a RAMSIC receiver on a frequency selective Rayleigh fading channel with f = 0.959 and synchronization error of 0.15T_c.

Fig. 4.C.28. The multi-cell performance of a RAMSIC receiver on a frequency selective Rayleigh fading channel with f = 1.57 and synchronization error of 0.15T_c.

Fig. 4.C.29. The multi-cell performance of a RAMSIC receiver on a frequency selective Rayleigh fading channel with f − 0.55 and synchronization error of $0.2T_c$.

Fig. 4.C.30. The multi-cell performance of a RAMSIC receiver on a frequency selective Rayleigh fading channel with f − 0.686 and synchronization error of $0.2T_c$.

Fig. 4.C.31. The multi-cell performance of a RAMSIC receiver on a frequency selective Rayleigh fading channel with f = 0.959 and synchronization error of $0.2T_c$.

Fig. 4.C.32. The multi-cell performance of a RAMSIC receiver on a frequency selective Rayleigh fading channel with f = 1.57 and synchronization error of $0.2T_c$.

4.10 Appendix 4D

This appendix illustrates the sensitivity of the RAMSIC receiver with quadriphase spreading to power control error. For all cases considered here, perfect synchronization as well as the IS-95 type power amplifier mask are assumed.
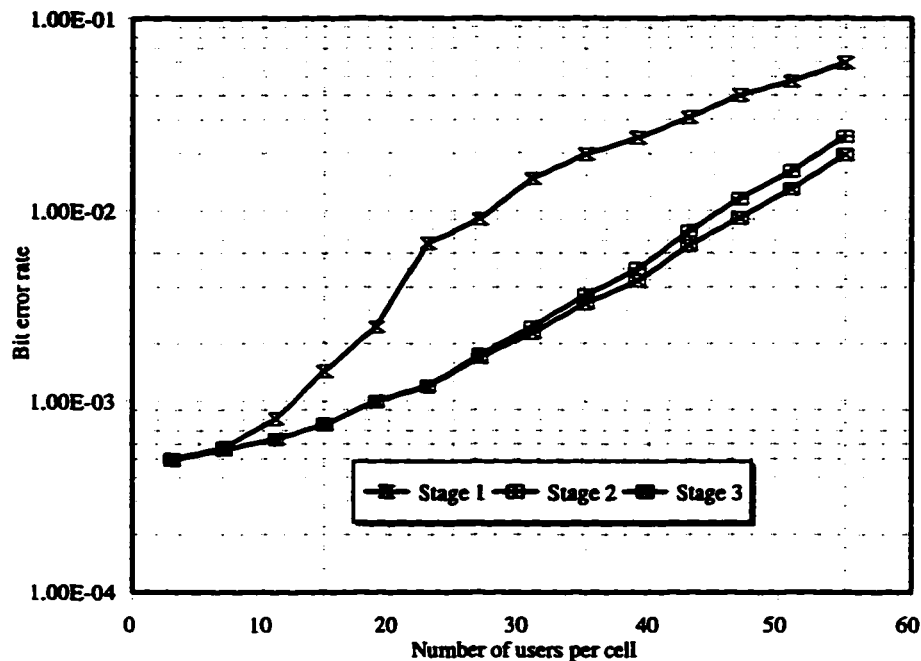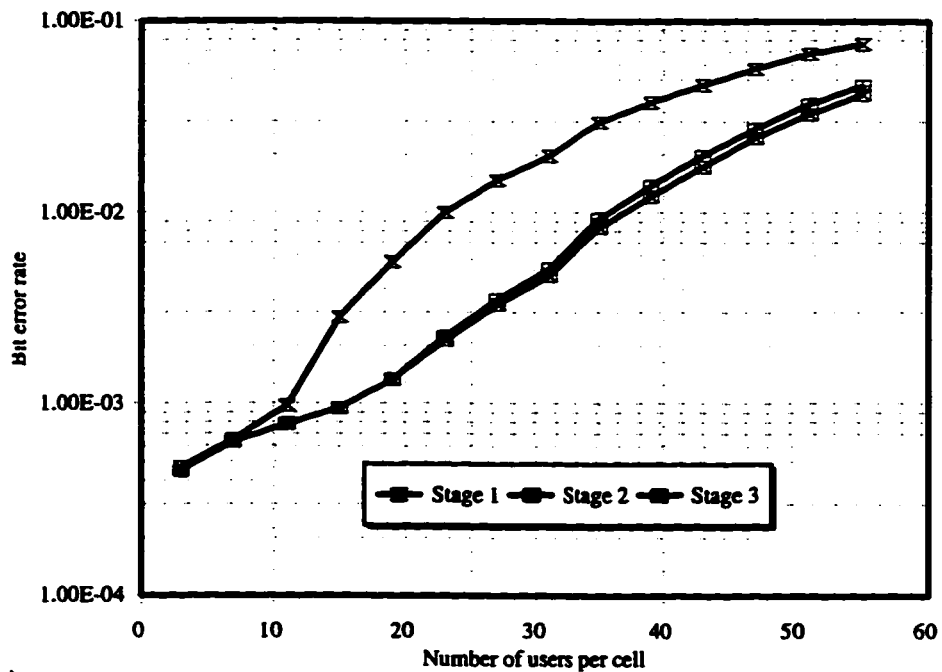

Fig. 4.D.1. The multi-cell performance of a RAMSIC receiver with quadriphase spreading on a flat Rayleigh fading channel with f = 0.686 and ideal power control.
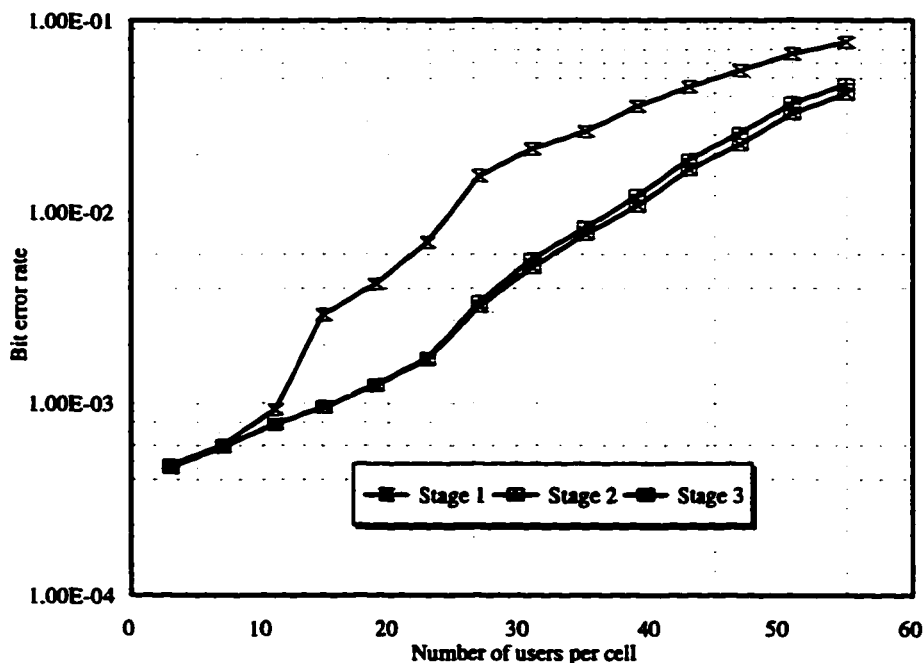
Fig. 4.D.2. The multi-cell performance of a RAMSIC receiver with quadriphase spreading on a flat Rayleigh fading channel with f = 0.959 and ideal power control.
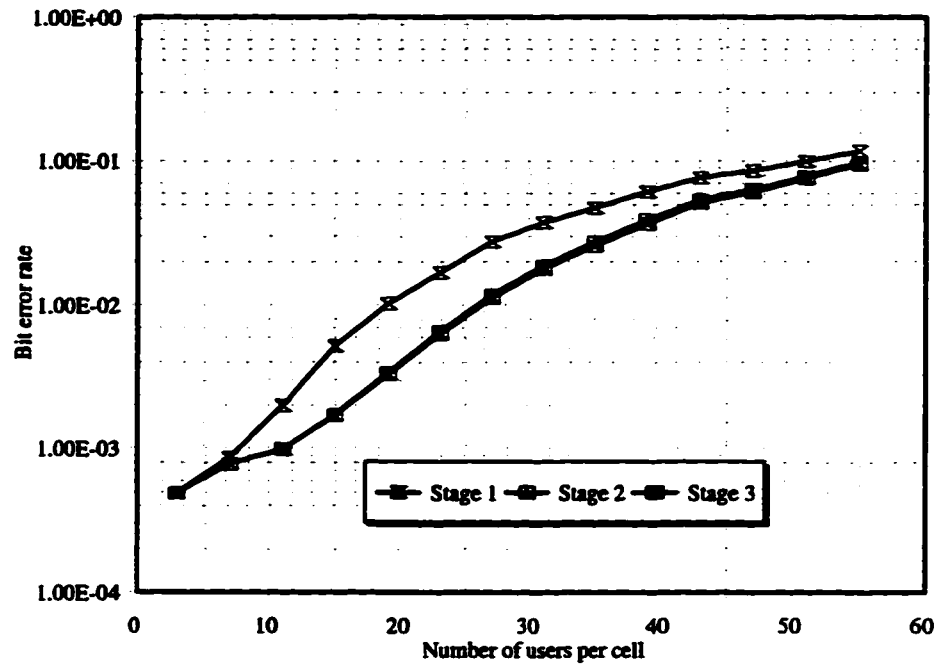
Fig. 4.D.3. The multi-cell performance of a RAMSIC receiver with quadriphase spreading on a flat Rayleigh fading channel with f = 1.57 and ideal power control.
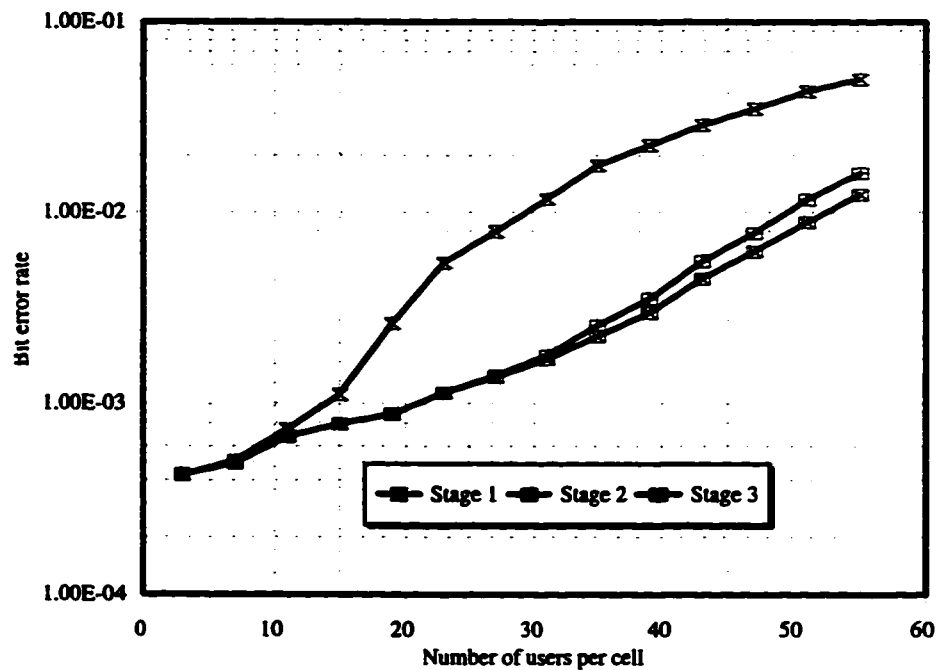
Fig. 4.D.4. The multi-cell performance of a RAMSIC receiver with quadriphase spreading on a flat Rayleigh fading channel with f = 0.55. Power control is non-ideal with standard deviation of its error equal to 0.7 dB.
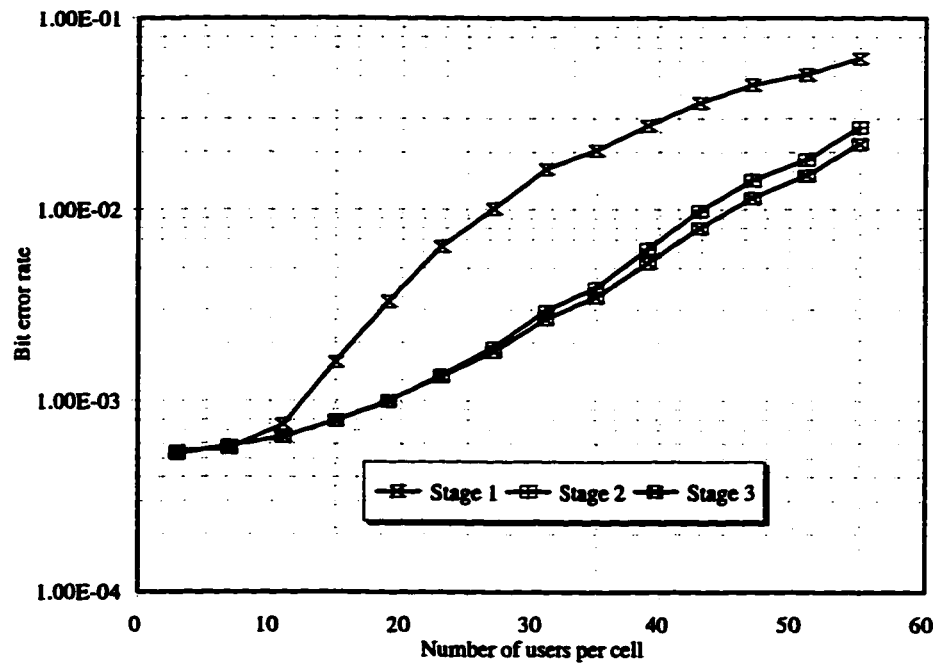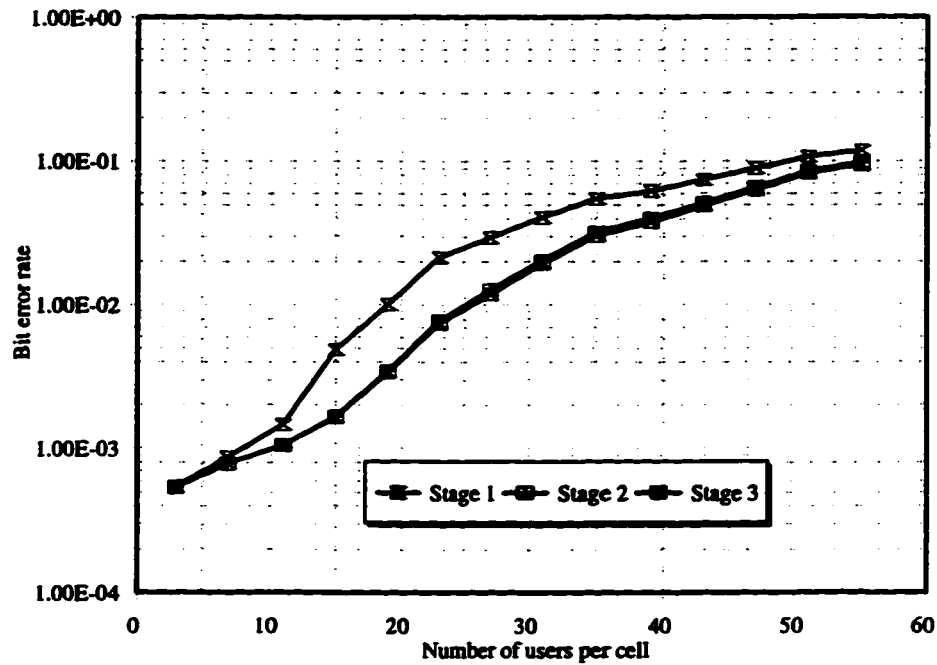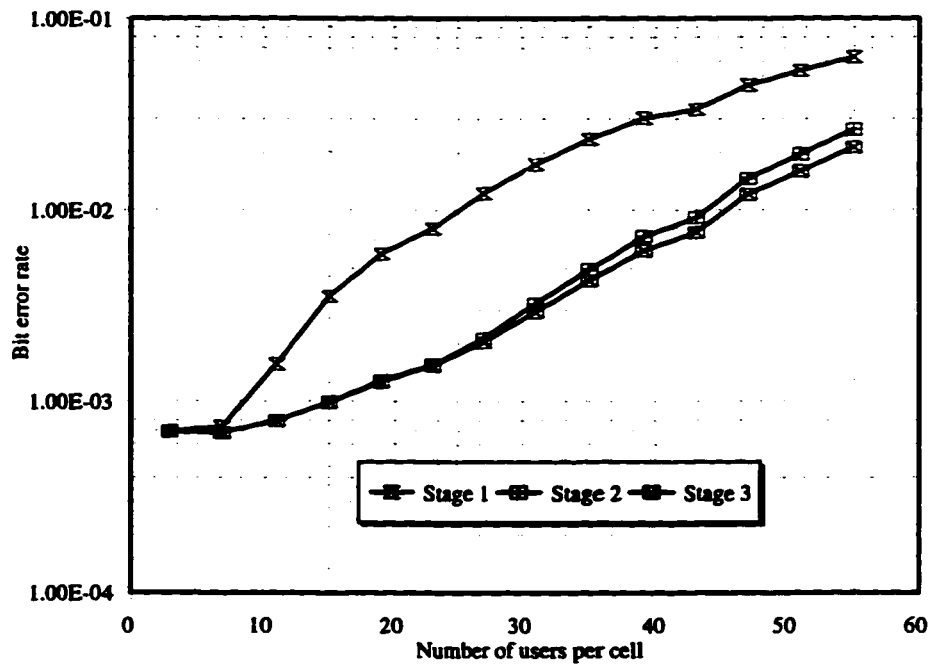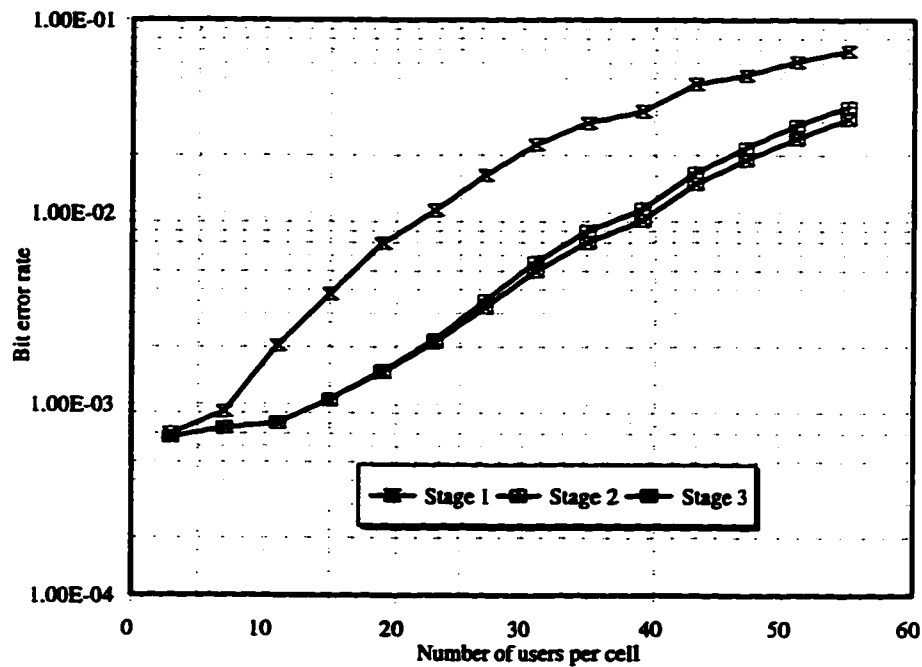
Fig. 4.D.5. The multi-cell performance of a RAMSIC receiver with quadriphase spreading on a flat Rayleigh fading channel with f = 0.686. Power control is non-ideal with standard deviation of its error equal to 0.7 dB.
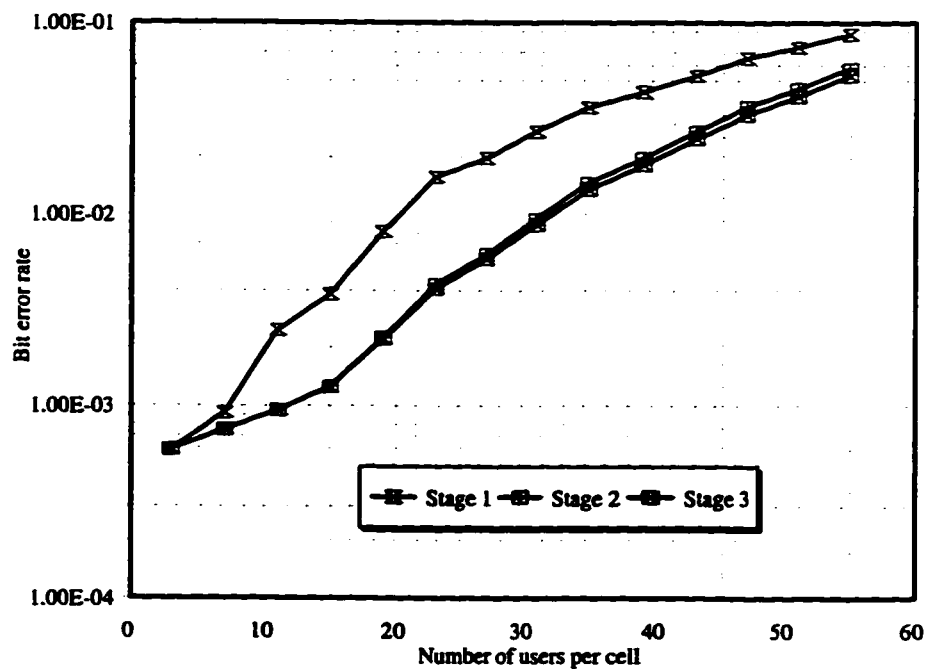

Fig. 4.D.6. The multi-cell performance of a RAMSIC receiver with quadriphase spreading on a flat Rayleigh fading channel with f = 0.959. Power control is non-ideal with standard deviation of its error equal to 0.7 dB.
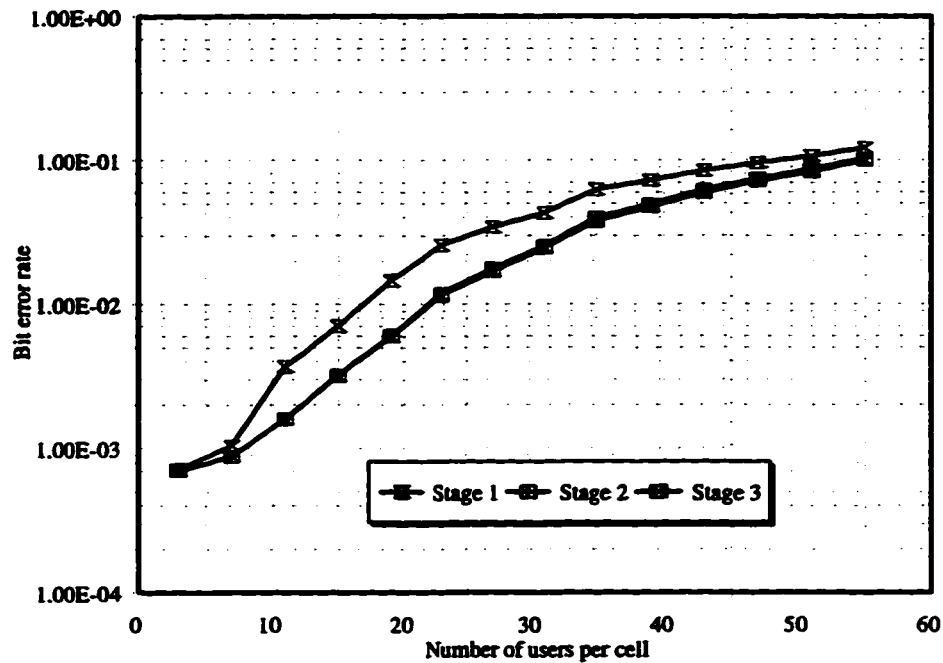
191

Fig. 4.D.7. The multi-cell performance of a RAMSIC receiver with quadriphase spreading on a flat Rayleigh fading channel with f = 1.57. Power control is non-ideal with standard deviation of its error equal to 0.7 dB.

Fig. 4.D.8. The multi-cell performance of a RAMSIC receiver with quadriphase spreading on a flat Rayleigh fading channel with f = 0.55. Power control is non-ideal with standard deviation of its error equal to 1.6 dB.
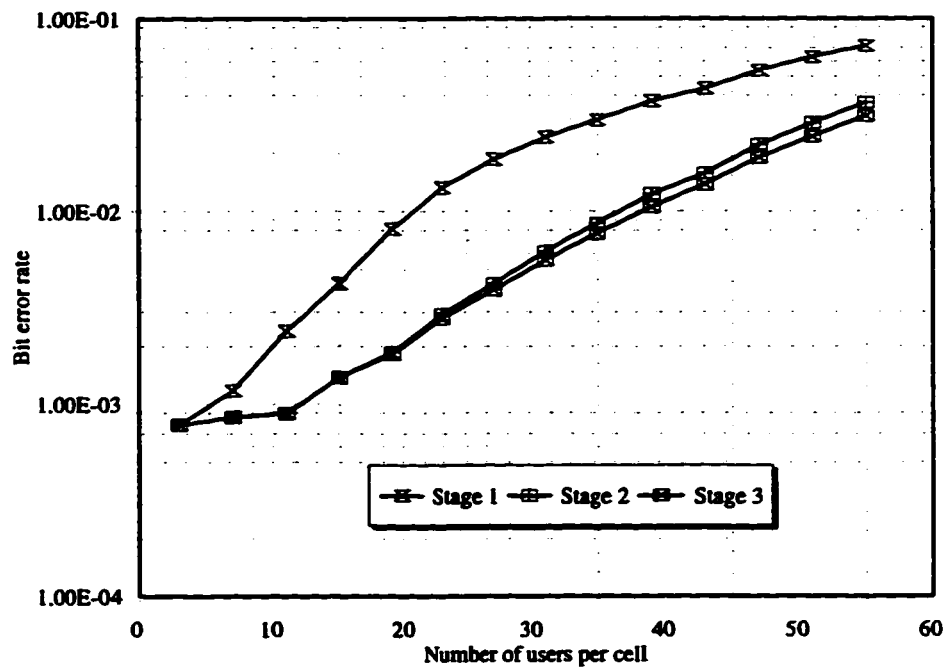
Fig. 4.D.9. The multi-cell performance of a RAMSIC receiver with quadriphase spreading on a flat Rayleigh fading channel with f = 0.686. Power control is non-ideal with standard deviation of its error equal to 1.6 dB.

Fig. 4.D.10. The multi-cell performance of a RAMSIC receiver with quadriphase spreading on a flat Rayleigh fading channel with f = 0.959. Power control is non-ideal with standard deviation of its error equal to 1.6 dB.
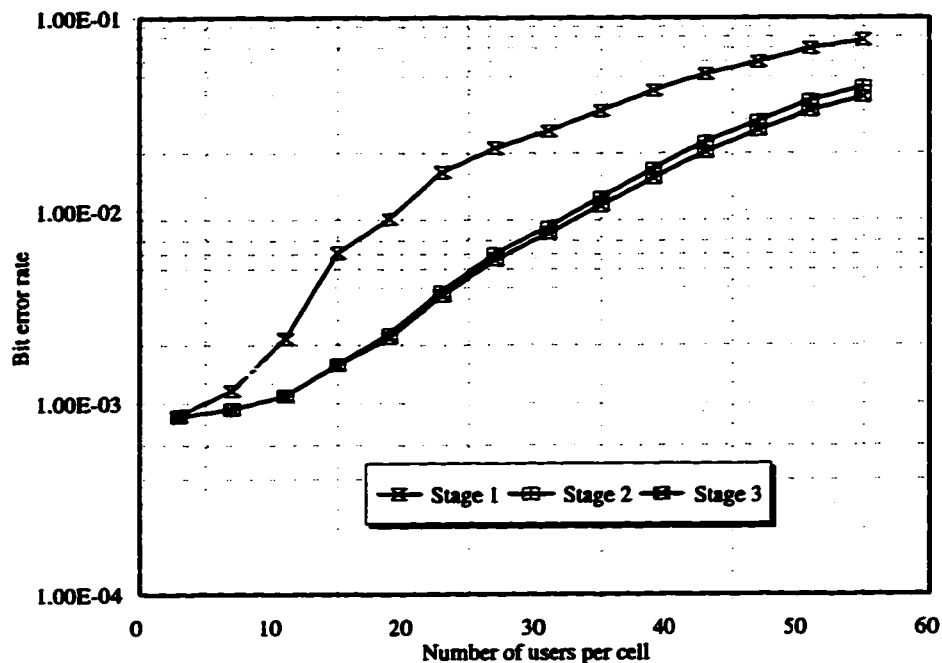
Fig. 4.D.11. The multi-cell performance of a RAMSIC receiver with quadriphase spreading on a flat Rayleigh fading channel with f = 1.57. Power control is non-ideal with standard deviation of its error equal to 1.6 dB.
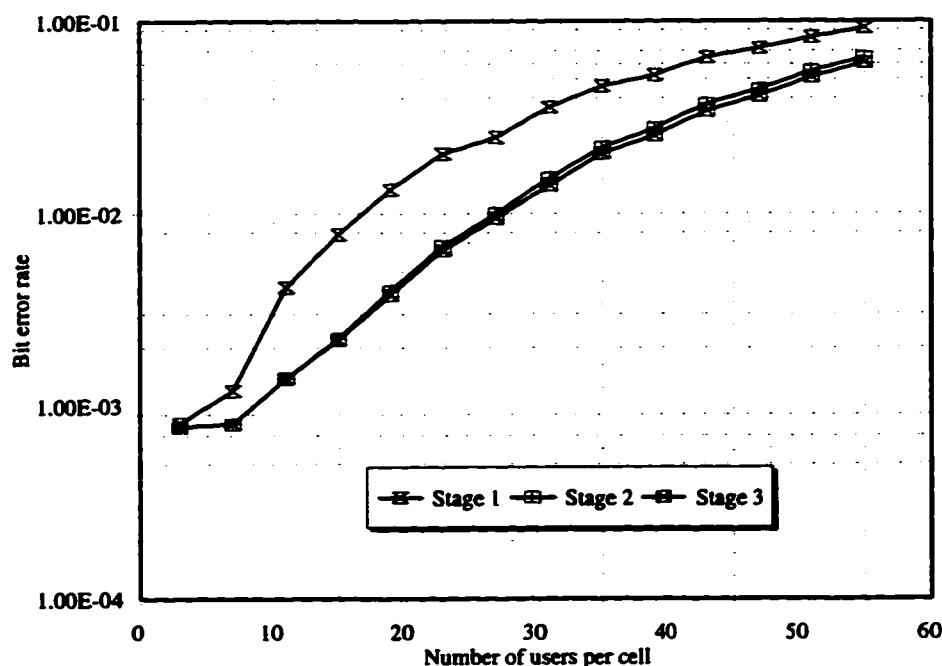

Fig. 4.D.12. The multi-cell performance of a RAMSIC receiver with quadriphase spreading on a flat Rayleigh fading channel with f = 0.55. Power control is non-ideal with standard deviation of its error equal to 2.2 dB.

Fig. 4.D.13. The multi-cell performance of a RAMSIC receiver with quadriphase spreading on a flat Rayleigh fading channel with f - 0.686. Power control is non-ideal with standard deviation of its error equal to 2.2 dB.
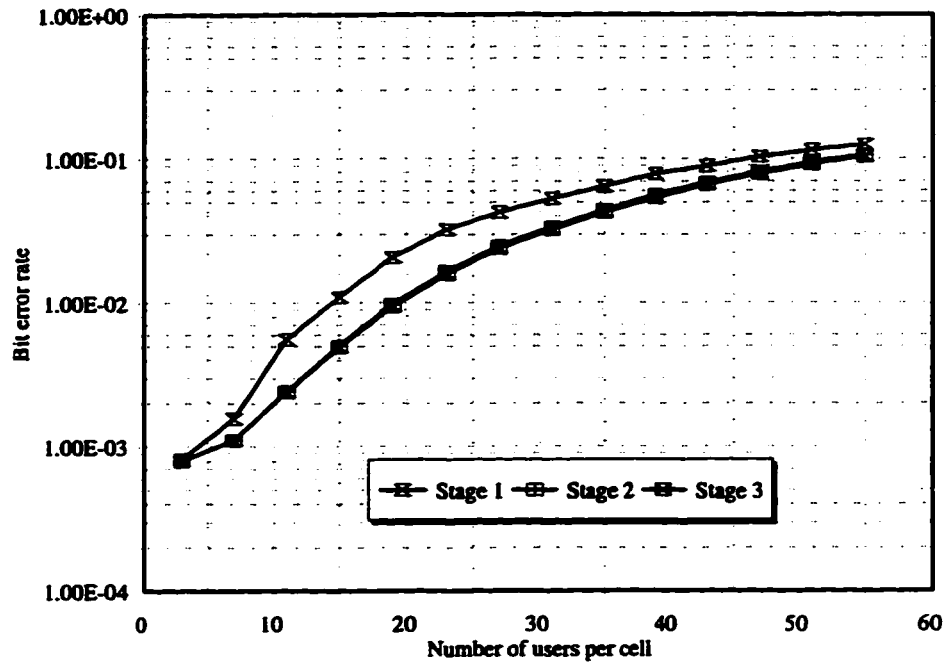

Fig. 4.D.14. The multi-cell performance of a RAMSIC receiver with quadriphase spreading on a flat Rayleigh fading channel with f - 0.959. Power control is non-ideal with standard deviation of its error equal to 2.2 dB.
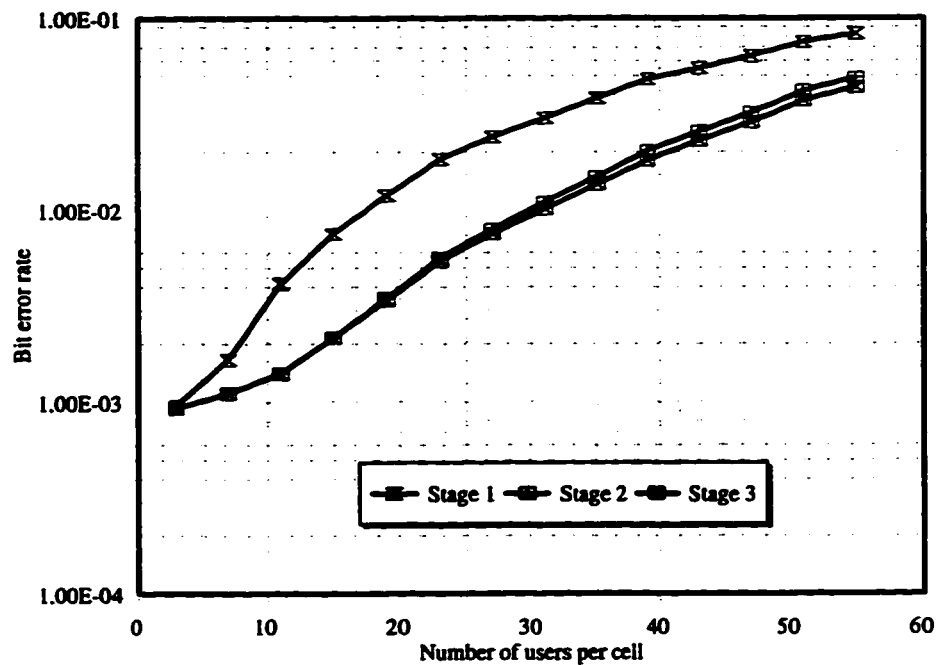
Fig. 4.D.15. The multi-cell performance of a RAMSIC receiver with quadriphase spreading on a flat Rayleigh fading channel with f = 1.57. Power control is non-ideal with standard deviation of its error equal to 2.2 dB.

Fig. 4.D.16. The multi-cell performance of a RAMSIC receiver with quadriphase spreading on a flat Rayleigh fading channel with f = 0.55. Power control is non-ideal with standard deviation of its error equal to 2.9 dB.
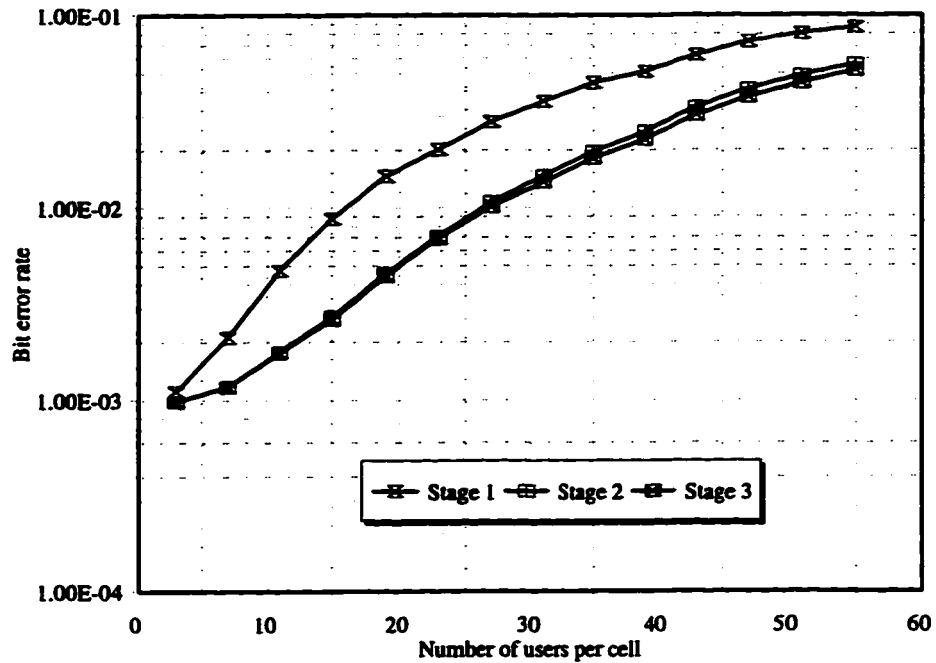
Fig. 4.D.17. The multi-cell performance of a RAMSIC receiver with quadriphase spreading on a flat Rayleigh fading channel with f = 0.686. Power control is non-ideal with standard deviation of its error equal to 2.9 dB.
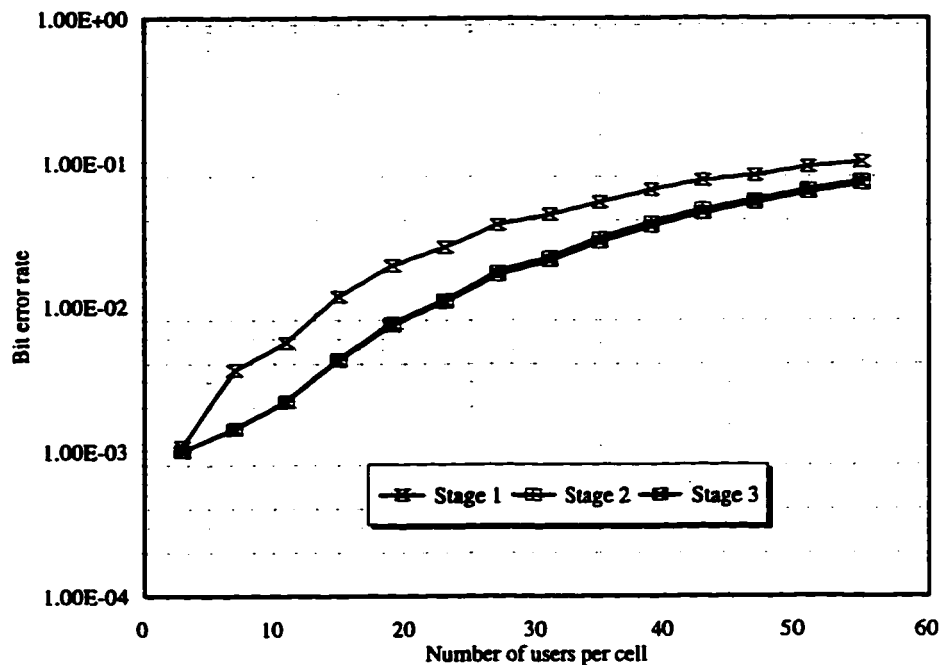

Fig. 4.D.18. The multi-cell performance of a RAMSIC receiver with quadriphase spreading on a flat Rayleigh fading channel with f = 0.959. Power control is non-ideal with standard deviation of its error equal to 2.9 dB.
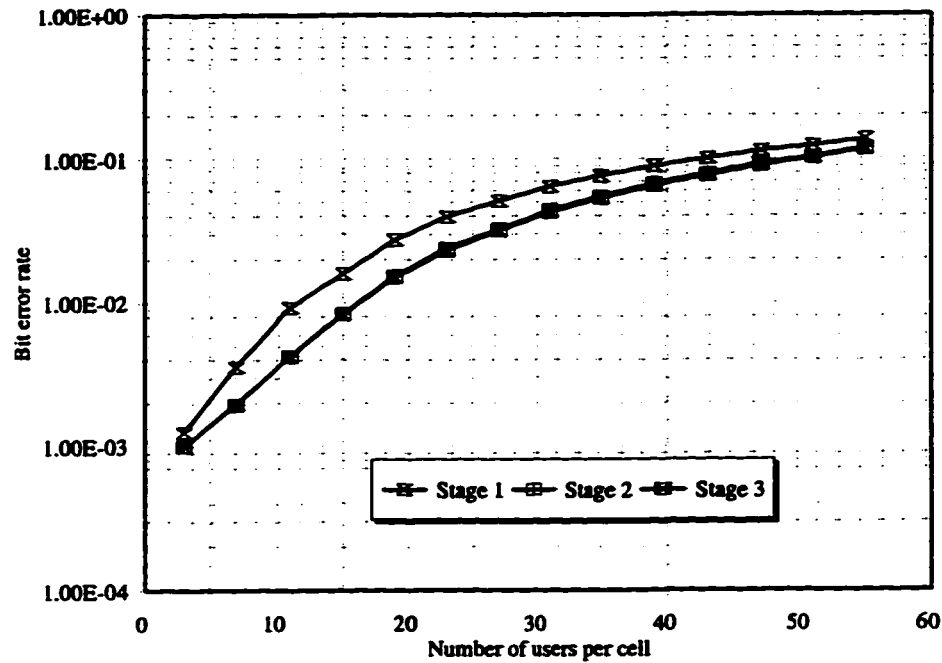
Fig. 4.D.19. The multi-cell performance of a RAMSIC receiver with quadriphase spreading on a flat Rayleigh fading channel with f = 1.57. Power control is non-ideal with standard deviation of its error equal to 2.9 dB.
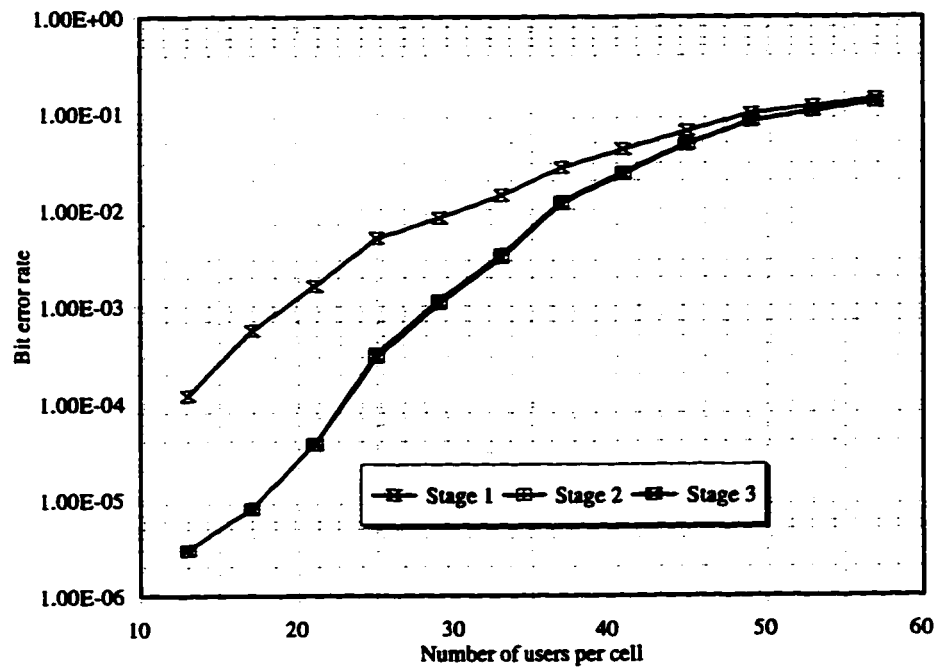

Fig. 4.D.20. The multi-cell performance of a RAMSIC receiver with quadriphase spreading on a frequency selective Rayleigh fading channel with f = 0.686 and ideal power control.
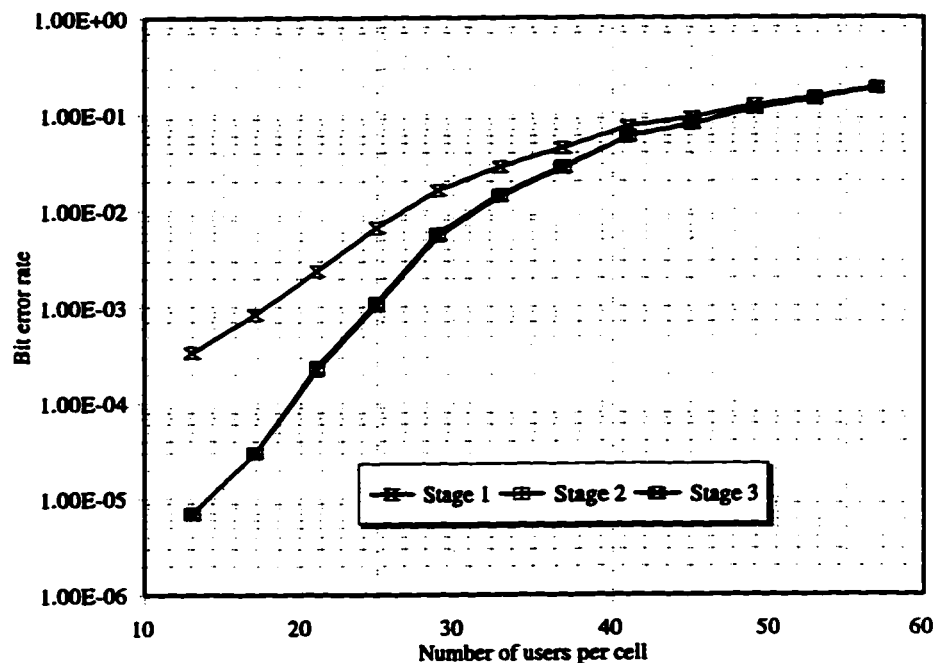
Fig. 4.D.21. The multi-cell performance of a RAMSIC receiver with quadriphase spreading on a frequency selective Rayleigh fading channel with f = 0.959 and ideal power control.

Fig. 4.D.22. The multi-cell performance of a RAMSIC receiver with quadriphase spreading on a frequency selective Rayleigh fading channel with f = 1.57 and ideal power control.
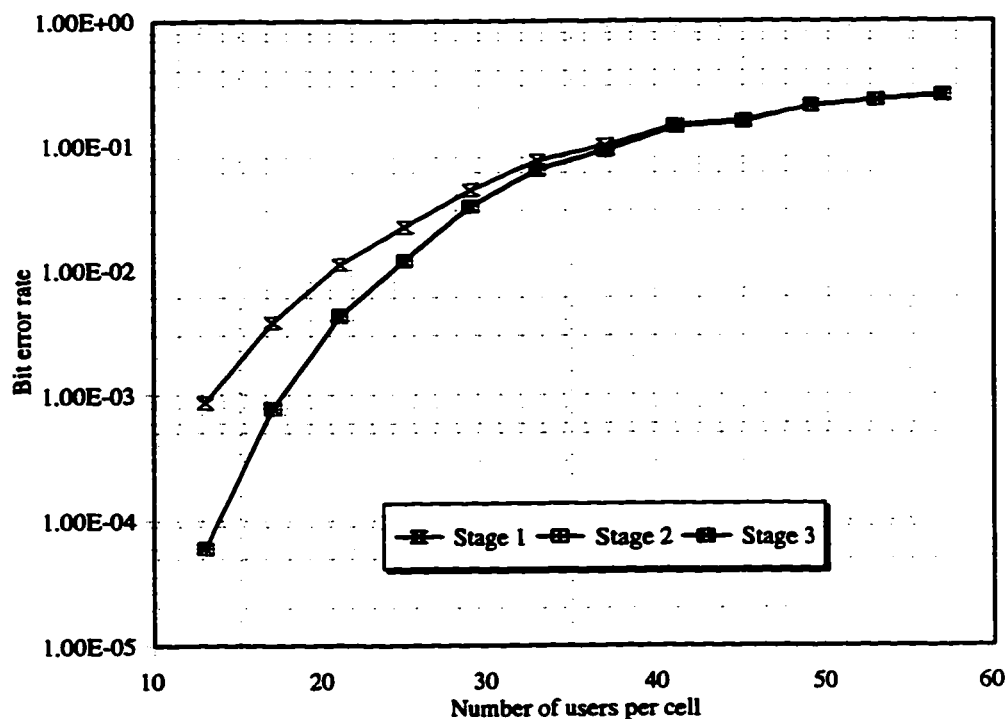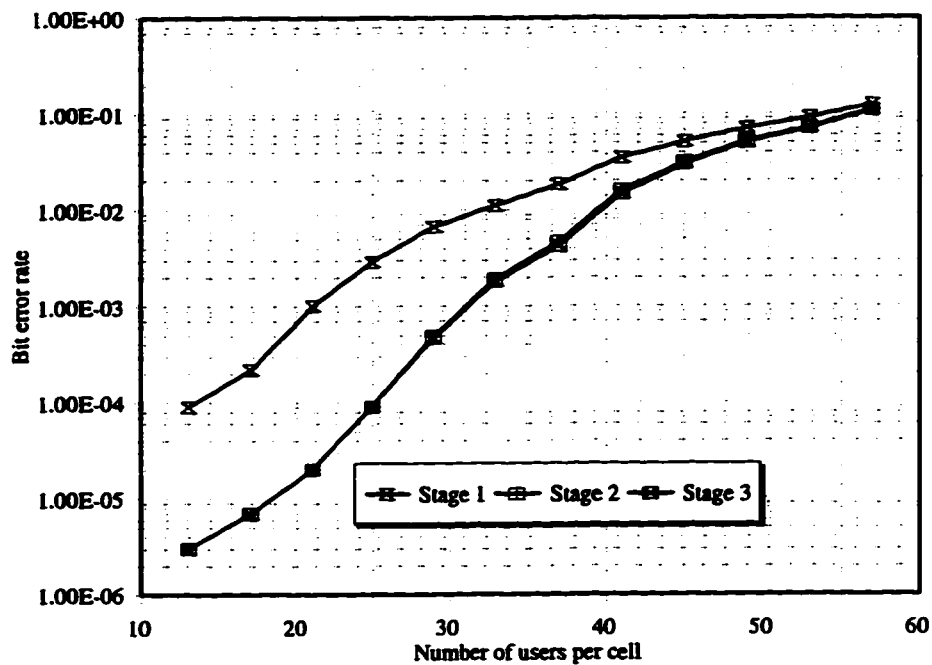
Fig. 4.D.23. The multi-cell performance of a RAMSIC receiver with quadriphase spreading on a frequency selective Rayleigh fading channel with f = 0.55. Power control is non-ideal with standard deviation of its error equal to 0.7 dB.

Fig. 4.D.24. The multi-cell performance of a RAMSIC receiver with quadriphase spreading on a frequency selective Rayleigh fading channel with f = 0.686. Power control is non-ideal with standard deviation of its error equal to 0.7 dB.

Fig. 4.D.25. The multi-cell performance of a RAMSIC receiver with quadriphase spreading on a frequency selective Rayleigh fading channel with f = 0.959. Power control is non-ideal with standard deviation of its error equal to 0.7 dB.
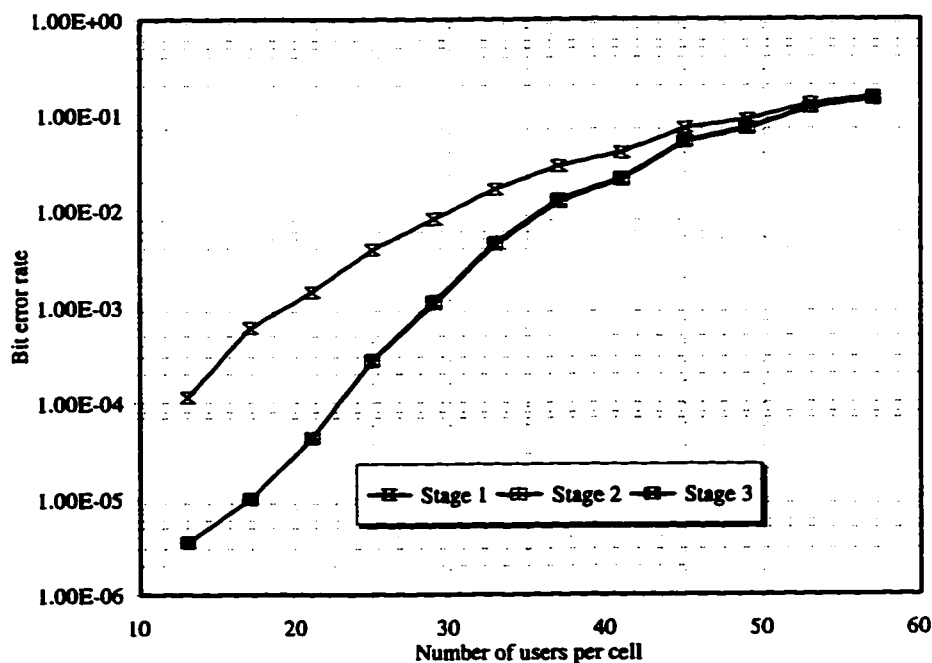

Fig. 4.D.26. The multi-cell performance of a RAMSIC receiver with quadriphase spreading on a frequency selective Rayleigh fading channel with f = 1.57. Power control is non-ideal with standard deviation of its error equal to 0.7 dB.
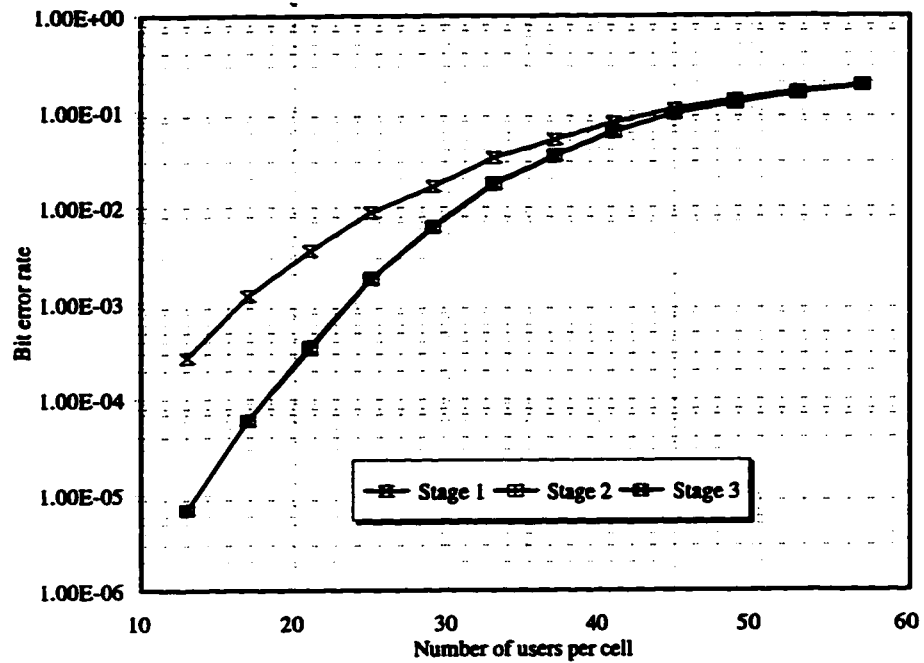
Fig. 4.D.27. The multi-cell performance of a RAMSIC receiver with quadriphase spreading on a frequency selective Rayleigh fading channel with f = 0.55. Power control is non-ideal with standard deviation of its error equal to 1.6 dB.

Fig. 4.D.28. The multi-cell performance of a RAMSIC receiver with quadriphase spreading on a frequency selective Rayleigh fading channel with f = 0.686. Power control is non-ideal with standard deviation of its error equal to 1.6 dB.

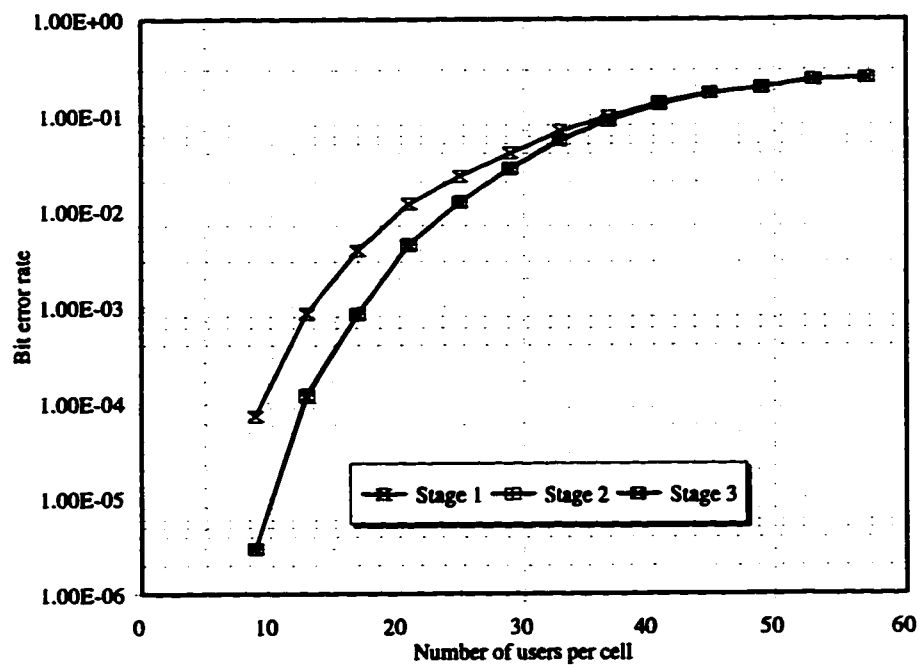Fig. 4.D.29. The multi-cell performance of a RAMSIC receiver with quadriphase spreading on a frequency selective Rayleigh fading channel with f = 0.959. Power control is non-ideal with standard deviation of its error equal to 1.6 dB.

Fig. 4.D.30. The multi-cell performance of a RAMSIC receiver with quadriphase spreading on a frequency selective Rayleigh fading channel with f = 1.57. Power control is non-ideal with standard deviation of its error equal to 1.6 dB.
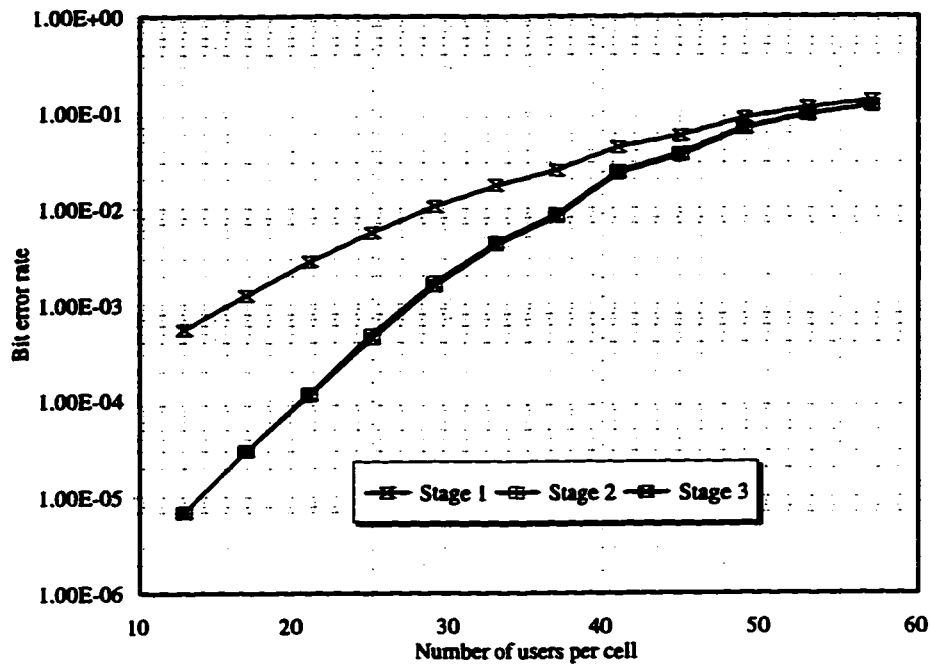
Fig. 4.D.31. The multi-cell performance of a RAMSIC receiver with quadriphase spreading on a frequency selective Rayleigh fading channel with f = 0.55. Power control is non-ideal with standard deviation of its error equal to 2.2 dB.
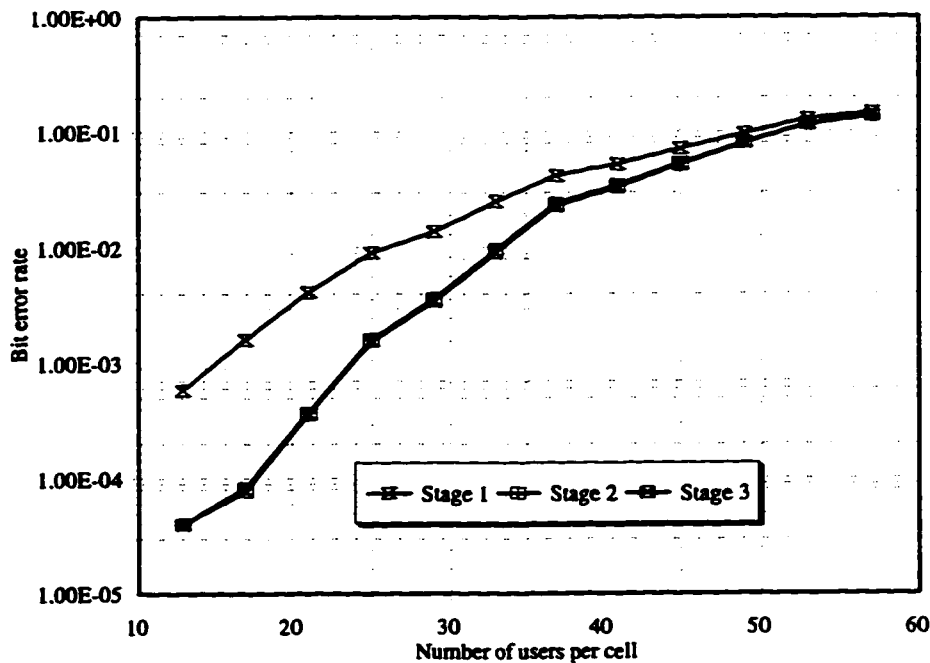

Fig. 4.D.32. The multi-cell performance of a RAMSIC receiver with quadriphase spreading on a frequency selective Rayleigh fading channel with f = 0.686. Power control is non-ideal with standard deviation of its error equal to 2.2 dB.
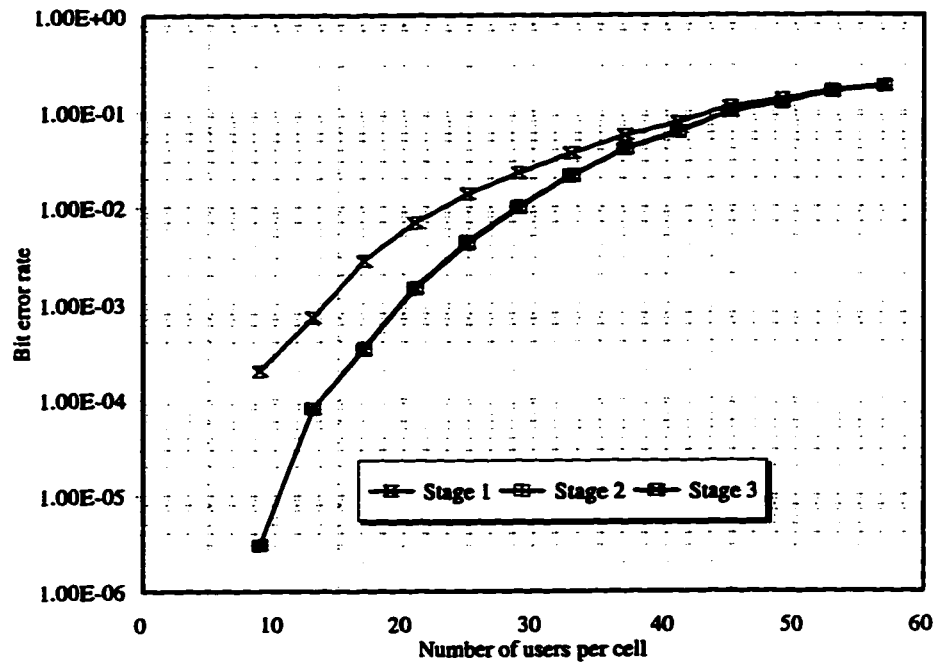
Fig. 4.D.33. The multi-cell performance of a RAMSIC receiver with quadriphase spreading on a frequency selective Rayleigh fading channel with f = 0.959. Power control is non-ideal with standard deviation of its error equal to 2.2 dB.
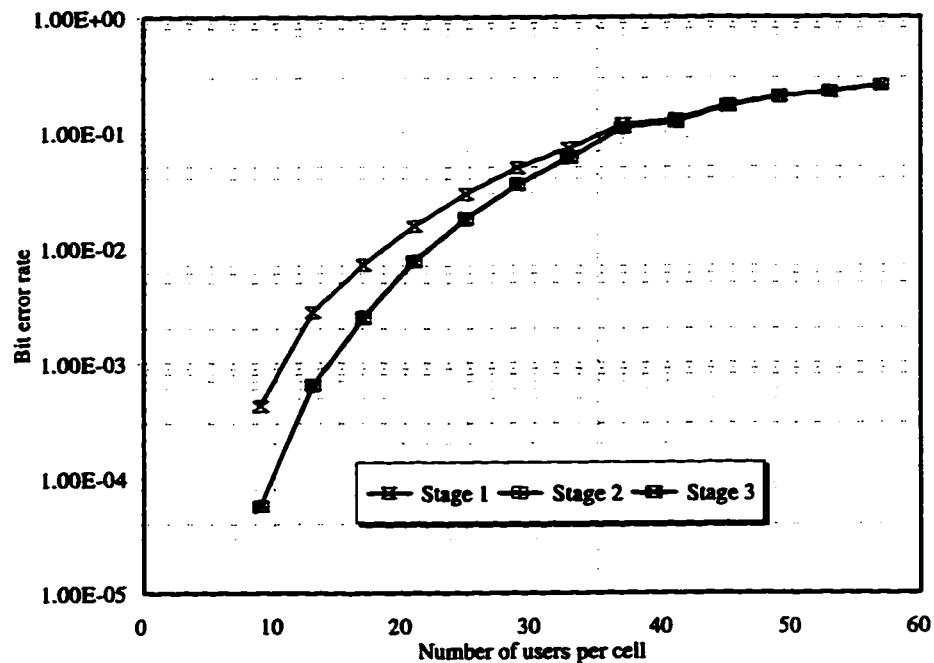

Fig. 4.D.34. The multi-cell performance of a RAMSIC receiver with quadriphase spreading on a frequency selective Rayleigh fading channel with f = 1.57. Power control is non-ideal with standard deviation of its error equal to 2.2 dB.
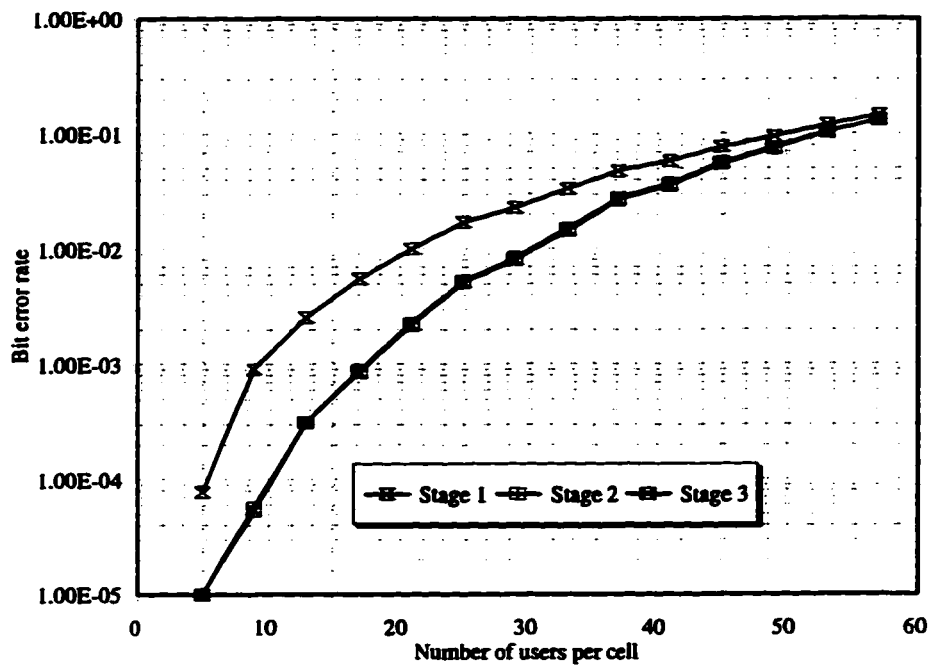
Fig. 4.D.35. The multi-cell performance of a RAMSIC receiver with quadriphase spreading on a frequency selective Rayleigh fading channel with f = 0.55. Power control is non-ideal with standard deviation of its error equal to 2.9 dB.
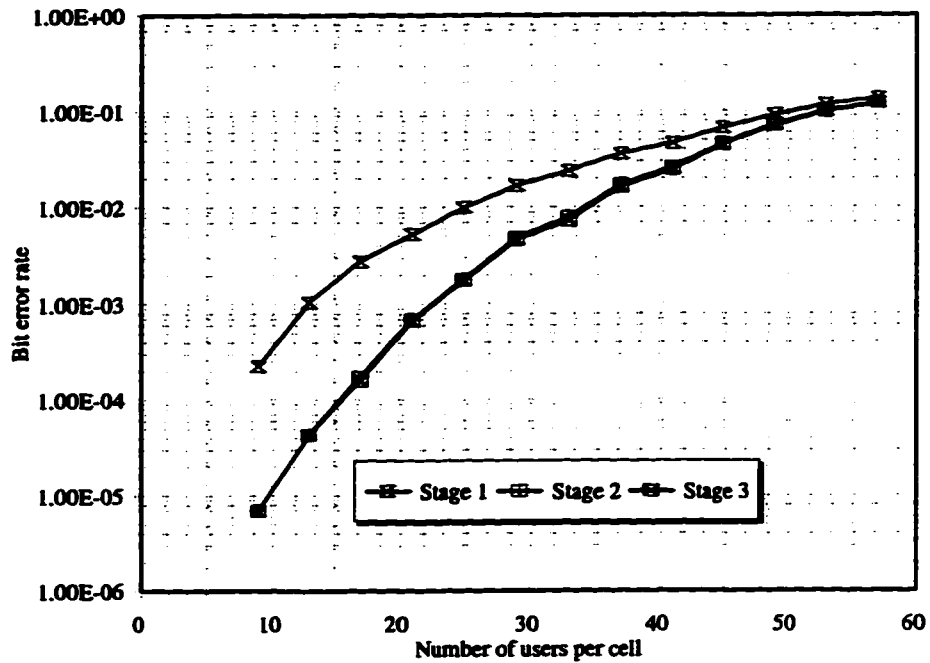

Fig. 4.D.36. The multi-cell performance of a RAMSIC receiver with quadriphase spreading on a frequency selective Rayleigh fading channel with f = 0.686. Power control is non-ideal with standard deviation of its error equal to 2.9 dB.

Fig. 4.D.37. The multi-cell performance of a RAMSIC receiver with quadriphase spreading on a frequency selective Rayleigh fading channel with f = 0.959. Power control is non-ideal with standard deviation of its error equal to 2.9 dB.
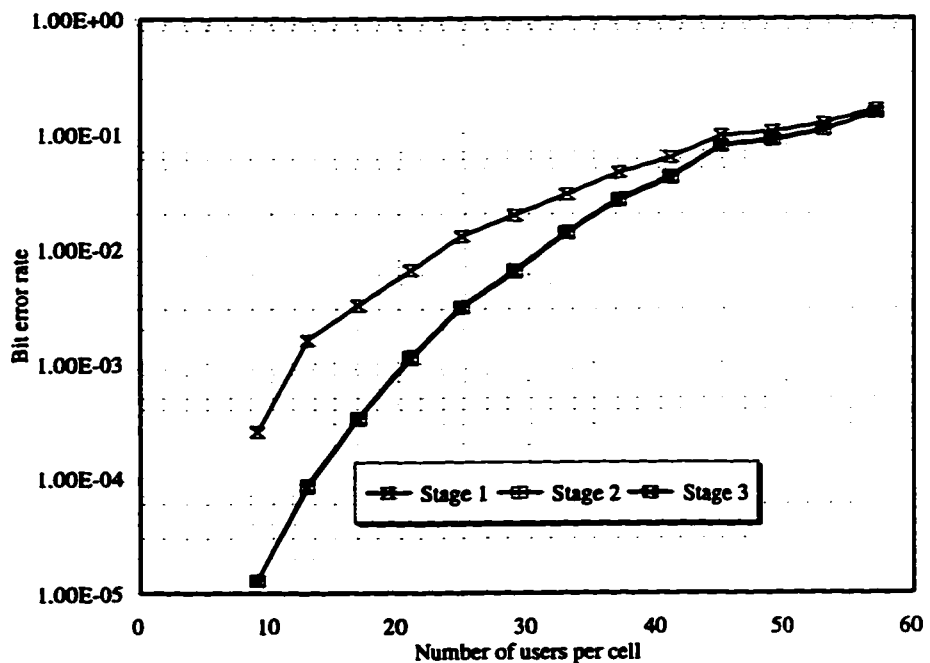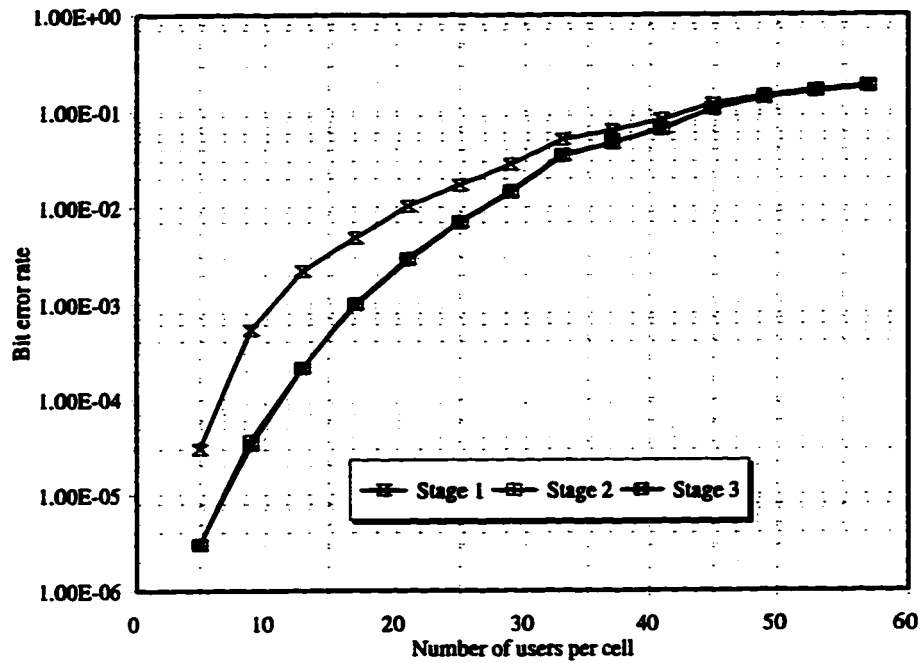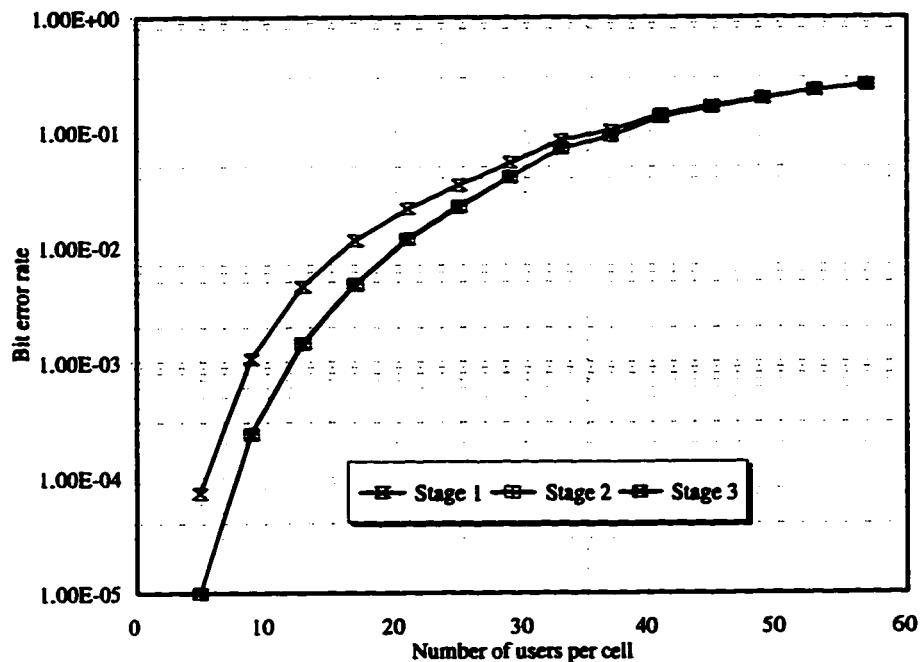

Fig. 4.D.38. The multi-cell performance of a RAMSIC receiver with quadriphase spreading on a frequency selective Rayleigh fading channel with f = 1.57. Power control is non-ideal with standard deviation of its error equal to 2.9 dB.

4.11 Appendix 4E

The performance curves illustrating the sensitivity of the RAMSIC receiver with quadriphase spreading to synchronization errors. For all figures, the output amplifier mask is of the IS-95 type and the power control is non-ideal with standard deviation of its error equal to 1 dB.

Fig. 4.E.1. The multi-cell performance of a RAMSIC receiver with quadriphase spreading on a flat fading channel with f = 0.55 and synchronization error of $0.05T_c$.

Fig. 4.E.2. The multi-cell performance of a RAMSIC receiver with quadriphase spreading on a flat fading channel with f = 0.686 and synchronization error of $0.05T_c$.

208

Fig. 4.E.3. The multi-cell performance of a RAMSIC receiver with quadriphase spreading on a flat fading channel with f = 0.959 and synchronization error of $0.05T_c$.

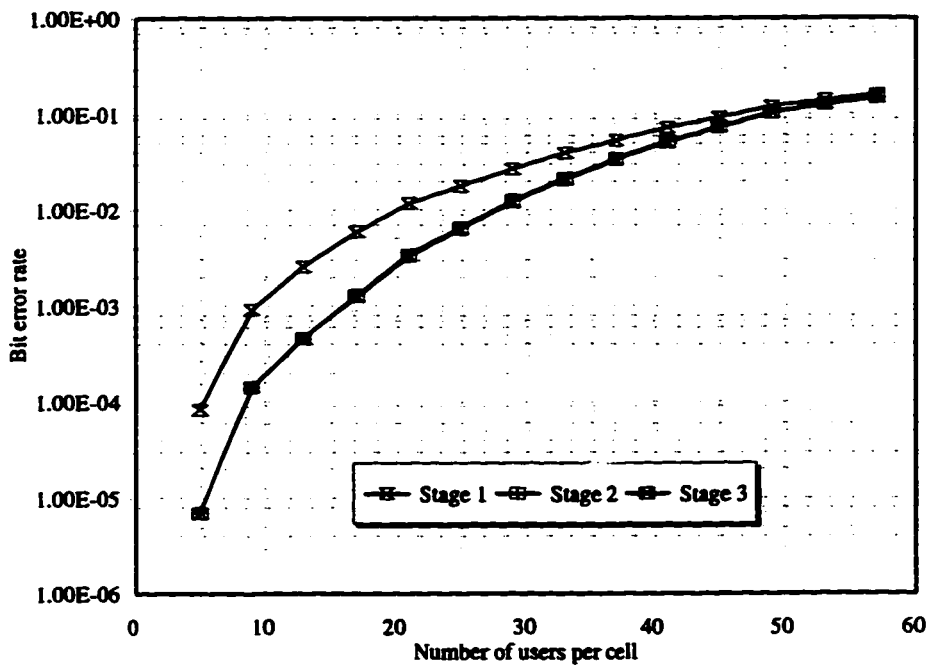Fig. 4.E.4. The multi-cell performance of a RAMSIC receiver with quadriphase spreading on a flat fading channel with f = 1.57 and synchronization error of $0.05T_c$.

Fig. 4.E.5. The multi-cell performance of a RAMSIC receiver with quadriphase spreading on a flat fading channel with f = 0.55 and synchronization error of $0.10T_c$.
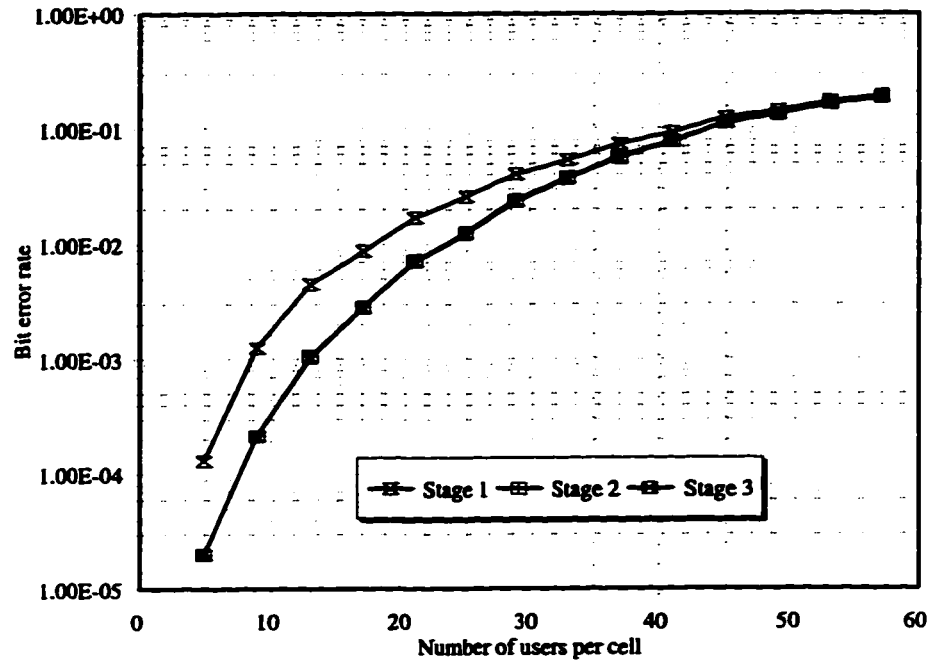

Fig. 4.E.6. The multi-cell performance of a RAMSIC receiver with quadriphase spreading on a flat fading channel with f = 0.686 and synchronization error of $0.10T_c$.

Fig. 4.E.7. The multi-cell performance of a RAMSIC receiver with quadriphase spreading on a flat fading channel with f = 0.959 and synchronization error of $0.10T_c$.

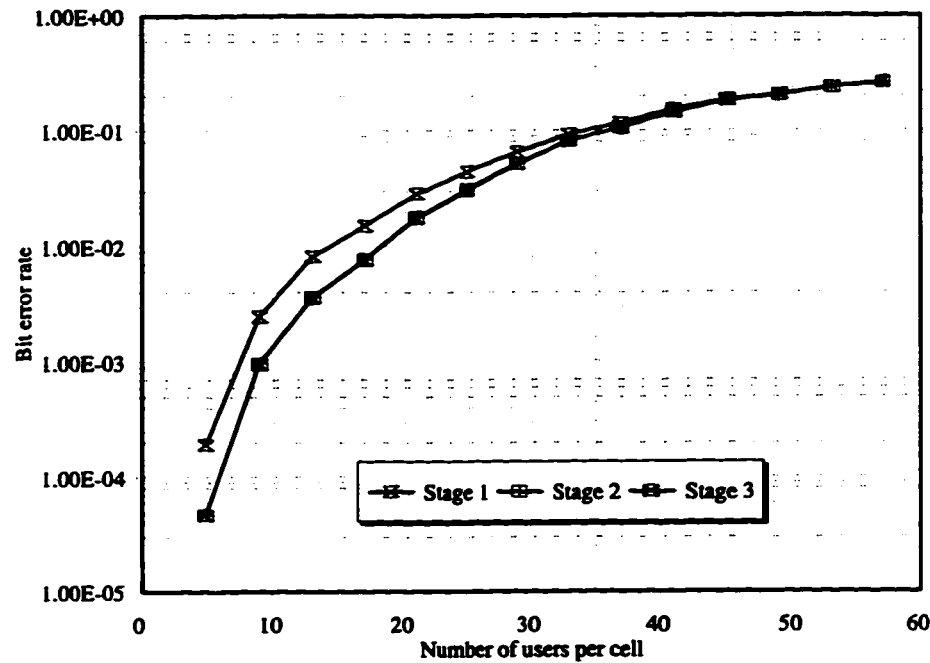Fig. 4.E.8. The multi-cell performance of a RAMSIC receiver with quadriphase spreading on a flat fading channel with f = 1.57 and synchronization error of $0.10T_c$.

Fig. 4.E.9. The multi-cell performance of a RAMSIC receiver with quadriphase spreading on a flat fading channel with f = 0.55 and synchronization error of $0.15T_c$.

Fig. 4.E.10. The multi-cell performance of a RAMSIC receiver with quadriphase spreading on a flat fading channel with f = 0.686 and synchronization error of $0.15T_c$.
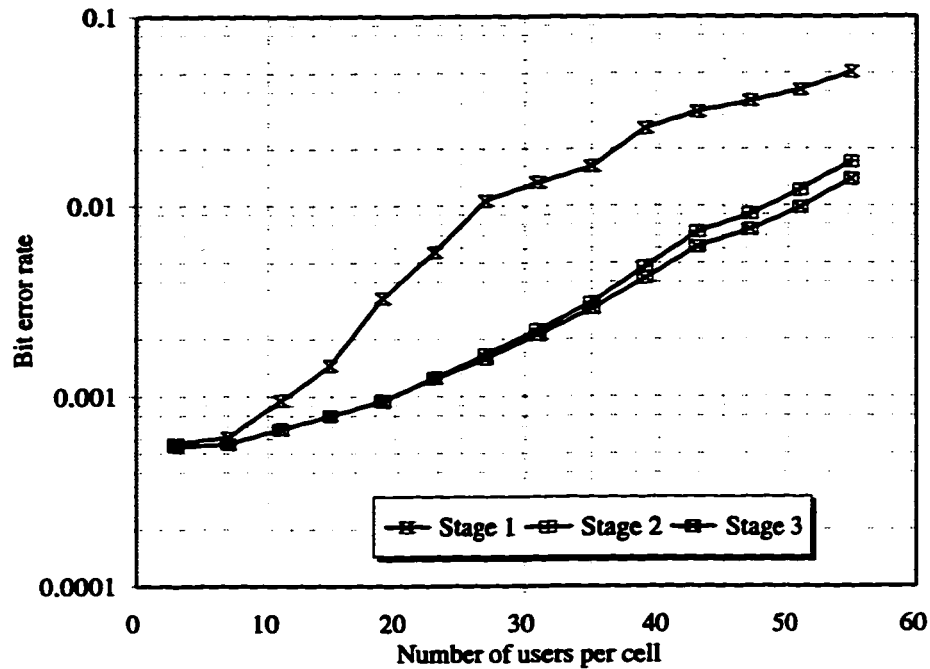
Fig. 4.E.11. The multi-cell performance of a RAMSIC receiver with quadriphase spreading on a flat fading channel with f = 0.959 and synchronization error of $0.15T_c$.

Fig. 4.E.12. The multi-cell performance of a RAMSIC receiver with quadriphase spreading on a flat fading channel with f = 1.57 and synchronization error of $0.15T_c$.

Fig. 4.E.13. The multi-cell performance of a RAMSIC receiver with quadriphase spreading on a flat fading channel with f = 0.55 and synchronization error of $0.20T_c$.
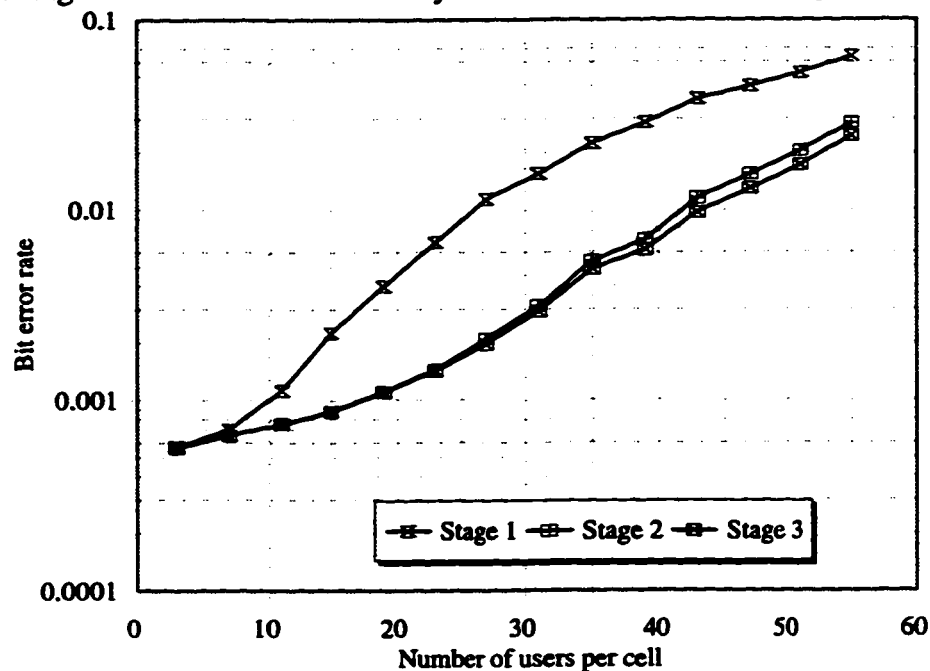

Fig. 4.E.14. The multi-cell performance of a RAMSIC receiver with quadriphase spreading on a flat fading channel with f = 0.686 and synchronization error of $0.20T_c$.
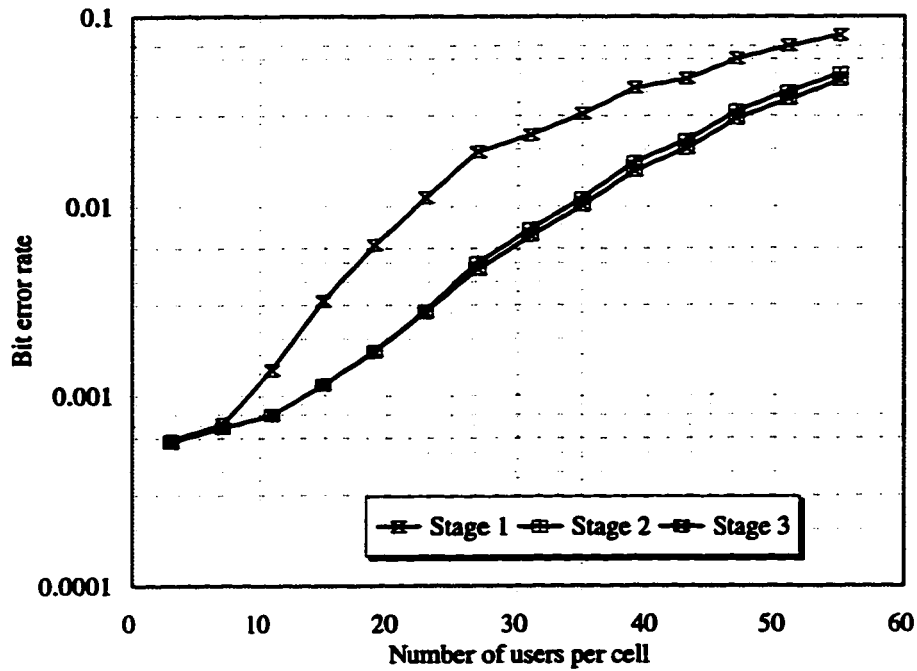
Fig. 4.E.15. The multi-cell performance of a RAMSIC receiver with quadriphase spreading on a flat fading channel with f = 0.959 and synchronization error of $0.20T_c$.
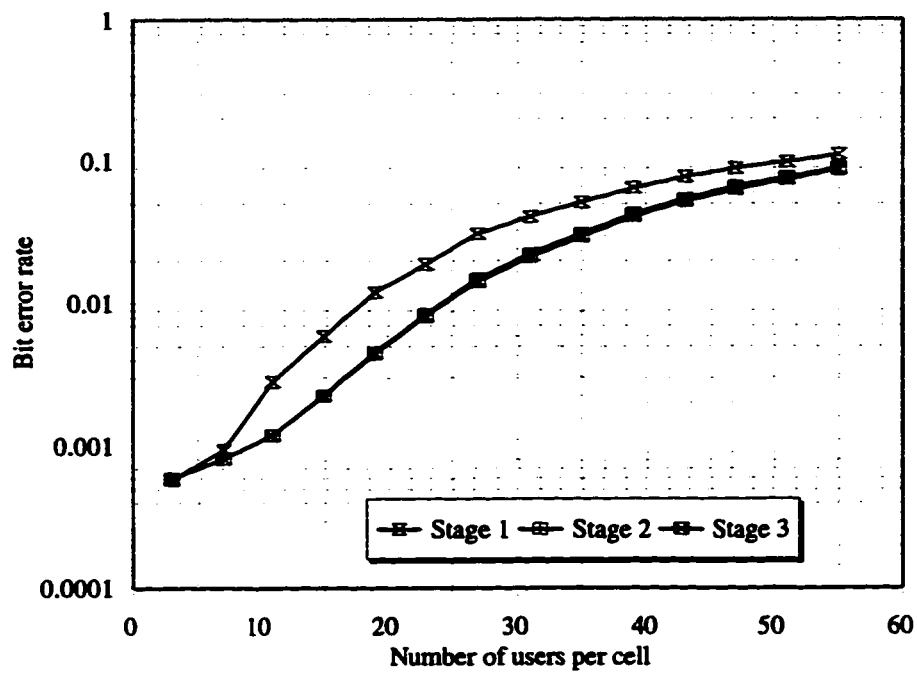

Fig. 4.E.16. The multi-cell performance of a RAMSIC receiver with quadriphase spreading on a flat fading channel with f = 1.57 and synchronization error of $0.20T_c$.
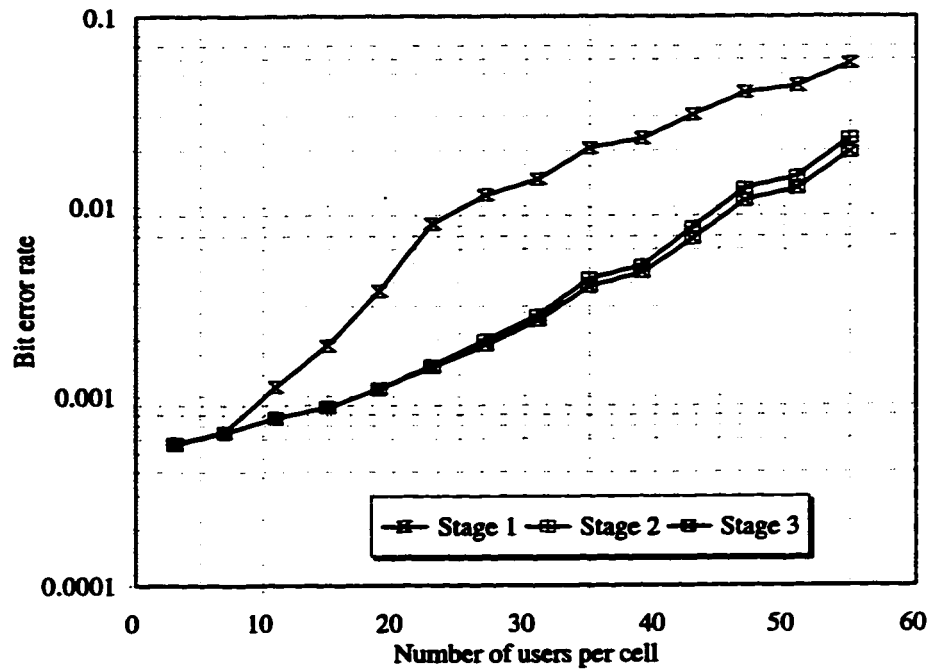
Fig. 4E.17. The multi-cell performance of a RAMSIC receiver with quadriphase spreading on a frequency selective fading channel with f = 0.55 and synchronization error of $0.05T_c$.
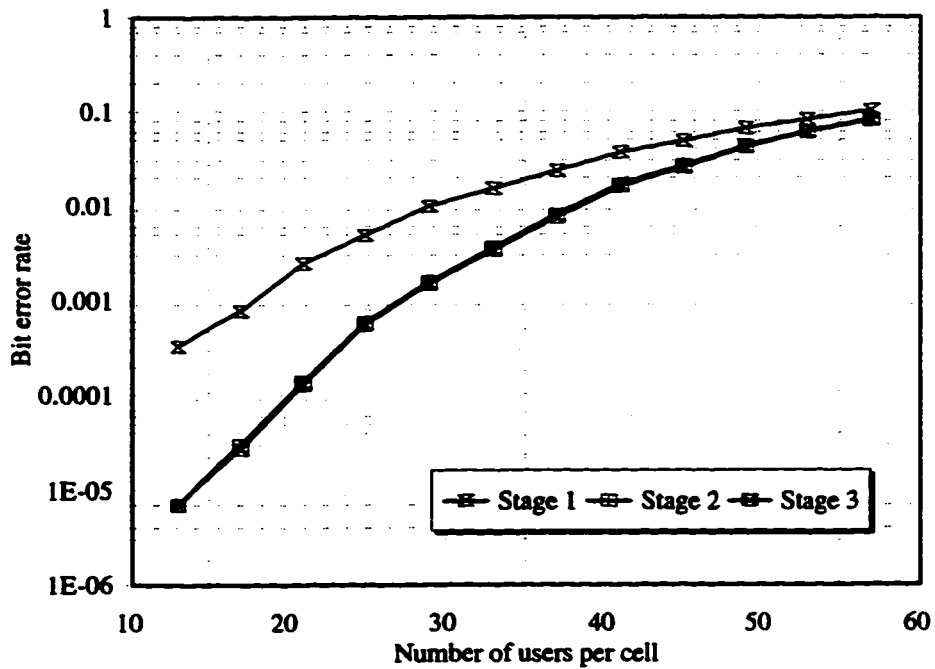
Fig. 4E.18. The multi-cell performance of a RAMSIC receiver with quadriphase spreading on a frequency selective fading channel with f = 0.686 and synchronization error of $0.05T_c$.
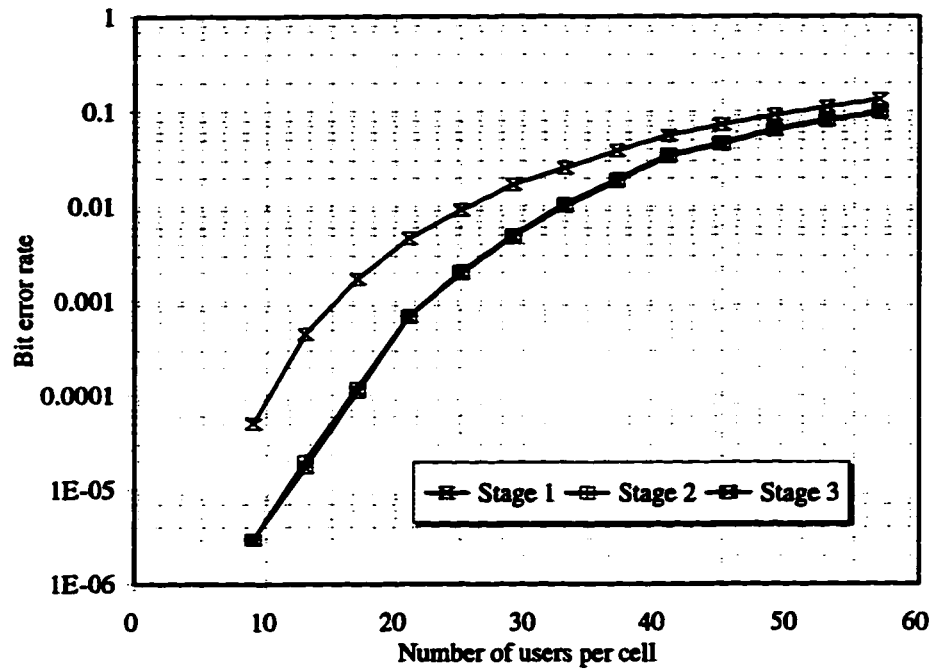
Fig. 4E.19. The multi-cell performance of a RAMSIC receiver with quadriphase spreading on a frequency selective fading channel with f = 0.959 and synchronization error of $0.05T_c$.
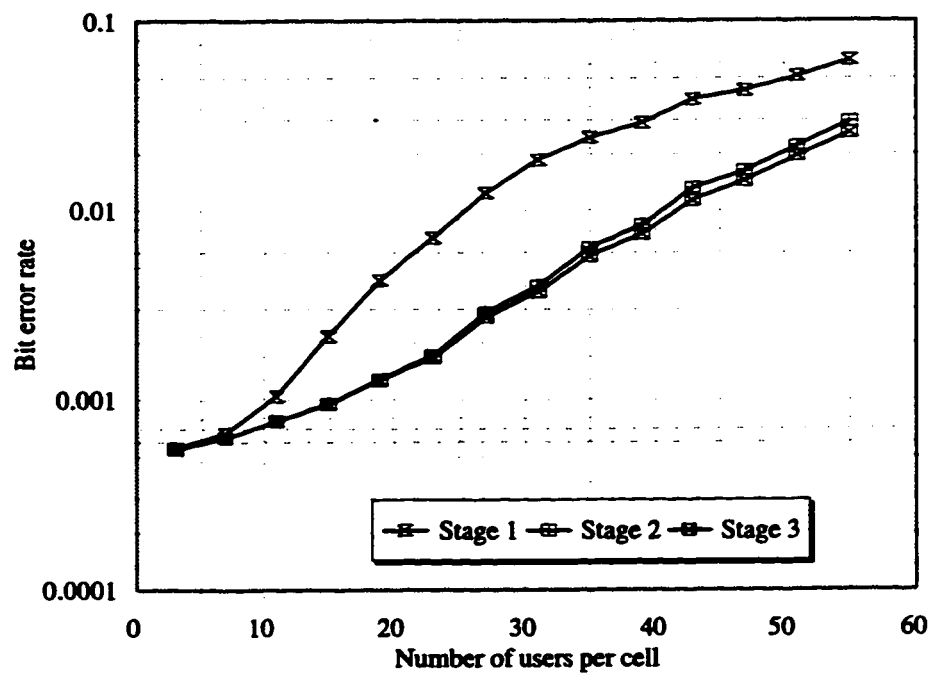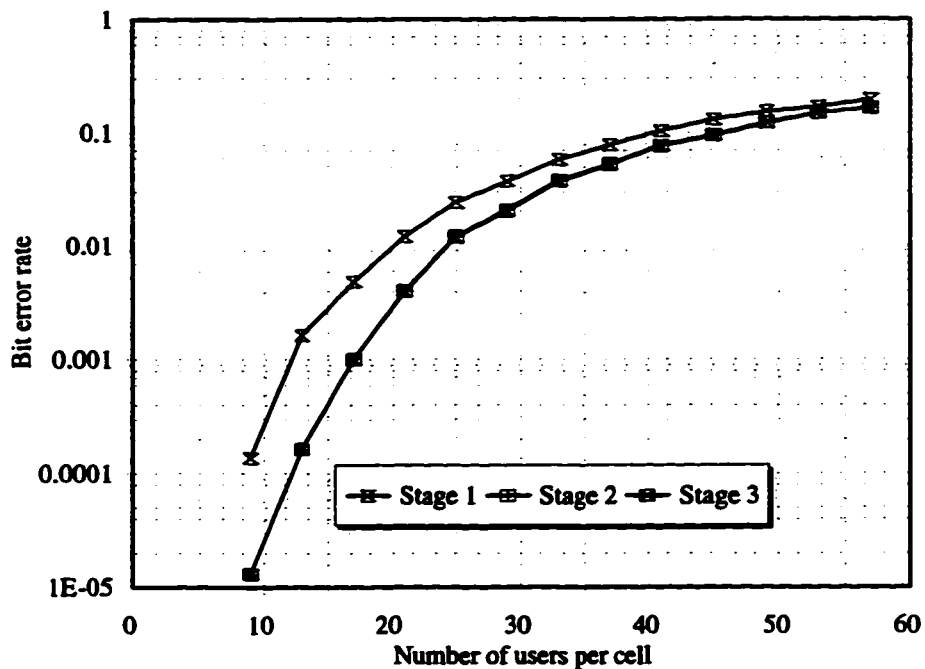

Fig. 4E.20. The multi-cell performance of a RAMSIC receiver with quadriphase spreading on a frequency selective fading channel with f = 1.57 and synchronization error of $0.05T_c$.
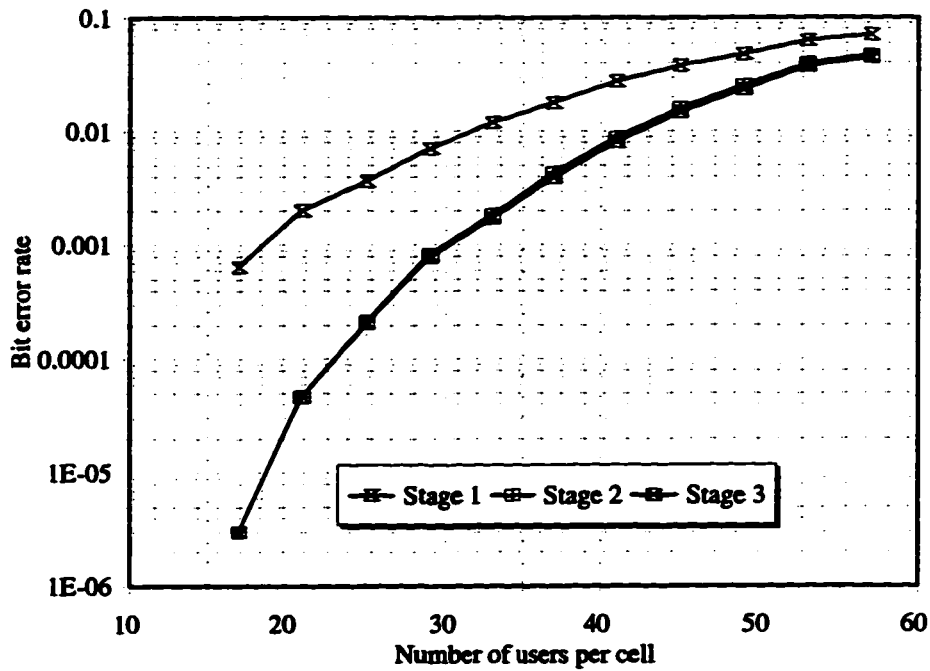
Fig. 4E.21. The multi-cell performance of a RAMSIC receiver with quadriphase spreading on a frequency selective fading channel with f = 0.55 and synchronization error of $0.10T_c$.
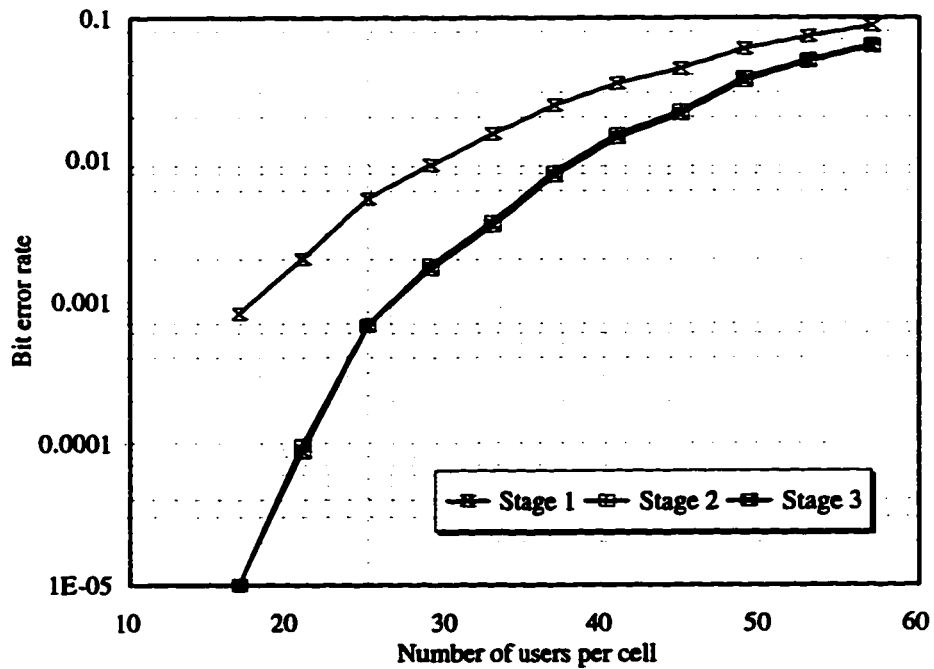
Fig. 4E.22. The multi-cell performance of a RAMSIC receiver with quadriphase spreading on a frequency selective fading channel with f = 0.686 and synchronization error of $0.10T_c$.
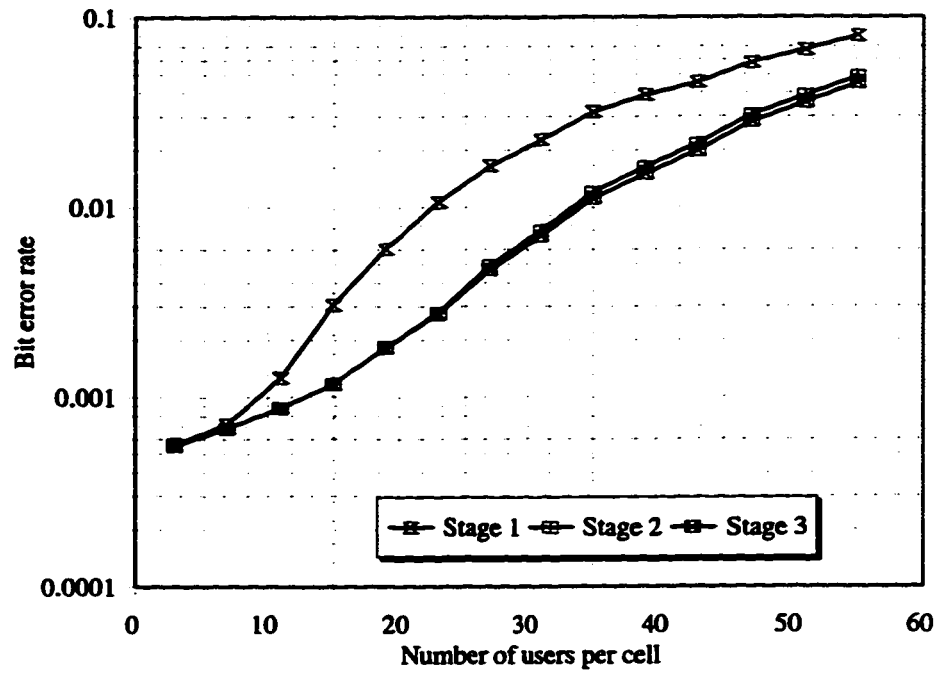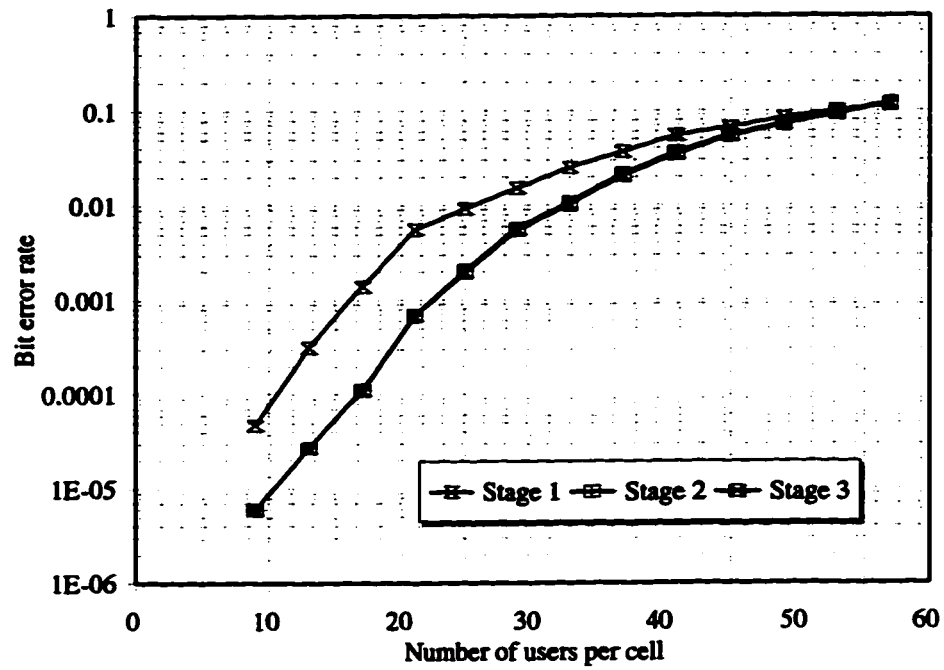
Fig. 4E.23. The multi-cell performance of a RAMSIC receiver with quadriphase spreading on a frequency selective fading channel with f = 0.959 and synchronization error of $0.10T_c$.
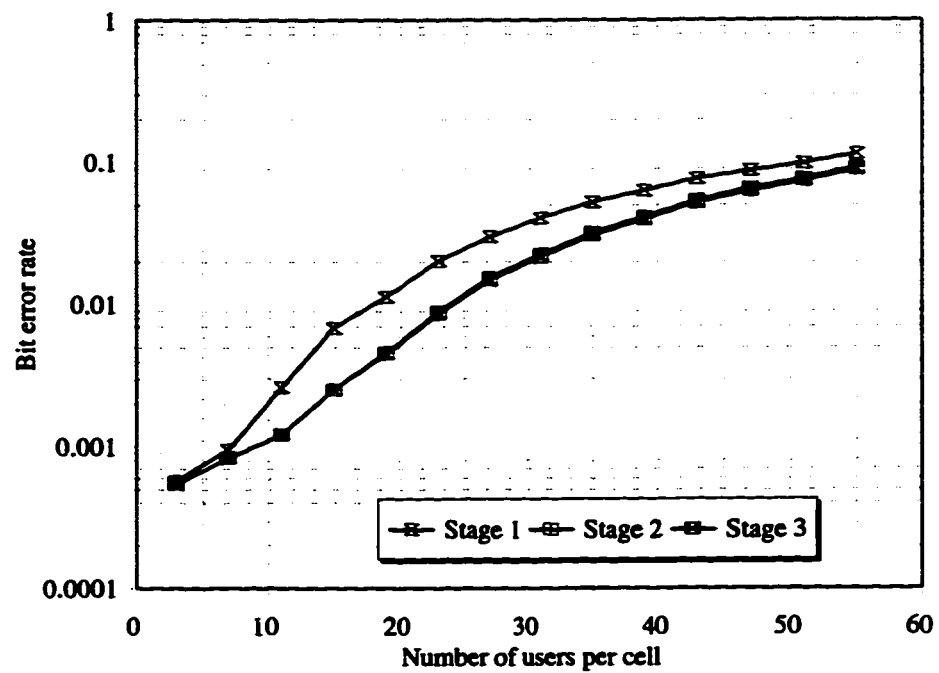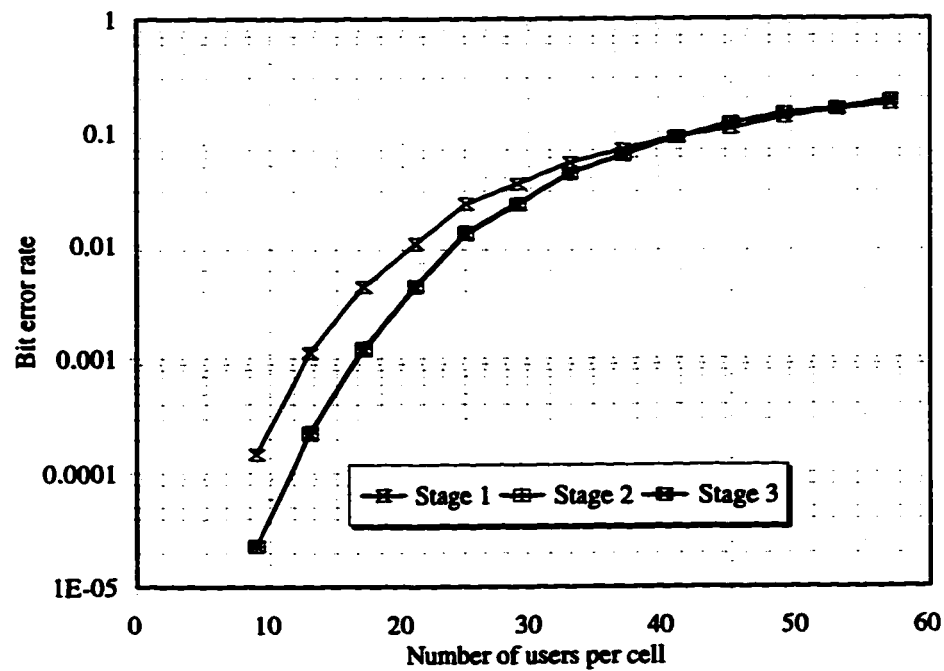

Fig. 4E.24. The multi-cell performance of a RAMSIC receiver with quadriphase spreading on a frequency selective fading channel with f = 1.57 and synchronization error of $0.10T_c$.
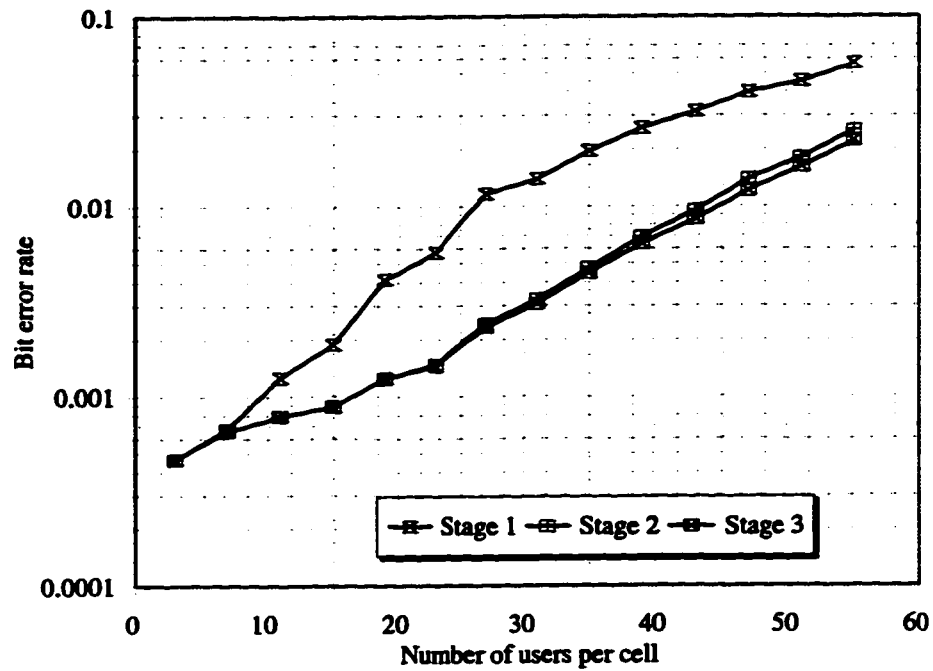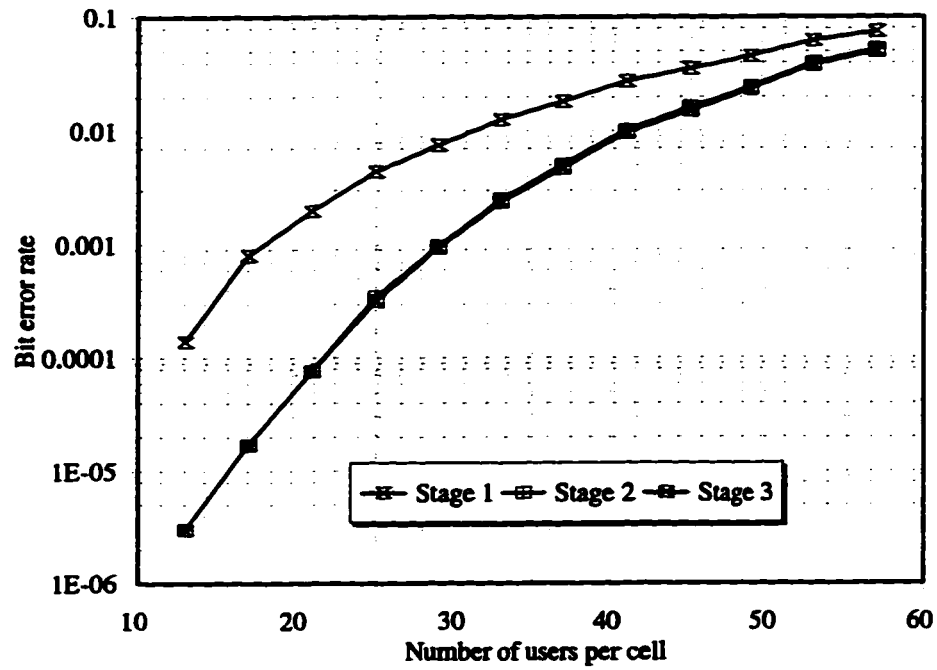
Fig. 4E.25. The multi-cell performance of a RAMSIC receiver with quadriphase spreading on a frequency selective fading channel with f = 0.55 and synchronization error of $0.15T_c$.
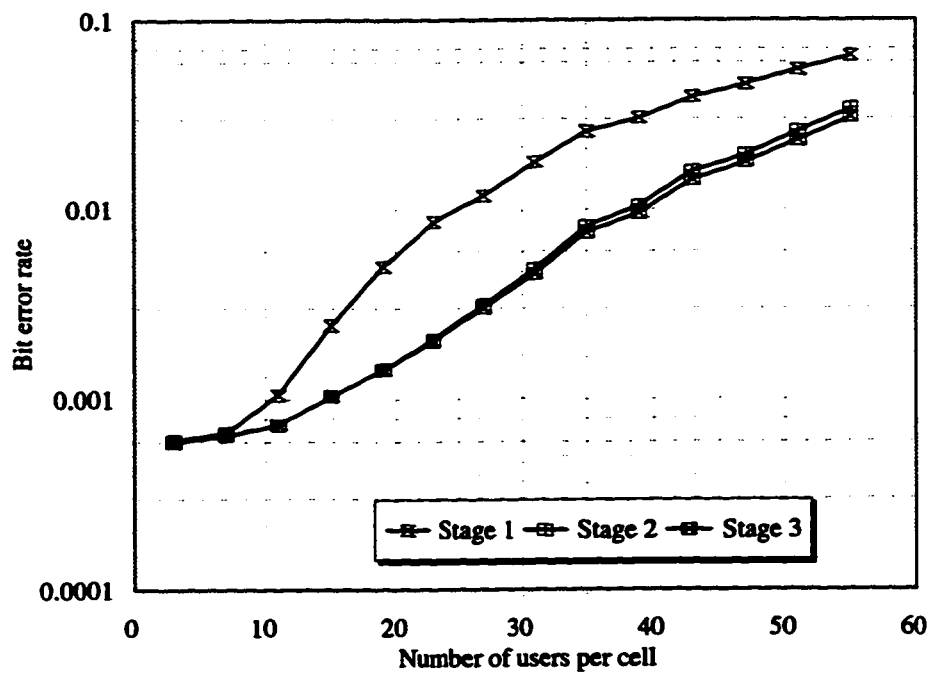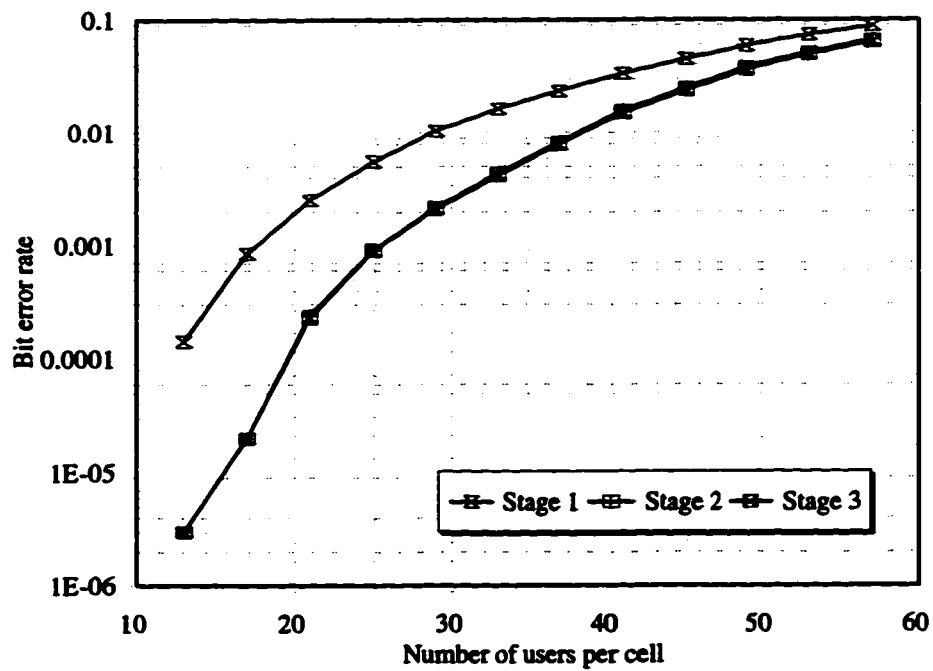

Fig. 4E.26. The multi-cell performance of a RAMSIC receiver with quadriphase spreading on a frequency selective fading channel with f = 0.686 and synchronization error of $0.15T_c$.
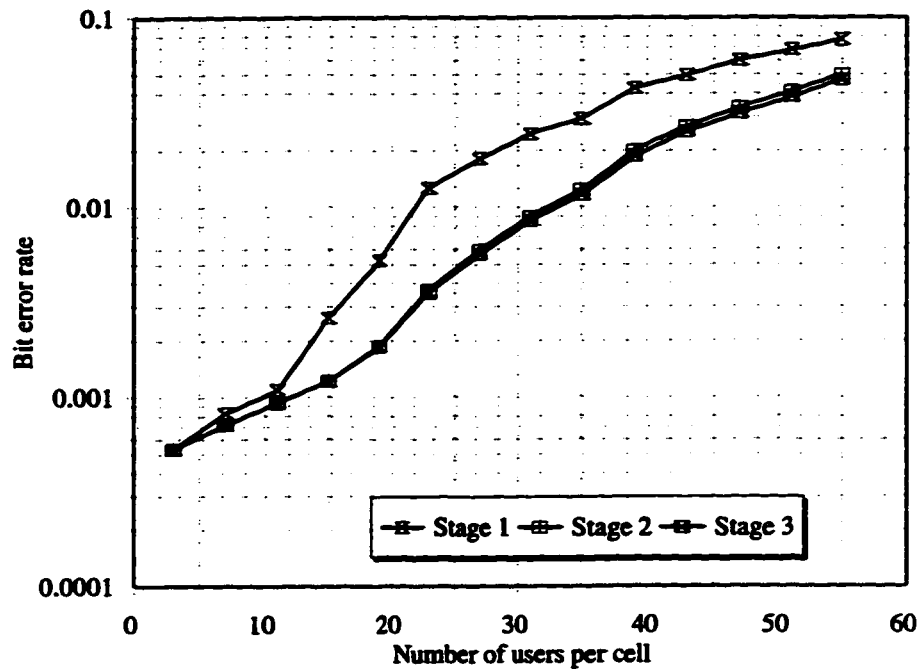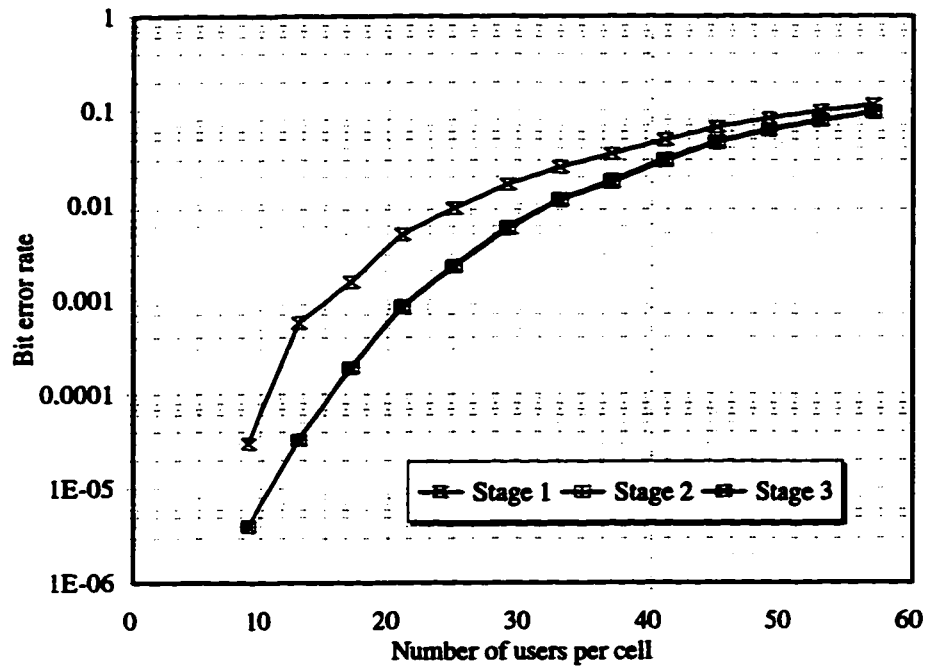
Fig. 4E.27. The multi-cell performance of a RAMSIC receiver with quadriphase spreading on a frequency selective fading channel with f = 0.959 and synchronization error of $0.15T_c$.
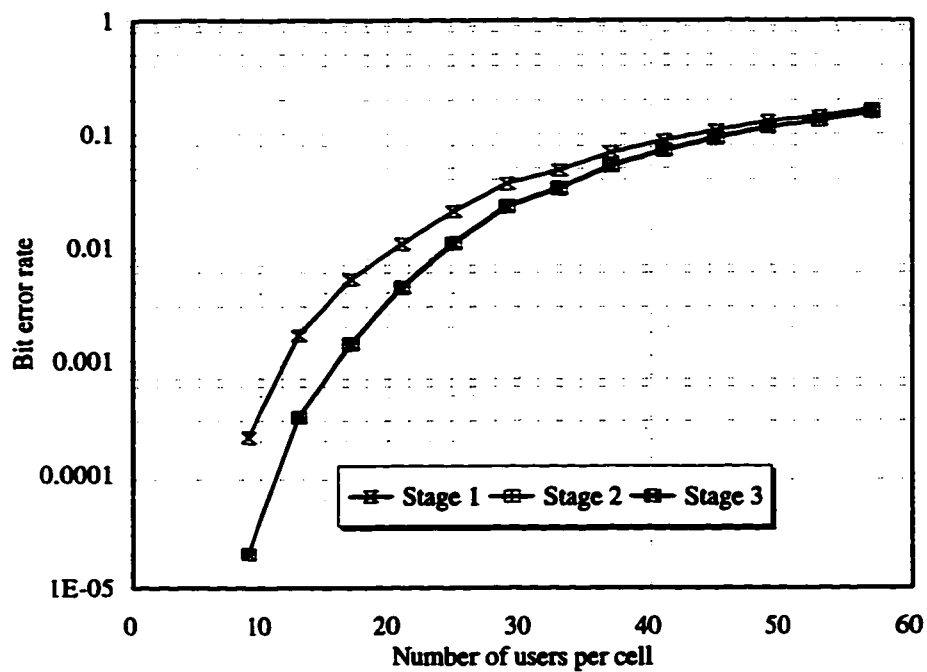
Fig. 4E.28. The multi-cell performance of a RAMSIC receiver with quadriphase spreading on a frequency selective fading channel with f = 1.57 and synchronization error of $0.15T_c$.
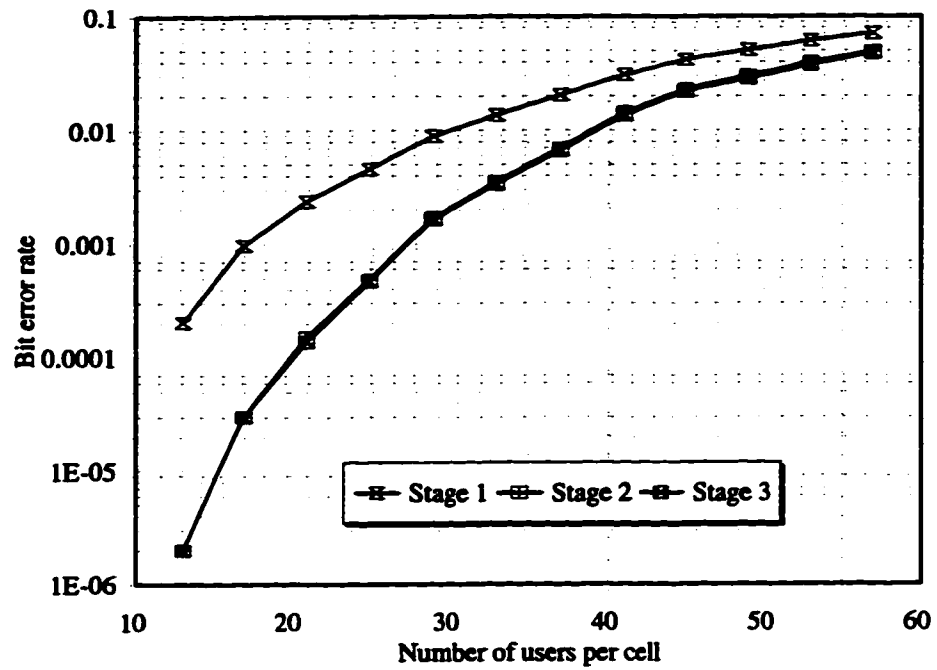
Fig. 4E.29. The multi-cell performance of a RAMSIC receiver with quadriphase spreading on a frequency selective fading channel with $f = 0.55$ and synchronization error of $0.20T_c$.
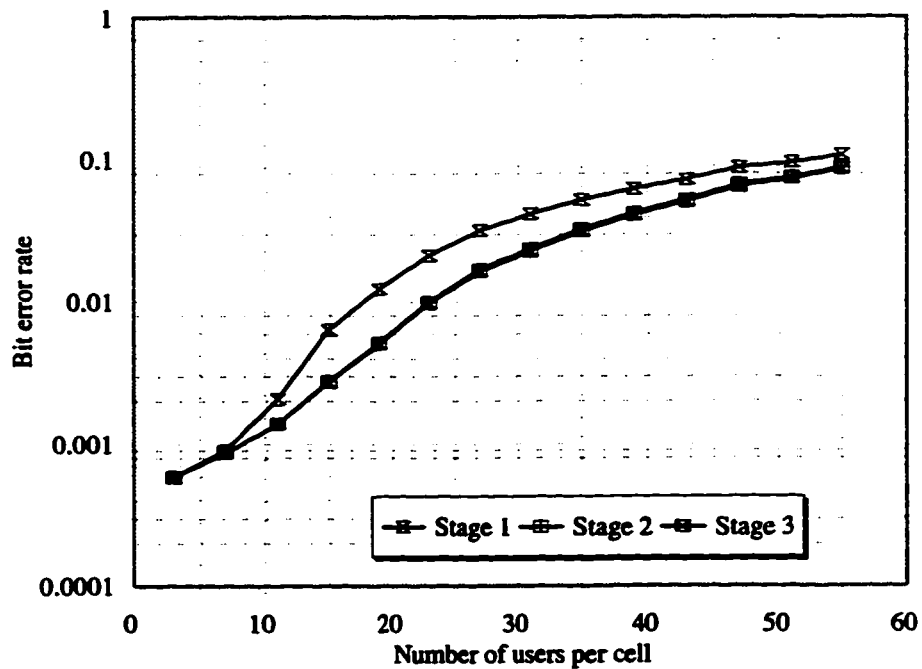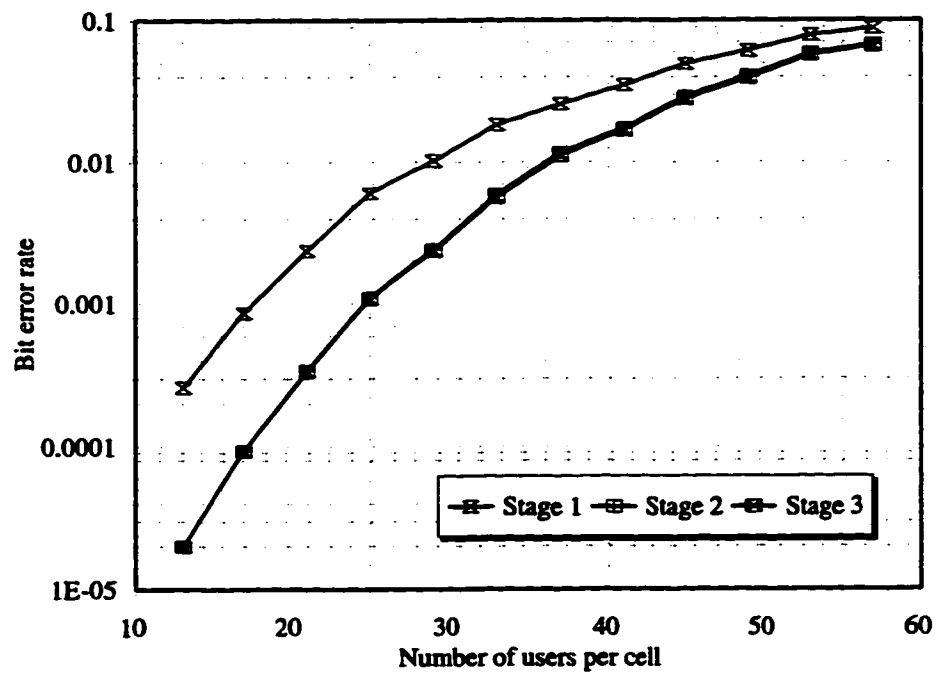

Fig. 4E.30. The multi-cell performance of a RAMSIC receiver with quadriphase spreading on a frequency selective fading channel with $f = 0.686$ and synchronization error of $0.20T_c$.
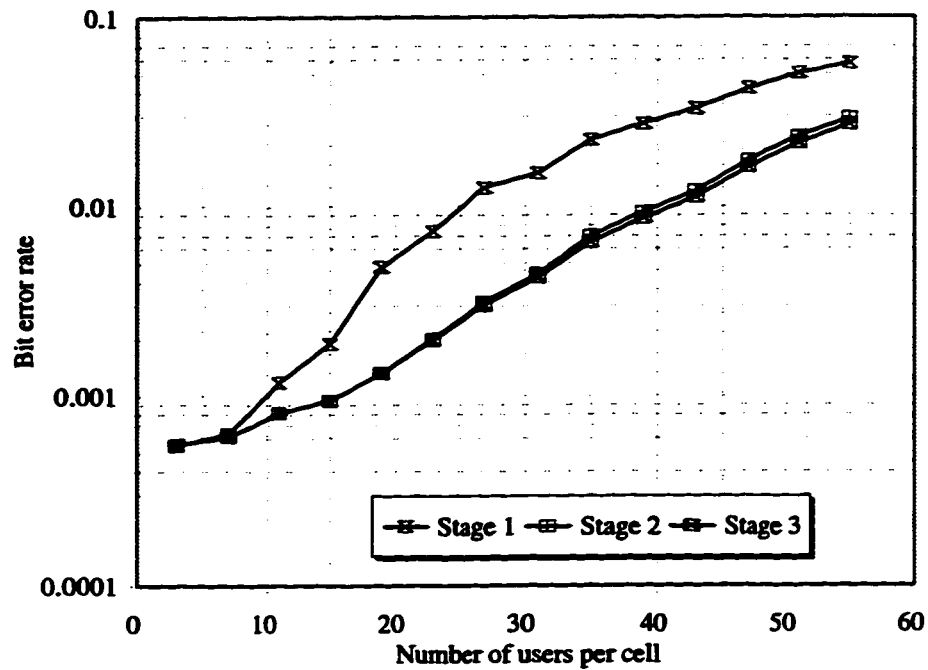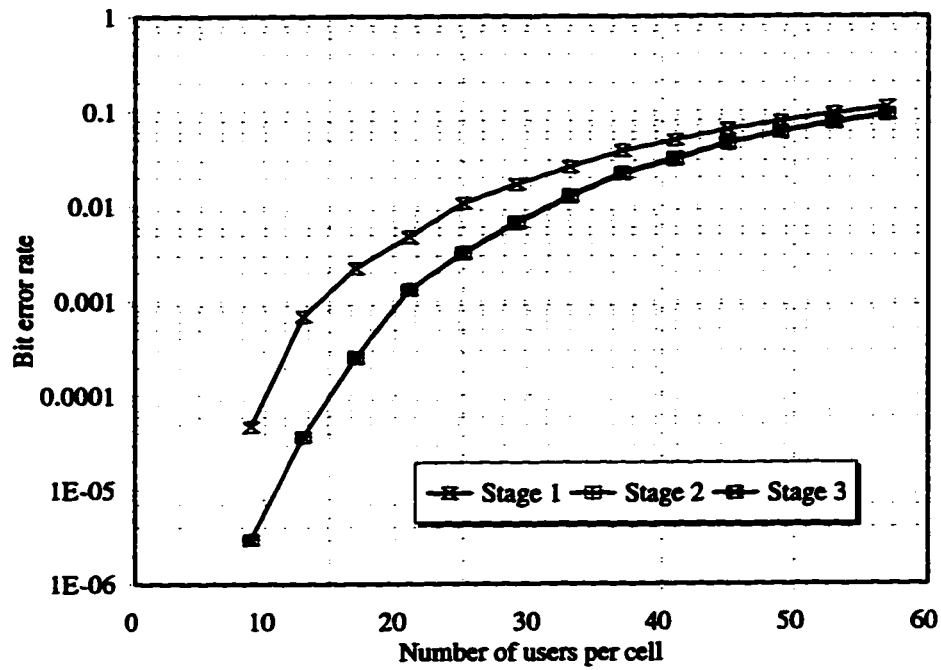
Fig. 4E.31. The multi-cell performance of a RAMSIC receiver with quadriphase spreading on a frequency selective fading channel with f = 0.959 and synchronization error of $0.20T_c$.
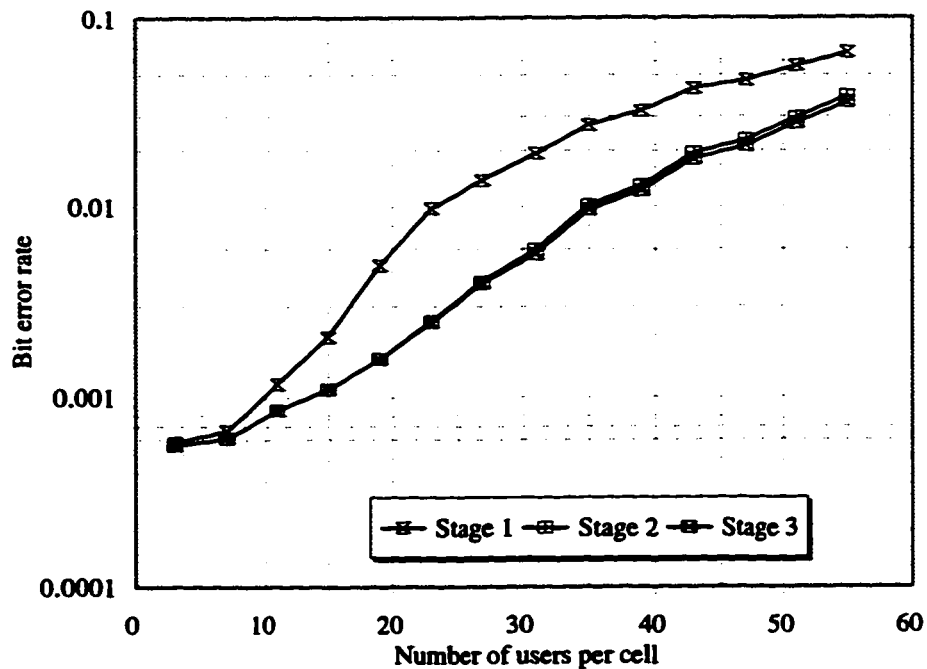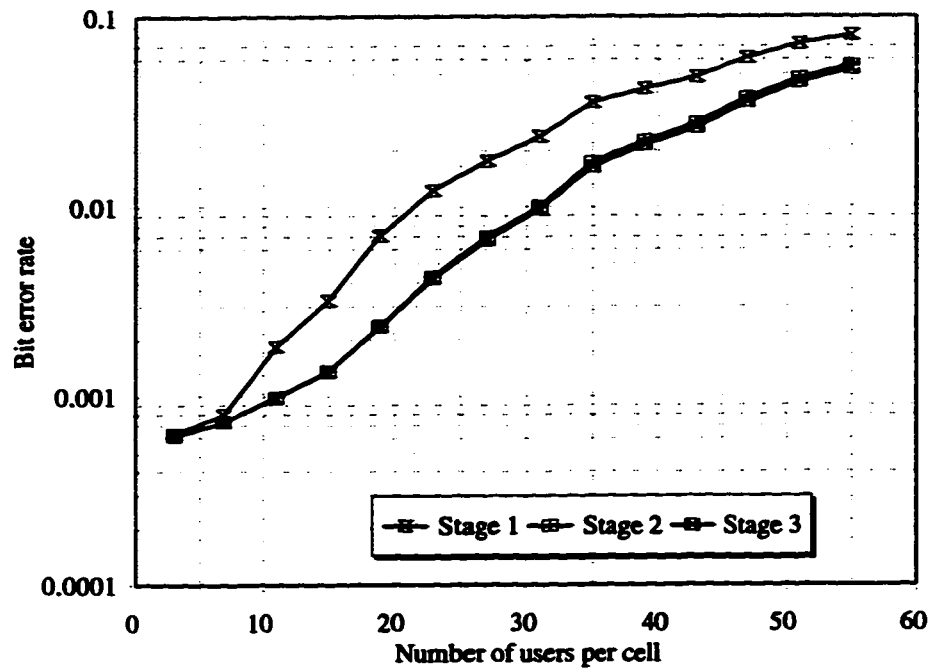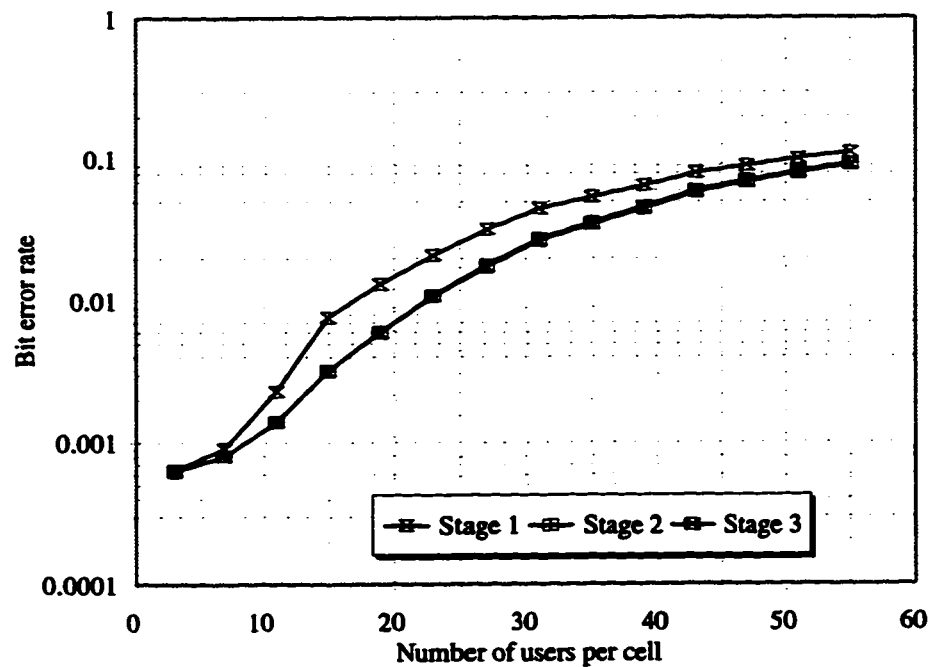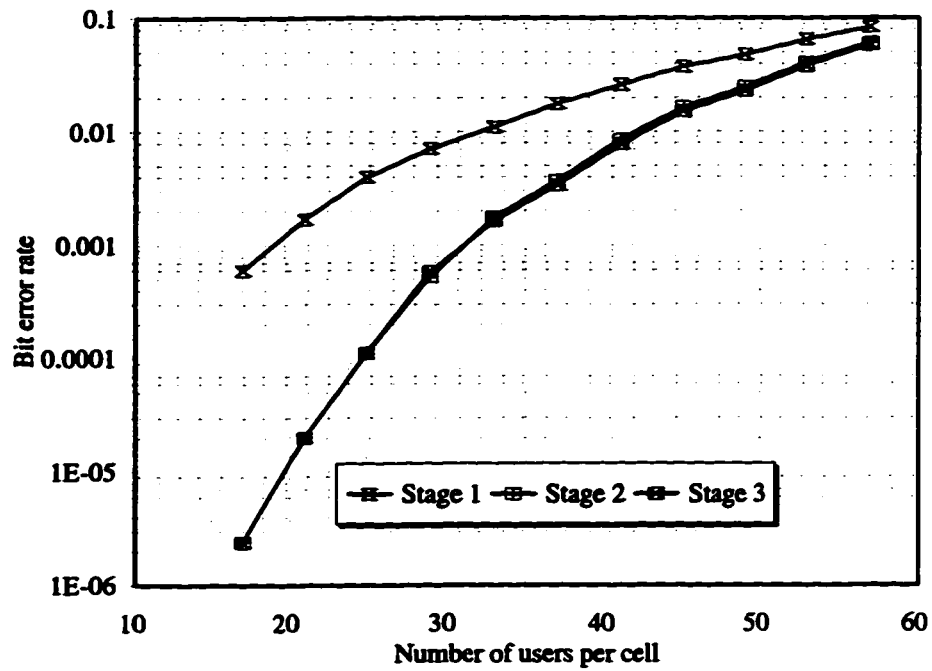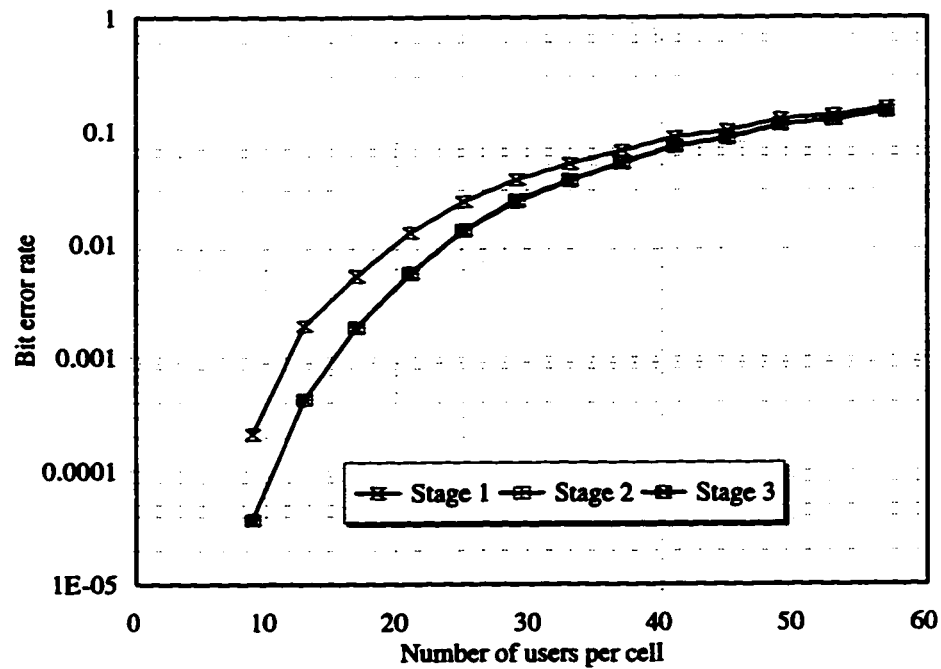

Fig. 4E.32. The multi-cell performance of a RAMSIC receiver with quadriphase spreading on a frequency selective fading channel with f = 1.57 and synchronization error of $0.20T_c$.

# 4.12 References

Cheng, F.C. and Holtzman, J.M. (1994): Effect of tracking error on DS/CDMA successive interference cancellation. *Proc. IEEE Globecom/CTMC*, pp. 166-170.

Gilhousen, K.S., Jacobs, I.M., Padovani, R., Viterbi, A.J., Weaver, L.A. and Wheatley III, C.E. (1991): On the capacity of cellular CDMA system. *IEEE Trans. Veh. Technol.*, vol. VT-27, pp 303-312.

Jakes, W.C. (1974): *Microwave Mobile Communications*, John Wiley: N.Y..

Ling, F. (1993): Coherent detection with reference-symbol based channel estimation for direct sequence CDMA uplink communications, *Proc. IEEE Vehicular Technology Conf.*, pp. 400-403.

Milstein, L.B. and Rappaport, T.S. (1992): Effects of radio propagation path loss on DS-CDMA cellular frequency reuse efficiency for the reverse channel. *IEEE Trans. Vehicular Technology*, vol. 41, no. 3, pp. 231-241.

Pursley, M.B. (1981): Spread-spectrum multiple-access communications. In Longo, G. (eds): *Multi-User Communication Systems*, New York: Springer-Verlag.

Sunay, M.O. andMcLane, P.J. (1995a): Performance of selection diversity for DS CDMA system with synchronization errors. *Proc. IEEE ICUPC*, pp. 431-435.

Sunay, M.O. andMcLane, P.J. (1995b): Effects of carrier phase and chip timing errors on the capacity of a quadriphase spread BPSK modulated DS CDMA system. *Proc. IEEE Globecom*, pp. 1114-1120.

Torrieri, D.J. (1992): Performance of direct-sequence systems with long pseudonoise sequences, *IEEE J. Select. Areas Commun.*, vol. 10, no. 4, pp. 770-781.

Viterbi, A.J., Viterbi, A.M., and Zehavi, E. (1993): Performance of power-controlled wideband terrestrial digital communication, *IEEE Trans. Commun.*, vol. 41, no. 4, pp. 559-569.

Yoon, Y.C., Kohno,R. and Imai, H. (1993): A spread-spectrum multiaccess system with cochannel interference cancellation for multipath fading channels. *IEEE J. Select. Areas Commun.*, vol. 11, no. 7, pp. 1067-1075.

Chapter 5: The effect of antenna diversity[*]

5.1 Introduction

The thrust of this thesis is to increase the capacity of direct sequence code division multiple access (DS-CDMA) wireless communication systems. Since the capacity of these systems is limited by multi-user access interference, significant capacity increase can be realized with receiver structures that are capable of mitigating this interference. The structure of the optimal multi-user receiver (Verdu, 1986) is too complex to be implementable in the foreseeable future. The interest, currently, is to develop suboptimal receiver structures that are more easily implementable while retaining some interference mitigation capabilities.

A relatively simple suboptimal multi-user receiver structure, the reference symbol assisted multistage successive interference cancelling (RAMSIC) receiver is proposed in Chapter 3. In all cases considered with biphase spreading, substantial traffic capacity increases over the conventional matched filter receiver are demonstrated. The sensitivity of the receiver to imperfect parameter estimation as well as the use of quadriphase spreading are investigated in Chapter 4. The results show that with quadriphase spreading, hexagonal cell geometry, path loss exponent of 4, tight power control and without any forward error correction coding, the capacity of the proposed system is between 1.17 and 1.67 times that of the IS-95 system. Further investigation with nonidealized cell geometries and other path loss exponents show substantial capacity improvement over that of non interference cancelling receivers. Investigation into the sensitivity of the

---

[*] Parts of this chapter were submitted for presentation at the 1997 IEEE International Conference on Universal Personal Communication.

225

receiver structure to imperfect parameter estimation has shown that the system is insensitive to imperfect amplifier gating and chip synchronization errors of the order expected for normal operation of the conventional detector. The system, however, is very sensitive to power control errors and additional diversity should be exploited to decrease these errors as much as possible. This may be especially important in high Doppler shift (fast fading) environments where tight power control is very difficult.

Performance of the system with antenna diversity is investigated in this chapter. The assumed power control error is as can be expected from the feedback power control algorithm described in the IS-95 standard. Although the fading signals received by different spatially separated antennas at the base station are usually correlated (Stüber, 1996), we will assume them to be uncorrelated to evaluate the maximum possible combining gain. A brief system description is given in Section 5.2. Performance results in Section 5.3 show that with dual antenna diversity significant traffic capacity improvement over an IS-95 like system, which also uses dual antenna diversity in the reverse link, can be achieved. Section 5.4 will demonstrate that the results with the high Doppler shift assumption can be considered worst case. The chapter is concluded by Section 5.5.

5.2 System description

The system considered in this chapter, with the exception of antenna diversity, is the same as the quadriphase spread CDMA system considered in Chapter 4. A description of the system can be found in Section 4.2.

Let us consider the reverse link of a quadriphase spread CDMA wireless system

226

with M users. The base station has K antennas and L paths per antenna. The baseband equivalent representation of the m-th user's transmitted signal is

$$s_m(t) = \sqrt{2P_m}\, d_m(t)\left[c_{I,m}(t)\cos\theta_m + jc_{Q,m}(t)\sin\theta_m\right] \qquad (5.1)$$

where $d_m(t)$ is the data waveform with reference symbols inserted, $c_{I,m}(t)$ and $c_{Q,m}(t)$ are respectively the in-phase and quadrature spreading waveforms and θ_m is the phase of the carrier. The data pulse and spreading chip shapes, as well as their normalization, are the same as in Chapter 3. The baseband received signal in the in-phase branch of the receiver is

$$
\begin{aligned}
r_I(t) &= \frac{1}{2}\sum_{m=1}^{M}\sum_{k=1}^{K}\sum_{l=1}^{L} a_{m,k,l}(t)\sqrt{2P_m}\, d_m(t-\tau_{m,k,l})\left[c_{I,m}(t-\tau_{m,k,l})\cos\varphi_m +\right.\\
&\qquad \left. c_{Q,m}(t-\tau_{m,k,l})\sin\varphi_m\right] + n(t)\\
&= \frac{1}{2}\sum_{m=1}^{M}\sum_{k=1}^{K}\sum_{l=1}^{L} d_m(t-\tau_{m,k,l})\left[c_{I,m}(t-\tau_{m,k,l})A_{I,m,k,l}(t)+c_{Q,m}(t-\tau_{m,k,l})A_{Q,m,k,l}(t)\right]\\
&\qquad + n(t)
\end{aligned}
\qquad (5.2)
$$

where

$$A_{I,m,k,l}(t) = a_{m,k,l}(t)\sqrt{2P_m}\,\cos\varphi_m , \qquad (5.3)$$

$$A_{Q,m,k,l}(t) = a_{m,k,l}(t)\sqrt{2P_m}\,\sin\varphi_m , \qquad (5.4)$$

$a_{m,k,l}$ is the channel gain and φ_m is the total phase shift. The background noise $n(t)$ is modelled as a zero mean Gaussian noise with two-sided power spectral density $N_0/2$. After n-1 stages of cancellation of all interfering multipath signals, and after cancelling the multipath signal of the $(x$-1)-th user in the n-th stage, the decision statistic calculated by the inphase branch of the receiver from the z-th path of the y-th antenna for the x-th user is

$$D_{I,x,y,z}^{(n)} = \frac{2}{T_s} \int_{\tau_{x,y,z}}^{\tau_{x,y,z}+T_s} \hat{r}_I^{(n)}(t) \left[\hat{A}_{I,x,y,z} c_{I,x}(t-\tau_{x,y,z}) + \hat{A}_{Q,x,y,z} c_{Q,x}(t-\tau_{x,y,z}) \right] dt$$

$$\approx \left| A_{x,y,z} \right|^2 d_m + A_{I,x,y,z} A_{Q,x,y,z} \frac{(I_{QI,x,y,z;x,y,z}(d_m) + I_{IQ,x,y,z;x,y,z}(d_m))}{T_s} + \qquad (5.5)$$

$$A_{I,x,y,z} N_{II,x,y,z} + A_{Q,x,y,z} N_{IQ,x,y,z} + \left[\left(1 + \frac{1}{Q}\right)\left(1 + \frac{2f_{cutoff}}{f_r}\right) \right]^{\frac{1}{2}} N_{I,x,y,z}$$

where

$$\hat{r}_I^{(n)}(t) = r_I(t) - \sum_{m=1}^{x-1} \hat{s}_{I,m}^{(n)}(t) - \sum_{m=x+1}^{M} \hat{s}_{I,m}^{(n-1)}(t) , \qquad (5.6)$$

$$\hat{A}_{I,x,y,z} = A_{I,x,y,z} + n_{a,I;x,y,z} , \qquad (5.7)$$

$$I_{QI,m,k,l;x,y,z}(d_m) = \int_{\tau_{x,y,z}}^{\tau_{x,y,z}+T_s} d_m(t-\tau_{m,k,l}) c_{Q,m}(t-\tau_{m,k,l}) c_{I,x}(t-\tau_{x,y,z}) dt , \qquad (5.8)$$

$N_{II,x,y,z}$ represents the part of the multiuser interference at the output of the inphase correlator associated with despreading by the inphase spreading code and has the following form

$$N_{II,x,y,z} = \left[\left(1 + \frac{1}{Q}\right)\left(1 + \frac{2f_{cutoff}}{f_r}\right) \right]^{\frac{1}{2}} \left\{ \sum_{\substack{l=1 \\ l \neq z}}^{L} \left[\frac{A_{I,x,y,l} I_{II,x,y,l;x,y,z}(d_m)}{T_s} \right. \right.$$

$$\left. + \frac{A_{Q,x,y,l} I_{QI,x,y,l;x,y,z}(d_m)}{T_s} \right] + \sum_{\substack{m=1 \\ m \neq x}}^{M} \sum_{l=1}^{L} \left[\frac{A_{I,m,y,l} I_{II,m,y,l;x,y,z}(d_m - \hat{d}_m^{(\rho)}(t))}{T_s} \right.$$

$$+ \frac{A_{Q,m,y,l} I_{QI,m,y,l;x,y,z}(d_m - \hat{d}_m^{(\rho)}(t))}{T_s} - \frac{n_{aI;m,y,l} I_{II,m,y,l;x,y,z}(\hat{d}_m^{(\rho)}(t))}{T_s}$$

$$\left. \left. \frac{n_{aQ;m,y,l} I_{QI,m,y,l;x,y,z}(\hat{d}_m^{(\rho)}(t))}{T_s} \right] \right\} , \qquad (5.9)$$

$N_{IQ,x,y,z}$ represents the part of the multiuser interference at the output of the inphase correlator associated with despreading by the quadrature spreading code and has the

228

following form

$$N_{IQ,x,y,z} = \left[\left(1+\frac{1}{Q}\right)\left(1+\frac{2f_{cutoff}}{f_r}\right)\right]^{\frac{1}{2}} \left\{ \sum_{\substack{l=1 \\ l\neq z}}^{L} \left[\frac{A_{I,x,y,l} I_{IQ,x,y,l;x,y,z}(d_m)}{T_s} \right. \right.$$

$$+ \frac{A_{Q,x,y,l} I_{QQ,x,y,l;x,y,z}(d_m)}{T_s} \right] + \sum_{\substack{m=1 \\ m\neq x}}^{M} \sum_{l=1}^{L} \left[\frac{A_{I,m,y,l} I_{IQ,m,y,l;x,y,z}(d_m - \hat{d}_m^{(\rho)}(t))}{T_s} \right. \qquad (5.10)$$

$$+ \frac{A_{Q,m,y,l} I_{QQ,m,y,l;x,y,z}(d_m - \hat{d}_m^{(\rho)}(t))}{T_s} - \frac{n_{al;m,y,l} I_{IQ,m,y,l;x,y,z}(\hat{d}_m^{(\rho)}(t))}{T_s}$$

$$\left. \left. \frac{n_{aQ;m,y,l} I_{QQ,m,y,l;x,y,z}(\hat{d}_m^{(\rho)}(t))}{T_s} \right] \right\} ,$$

$$\rho = \begin{cases} n & m < x \\ n-1 & m > x \end{cases} , \qquad (5.11)$$

$$A_{x,y,z} = A_{I,x,y,z} + jA_{Q,x,y,z} , \qquad (5.12)$$

$\hat{s}_{I,m}^{n}(t)$ is the baseband regenerated signal in the in phase branch of the receiver for the m-th user after n stages of cancellation, $\hat{d}_m^{(\rho)}$ is the ρ stage decision estimate for the m-th user, $n_{aI;x,y,z}$ is the noise corrupting the channel estimate $\hat{A}_{I,x,y,z}$, f_r is the reference symbol insertion frequency, $f_{cut-off}$ is the cut off frequency of the low pass filter used to reduce the noise corrupting the channel estimate, Q is the number of data symbols after which a reference symbol is inserted and $N_{I,x,y,z}$ represents the effect of the background noise on the inphase decision statistic. Equation (5.5) is approximate because the second order noise terms are assumed negligible and the channel parameters are assumed constant over one symbol interval, T_s. The first term in (5.9) and (5.10) is the noise enhancement factor due to channel estimation (Ling, 1993) and the other terms represent self interference and

residual interference from users that have been cancelled, respectively.

The low pass filtered received signal on the quadrature branch of the receiver is

$$r_Q(t) = \frac{1}{2} \sum_{m=1}^{M} \sum_{k=1}^{K} \sum_{l=1}^{L} d_m(t - \tau_{m,k,l}) \Big[c_{Q,m}(t - \tau_{m,k,l}) A_{I,m,k,l}(t)$$

$$- c_{I,m}(t - \tau_{m,k,l}) A_{Q,m,k,l}(t) \Big] + n(t) \tag{5.13}$$

The decision statistic calculated by the quadrature branch at the n-th stage from the z-th path of the y-th antenna for the x-th user is

$$D_{Q,x,y,z}^{(n)} = \frac{2}{T_s} \int_{\tau_{x,y,z}}^{\tau_{x,y,z}+T_s} \hat{r}_Q^{(n)}(t) \Big[\hat{A}_{Q,x,y,z} c_{I,x}(t - \tau_{x,y,z}) + \hat{A}_{I,x,y,z} c_{Q,x}(t - \tau_{x,y,z}) \Big] dt$$

$$\approx |A_{x,y,z}|^2 d_m - A_{I,x,y,z} A_{Q,x,y,z} \frac{(I_{QI,x,y,z;x,y,z}(d_m) + I_{IQ,x,y,z;x,y,z}(d_m)}{T_s} + \tag{5.14}$$

$$A_{Q,x,y,z} N_{QI,x,y,z} + A_{I,x,y,z} N_{QQ,x,y,z} + \left[\left(1 + \frac{1}{Q} \right) \left(1 + \frac{2 f_{cutoff}}{f_r} \right) \right]^{\frac{1}{2}} N_{Q,x,y,z}$$

where $N_{Q,x,y,z}$ represents the effect of thermal noise, $N_{QI,x,y,z}$ represents the part of the multiuser interference at the output of the quadrature correlator associated with despreading by the inphase spreading code and has the following form

$$N_{QI,x,y,z} = \left[\left(1 + \frac{1}{Q} \right) \left(1 + \frac{2 f_{cutoff}}{f_r} \right) \right]^{\frac{1}{2}} \left\{ \sum_{\substack{l=1 \\ l \neq z}}^{L} \left[\frac{A_{Q,x,y,l} I_{II,x,y,l;x,y,z}(d_m)}{T_s} \right. \right.$$

$$\left. + \frac{A_{I,x,y,l} I_{QI,x,y,l;x,y,z}(d_m)}{T_s} \right] + \sum_{\substack{m=1 \\ m \neq x}}^{M} \sum_{l=1}^{L} \left[\frac{A_{Q,m,y,l} I_{II,m,y,l;x,y,z}(d_m - \hat{d}_m^{(\rho)}(t))}{T_s} \right.$$

$$- \frac{A_{I,m,y,l} I_{QI,m,y,l;x,y,z}(d_m - \hat{d}_m^{(\rho)}(t))}{T_s} - \frac{n_{aQ;m,y,l} I_{II,m,y,l;x,y,z}(\hat{d}_m^{(\rho)}(t))}{T_s}$$

$$\left. \left. \frac{n_{aI;m,y,l} I_{QI,m,y,l;x,y,z}(\hat{d}_m^{(\rho)}(t))}{T_s} \right] \right\} , \tag{5.15}$$

230

$N_{QQ,x,y,z}$ represents the part of the multiuser interference at the output of the quadrature correlator associated with despreading by the quadrature spreading code and has the following form

$$N_{QQ,x,y,z} = \left[\left(1+\frac{1}{Q}\right)\left(1+\frac{2f_{cutoff}}{f_r}\right)\right]^{\frac{1}{2}}\left\{\sum_{\substack{l=1\\l\neq z}}^{L}\left[\frac{A_{Q,x,y,l}I_{IQ,x,y,l;x,y,z}(d_m)}{T_s}\right.\right.$$

$$\left.+\frac{A_{I,x,y,l}I_{QQ,x,y,l;x,y,z}(d_m)}{T_s}\right]+\sum_{\substack{m=1\\m\neq x}}^{M}\sum_{l=1}^{L}\left[\frac{A_{Q,m,y,l}I_{IQ,m,y,l;x,y,z}(d_m-\hat{d}_m^{(\rho)}(t))}{T_s}\right.$$

(5.16)

$$+\frac{A_{I,m,y,l}I_{QQ,m,y,l;x,y,z}(d_m-\hat{d}_m^{(\rho)}(t))}{T_s}-\frac{n_{aQ;m,y,l}I_{IQ,m,y,l;x,y,z}(\hat{d}_m^{(\rho)}(t))}{T_s}$$

$$\left.\left.\frac{n_{aI;m,y,l}I_{QQ,m,y,l;x,y,z}(\hat{d}_m^{(\rho)}(t))}{T_s}\right]\right\} \ .$$

The overall decision variable for the m-th user in the n-th stage is then

$$D_x^{(n)} = \sum_{y=1}^{K}\sum_{z=1}^{L}D_{I,x,k,l}^{(n)} + D_{Q,x,k,l}^{(n)}$$

$$\approx \sum_{y=1}^{K}\sum_{z=1}^{L}2|A_{x,y,z}|^2 d_m + A_{I,x,y,z}N_{II,x,y,z} + A_{Q,x,y,z}N_{IQ,x,y,z} + A_{Q,x,y,z}N_{QI,x,y,z} \quad (5.17)$$

$$+A_{I,x,y,z}N_{QQ,x,y,z}+\left[\left(1+\frac{1}{Q}\right)\left(1+\frac{2f_{cutoff}}{f_r}\right)\right]^{\frac{1}{2}}(N_{I,x,y,z}+N_{Q,x,y,z}) \ .$$

The signal to noise ratio of the decision variable, which is the square of the signal part (the first term) of (5.17) divided by the variance of the noise term, is given by

$$\gamma_x^{(n)} = \left[\sum_{y=1}^{K}\sum_{z=1}^{L}2|A_{x,y,z}|^2\right]^2\left\{\sum_{y=1}^{K}\sum_{z=1}^{L}A_{I,x,y,z}^2\left(\eta_{II,x,y,z}+\eta_{QQ,x,y,z}\right)+A_{Q,x,y,z}^2\left(\eta_{IQ,x,y,z}\right.\right.$$

(5.18)

$$\left.+\eta_{QI,x,y,z}\right)+\left[\left(1+\frac{1}{Q}\right)\left(1+\frac{2f_{cutoff}}{f_r}\right)\right]\left(\frac{2N_0}{T_s}\right)\right\}^{-1} \ .$$

231

where

$$\eta_{IQ,x,y,z} = VAR\left(N_{IQ,x,y,z} | \mathbf{A}, \hat{\mathbf{d}}, \tau\right),$$ (5.19)

A denotes the set of complex channel parameters, $\{A_{x,y,z}\}$, $\hat{\mathbf{d}}$ denotes the set of estimated data, $\left\{\hat{d}_{m}^{(\rho)}\right\}$ and τ denotes the set of all delays, $\{\tau_{x,y,z}\}$. The conditional error probability, using the Gaussian approximation, can then be written as

$$P_{e,x}^{(n)}(\mathbf{A}, \hat{\mathbf{d}}, \tau) = \frac{1}{2} erfc\left[\sqrt{\frac{1}{2}\gamma_{x}^{(n)}}\right].$$ (5.20)

In principle, the average unconditional probability of error can be obtained by integration. Unfortunately, the evaluation of the exact probability of error is computationally intensive because the various decision estimates used for interference cancellation are not independent, and that the decision statistic is a nonlinear function of these variables. Therefore the calculation of the unconditional probability of error requires the evaluation of nM nested integrals and thus depends exponentially upon the number of users (Varanasi and Aazhang, 1990). Hence, there is no clear advantage to the numerical evaluation, and consequently computer simulation has been used to determine the unconditional probability of error.

5.3 Performance with dual antenna diversity

The performance of the RAMSIC receiver with dual antenna diversity operating in a flat Rayleigh fading environment is investigated via computer simulation. Two cases are considered: dual receive antenna diversity and dual receive antenna diversity with 2 artificial multipaths created by the transmitter. The specifics of the simulated system are as

follows:

- information bit rate = 9600 bits/s;

- system chip rate = 1.23 Mchips/s;

- Doppler frequency for each user = 100 Hz;

- Rayleigh fader modelled as in (Jakes, 1974);

- pilot insertion parameter is set at the optimal rate determined in Chapter 3 (Q = 12);

- filters are the optimal low pass filters used in Chapter 3;

- intercell interference is modelled as a zero mean complex white Gaussian process with variance which is related to the intercell to intracell interference ratio f.

The intercellular interference is approximated as a Gaussian process because it originates from a large number of relatively distant users in surrounding cells, and hence approximately satisfies the assumptions of the central limit theorem. Frequency reuse factors half way between the upper and lower bounds given in Milstein and Rappaport (1992) for path loss exponent of 4 and hexagonal cells (corresponding to f = 0.55), as well as nonidealized cell geometries with path loss exponents of 2, 3, 4 (corresponding to f = 1.57, 0.959 and 0.686, respectively) are considered. The IS-95 transmitter gating mask is used to implement guard intervals in all cases discussed in this section. The power control error is modelled as a sum of Rayleigh distributed random variables. Such approach has been adopted at high fading rates following the findings of Ariyavisitakul and Chang (1993). This model is different from that in Chapters 3 and 4 because it was assumed in those chapters that a power control algorithm capable of mitigating fast fading exist. Whereas in this chapter the performance of a RAMSIC receiver with the IS-95 power

Fig. 5.1. Multi-cell performance of the RAMSIC receiver with two receive antennas on a flat Rayleigh fading channel. The power control is imperfect, Doppler frequency is 100 Hz and $f = 0.55$.

control algorithm is investigated.

The multi-cell performance of the RAMSIC receiver operating in a flat Rayleigh fading channel with two receive antennas, hexagonal cell geometry and path loss exponent of 4 ($f = 0.55$) is shown in Figure 5.1. Only dual receive antenna diversity is considered, because receivers with larger number of receive antennas may not be commercially viable. It can be seen that increasing the number of cancellation stages beyond two results in no significant improvement in the performance of the receiver. The capacity of the system is 29 users per cell. In Chapter 4, it is demonstrated that with the power control error

Fig. 5.2. Multi-cell performance of the RAMSIC receiver with two receive antennas on a flat Rayleigh fading channel. The power control is imperfect, Doppler frequency is 100 Hz and $f = 0.686$.

standard deviation of 2.9 dB (which is less than that considered here), the system can only accommodate three users per cell. Therefore, we may conclude that dual antenna diversity can be used to compensate for imperfect power control, and results in substantial increase of traffic capacity. Moreover, the capacity of 29 users represents a 1.6 fold increase in capacity over that reported by Gilhousen *et al.* (1991).

The assumptions of hexagonal cell geometry and path loss exponent of 4 are somewhat idealistic. Figures 5.2, 5.3 and 5.4 demonstrate the performance of the RAMSIC receiver in a flat Rayleigh fading channel with dual antenna diversity, non-
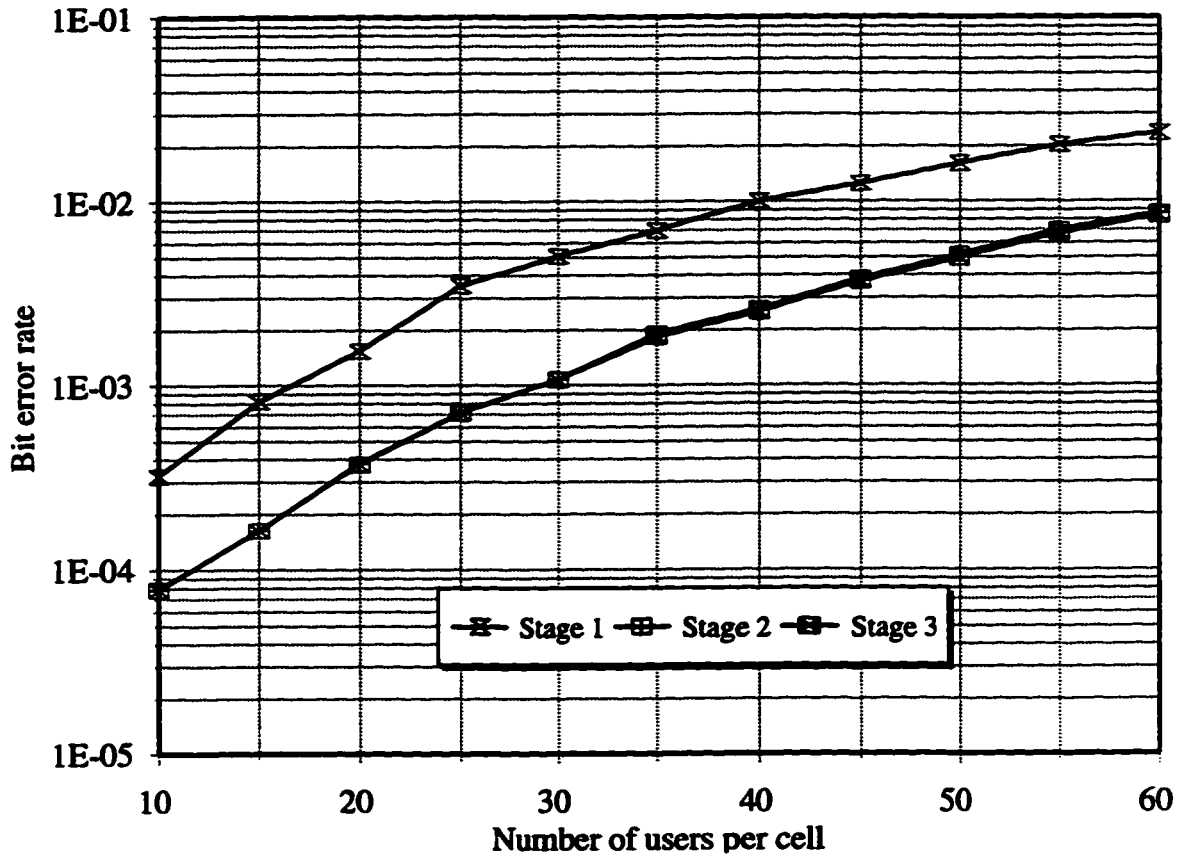
Fig. 5.3. Multi-cell performance of the RAMSIC receiver with two receive antennas on a flat Rayleigh fading channel. The power control is imperfect, Doppler frequency is 100 Hz and $f = 0.959$.

idealized cell geometry and path loss exponent of 4 ($f = 0.686$), 3 ($f = 0.959$) and 2 ($f = 1.57$) respectively. Similar to that for $f = 0.55$, the performance curves show that increasing the number of cancellation stages beyond two results in no gain in performance. The capacity for a BER of 10^{-3} is 26 for path loss exponent 4, 22 for path loss exponent 3 and 15 for path loss exponent 2. As expected, the system traffic capacity decreases with increasing intercell interference. The system, nevertheless, still have significant capacity even when the path loss exponent is 2.

Another possible form of diversity that may be employed in a flat fading channel is that of artificial multipaths created with multiple transmitter antennas. Since increasing the
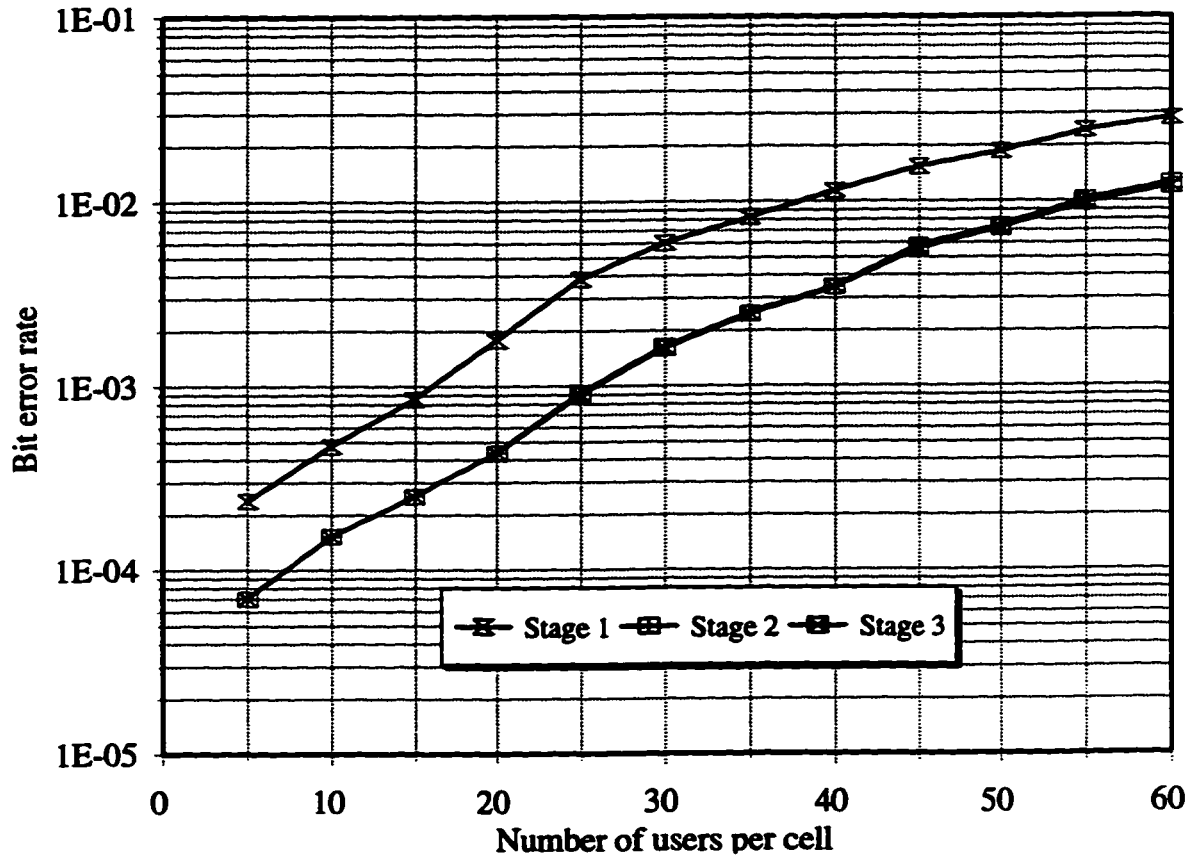
236

Fig 5.4. Multi-cell performance of the RAMSIC receiver with two receive antennas on a flat Rayleigh fading channel. The power control is imperfect, Doppler frequency is 100 Hz and $f = 1.57$.

number of multipaths will make interference cancellation more difficult (more multiple access interference will need to be cancelled), it is not intuitively obvious whether artificial multipaths are beneficial to the performance of the RAMSIC receiver. Figures 5.5 to 5.8 show the performance of the RAMSIC receiver with dual receive antenna diversity operating under the same conditions as those assumed in Figure 5.1 to 5.4 respectively, and two artificially created propagation paths (i.e. transmitter diversity). Only two artificial multipaths are considered because a handset with more than two transmitter antennas unlikely to be used. It can be seen from the figures that the capacity of the system for BER
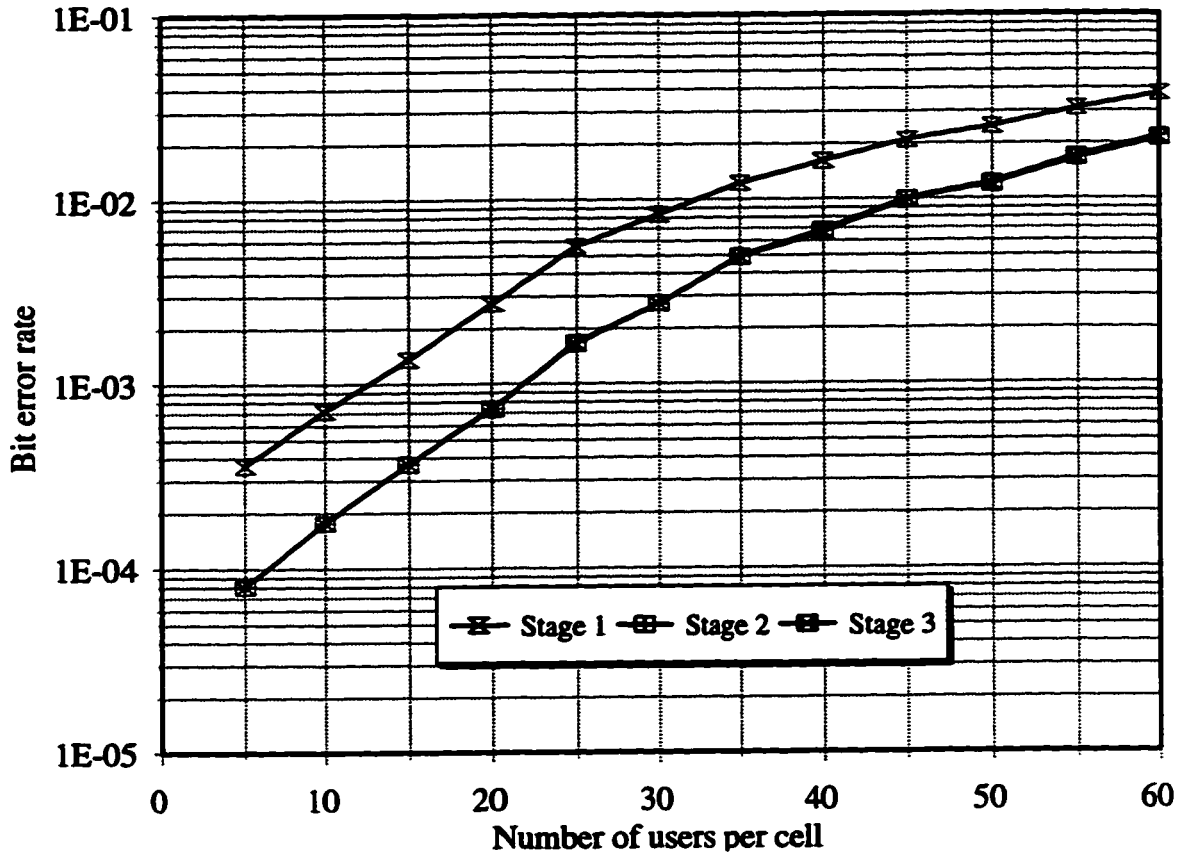
Fig 5.5. Multi-cell performance of the RAMSIC receiver with two receive antennas on a flat Rayleigh fading channel. Dual artificial multipath is created by the transmitter. The power control is imperfect, Doppler frequency is 100 Hz and $f = 0.55$.

of 10^{-3} is 27, 24, 18 and 13 users per cell for $f = 0.55$, 0.686. 0.959 and 1.57 respectively. Comparing with the previous results, it can be seen that the capacity with artificial multipath is less than that without artificial multipath. Thus it can be concluded that although the addition of artificial multipaths decrease the standard deviation of the power control error, the increase multiple access interference more than offsets possible gains. However, comparision of the performance curves with those of Figures 5.1 to 5.4 also shows that if a lower BER is required (say 10^{-4} or less), there is a performance gain with artificial multipath. This is because with a lower required BER, the system is smaller and

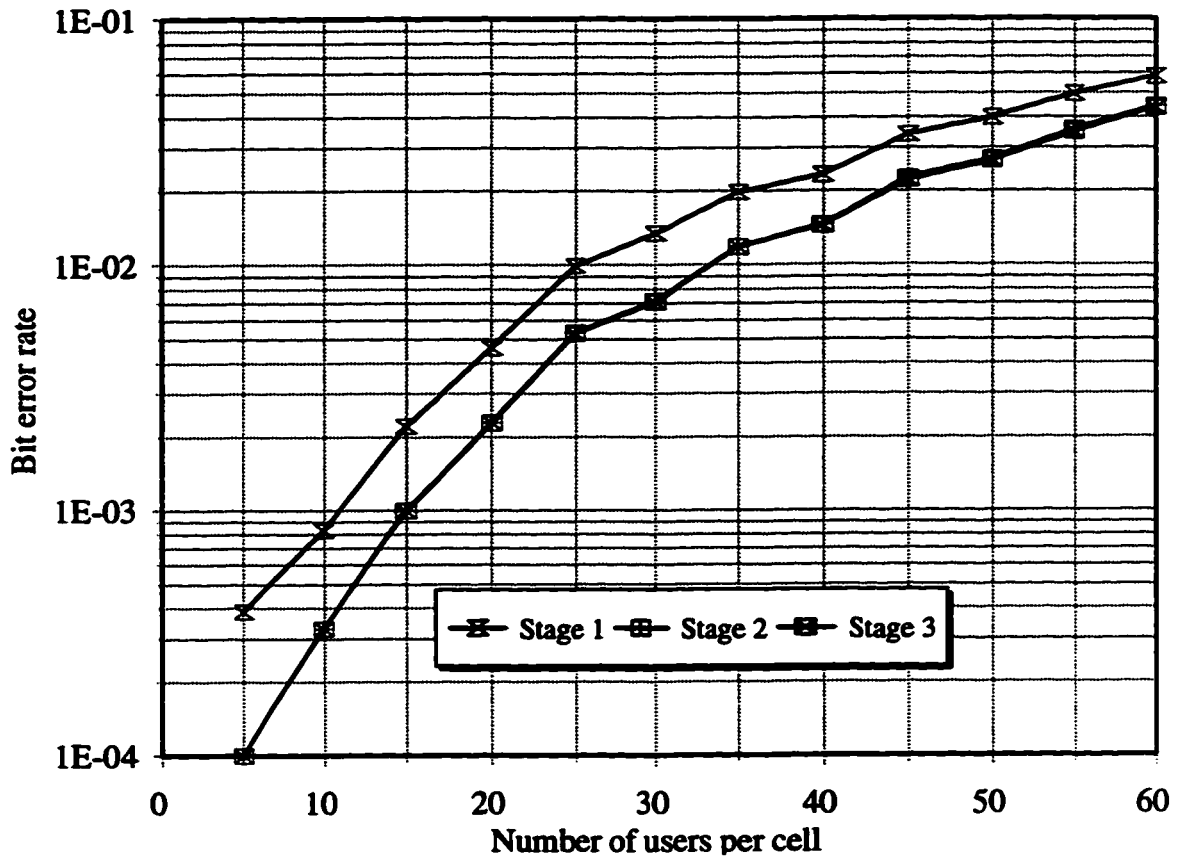Fig 5.6. Multi-cell performance of the RAMSIC receiver with two receive antennas on a flat Rayleigh fading channel. Dual artificial multipath is created by the transmitter. The power control is imperfect, Doppler frequency is 100 Hz and $f = 0.686$.

hence the additional multiple access interference due to artificially created multipath is easier to handle. Under such circumstances, performance gains obtained from decreased power control error due to artificial multipath more than offset the loss caused by additional interference.

Fig 5.7. Multi-cell performance of the RAMSIC receiver with two receive antennas on a flat Rayleigh fading channel. Dual artificial multipath is created by the transmitter. The power control is imperfect, Doppler frequency is 100 Hz and $f = 0.959$.
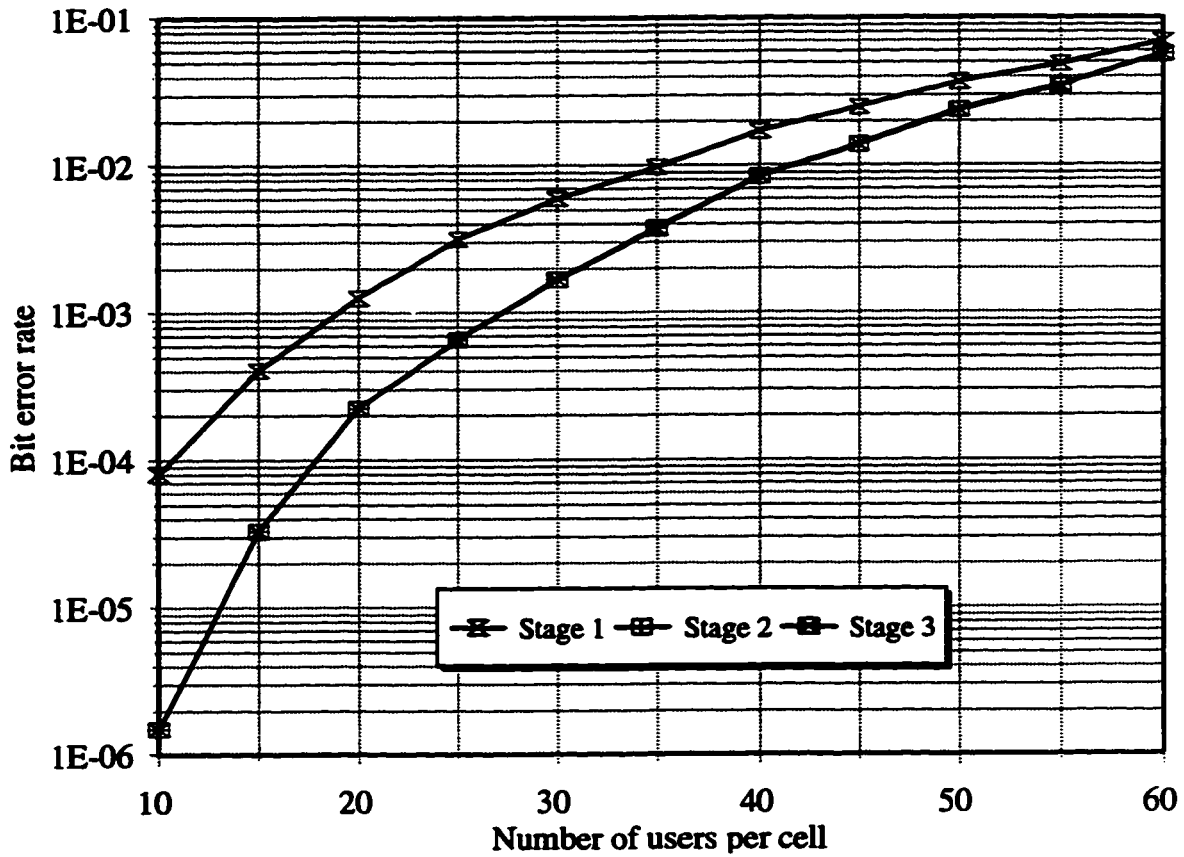
Fig 5.8. Multi-cell performance of the RAMSIC receiver with two receive antennas on a flat Rayleigh fading channel. Dual artificial multipath is created by the transmitter. The power control is imperfect, Doppler frequency is 100 Hz and $f = 1.57$.

5.4 Performance in low Doppler environment

All previously presented results were obtained at high Doppler shifts (in fast fading). The performance of the RAMSIC receiver in low Doppler shift environment is now investigated. The system parameters are the same as those in Section 5.3 with the following exceptions: Doppler shift is now set at 10 Hz and the power control error is modelled as a log-normal variable, because the IS-95 feedback power control algorithm is now capable of eliminating Rayleigh fading. The standard deviation of the power control error is the same as that determined by Naguib (1995) ($\sigma = 1.1$ for dual receive antenna

diversity and $\sigma = 0.5$ for dual receive antenna diversity with dual artificial multipaths).

Performance with dual receive antenna diversity for different intercell to intracell interference ratios is shown in Figures 5.9 to 5.12. The traffic capacity at a BER of 10^{-3} is 67, 57, 45 and 30 users per cell for $f = 0.55$, 0.686, 0.959 and 1.57 respectively. Comparing the capacity with that given in Section 5.3 shows that decreasing the Doppler frequency significantly increases the traffic capacity. Therefore it is reasonable to interpret earlier results as the worst case ones.

Figures 5.13 to 5.16 detail the multi-cell performance of the RAMSIC receiver with dual antenna diversity and dual artificial multipaths for different values of intercell to
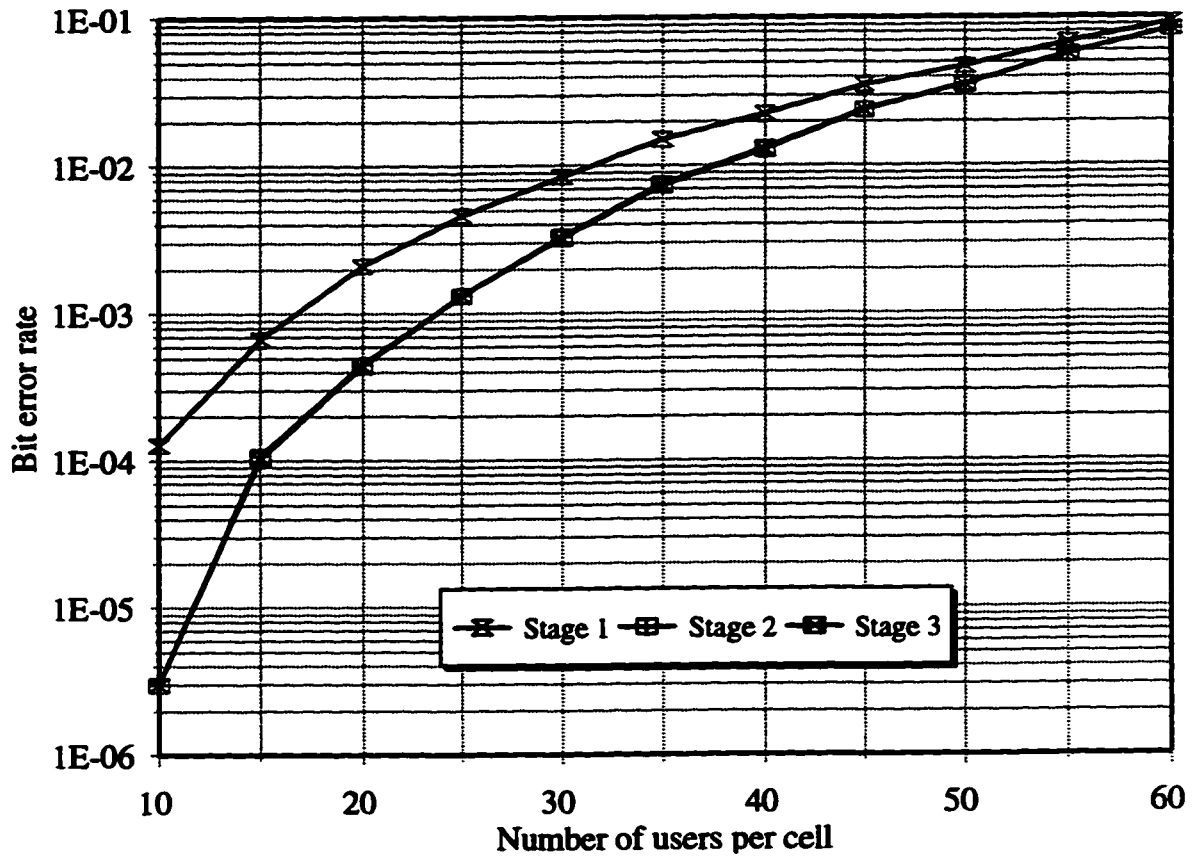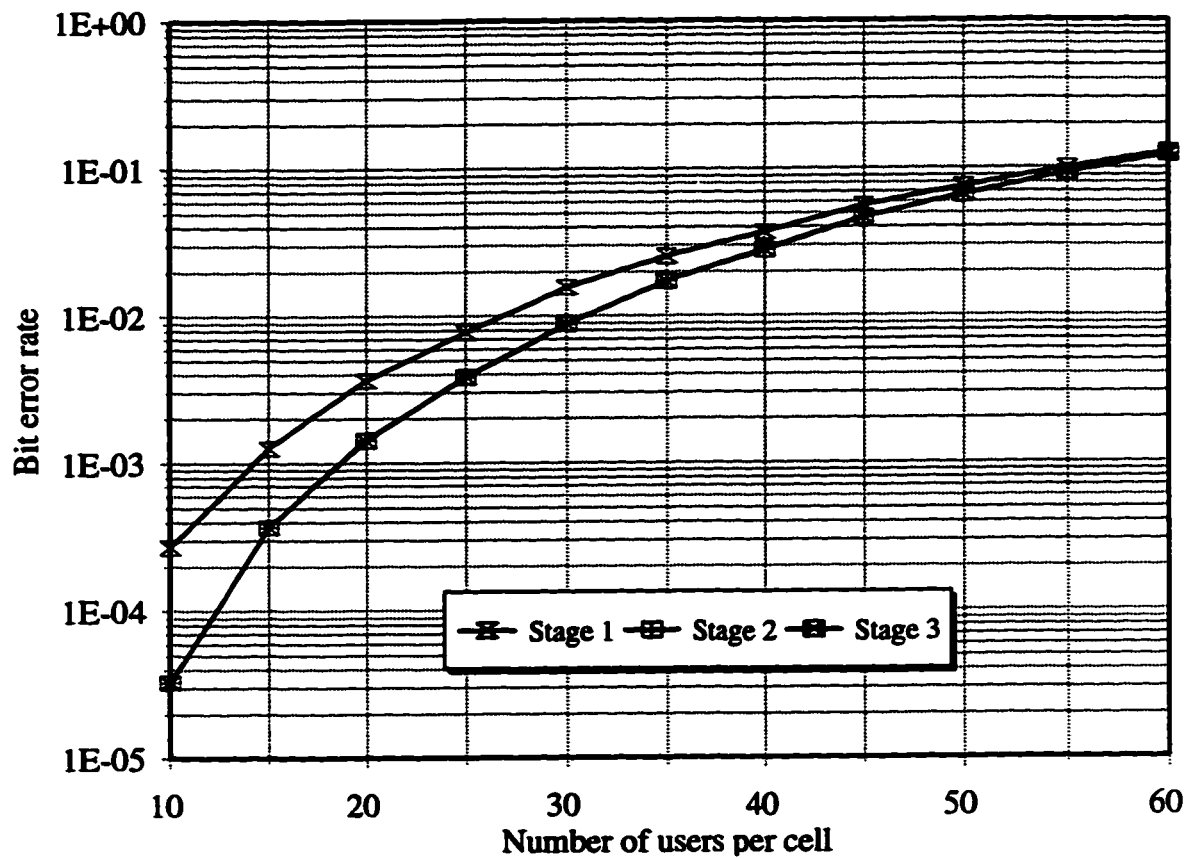

Fig. 5.9. Multi-cell performance of the RAMSIC receiver with two receive antennas on a flat Rayleigh fading channel. The power control is imperfect, Doppler frequency is 10 Hz and $f = 0.55$.
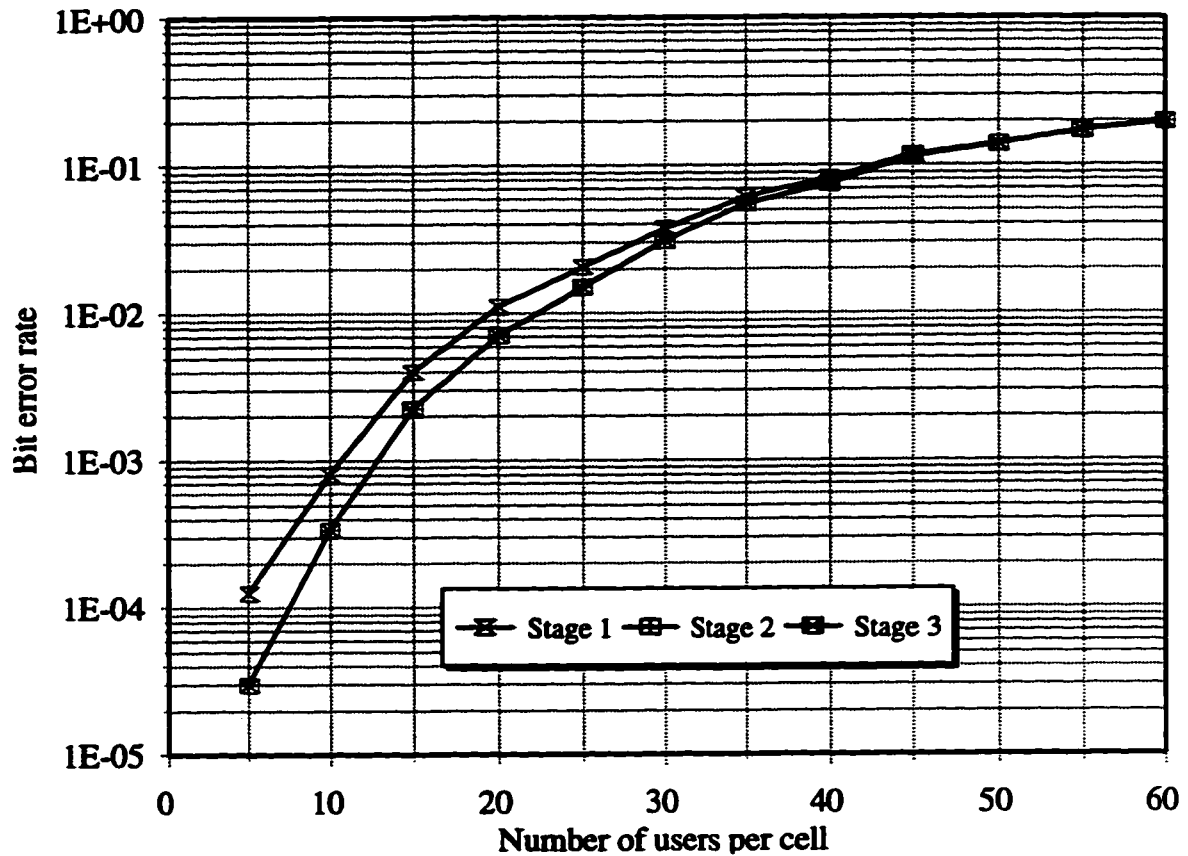
Fig. 5.10. Multi-cell performance of the RAMSIC receiver with two receive antennas on a flat Rayleigh fading channel. The power control is imperfect, Doppler frequency is 10 Hz and $f = 0.686$.

intracell interference ratios. The capacity at a BER of 10^{-3} is 41, 36, 29 and 19 users per cell for $f = 0.55$, 0.686, 0.959 and 1.57 respectively. Since the capacity is much larger than that of the comparable system in Section 5.3, the results obtained there may again be considered as the worst case ones. Moreover, comparison with the results from Figures 5.9 to 5.12 demonstrates that at BER of 10^{-3}, the introduction of artificial multipath does not result in capacity increase because of the corresponding increase of multiple access interference. On the other hand, similarly to the results in Section 5.3, in systems requiring a lower BER artificial multipaths can be used to improve the performance.

Fig. 5.11. Multi-cell performance of the RAMSIC receiver with two receive antennas on a flat Rayleigh fading channel. The power control is imperfect, Doppler frequency is 10 Hz and $f = 0.959$.
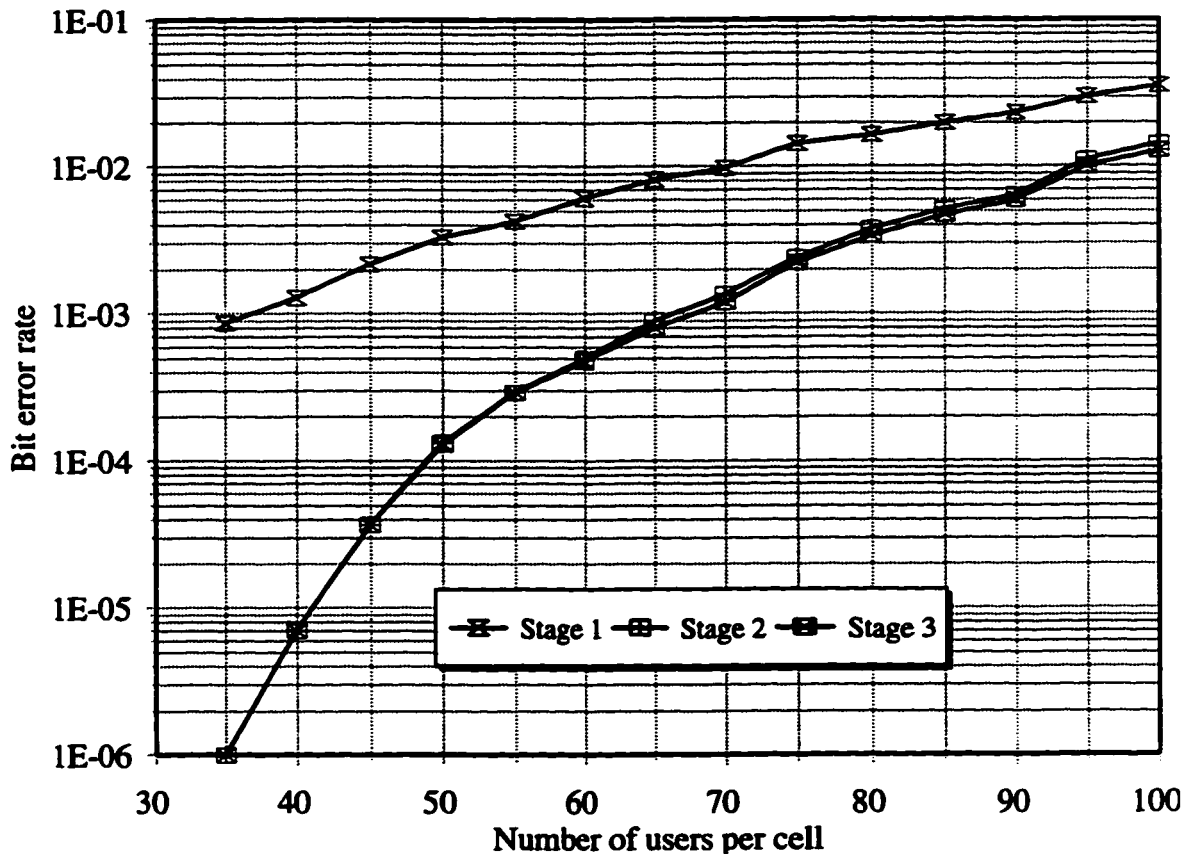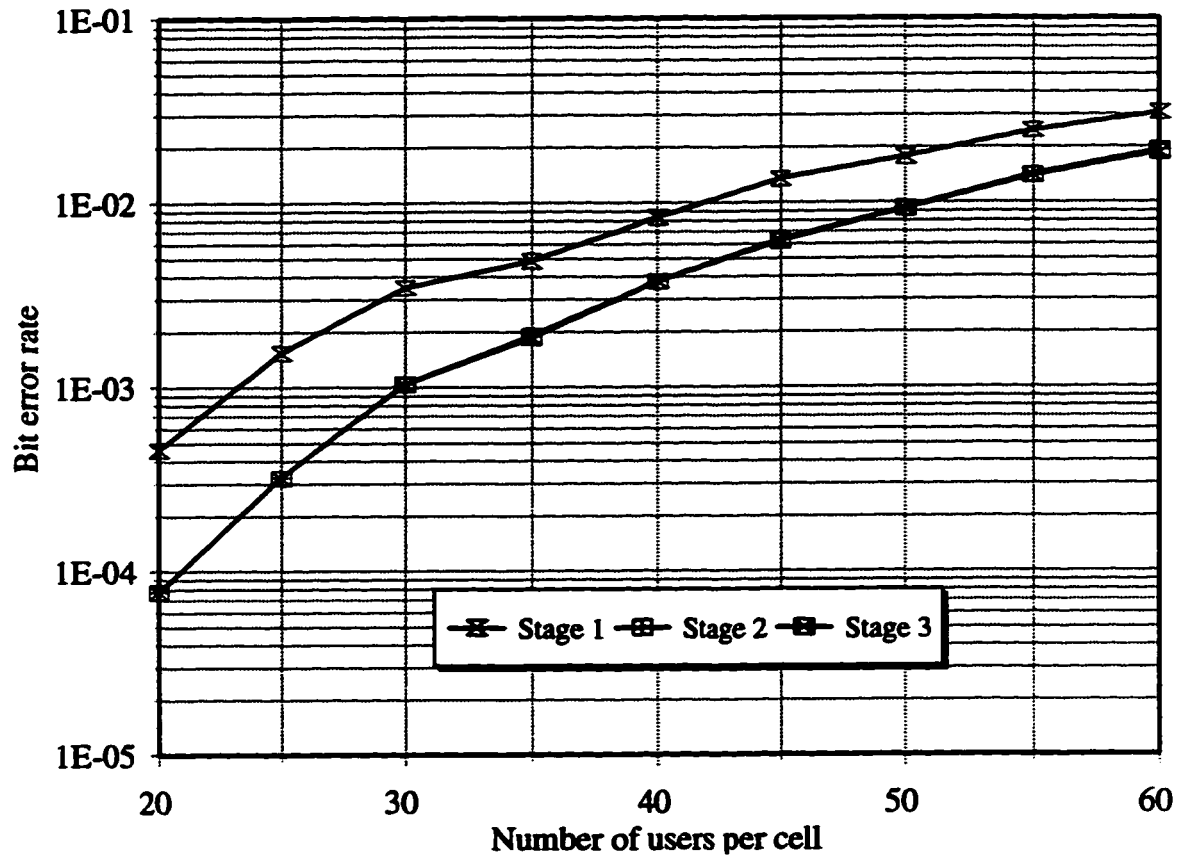
Fig. 5.12. Multi-cell performance of the RAMSIC receiver with two receive antennas on a flat Rayleigh fading channel. The power control is imperfect, Doppler frequency is 10 Hz and $f = 1.57$.
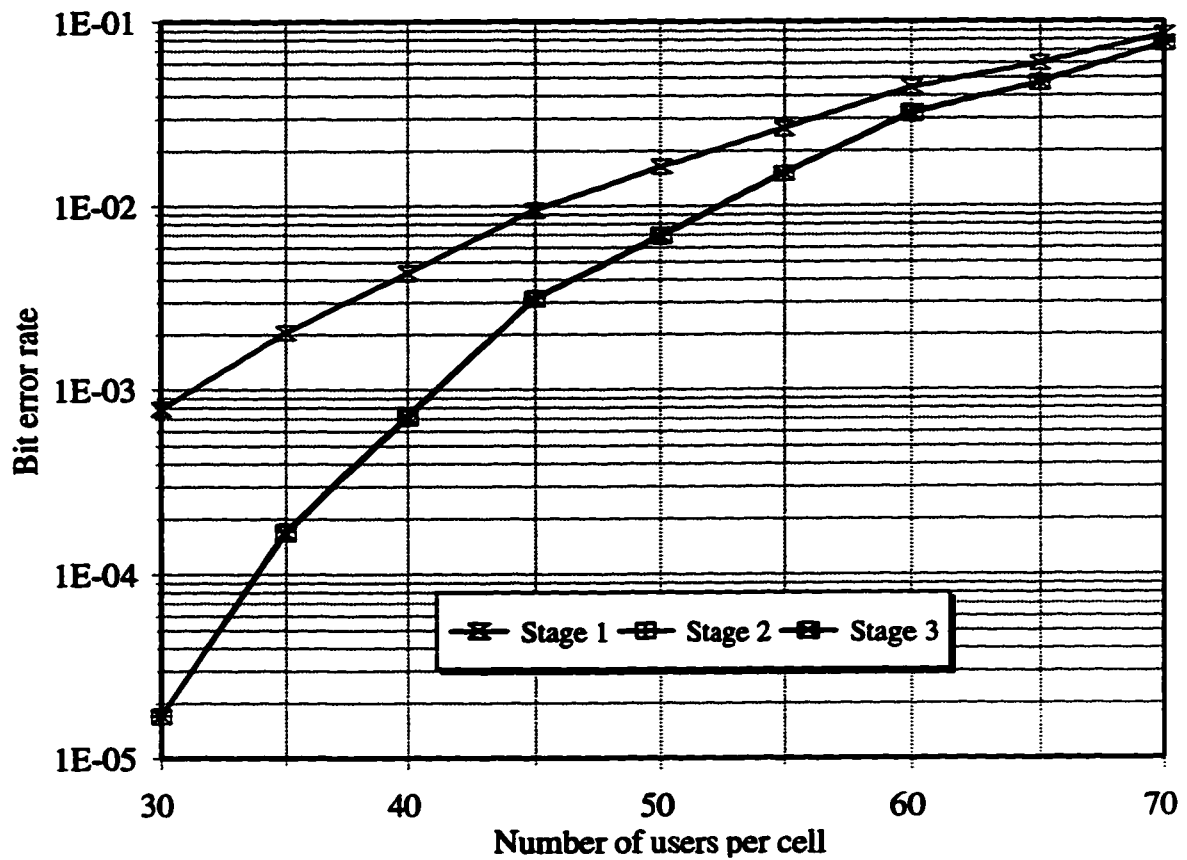
Fig 5.13. Multi-cell performance of the RAMSIC receiver with two receive antennas on a flat Rayleigh fading channel. Dual artificial multipath is created by the transmitter. The power control is imperfect, Doppler frequency is 10 Hz and $f = 0.55$.
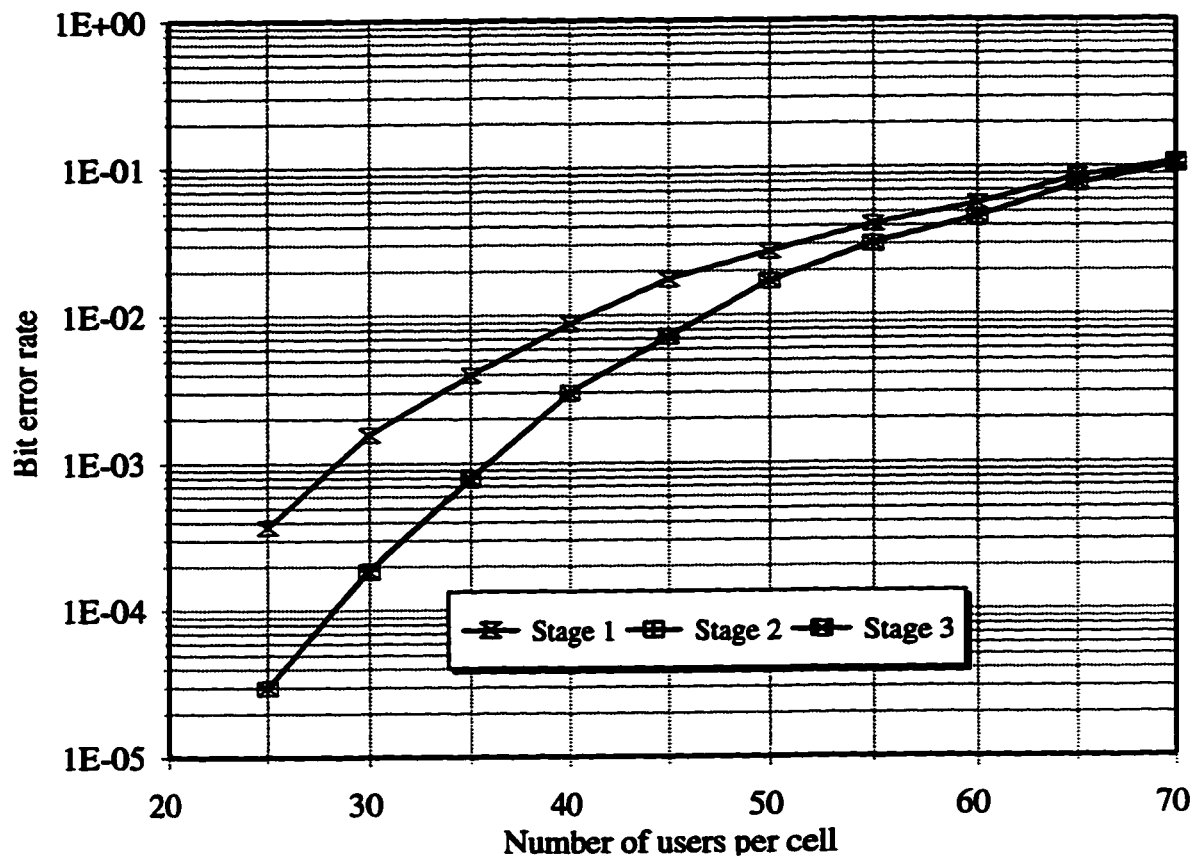
Fig 5.14. Multi-cell performance of the RAMSIC receiver with two receive antennas on a flat Rayleigh fading channel. Dual artificial multipath is created by the transmitter. The power control is imperfect, Doppler frequency is 10 Hz and $f = 0.686$.
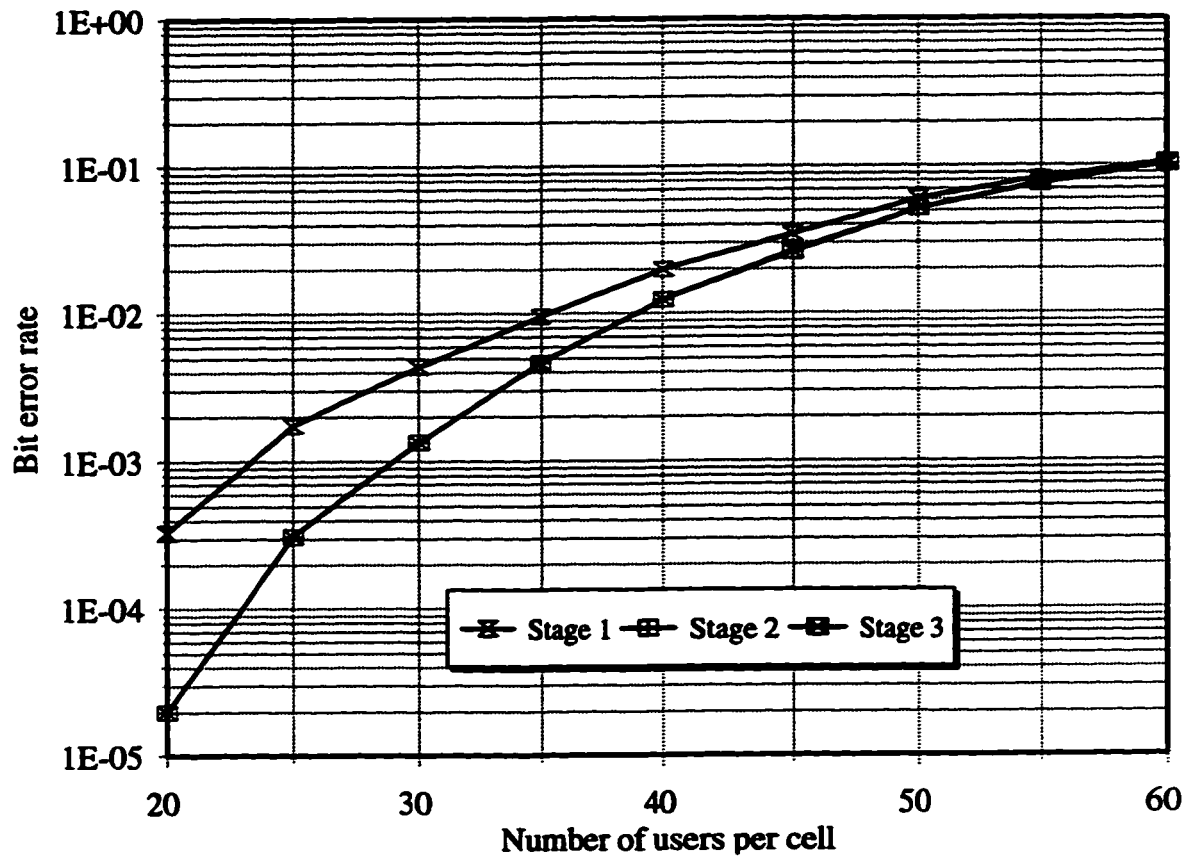
Fig 5.15. Multi-cell performance of the RAMSIC receiver with two receive antennas on a flat Rayleigh fading channel. Dual artificial multipath is created by the transmitter. The power control is imperfect, Doppler frequency is 10 Hz and $f = 0.959$.
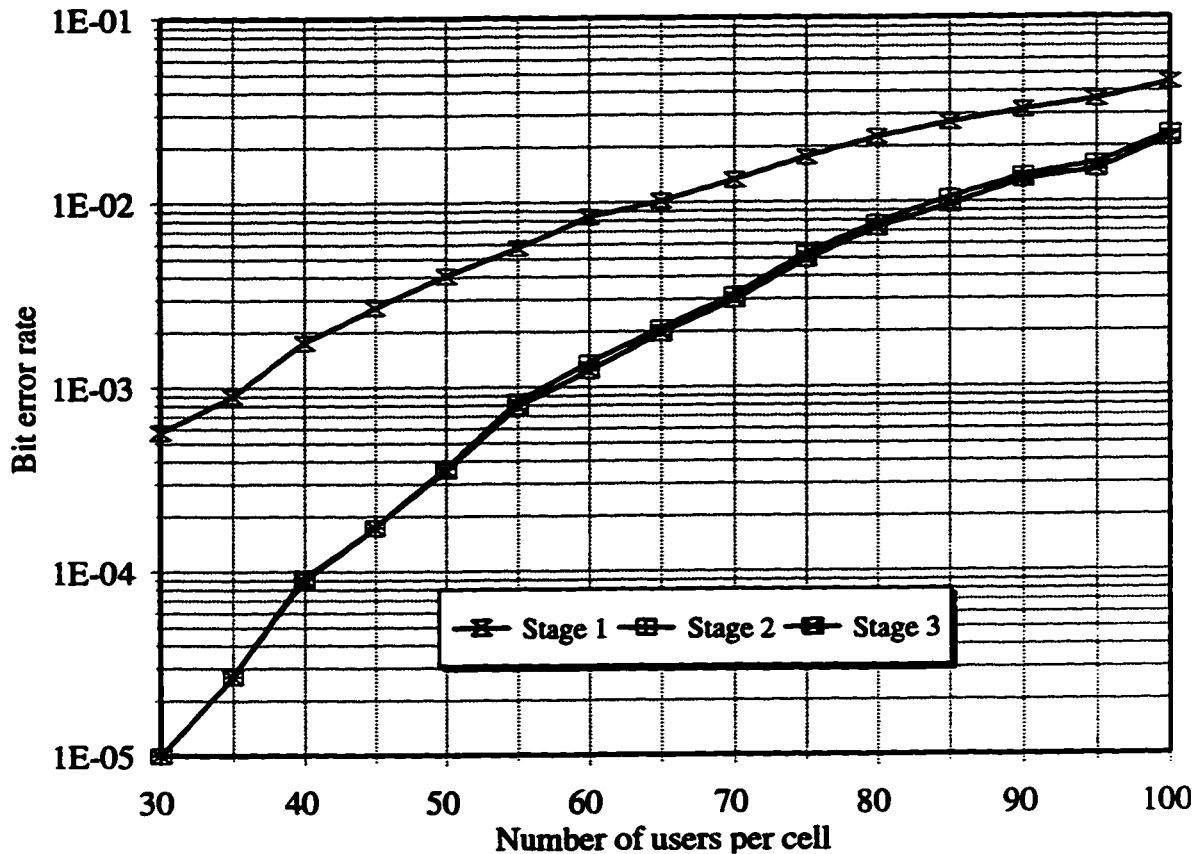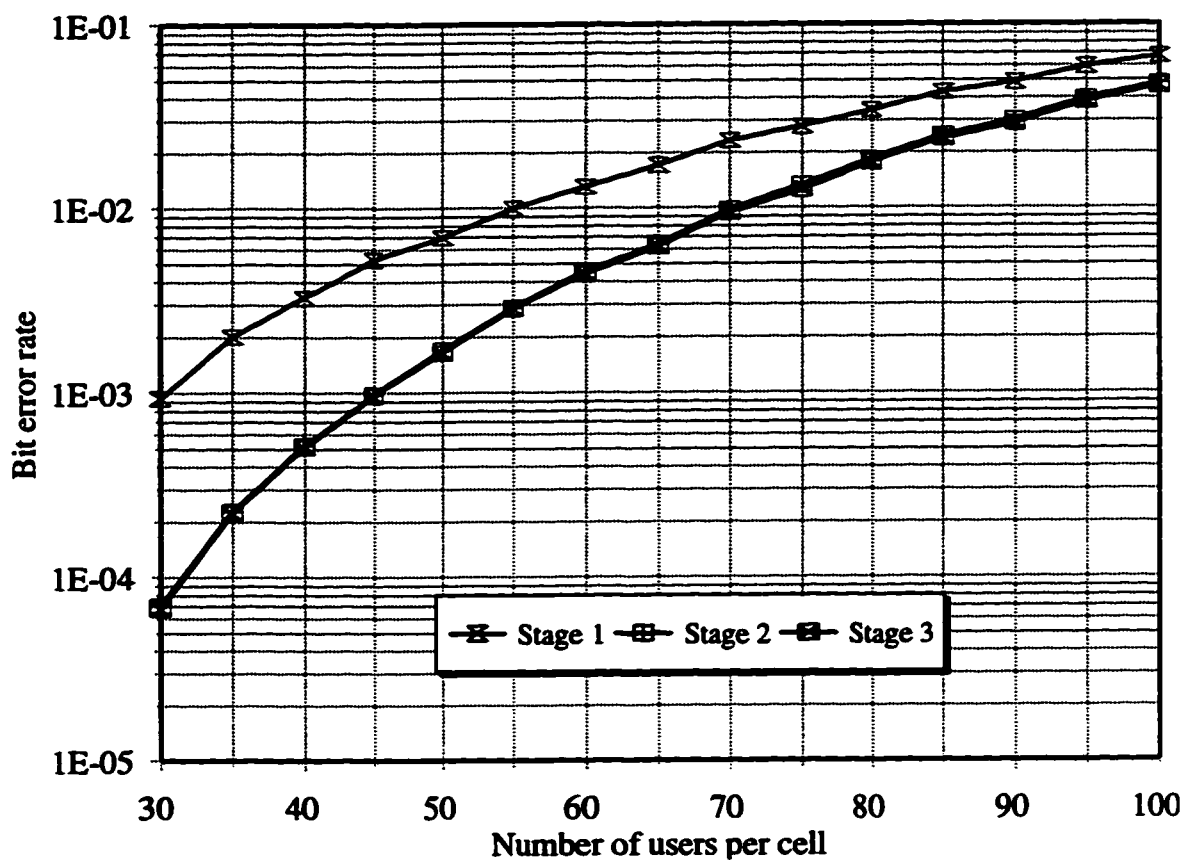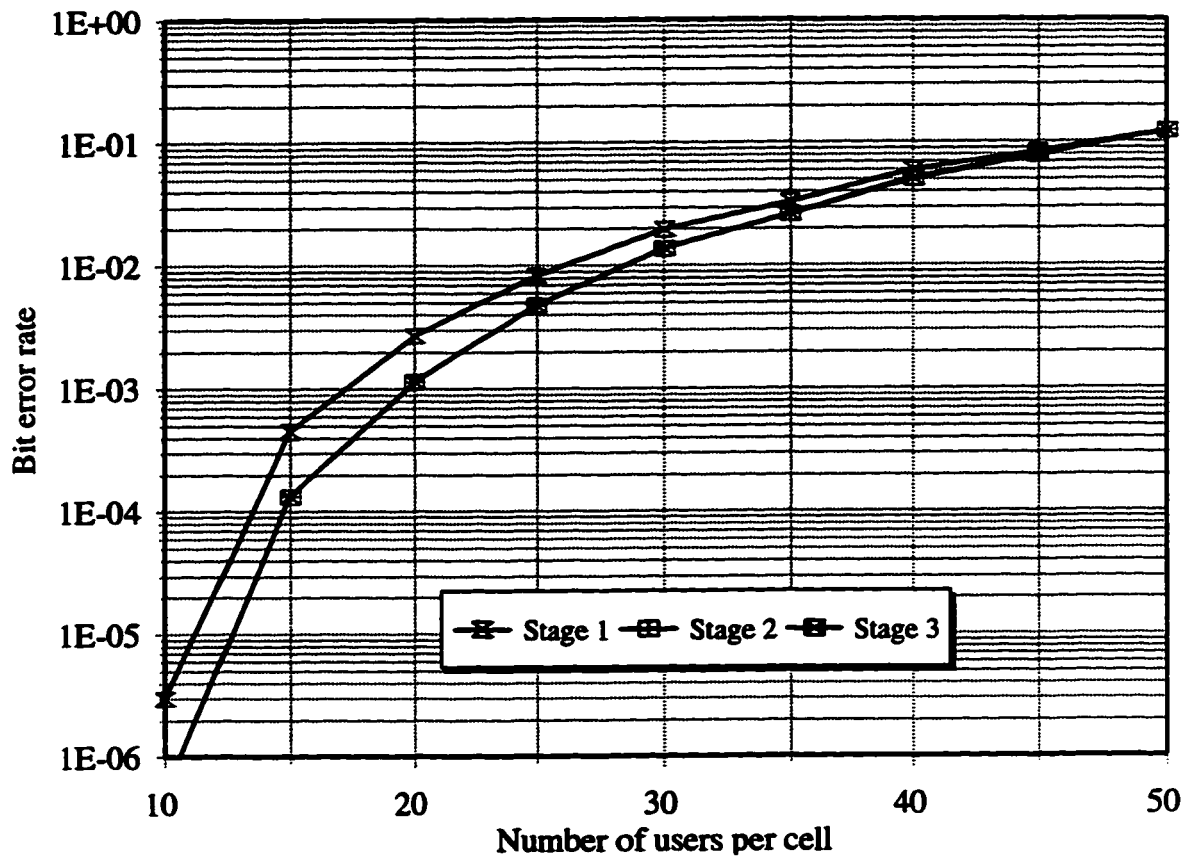
Fig 5.16. Multi-cell performance of the RAMSIC receiver with two receive antennas on a flat Rayleigh fading channel. Dual artificial multipath is created by the transmitter. The power control is imperfect, Doppler frequency is 10 Hz and $f = 1.57$.

5.5 Conclusion

This chapter has discussed performance of the RAMSIC receiver with antenna diversity. It has been shown that with dual receive antenna diversity, the capacity of the system with a realistic power control algorithm can be increased 1.6 times over that of the system investigated by Gilhousen *et al.* (1991). Investigation into the performance of the receiver in a small Doppler shift environment shows that the capacity increased dramatically with decreasing Doppler shift. Therefore, the 1.6 fold advantage of the RAMSIC receiver may be interpreted as the worst case performance advantage. The

results also show that for systems requiring BER of 10^{-3}, as in voice communication, the introduction of artificial multipath decreases capacity while for systems requiring lower BER (say 10^{-4} or less), as in image and video communication, artificial multipath can be used to increase capacity.

.

5.6 References

Ariyavisitakul S. and Chang, L.F. (1993): Signal and interference statistics of a CDMA system with feedback power control, *IEEE Trans. Commun.*, vol. 41, no. 11, pp.1626-1634.

Gilhousen, K.S., Jacobs, I.M., Padovani, R., Viterbi, A.J., Weaver, L.A. and Wheatley III, C.E. (1991): On the capacity of cellular CDMA system. *IEEE Trans. Veh. Technol.*, vol. VT-27, pp 303-312.

Jakes, W.C. (1974): *Microwave Mobile Communications*. New York: John Wiley, 1974.

Ling, F. (1992): Coherent detection with reference-symbol based channel estimation for direct sequence CDMA uplink communications. *Proc. IEEE Vehicular Technology Conf.*, pp. 400-403.

Milstein, L.B. and Rappaport, T.S. (1992): Effects of radio propagation path loss on DS-CDMA cellular frequency reuse efficiency for the reverse channel. *IEEE Trans. Vehicular Technology*, vol. 41, no. 3, pp. 231-241.

Stüber, G.L. (1996): *Principles of Mobile Communication*. Boston: Kluwer Academic Press.

Varanasi, M.K. and Aazhang, B. (1990): Multistage detection in asynchronous code-division multiple-access communications. *IEEE Trans. Commun.*, vol. 38, no. 4, pp. 509-519.

Verdu, S. (1986): Minimum probability of error for asynchronous Gaussian multiple-access channels. *IEEE Trans. Infrom. Theory*, vol. IT-32, no. 1, pp. 85-96.

Naguib, A.F. (1995) Power control in wireless CDMA: performance with cell site antenna arrays. *Proc. IEEE Globecom*, pp. 225-229.

Chapter 6: Conclusion

6.1 Introduction

Code division multiple access (CDMA) is, at least in North America, a leading multiple access candidate for third generation wireless cellular telephone systems. However, even with the capacity improvement that is realizable with the current CDMA standard (TIA IS 95), it is anticipated that, because of the recent explosion in the demand for cellular service, traffic congestion over the allotted spectrum will still be of prime concern. Therefore, the main objective of this thesis has been to develop a receiver structure that is capable of significantly increasing the traffic capacity of wireless CDMA systems.

6.2 Conclusions

It was evident from the review of the literature in Chapter 2 that, in the last decade, significant efforts were devoted to developing receiver structures that were resistant to multiple access interference. This is because of the fundamental fact that the capacity of CDMA systems is limited by multiple access interference. The optimal multiuser receiver structure is capable of significantly increasing traffic capacity (Verdu, 1986). However, the structure of this receiver is too complex to be implemented in the foreseeable future. Recent efforts have been focused on suboptimal receiver structures that are more easily implemented.

It can be argued that of all the different receiver structures described in the literature (a review can be found in Chapter 2), the least complex and thus most practical class of

252

multi-user receivers is the successive interference cancelling type. Since estimation of the channel parameters is critical to the performance of this class of receiver, Chapter 3 introduced the reference symbol assisted multistage successive interference cancelling (RAMSIC) receiver. The results of a single cell multi-user investigation demonstrated increased traffic capacity. However, this increase was initially very moderate due to corruption of the channel estimates by interference from symbols not yet demodulated and cancelled. A modification in the transmitted signal structure addressing this problem was proposed. The results of a single cell analysis of the modified cancellation scheme demonstrated that the system's traffic capacity reached approximately 80% of that of a multistage successive interference cancelling receiver operating with the perfect knowledge of channel parameters. Subsequent multi-cell investigation showed that for hexagonal cell geometry with path loss exponent of 4 and without any forward error correction coding or cell sectorization, capacity of the system compared very favourably with that of the IS 95 system, employing powerful error control coding. Capacities with other path loss exponents and cell geometries were also investigated. The results showed substantial traffic capacity increase over that of a comparable receiver without interference cancellation.

Chapter 4 investigated the sensitivity of a reference symbol assisted multi-stage successive interference cancelling (RAMSIC) receiver to system imperfections. The reverse link of a CDMA system with binary antipodal modulation and coherent detection was considered. Performance of the system using either biphase or quadriphase spreading was compared under different operating conditions. Analysis of a conventional matched

filter receiver operating on an AWGN channel revealed that when the number of users was small (such that the multiple access interference could not be accurately modelled as Gaussian), quadriphase spreading had a significant advantage over biphase spreading. This advantage, however, disappeared when the number of users per sector was large (of the order necessary for the multiple access interference to be considered Gaussian). Results for the RAMSIC receiver with quadriphase spreading, on the other hand, showed that for hexagonal cell geometry with path loss exponent of 4 and without any forward error correction coding, the traffic capacity was between 1.17 and 1.67 times that of the IS-95. These numbers represented a significant increase over those obtained with biphase spreading. Further investigation with nonidealized cell geometries and other path loss exponents also showed substantial capacity improvement over that of conventional correlator receivers. Performance losses due to nonideal transmitter power amplifier gating, imperfect power control and synchronization errors in the RAKE receiver were also determined. The results for biphase spreading showed that for path loss exponent of 4, imperfect amplifier gating caused relatively minor decrease in the traffic capacity, while no such effect was observed for path loss exponents of 2 and 3. As expected, relaxing power control for both biphase and quadriphase spreading had a similar capacity reducing effect. In spite of these two effects the resultant capacity was still significantly higher than that with the conventional matched filter receiver. Capacity increase with quadriphase over biphase spreading was between 1.4 and 2.0 times. Chip synchronization errors of the order to be expected in a properly designed conventional CDMA system also had only minimal effect on performance. Therefore, we concluded that conventional synchronization

algorithms should perform adequately with successive interference cancelling receivers considered in the paper.

The results of Chapter 4 lead to the realization that additional diversity should be employed to minimize the power control error in order to maximize the capacity improvement possible with the RAMSIC receiver. The prime candidate, which was investigated in Chapter 5, was receiver antenna diversity because of its additional advantage over multipath diversity of not introducing self interference. The results showed that with the power control algorithm as in the IS 95 standard and dual antenna diversity, the capacity of the system operating in a high Doppler environment could be increased by a factor of 1.6 over the system investigated in Gilhousen *et al.* (1991). Moreover, performance results in a low Doppler environment showed that capacity increased significantly with decreasing Doppler shift. This result was expected because the system considered in this thesis did not employ forward error correction coding. Therefore we may interpret the high Doppler shift results in this thesis as the worst case.

6.3 Future work

Although this thesis has demonstrated that the RAMSIC receiver can significantly increase the capacity of wireless CDMA systems, there are several questions about its performance that are still unanswered. One of the most obvious questions is: what is the performance of the RAMSIC receiver employing powerful forward error correction coding such as convolutional coding? Error correction coding has the capability of significantly increasing the capacity of the system. But its integration with the RAMSIC

255

algorithm requires further study.

Another open question relates to handoffs which are critical to the success of any cellular system. At present, the best way to transmit the reference symbols and to estimate the channel during soft handoffs is not clear. Clearly more work is necessary before the handoff algorithm suitable for integration with the RAMSIC receiver can be specified.

How does a wireless communication system employing a RAMSIC receiver take advantage of voice activity level is another open question. Recall that in IS-95 systems, the algorithm for taking advantage of voice activity level is different in the forward and reverse links. During intervals of low voice activity, the transmitter power is reduced and the symbol time is lengthened in the forward link while in the reverse link, power control groups are deleted to reduce the multiple access interference. The natural question that needs to be answered is which algorithm is better in a system with the RAMSIC receiver. Intuitively, voice activity should be handled similarly to that in the forward link of IS-95 systems because reference symbols are transmitted regularly resulting in better tracking of the time variant channel. However, this needs to be demonstrated explicitly.

Research on improving the RAMSIC receiver is currently underway at Simon Fraser University in British Colombia (Nesper and Ho, 1996a, b). Since this thesis shows that the performance of the RAMSIC receiver can be improved if the channel estimates can be refined, they suggest changing the interference cancellation algorithm during estimation of the channel parameters. Their results show that, at least for a single cell system, employing a decorrelating receiver during channel estimation can significantly improve the performance of the RAMSIC receiver. This immediately leads to two questions: a) what is

the best interference algorithm for channel estimation? and b) will the performance advantage be significant in the multi-cell environment where most of the interference is from out of cell and thus cannot be easily cancelled?

As can be seen in this section, much work is still needed before the implementation of the RAMSIC receiver becomes possible. Nevertheless, this thesis has demonstrated the intriguing possibility of using the RAMSIC receiver to improve the capacity of CDMA wireless systems. The relative simplicity of this receiver structure makes it a prime candidate for commercial development.

6.4 References

Nesper, O. and Ho, P. (1996a): A reference symbol assisted interference cancelling hybrid receiver for an asynchronous DS/CDMA system. *Proc. IEEE PIMRC* , pp. 108-112.

Nesper, O. and Ho, P. (1996b): A pilot symbol assisted successive interference cancellation scheme for an asynchronous DS/CDMA system. *Proc. IEEE GLOBECOM*, pp. 1447-1451.